The Role of Aurora Kinases at the Crossroads of Cancer and Differentiation

A Thesis Submitted for the Degree of

Doctor of Philosophy

By

Arnab Bose

To

Molecular Biology and Genetics Unit

Jawaharlal Nehru Centre for Advanced Scientific Research

Jakkur, Bangalore-560064, India

OCTOBER, 2018

TABLE OF CONTENTS

1.3.4. Metabolic reprogramming in cancer

1.3.5. T-cell activation

1.3.6. Functions in ciliary resorption

1.3.7. Cellular quiescence

1.3.8. Regulation of Transcription Factors

1.3.9. Regulation of oncogenic signalling

1.3.9.1. NFkB signalling activation

1.3.9.2. c-Fos complex formation

1.3.9.3. N-Myc stability and function

1.3.9.4. c-Myc oncogenic activity

1.3.9.5. Androgen receptor activation

1.3.10. Regulation of tumour suppressor pathways

1.3.10.1. Wnt signal transduction pathway

1.3.10.2. p53 family inhibition

1.4. Regulation Of Aurora Kinases By Extracellular Signalling

1.5. Regulation Of Aurora Kinases By Post Translational Modifications

1.5.1. Phosphorylation

1.5.2. Poly(ADP-ribosyl)ation

1.5.3. SUMOylation

1.5.4. Acetylation

1.5.5. Ubiquitination

1.6. Impact Of DNA Damage And Repair On Aurora Kinases

1.7. Role Of Aurora Kinases In Cellular Differentiation

1.7.1. Neuronal processes

1.7.1.1. Neuronal plasticity

1.7.1.2. Axonal outgrowth

2.3. Cell culture

2.3.1. Mammalian Cell culture

2.3.2. Insect Cell Culture

2.3.3. Culture and differentiation of C2C12 myoblasts

2.3.3. Mammalian cell Transfection

2.3.3.1. Transfection of plasmid DNA

2.3.3.2. Transfection of siRNA

2.3.4. Generation of stable cell lines

2.3.4.1. Stable knockdown of Tip60

2.3.4.1. Stable knockdown of Aurora kinase B

2.3.5. Indirect Immunocytochemistry

2.3.6. Cell Synchronization for mass spectrometry mediated identification of Aurora kinase B acetylation sites

2.3.6.1. G0/G1 block

2.3.6.2. G1/S block

2.3.6.3. G2/M block

2.4. Protein purification

2.4.1. Purification of recombinant proteins from baculovirus-infected Sf21 cells

2.4.2. His_6-tag fusion protein purification

2.4.2.1. Purification of recombinant His_6-tag fusion proteins from soluble fraction of E. coli lysate

2.4.2.1. Purification of recombinant His_6-Myc fusion proteins from inclusion bodies of E. coli

2.4.3. Flag-tag fusion protein purification

2.4.3.1. For mass spectrometric analysis

2.4.3.2. For studying the interactions with other protein partners

2.5. In vitro Assays

2.5.1. Kinase assay

2.5.2. In vitro mass phosphorylation of mPOU

2.5.3. Histone Acetyltransferase (HAT) gel assay

2.6. Generation of polyclonal antisera

2.6.1. Against K85-K87 acetylated peptide of Aurora kinase B in rabbit

2.6.2. Against phosphorylated oligopeptide of Ser-197 POU6F1 in rabbit

2.7. Mass spectrometry

2.7.1. Preparation of protein samples

2.7.1.1. In vitro acetylation of Aurora kinase B by Tip60

2.7.1.2. Immuno-purification of Flag-Max from HeLa cells

2.7.1.3. Immuno-purification of Flag-Max from HeLa cells upon Aurora kinase inhibitor treatment

3.1.6. Aurora kinases exhibit subtype specific alteration in breast cancer

3.1.7. Impact of AurkB knockdown or inhibition on c-Myc/Max dependent target gene expression

3.2. Acetylation dependent regulation of AurkB and a probable role of the dysregulated kinase in dictating the outcome of DNA damage repair pathway choice

3.2.1. Biochemical screening for the putative KAT(s) of AurkB

3.2.2. AurkB is a substrate of Tip60

3.2.3. Tip60 acetylate AurkB at two highly conserved lysine residues

3.2.4. Tip60 and p300 may not possess overlapping acetylation sites on AurkB

3.2.5. Tip60 interacts with and acetylates AurkB in cells

3.2.6. Tip60 regulate protein levels of AurkB in cells

3.2.7. Tip60 mediated acetylation inhibit the kinase activity of AurkB

3.2.8. Tip60 and AurkB follow inverse pattern of expression in breast cancer cells and modulate DNA damage response

3.2.9. AurkB regulates γH2AX levels by influencing Tip60 gene transcription

3.2.10. AurkB influences the choice of DNA damage repair

3.3. Reciprocal regulation of skeletal muscle differentiation by Aurora A kinase and POU6F1

3.3.1. mPOU is phosphorylated at Ser-197 in cells

Acknowledgements

It is with immense appreciation and pleasure that I acknowledge the contribution of my mentor, Prof. Tapas K. Kundu, in shaping my professional and personal outlook towards life. His rigour and perspectives have shattered all my dogmatic idealism and has rightfully propelled my thinking towards real and practical issues. His scientific and personal ambitions are intriguing and the planning to achieve the same, is thought provoking. Prof. Kundu is one of such bright examples who has outweighed his humble upbringing in undertaking one of the most daunting tasks of taking forward his life and scientific understanding, not only to the international podium through successful collaborations, but has also attempted in popularizing science by taking it to the school kids of some of the remotest villages of India. His management skills also display an interesting array of discipline and dedication and presents oneself an option to follow. I draw sincere inspirations from these aspects of his life and firmly believe that our brief philosophical interactions will definitely guide me to carry forward the responsibility I graciously bear for the betterment of the society, scientifically and otherwise. I am also grateful to him for not only providing me the opportunity to initiate my scientific career with an extremely captivating yet very competitive field of Myc biology, which has thoroughly smitten my scientific imagination, but also in giving me enough freedom to pursue the experiments I designed for all the subsequent lines of research. Although our interactions have not been without differences in opinion, but I steadily admit that these differences have enlightened and guided me to evolve and evaluate myself, in retrospect. I cherish my colourful experiences with him over these years and I take this opportunity to express my heartfelt gratitude.

It gives me great pleasure in acknowledging the erstwhile MBGU Chairman, Prof. Anuranjan Anand for providing excellent core departmental facilities and the present Chairman, Prof. Ranga Uday Kumar, in taking the extra step in adding to the existing ones. I also acknowledge the positive criticisms extended by Prof. M.R.S. Rao, Prof. Anand, Prof. Ranga, Prof. Kaustuv Sanyal, Prof. Maneesha Inamdar and Prof. Ravi Manjithaya in the course of my research in terms of experimental designing, suggestions and feasibility of the outcome. I also acknowledge the contributions of all the MBGU faculties with whom I interacted at various times during my stay in JNCASR and who have been kind enough in suggesting ways to improve the quality of my

work. I owe my gratitude to Prof. Umesh Varshney (Indian Institute of Science) and Prof. P.N. Rangarajan (Indian Institute of Science) for the valuable suggestions during my comprehensive examination.

I am thankful to my collaborators, Prof. Kazuhiko Igarashi, Tohoku University, Japan and Prof. N. Ganesh, Department of Biochemistry, IISc for extending their instant support and contribution to my work. It is very difficult to find a very good scientist who is also an amazing human being like Prof. Igarashi and I really cherish my brief association with him. I appreciate Dr. Hiroki Shima, Prof. Muto, Dr. Tamahara and Dr. Ochiai for making my stay in Japan, enjoyable. I acknowledge Sharmi with whom I got the opportunity to work and must admit the pleasure of discussing my work with her and thank her for helping me in understanding the field of DNA damage and repair.

I am indebted to my teachers, Ms. Bharaty Ghosh and Prof. Maitrayee Dasgupta, who instilled confidence and self-worth in myself. Ms. Ghosh has been instrumental during my school days and her encouragement on a daily basis had been humbling and motivating at the same time. Prof. Dasgupta has been a fantastic teacher whose patience and approach to answer the queries of my curious mind will always be remembered and appreciated. Scientifically, she has been an extremely open person and personally, her motherly affections have touched me.

I owe my deepest gratitude to Deepthi and Pallabi, whom by all means I adore as friends and possess enormous respect from the deepest core of my heart. Their sense of worldly understanding had helped me sail through some of the roughest patches and grow both as a professional and a personal entity. I am truly indebted to Vinay for helping me in several of the experiments that have become an integral part of this thesis. Kushaghra and Dr. Sadhan have been compassionate brother-like figures for me and I truly adore their company. Utsho has modified my understanding of politics in and politics of science and our interactions have strengthened my views on the necessity of diplomacy, good scientific policies and their rigorous implementation in order to make India globally accepted in Biological Sciences. Finally, I acknowledge my school and college friends- Ayan, Srijit, Abir, Satrajit and Sayan for creating some of the wonderful memories which I really cherish.

I sincerely acknowledge the help and support of my seniors, Dr. Karthigeyan and Dr. Parijat, for their guidance and support during the initial years of my research. I am truly and highly indebted

to so many people that the words might be limiting. I learned, gained, and enjoyed from my experiences in the Transcription and Disease Laboratory for which I acknowledge the contribution of my past and present lab members- Dr. Sharmishtha, Dr. Mahadev, Raktim, Debanjan, Dr. Snehajyoti, Dr. Sujata, Dr. Rahul, Dr. Jeelan, Dr. Stephanie, Dr. Amit, Dr. Surabhi, Suchismita, Siddharth, Aditya, Akash, Dr. Shrinka, Akshay, Dr. Somnath, Dr. Manoj, Dr. Sourav, Dr. Sweta, Padmalaya, Shubham, Nikitha, Vishakha, Dr. Amrutha, Moumita, Smita, Ila, Koel, and Dharaneeshwar. I really appreciate the contributions of Gowda, Salauddin and Sunil whose constant assistance on a daily basis has simplified my lab life.

I am thankful to Ms. Suma for helping me with confocal imaging, Ms. Anita for sequencing, and Dr. Uttara, Ms. Swaroopa and Dr. Narendra for the Flow Cytometry facility, which have been really helpful and necessary in shaping the present thesis. I acknowledge CSIR, DBT, DST, and JNCASR for all the financial support for the Ph.D. programme.

I feel privileged to have such affectionate and wonderful parents and brother, as my family. My mother has always been extremely instrumental in impregnating my young and naïve mind with the idea of “impossible is nothing”. Although, as I grew older I could feel the brunt of this overt optimism, but it still makes me believe that giving up is NOT an easy option. My father made sure that we have a modest upbringing despite all the financial problems and has always emphasized that education is never compromised. He always kept giving, asking for nothing in return. My thanking of these truly wonderful human beings will never be enough, but I extend my deepest gratitude for the unconditional love and affection they have extended to me over many, many years. I feel privileged to have a very cool and supportive brother in my unnecessarily serious life. His lovely company makes me understand the immense necessity of a more balanced life. Finally, I acknowledge the contribution of Pooja. She has been more of a friend, than everything else. I thank her for tolerating me and providing a fantastic company. Her unwavering love, support and encouragement are invaluable to me and I cherish her presence in my life.

Last, but never the least, I acknowledge my inspirations- Sidney Farber, Michael Bishop and Swami Vivekanada, whose lives have inculcated in me the necessity of patience and perseverance, the requirement of good scientific vision and the importance of kindness and dedication.

Abbreviations

µg- Microgram

µM- Micromolar

µm- Micrometre

ºC- Degree Celsius

ac- Acetylated

APS- Ammonium persulfate

ATCC- American Type Culture Collection

ATP-Adenosine triphosphate

AurkA- Aurora kinase A

AurkB- Aurora kinase B

AZD1152 HQPA- 2-[3-[[7-[3-[ethyl(2-hydroxyethyl)amino]propoxy]-4-quinazolinyl]amino]-1H-pyrazol-5-yl]-N-(3-fluorophenyl)acetamide

BOD-Biological oxygen demand

BRN5- Brain5

ChIP seq- Chromatin immunoprecipitation coupled to massively parallel DNA sequencing

CHX- Cycloheximide

CKII- Casien kinase 2

cm- Centimetre

CO_2- Carbon dioxide

CTD- C-terminal domain

DDR- DNA damage response

DMEM-Dulbecco's Modified Eagle medium

DMSO- Dimethyl sulfoxide

DTT- Dithiothreitol

EDTA- Ethylene diamine tetra acetate

EGTA- Ethylene glycol tetra acetate

EMSA- Electrophoretic mobility shift assay

FACS- Fluorescence activated cell sorting

FBS- Fetal bovine serum

HA- Haemaglutinin

HAT- Histone acetyltransferase

HDAC- Histone deacetylase

IPTG- Isopropyl β-D thiogalactoside

KAT- Lysine acetyltransferase

kDa- KiloDalton

mPOU- Muscle POU

MLN8237- 4-[[9-chloro-7-(2-fluoro-6-methoxyphenyl)-5H-pyrimido[5,4-d][2]benzazepin-2-yl]amino]-2-methoxybenzoic acid

ng- Nanogram

NTD- N-terminal domain

Ni-NTA- Nickel Nitrilotriacetic acid

NP40- Nonidet P-40

$O.D._{600}$- Optical density at 600nm

ph- Phosphorylated

PAGE- Polyacrylamide gel electrophoresis

PBS- Phosphate buffer saline

PMSF- Phenyl methyl sulphonyl fluoride

PTM- Post translational modification

PVDF- Polyvinylidene fluoride

RA- Retinoic acid

RT- Reverse transcriptase

RT-Room temperature

siRNA- Silencing RNA

SDS- Sodium dodecyl sulphate

TBS- Tris buffered saline

TCF β1- T cell binding factor β1

TEMED- N, N, N', N'- tetramethyl ethylene diamine

TNBC- Triple negative breast cancer

Tris- tris-(hydroxymethyl)-aminomethane

w/v- Weight by volume

v/v- Volume by volume

CHAPTER 1: INTRODUCTION

Chapter outline

1.1. Introduction To Cell Division Cycle

Organismal growth and reproduction stems from the basic, microscopic mode of cell division, initially proposed as the "Cell Theory" by Theodore Schwann and Matthias Schleiden and later posed by Rudolf Vircho was a maxim- *Omnis cellula e cellula*. Cell cycling is broadly categorized into two phases- interphase and mitosis. While the interphase is sub-divided into two Gap-phases (G1 and G2) and Synthesis phase (S), the mitotic phase (M) considers the ultimate division into two identical daughter cell clones. Each of the phases is characterized by unique molecular events whose macroscopic manifestation culminates into error-free cell division.

Eukaryotic cell cycle clock represents an intricately orchestrated mean of sensing the external environment, which may include mating factors (in yeasts), nutritional status, presence of mitogens or inhibitory factors, and a subsequent "all-or-none" response to the stimuli. This response is determined during the first two-thirds of the time period in G1-phase which dictates whether a cell will proliferate or undergo quiescence. Suitable proliferative environments and presence of growth factors generate signal transduction cascades emanating from the cell surface toward the cell interior (N B Ruderman et al., 2008; Auger KR et al., 1989), activating pre-existing transcription factors and chromatin re-modellers, which in turn transactivate multiple genes, broadly divided into two classes- *immediate early response (IER)* or *delayed response (DR)* genes, named according to the kinetics and chronology of their expression. Mitogenic stimulation transactivate the IER genes (c-Myc, or c-Jun transcription factors) within a few minutes (Bahrami S et al., 2016; Yang SH et al., 2013; Davie JR et al., 2010; Carbone M et al., 2008; Mostocotto C et al., 2014). The IER proteins are then translated from these early transcripts and act to relay the baton to the DR genes through successive transactivation of these genes. The IER factors themselves witness a decline in the levels, as the DR products peak, either through mRNA or protein degradation. The lower levels of the IER transcripts and proteins are, however, being maintained as long as growth factors are present in the surrounding. Some of the DR genes express transcription factors, while others encode factors which play pivotal roles in sailing through the G1-phase, namely the mid- and late-G1-phase cyclins and the cyclin dependent kinases (CDKs). G1-phase also serves as an important phase for cellular growth and accumulation of biomass through the activation of the mTOR pathway (Scott PH et al., 1998). It is only when a cell has reached a certain size that it proceeds irrevocably to the S-phase.

S-phase entry is an outcome of the inputs assimilated from the cellular environment and defined by uniform molecular events at the level of gene expression, protein-protein interactions and protein degradation which occurs during the mid to late G1-phase. This gateway is coined START in yeast (Leland H. Hartwell et al., 1970) and Restriction Point in mammalian cells (Pardee AB et al., 1974; A Zetterberg et al., 1985; Pardee AB, 1989). If growth factors are withdrawn before passage through the Restriction Point, transcription of G1-cyclins and CDKs thwart. Since these factors are highly unstable, their concentrations fall precipitously and the cell cannot enter the S-phase. The Restriction Point, therefore, serves as a "unidirectional valve" in allowing a cell to replicate its hereditary material. Cyclin-CDK complexes represent the core functional module of cell cycle regulation and an overview of the different cyclin-CDKs of the vertebrates is highlighted in Table 1.

Mid-G1-phase CDKs	**CDK4, CDK6**
Late-G1 and S-phase CDK	**CDK2**
Mitotic CDKs	**CDK1**
Mid-G1 cyclins	***D-type cyclins***
Late-G1 and S-phase cyclin	***Cyclin E***
S-phase and mitotic cyclin	***Cyclin A***
Mitotic cyclins	***Cyclin A, cyclin B***

Table 1: Tabulation of various cyclin-CDK complexes of metazoans involved in the regulation of different cell cycle phases.

One of the important regulators of the transition through the Restriction Point depends on the first tumor suppressor identified- the retinoblastoma protein (pRb), whose discovery and characterization in itself laid a significant step forward for studies related to both cell cycle regulation and understanding cancer biology (Friend SH et al., 1986; Lee WH et al., 1987; Fung YK et al., 1987). Extensive analysis unravelled the mechanism that operates between pRb and the E2F transcription factors in determining the S-phase entry (Figure 1.1).

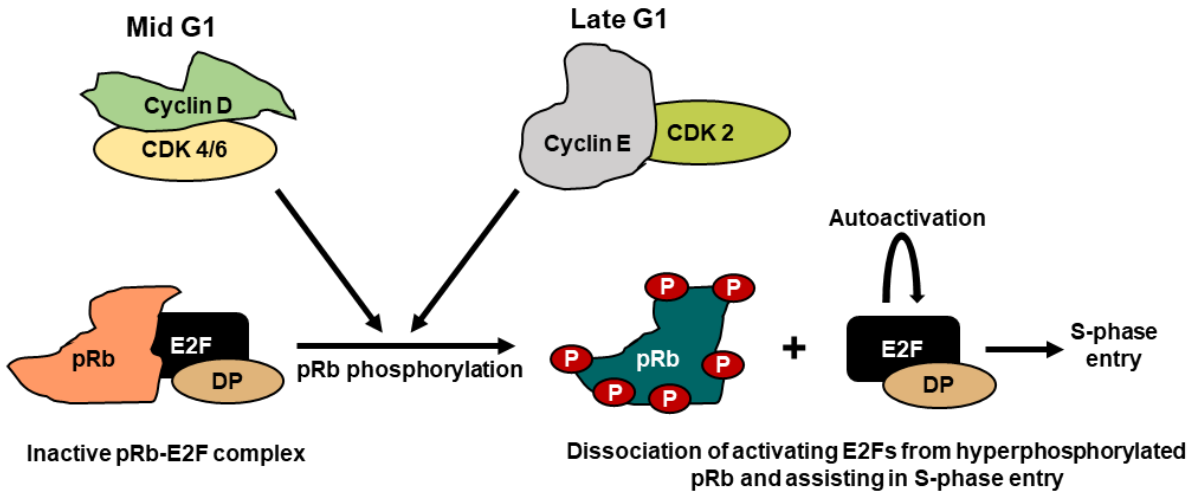

Figure 1.1: Regulation of Rb and E2F activities in mid-late G1. *Stimulation of G0 cells with mitogens induces the expression of CDK 4/6, cyclin-D and the E2F transcription factors, all encoded by delayed response genes, although E2F1 is necessary for timely G0 exit and entry into G1 (Wang ZM et al., 1998). pRb forms a complex with the activating E2Fs on the chromatin and inhibits transactivation of the target genes. Sustenance of mitogenic stimulation till the late-G1-phase causes the initial surge of inactivating phosphorylation of pRb by cyclin D-Cdk4/6 complexes (De Gregori J et al., 1995; Ewen ME et al., 1993 a & b; Kato J et al., 1993; Lees JA et al., 1991). This causes a partial dissociation of E2Fs from pRb and leads to further transcription enhancement of notable growth control genes like c-myc, B-myb, cdc2, dihydrofolate reductase, thymidine kinase, its own gene (E2F1) (Nevins JR, 1992; La Thangue NB, 1994) along with the late G1-phase cyclin, cyclin E (Ohtani K et al., 1995). Cyclin E- Cdk2 complex not only hyper phosphorylates pRb leading to complete dissociation from the E2F protein but also phosphorylates E2F and stimulates transcription and cell-cycle progression by the recruitment of the p300/CBP family of co-activators (Morris L et al., 2000), thus freeing the E2Fs in activating the set of genes necessary for the irreversible S-phase entry (Bertoli C et al., 2013).*

High levels of E2F1 is necessary to activate transcription of the S-phase cyclin, cyclin A, as cells approach G1-S transition (A Schulze et al.¸1995; Soucek T et al., 1997). The late G1- and S-phase cyclin-CDK complexes (cyclin E/A-CDK2) are susceptible to regulations which confers abrupt outcomes in terms of stability and kinase activity. The first layer of complexity is endowed by three related CDK inhibitory proteins (CKIs) or kinase inhibitory proteins (KIP), namely $p27^{KIP}$, $p21^{KIP}$ and $p57^{KIP}$ which regulate the precise timing of S-phase entry. As the S-

phase cyclin-CDK heterodimers accumulate in late G1, they are immediately inactivated by binding to the CKIs, that are expressed early in G1. CKIs specifically target B-type cyclin (cyclin A)-CDK complexes and hence do not affect either D-type early G1-phase cyclins or late G1-cyclin (cyclin E). S-phase entry is characterized by degradation of the CKI, majorly through SCF^{Skp2} E3- ubiquitin ligase pathway (Bornstein G et al., 2003; Tsvetkov LM et al., 1999; Kamura T et al., 2003), or PCNA dependent CRL4Cdt2 ubiquitin ligase complex (Kim Y et al., 2008; Abbas T; 2008) (Figure 1.2).

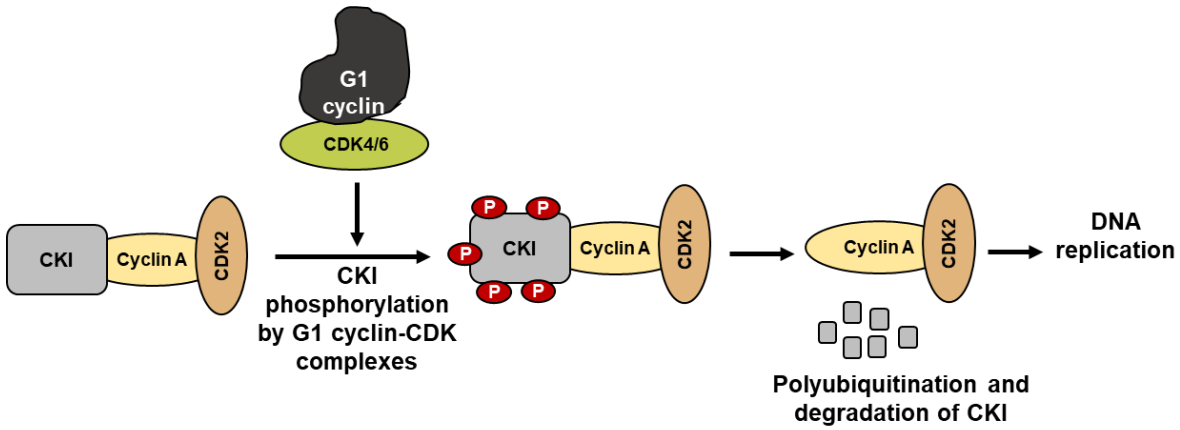

Figure 1.2: Control of the precise timing for S-phase entry. *CDK inhibitory proteins (CKIs- p21, p27 and p57) form a stable association with B-type cyclin-CDK complexes throughout G1-phase, making them inactive. Once the cell reaches late G1, the CKIs are polyubiquitinated and degraded through the proteasome dependent degradation pathway, thus freeing the S-phase cyclin-CDK complexes and help ensue DNA replication.*

The second layer of regulation is conferred by phosphorylation and dephosphorylation mechanisms (Figure 1.3). Both these regulations act to permit abrupt activation of a large number of protein complexes for rapid transition to the S-phase, as opposed to a gradual build-up of kinase activity that would occur if phase specific transcription were to emanate.

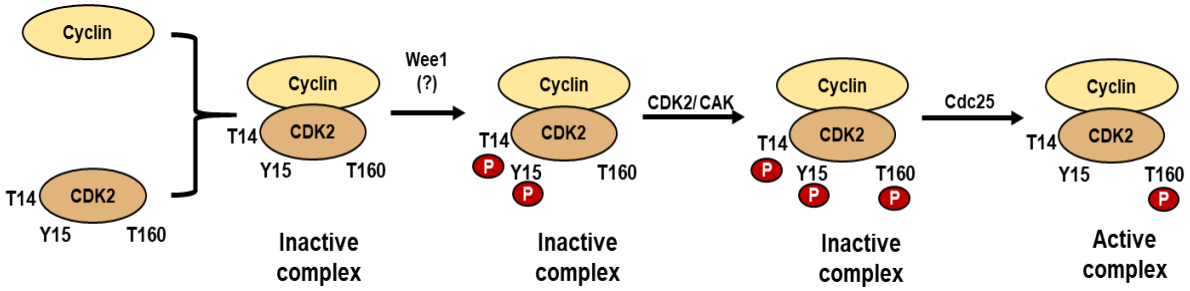

Figure 1.3: Regulation of kinase activity of cyclin-CDK2 complex. *Wee-1 or Wee-1 like kinases phosphorylate Y15 [and T14 (to a lesser extent)] of mammalian CDK2 and inactivates the cyclin-CDK2 heterodimeric complex (Gu Y et al., 1992; Chow JP et al., 2003). CDK activating kinase (CAK) acts on this inactive complex and phosphorylates an activating threonine residue-T160. CDK2 is also suggested to autophosphorylate T160 and cause autoactivation (Abbas T et al., 2007). This activating phosphorylation is however insufficient to drive active cyclin-CDK2 complex formation as the inhibitory Y15 phosphorylation blocks the access of substrates. Cdc25 phosphatases, which are activated late in G1, removes the inhibitory phosphate from CDK2 and assist in the activation of the cyclin E-CDK2 activity (Sebastian B et al., 1993; Ida Blomberg et al., 1993; Gabrielli BG et al., 1992; Chow JP et al., 2003).*

DNA replication ensues upon the activation of late G1- and S-phase cyclin-CDK complexes, through a phosphorylation of the pre-replication complexes at the replication origins. Evidence suggests that cyclin E-CDK2 cooperates with Cdc6 and initiates the assembly of the pre-replicative complexes onto the replication origins and makes the G1 cell nuclei competent and receptive to replication initiation. Cyclin A displaces cyclin E in the S-phase and forms the cyclin A-CDK2 complex which serves two different functions. Firstly, it activates DNA synthesis from pre-assembled replication complexes and secondly, it inhibits re-assembly of new complexes thus preventing re-initiation of DNA synthesis (Coverley D et al., 2002; Machida YJ et al., 2005; Bell SP et al., 2002). Replication re-initiation in metazoans is inhibited by another protein called geminin which acts by preventing the loading of MCM proteins onto chromatin without interfering with ORC and Cdc6p association (McGarry TJ et al., 1998). *Geminin* is expressed in late G1-phase, accumulates to high levels as S-phase proceeds until M-phase when it undergoes anaphase promoting complex/cyclosome (APC/C)-mediated degradation [the core component of the ubiquitin-dependent proteolytic machinery], dependent on its N-terminal destruction box.

The maestro of mitosis, CDK1, forms a heterodimeric complex with G2- and S-phase cyclins and is regulated by Wee1 and Myt kinases, CAK and Cdc25 phosphatase, in a manner similar to CDK2 (detailed above). The cyclin A/B-CDK1 complexes are also termed as mitosis/maturation promoting factor (MPF) owing to their quintessential roles in the mitotic phase. Activated Cdk1–cyclin complexes phosphorylate nuclear lamins necessary for nuclear envelop disassembly, kinesin-related motors and other microtubule-binding proteins required for centrosome maturation and separation, condensins for spindle assembly and chromosome condensation and Golgi matrix components for Golgi fragmentation (Andersen SS et al., 1991; Lowe M et al., 1998; Kimura K et al., 1998; Nigg EA et al., 1995). Furthermore, cyclin-CDK1 complexes contribute to regulate the APC/C, that controls the timely degradation of critical mitotic regulators, in particular inhibitors of anaphase onset (securins) and cyclins (Kramer ER et al., 2000). Degradation of M-phase cyclin inactivates CDK1, thus setting the stage for mitotic exit and cytokinesis. CDK1 inactivation also allows the reformation of pre-initiation complexes at origins of replication, thereby licensing cellular chromatin for the next round of replication (Noton E et al., 2000).

1.2. Regulation Of Mitosis By Aurora And Other Major Mitotic Kinases

Although CDK1 activity earmarks mitosis, the mitotic phase is not exempted from the involvement of other kinases which are pivotal for mitotic entry and exit and the perturbation of which affects mitosis at different stages. This coordinated regulation is brought about by Aurora kinase (Aurk)s, Polo-like kinase (Plk)s, Never In Mitosis in *Aspergillus nidulans* (NIMA) kinase, NIMA related kinase (Nek)s, Haspin kinase and vaccinia-related kinase 1 (VRK1). These kinases have profound impact on mitosis, which can be sub-divided into the following stages and has been discussed in detail below.

1.2.1. Early Mitotic Events

1.2.1.1. Centrosome Maturation And Separation

Centrosomes in animal cells are major microtubule organizing centre (MTOC) for cytoskeleton maintenance during interphase and mitotic spindle assembly with the onset of mitosis. It comprises of a pair of centrioles surrounded by an amorphous pericentriolar material (PCM); each of the centrioles are conserved organelles comprising of nine microtubule triplets that are organized in a symmetric ‘cartwheel’ (Kitagawa D et al., 2011). The centrosome duplicates only once per cell cycle in order to avoid an uncontrolled centriole number, thereby ensuring

mitotic spindle fidelity. Centrosome duplication is coordinated with cell cycle progression, occurring at the S-phase entry where the nucleation starts as small pro-centrioles and depends on the activity of CyclinA-Cdk2 and the presence of E2F transcription factors (Meraldi P et al., 1999). The duplicated centrosomes remain closely associated throughout the S-phase and into the G2 phase, and functions as a single MTOC, until after G2 when they separate and recruit γ-tubulin ring complexes (γ-TuRC) which serve as a seed for nucleation of microtubules.

Aurora A play pivotal roles in centrosome maturation and microtubule assembly. Centrosomal recruitment of Aurora A is dependent on "Golgi- mitotic checkpoint" in which, an improper Golgi fragmentation in the G2-phase inhibits Aurora A activation (Persico A et al., 2010). Phosphorylation of Aurora A at a crucial tyrosine residue (Y148) by Src kinase on the Golgi lead to enhanced recruitment of Aurora A onto the centrosomes and activates it in a phosphorylation dependent manner (Barretta ML et al., 2016). At the centrosome, Aurora A interacts with and phosphorylates the γ-TuRC adaptor protein NEDD1. Phosphorylation is not necessary for centrosomal microtubule (MT) nucleation but is critical for MT nucleation in the vicinity of the chromosomes in mitotic cells (Pinyol R et al., 2013). Aurora A also phosphorylates Nuclear distribution protein nudE-like 1 (NDEL1) in late G2/prophase, which is required to recruit NDEL1 to the centrosome. NDEL1 is required for organization of the cellular microtubule array and microtubule anchoring at the centrosome. It interacts with TACC3 and targets it to the centrosomes (Kinoshita K et al., 2007). Centrosomal targeting of TACC3 is also suggested to be dependent on phosphorylation by Aurora A (Kinoshita K et al., 2005). TACC3 can only bind MTs when complexed with the MT-stabilising protein-TOG/XMAP215 (TOG), and opposes the MT-destabilising activity of MCAK/XKCM1 (MCAK). Aurora kinase A mediated phosphorylation of TACC3 promotes the binding ofTACC3/TOG to MT minus-ends, where they protect MTs from MCAK-induced destabilisation. TACC3/TOG determine the number and hence, the strength of microtubules associated with the centrosomes. Aurora A kinase activity dependent events therefore determines the extent of assembly of the microtubules during mitotic entry.

At the onset of mitosis, the PCM undergoes dramatic increase in size, a phenomenon termed as centrosomal maturation, and requires the activity of Polo-like kinase (Plk). PCM expansion occurs by the recruitment of proteins like the γ-TuRCs and centrosomin (Cnn). Plk1is critical for centrosome maturation as its inhibition results in a monopolar spindle with reduced microtubule-organizing activity. (Lane HA et al., 1996; Lénárt P et al., 2007; Qian YW et al.,

1998). Pericentriolar material 1(PCM1) recruits Plk1 to the PCM in a dynein-dynactin complex-dependent manner. The interaction between PCM1 and Plk1 is phosphorylation dependent, and CDK1 functions as the priming kinase for PCM1 to facilitate the interaction (Wang G et al., 2013). Aurora A phosphorylates Plk1 in the activation loop at the critical T210 residue (Macůrek L et al., 2008), an event which also requires the coactivating protein Bora (Seki A et al., 2008). Phosphorylation of T210 of Plk1 by Aurora A occurs upon release of an inhibitory intramolecular interaction between the N-terminal catalytic domain of Plk1 and the C-terminal "polo-box" domain (PBD). The latter is a phospho-serine/threonine recognition domain which binds to phospho-Bora T252 generated by the cyclin B-CDK1 and impairs the interaction with the N-terminal catalytic domain, thus stimulating Plk1 activation. Plk1 activation is thus triggered by a priming kinase like CDK1 (Petronczki M et al., 2008). Recent evidence, however, emphasize that cyclin A-CDK1 complex, and not the cyclin B-CDK1 heterodimer, phosphorylates Bora at S110 which is sufficient for mitotic entry (Vigneron S et al., 2018) (Figure 1.4).

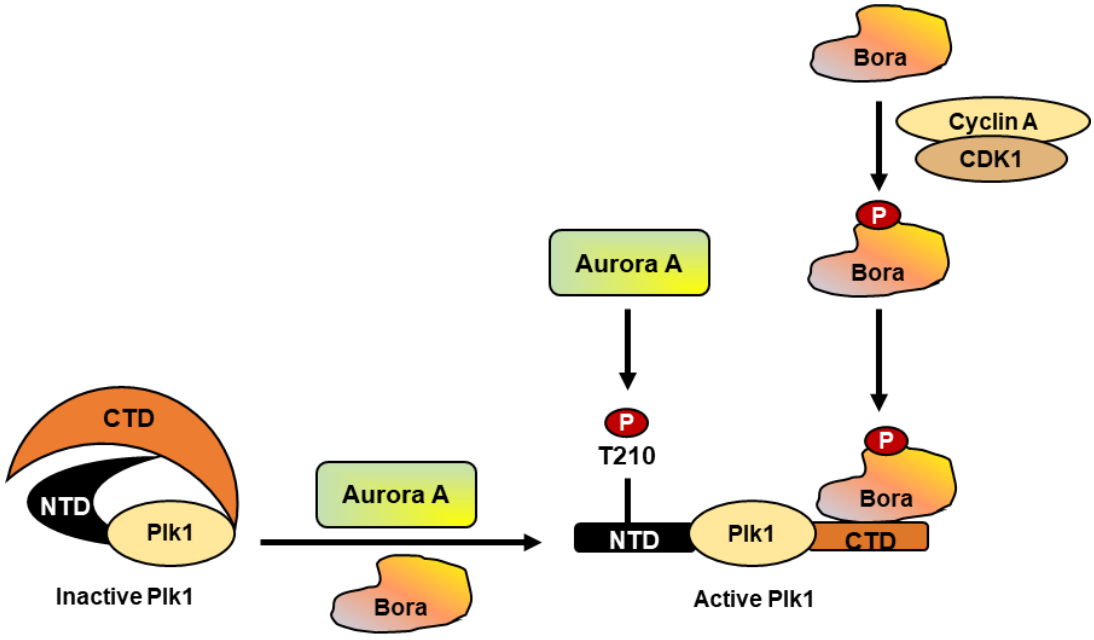

Figure 1.4: Schematic representation for the activation of Plk1. *Activation of Plk1 is stringently regulated by two phosphorylation events. Intramolecular interaction between the N-terminal kinase domain and the C-terminal the phospho-ser/thr recognition domain of Plk1 restricts its activation. Cdk1 phosphorylates Bora which then binds to CTD. This interaction frees the NTD which is now been phosphorylated at Thr-210 by Aurora A for activation.*

Plk functions at multiple levels during centrosomal maturation. Firstly, it regulates the Asp ("Abnormal Spindle") protein which binds to the γ-TuRC as a clamp and holds them onto the

mitotic centrosomes. Secondly, increase in PCM size is mediated by Plk dependent phosphorylation of Cnn protein scaffold specifically at the centrosome which promotes the assembly of a Cnn scaffold around the centrioles at a definite pace, with Cnn molecules recruited continuously around the centrioles as the scaffold spreads slowly outward. It is further supported by phospho-deficient or mimetic mutations of Cnn protein that block scaffold assembly or help multimerize and rapidly form cytoplasmic scaffolds that organize microtubules independently of centrosomes (Conduit PT et al., 2014). Finally, Plk1 phosphorylate pericentrin and help recruit various PCM proteins like γ-tubulin, GCP-WD (γ-complex protein with WD repeats), CEP192, Aurora A, and PLK1at the centrosomes during mitosis (Lee K et al., 2011). Once Aurora A is recruited to the centrosomes, it phosphorylates and activates Cdc25B which in turn dephosphorylates CDK1, thus assisting in mitotic entry (Cazales M et al., 2005). Aurora A activity at the centrosomes is also maintained by Plk1 mediated phosphorylation and inhibition of PP6 phosphatase (Kettenbach AN et al., 2018).

Certain complex phosphorylation-dephosphorylation events controlled by Nek kinases are also important for centrosome maturation. Nek kinases are comprised of at least seven members (Nek1-Nek7) (Kandli M et al., 2000). The orthogonal orientation between a mother and a daughter centriole, established at the time of centriole duplication, inhibits re-duplication of the mother centriole. Loss of orthogonal orientation (disengagement) between two centrioles during anaphase is considered a licensing event for the next round of centriole duplication. Nek2 phosphorylates the centrosomal protein C-Nap1early in G2/M transition and aids in loosening and dissociation of the duplicated tethered centrosomal complex (Fry AM et al., 1998). Disengagement also requires the activity of Polo-like kinase 1 (Plk1) wherein it triggers re-duplication of the separated centrioles for the next round of mitosis (Shukla A et al., 2015).

Centrosomal aberrations (CA) have been observed in multiple cancer types. CA in the form of supernumerary centrosomes was proposed by Theodor Boveri over a century ago, to be a cause of malignancy (Boveri T et al., 2008). Recent evidences prove that centrosomal amplifications are sufficient to cause aneuploidy and drive high grade cancer in ectopic Plk4 overexpressing cell line and mouse models (Denu RA et al., 2016; Levine MS et al., 2017). These results highlight the significance of regulation of centrosomal duplication and maturation by various mitotic kinases and the probable pathophysiological events that may arise owing to dysregulation.

1.2.1.2. Nuclear Envelope Breakdown

Nuclear envelope breakdown is a characteristic of open mitosis that occur in metazoans and occurs shortly after centrosome separation. Mitotic onset lead to hyperphosphorylation of the karyoskeletal structure known as the nuclear lamina, by the cyclin B-CDK1 complex (Nigg EA et al., 1995). Lamina disassembly reduces nuclear envelope stability but is not in itself sufficient to cause nuclear envelope breakdown, the mechanism of which is poorly understood.

1.2.1.3. Chromosome Condensation

Condensation of the chromosomes is triggered by robust phosphorylation of both histone and non-histone proteins. Phosphorylation of histone H3at the onset of mitosis and at multiple sites is long known (Gurley LR et al., 1975). Subsequent efforts unveiled the involvement of H3S10 (Wei Y et al., 1999) and H3S28 phosphorylation (Goto H et al., 1999) in mitotic chromosome condensation. While H3S10 phosphodeficient mutation led to defective chromosome condensation and segregation errors in Tetrahymena (Wei Y et al., 1999), no such defect was evident in yeast (Hsu JY et al., 2000). This apparent contradiction with H3S10 phosphorylation can be resolved by considering the high extent of functional redundancy of the mitotic kinases.H3S10 phosphorylation is mediated by multiple kinases including Ipl1 in yeast (Hsu JY et al., 2000) or NIMA kinase in *Aspergilus*, during mitosis (De Souza CP et al., 2000). Ipl1 is also capable of phosphorylating H2B (Hsu JY et al., 2000). Loss of H3S10 phosphorylation owing to mutation might re-direct Ipl1 to other sites on H2B to bring about chromosome condensation. The fact that S14 and S32 of H2B, which fall within the consensus phosphorylation motif of Ipl1, are not conserved in Tetrahymena further boosts the possibility of functional redundancy in yeasts, but not in Tetrahymena (Cheung P et al., 2000). Furthermore, the employment of different mitotic kinases like Ipl1 and NIMA in invoking mitotic chromosome condensation and segregation in different organisms emphasize the underlying necessity of the process at the dispense of the kinases.

In mammalian cells, Aurora B is strategically targeted to the centromeres with the help of Survivin/BIR1 (Speliotes EK et al., 2000), which in turn is recruited by Haspin kinase dependent phosphorylation of H3T3 (Wang F et al., 2010). Aurora B faithfully phosphorylates H3S10 and aids in initiation of chromosome condensation (Crosio C et al., 2002). Another kinase, VRK1, localizes to the chromatin and phosphorylates H3T3 and H3S10 in a cell cycle phase dependent manner. Overexpression of VRK1 was also observed to dramatically

condense the cell nuclei (Kang TH et al., 2007). The mechanism by which H3S10 phosphorylation brings about chromosome condensation is fascinating. It is observed that the N-terminus H4 tail contacts the negatively charged acidic-patch formed at the interface of the H2A-H2B dimer of the neighbouring nucleosome and is crucial for higher-order chromatin structures. Acetylation of H4K16, however, counteracts and disrupts this condensation process (Shogren-Knaak M et al., 2006; Robinson PJ et al., 2008; Gordon F et al., 2005). H3S10 phosphorylation mediates the recruitment of HST2, a SIR2 homolog in yeast, which deacetylates H4K16 and initiates chromosome condensation (Wilkins BJ et al., 2014).

Prominent among other trans-acting factors involved in chromosome condensation are topoisomerase II and a multiprotein complex known as condensin, both of which are regulated by phosphorylation. Evidence suggests that cyclin B-CDK1phosphorylate the five membered condensin complex and regulates its DNA supercoiling activity in Xenopus extracts (Kimura K et al., 2005) and its cell-cycle-regulated nuclear accumulation in yeast (Sutani T et al., 1999).

1.2.2. Late Mitotic Events

1.2.2.1. Kinetochore-Microtubule Attachment And Chromosomal Dynamics

Spindle assembly and directed chromosomal movements during mitosis represent an outcome of a combination of multiple factors as detailed below.

1.2.2.1.1. A balance between microtubule stabilizing and destabilizing proteins

Microtubule dynamics are extensively regulated by microtubule-stabilizing and destabilizing proteins, most of which are controlled by phosphorylation. Prominent among these proteins is stathmin, whose microtubule-destabilizing activity is turned off during mitosis by sequential phosphorylation involving cyclin B-CDK1 complex (Larsson N et al., 1997). Throughout mitosis, microtubule–kinetochore interactions are highly dynamic and maintained by the countering actions of MCAK complex and TACC/TOG complex as detailed previously.

INCENP, Borealin and Survivin aid in the recruitment of Aurora B to the centromere and together, form the chromosome passenger complex (CPC) (Adams RR et al., 2000). As the cell cycle progresses to metaphase, the amount of CPC localized to the chromosome arms decreases and it is mainly detected at the inner centromere, an event which is dependent on the C-terminus

of borealin. When sister chromatids separate in anaphase, the CPC dissociates from centromeres and re-localizes to the spindle midzone and is dependent on the N-terminus of borealin (Beardmore VA et al., 2004; Jeyaprakash AA et al., 2007). The CPC acts as one of the most upstream regulators of centromere/kinetochore function. In metaphase, the CPC recruit numerous proteins which function at different strata of the kinetochore: outer kinetochore proteins, including those involved in spindle assembly checkpoint (SAC) signalling (Ditchfield C et al., 2003; Lens SM et al., 2003); proteins responsible for microtubule–kinetochore interactions (Pouwels J et al., 2007; Ohi R et al., 2004; Emanuele MJ et al., 2008; Andrews PD et al., 2004; Goto H et al., 2006 Lan W et al., 2004) and certain inner kinetochore proteins (Huang H et al., 2007; Kawashima SA et al., 2007). Consequently, a compromise in the functioning of the CPC results in improperly attached chromosomes to the kinetochore owing to a failure to detach. Several lines of evidence indicate that Aurora B kinase activity is necessary to destabilize improper microtubule attachments. Microtubules attach to the outer kinetochore through the Ndc80/Hec1 complex. Aurora B phosphorylates Ndc80 in the absence of tension, and reduces its affinity for microtubules (Cheeseman IM et al., 2006; DeLuca JG et al., 2006). Furthermore, Dam1, a protein that allows kinetochores to track depolymerizing plus ends of microtubules in budding yeast, is negatively regulated by Ipl1 (Aurora B)-mediated phosphorylation (Gestaut DR et al., 2008).

1.2.2.1.2. The action of microtubule-dependent motors proteins

Spindle assembly and function throughout mitosis depend on several distinct kinesin-related motor proteins (KRPs) and cytoplasmic dynein (Rieder CL et al., 1998). Aurora B aids in the proper localization of dynein to the kinetochores during prometaphase and astral microtubules during metaphase in a kinase activity dependent manner as a kinase dead, dominant negative mutant of Aurora B showed abnormally reduced dynein levels at the proper places. Furthermore, the centromeric localization of CENP-E, a kinesin-like motor, was also found to be disrupted in the kinase dead mutant of Aurora B (Murata-Hori M et al., 2002). These results exemplify the role of Aurora B in spatio-temporal regulation of motor proteins necessary for the dynamicity of the chromosomes during metaphase to anaphase transition.

1.2.2.1.3. Dynamicity of MT polymers

Dynamic instability is particularly important at the anaphase stage, when the catastrophe rate (the frequency of transitions between rapid growth and shrinkage of microtubules to assist chromosome separation into two daughter nuclei) is markedly increased. This transition can be triggered in vitro by several kinases, including cyclin A-CDK1 and mitogen-activated kinase (MAP kinase) (Andersen SS et al., 1999).

1.2.2.2. Onset Of Anaphase And Mitotic Exit

Chromosome biorientation is intricately dependent on Aurora B activity as it inhibits premature exit of the SAC (Krenn V et al., 2015; Gurden MD et al., 2016). Proper bipolar attachment of all the chromosomes to the microtubules signals the initiation of the next mitotic stage, anaphase, which is characterized by the simultaneous separation of all sister chromatids resulting from a loss of sister-chromatid cohesion. In vertebrates, different mechanisms destroy cohesion at chromosome arms and centromeres. The bulk of cohesin is removed from chromosome arms during prophase to permit the extensive chromosome condensation typical of vertebrate mitosis. Importantly, this first surge of cohesin removal does not depend on APC/C and instead requires phosphorylation of cohesin, possibly by CDK1 (Sumara I et al., 2000; Losada A et al., 2000). Residual cohesin remaining at vertebrate centromeres is then removed at the metaphase-anaphase transition. This second step is dependent on APC/C, and presumably follows the securin–separase pathway (Waizenegger IC et al., 2000).

APC/C not only primes anaphase onset inhibitors for degradation, but also the M-phase cyclin-CDK1 complex, Plks (Shirayama M et al., 1998; Charles JF et al., 1998; Fang G et al., 1998), NIMA kinases (Ye XS et al., 1998; Pfleger CM et al., 2000) and Aurora kinases (Honda K et al., 2000). Two different forms of APC/C are activated sequentially through the association of two distinct proteins, namely Cdc20 and Cdh1 which modulate the temporal regulation of mitotic exit in a vertebrate cell as APC/C^{Cdc20} is active at the metaphase–anaphase transition, while APC/C^{Cdh1} is turned on later in mitosis and remains active throughout the subsequent G1 phase (Morgan DO et al., 1999). These events, collectively, guide the exit of cells from mitosis and into the interphase for a whole new, but repetitive, set of molecular events.

1.3. Extra-Mitotic Roles Of Aurora Kinases

Recent evidences emphasize the influence of Aurora kinases in a wide range of non-mitotic yet physiologically important cellular functions. The intricate involvement of the Aurora kinases fosters a necessity for the detailed examination of functions of Aurora kinases outside the mitotic window. Each of the roles are briefly described below.

1.3.1. Maintenance of Golgi structure

The Golgi apparatus plays roles in secretary pathway, cell polarity, and directional cell migration. The dependence on a Golgi-mitotic checkpoint for Aurora A activation (described above) during mitotic entry accentuates the relationship between the two. Aurora A, in turn, aids in maintenance of Golgi cisternae structure as Aurora downregulation or inhibition leads to Golgi dispersal during the interphase, while no effect was observed for Golgi vesiculation during mitosis. Conversely, overexpression of Aurora A leads to tightly packed Golgi apparatus (Kimura M et al., 2018). The molecular pathway for such an outcome during the interphase, however, is presently unclear.

1.3.2. Telomere structure and function maintenance

As with proper chromosome separation, Aurora kinases guard against telomeric fusions to prevent aneuploid cells. It is observed that Ark1 (fission yeast Aurora kinase) promotes telomere dispersion and disjunction during mitosis. Ark1 controls telomere dispersion in metaphase by promoting the dissociation of Swi6/HP1 and cohesin Rad21from telomeres. It also phosphorylates the condensin subunit, Cnd2, and promotes telomere disjunction and chromosome arm separation (Reyes C et al., 2015). In mouse embryonic stem cells (mESCs), Aurora B is found to activate telomerase function in two different ways. Firstly, Aurora B mediated H3S10 phoshorylation during the S phase at centromeric and (sub)telomeric loci promotes the expression of non-coding minor satellite RNA (cenRNA). Inhibition of Aurora B leads to the silencing of cenRNA and establishment of a repressive heterochromatin state through H3K9me3 and HP1 accumulation, which results in gradual shortening of the telomeres. Furthermore, Aurora B interacts with both telomerase and cenRNA and activates telomerase in trans (Mallm JP et al., 2015). Secondly, Aurora B localizes to the telomeres in mESCs and phosphorylates Telomeric repeat binding factor 1 (TRF1, a component of the six membered telomeric shelterin complex, negatively regulates telomere elongation by telomerase and promotes efficient DNA replication at telomeres) at S404 residue.

Overexpression of phosphorylation mutants of TRF1 was observed to form fragile telomeres in vivo, thus demonstrating Aurora B to be an important regulator of telomere structural integrity (Chan FL et al., 2017). TRF1 in turn regulates Aurora B as TRF1depletion abolishes the recruitment of Aurora B to the centromere and leads to a wide range of mitotic defects and aneuploidy (Ohishi T et al., 2014).

1.3.3. PI3K-AKT-mTOR pathway modulation

Mechanistic target of rapamycin (mTOR)- complex 1 and 2 (mTORC1/2) represent a fundamental nodal point of convergence of signalling cascades emanating from extracellular stimuli, like growth factors (insulin and epidermal growth factor), oxygen tension, availability of amino acids, or negative regulators which guide the growth of cells through protein, lipid and nucleotide bio-synthesis and by inhibiting autophagy (Saxton RA et al., 2017). mTORC1 functions as a downstream effector for many frequently mutated oncogenic pathways, including the PI3K/Akt pathway as well as the Ras/Raf/Mek/Erk (MAPK) pathway, which results in mTORC1 hyperactivation in many human cancers. Rapamycin analogues targeting mTOR, or PI3K pathway inhibitors are actively being pursued for usage as anti-cancer agents, however, with reduced efficacy owing to mutations. A recent observation corroborates the involvement of Aurora A as one of the genes which is overexpressed in breast cancers with acquired PI3K inhibitor-resistance (Donnella HJ et al., 2018). Furthermore, Aurora A activity was found to be necessary for Akt activation as small molecule inhibitor mediated inhibition of Aurora A also reduces the activated, phosphorylated form of Akt necessary for proliferation (Xu DR et al., 2011; Yao JE et al., 2009. Independently, a loss-of-function RNAi screen elucidated Aurora B to be one of the genes whose expression causes resistance to rapamycin activity (Ou O et al., 2014). It was also observed that the mTOR-AKT pathway plays essential role in Aurora mediated cellular transformation (Taga M et al., 2009). Finally, Aurora A induces epithelial to mesenchymal transition (EMT) by hijacking the use of PI3K-AKT pathway, converging onto the promoter of the EMT regulator Twist (Liu X et al., 2016). These results collectively highlight the intricate regulation of a proliferation oriented PI3K-AKT-mTOR pathway by the mitotic Aurora kinases and the modes by which this pathway, in turn, regulate Aurora.

1.3.4. Metabolic reprogramming in cancer

Cancer cells undergo metabolic reprogramming which involves enhancement in the generation of lipids and proteins necessary for increased proliferation besides altered energy needs, which requires higher mitochondrial respiration. Aurora A is shown to possess a cryptic mitochondrion targeting sequence in its N-terminus and undergoes direct interaction with TOM (translocase of outer membrane) 20 and TOM 70 proteins of the TOM complex that plays a role in mitochondrial import. Mitochondrial localization of AurkA is necessary as its knockdown or inhibition leads to perturbed mitochondrial fission before mitotic entry. (Grant R et al., 2018). Independently, Aurora A co-localizes with the mitochondrial processing peptidase PMPCB and is imported to mitochondria during the interphase, where it induces mitochondrial fragmentation. Overexpression of Aurora A (dysregulated Aurora A levels in cancer cells) enhances mitochondrial fusion and ATP production, a necessity to be met for a cancer cell's growth and proliferation, and therefore, contributes to metabolic reprogramming by altering mitochondrial interconnectivity (Bertolin G et al., 2018).

1.3.5. T-cell activation

Activation of a T-cell depends on the ability of the T-cell receptor (TCR) to recognize specific antigen peptides presented by the major histocompatibility complex protein (MHCp) on the antigen-presenting cell (APC) (Chakraborty AK et al., 2014). Engagement of TCR to MHCp promotes the formation of an immune synapse (IS) where, the TCR and its associated molecules localize to a central area of the T cell–APC contact. The formation of the IS also triggers changes in the cytoskeleton organization, including the translocation of the MTOC to the IS (Vicente-Manzanares M et al., 2004; Dustin ML, 2014. Owing to its role in controlling MT dynamics, Aurora A play a crucial role in the activation of T-cells during IS formation. Aurora A is activated upon TCR stimulation and controls the dynamics of MT at the IS. The absence of Aurora A activity causes delocalized clustering and decreased phosphorylation and hence active levels of the tyrosine kinase, Lck, at the IS and impairs the activation of early signalling molecules downstream of the TCR and finally the expression of various signalling molecules and interleukins. These findings implicate Aurora A in the propagation of the TCR activation dependent signalling [Blas-Rus N et al., 2016).

1.3.6. Functions in ciliary resorption

The mammalian cilium acts as a sensor of environmental cues. Defects in cilia-associated signalling proteins cause a varied range of developmental disorders and pathological conditions. Aurora A is shown to be directly involved in controlling cilia disassembly. It is observed that the pro-metastatic scaffolding protein HEF1/CasL/NEDD9 interacts with Aurora A at the basal body of cilia and activates it, which leads to the phosphorylation of tubulin deacetylase, HDAC6 and ciliary disassembly (Pugacheva EN at al., 2007).The authors propose an intriguing possibility that utilization of an Aurora A-HEF1-HDAC6 switch at the basal body of quiescent cells and the centrosome of G2/M cells may serve as part of cilia-or centrosome-dependent checkpoint mechanism coordinating responsiveness to extracellular cues at different points in cell cycle. Furthermore, elevated levels of HEF1 or Aurora A in tumours may destabilize cilia, thus severing cellular response to external cues and impacting environmental cue-independent pathways.

1.3.7. Cellular quiescence

Reversible cellular quiescence is characterized by a reduction in cell size and transcriptional activity with a retention in the ability to respond to cues suitable for proliferation. It is observed that Aurora B is essential in regulating transcriptionally active genes in quiescent lymphocytes. In association with the polycomb group of protein Ring1B, Aurora B binds to a varied range of active promoters in resting B and T lymphocytes. Conditional knockout of either of the proteins decreased cell viability through a gross reduction in RNA polymerase II recruitment and gene transcription (Frangini A et al., 2013). The results implicate the dependence of the choice between proliferation and quiescence on epigenetic regulation by Aurora B.

1.3.8. Regulation of Transcription Factors

Aurora kinases exhibit phosphorylation dependent and independent activities against a wide range of transcription factors (TFs) which form a significant aspect of their extra-mitotic role. Interestingly, the broader theme of the modulation of the TFs by Aurora kinases strongly suggest a role in malignancy.

1.3.9. Regulation of oncogenic signalling

Aurora kinases modulate multiple oncogenic pathways, directly or indirectly, through the regulation of master transcription factors like NFκB, N-Myc, c-Myc, c-Fos and androgen receptor, each of which are briefly discussed below:

1.3.9.1. NFκB signalling activation

It was identified that Aurora A activates NFκB by phosphorylating IκBα and inducing its degradation. IκBα binds and sequesters NFκB in the cytoplasm and inhibits its transactivation function. Aurora A mediated phosphorylation, therefore, releases NFκB which can now translocate into the nucleus and activate its target pro-inflammatory genes, contributing to the oncogenic effect of Aurora-A in human tumours (Briassouli P et al., 2007).

1.3.9.2. c-Fos complex formation

c-Fos heterodimerizes with c-Jun and forms the mature AP1 complex that engage promoter and enhancer elements to control transcription of various genes (Lee W et al., 1987; Turner R et al., 1989). Aurora A carries out mitosis specific phosphorylation of c-Fos and, via an incompletely understood process, induces higher order complex formation by c-Fos, the implication(s) of which is unclear (Yu CT et al., 2008). However, the result is particularly interesting as it invites the possibility of association of c-Fos with co-activator or co-repressor complexes in gene transcription regulation.

1.3.9.3. N-Myc stability and function

MYC oncoproteins are involved in the genesis and maintenance of the majority of human tumours but are considered undruggable. The effects of Aurora kinases on Myc addicted cancers are immense. Aurora A is shown to interact with N-Myc and inhibit its interaction with the ubiquitin ligase, SCF^{Fbxw7}, thus prohibiting its turnover. This kinase-independent event causes an accumulation of mono-ubiquitylated N-Myc which is capable of transactivating its downstream targets necessary for the maintenance of cellular transformation (Otto T et al., 2009). Subsequent efforts have translated to the development of allosteric inhibitors which binds and causes structural alterations in Aurora A, thus inhibiting its interaction with N-Myc and dampening the transcriptional response (Gustafson WC et al., 2014; Richards MW et al., 2016; Brockmann M et al., 2016). Furthermore, Aurora A is also responsible for N-Myc dependent RNA pol II pause release through inhibition of N-Myc binding to TFIIIC, RAD21

and TOP2A (Büchel G et al., 2017) and therefore, controls N-MYC function during the S-phase of the cell cycle.

1.3.9.4. c-Myc oncogenic activity

Aurora kinases are also believed to contribute heavily to c-Myc driven cancers. Nuclear accumulation of Aurora A upregulates *c-myc* transcription by either binding a highly conserved nuclear hypersensitive region (NHE) region in the Myc promoter (Lu L et al., 2015) or through a direct interaction with hnRNP protein which recruits it onto the myc promoter (Zheng F et al., 2016) .Intriguingly, Aurora A and c-Myc interact in hepatocellular carcinoma (HCC) cells and the disruption of this interaction, using small molecule inhibitors, represent a promising therapy in p53 mutated HCC patients (Dauch D et al., 2016). High c-Myc expressing cells become dependent on Aurora kinases and in turn, upregulate them to maintain oncogenicity (den Hollander J et al., 2010). These cells can be selective triggered to undergo apoptosis by pan Aurora A/B kinase inhibitors, but can be bypassed by expressing inhibitor-resistant Aurora B mutant. This result highlights that Aurora B inhibition may serve as a therapeutic vulnerability for high Myc expressing tumours. Independently, other evidences also indicate that Aurora B inhibition acts in a synthetic lethal manner, inducing lethal autophagy mediated cell death for high c-Myc expressing cells (Yang D et al., 2010). Collectively, these results implicate the intricate relationship these two oncogenes elicit in the genesis and maintenance of malignancy.

1.3.9.5. Androgen receptor activation

Androgens represent a group of naturally occurring or synthetic steroid hormones which include testosterone and dihydro-testosterone as the active components possessing physiological effects in humans. Androgens exhibit their activity by binding to androgen receptor (AR). Although they play vital roles in regulating the development and maintenance of male characteristics in vertebrates, androgens are also necessary for the initiation and progression of prostate cancer in humans (Heinlein CA et al., 2004). Androgen ablation therapy or the use of anti-androgens have been a promising therapeutic option in prostate cancer. However, many of these tumours proceed to mutate and become refractory to androgens or anti-androgens, which cause androgen-independent growth of the malignant prostrate tissues. Aurora A contributes to androgen-independent cell growth and proliferation of androgen-refractory prostate cancer cells through phosphorylation of androgen receptor (AR) and

inducing its transactivation properties toward its downstream target genes (Shu SK et al., 2016).

1.3.10. Regulation of tumour suppressor pathways

Aurora kinases exhibit equally fascinating activities against a multitude of tumour suppressors, which contribute to the oncogenic functions of these kinases, and has been briefly highlighted below.

1.3.10.1. Wnt signal transduction pathway

β-catenin forms an integral component of adherens junctions and is also a pivotal member of the Wnt signalling pathway. Dysregulation of β-catenin, especially in terms of mutations and overexpression, disrupt the function of adherens junctions. Elevated expression of β-catenin has also been suggested to be a crucial transforming event in the genesis of a number of malignancies (Morin PJ et al., 1997).

Glycogen synthase kinase (GSK)-3β is a cytoplasmic protein that exists in a complex with adenomatous polyposis coli (APC) tumor suppressor protein, and axin to form the β-catenin destruction complex. In the absence of Wnt signalling, GSK3β phosphorylates β-catenin and induces its degradation by the proteasomal pathway, thus restricting its cytoplasmic accumulation. However, Wnt signalling activation relays a cascade of events that induce GSK3β phosphorylation at ser-9 residue and destabilize the destruction complex, leading to β-catenin accumulation in the cytosol (Giles RH et al., 2003). β-catenin then translocate to the nucleus and associates with TCF/LEF family of transcription factors which in turn causes an activation of a large set of genes that are relevant for carcinogenesis and metastasis (Crawford HC et al., 1999; Shtutman M et al., 1999; He TC et al., 1998). Aurora A was found to mediate ser-9 phosphorylation of GSK3β which inhibit its function. This also led to the concomitant accumulation of β-catenin which undergoes nuclear translocation and activation of the genes in a β-catenin/TCF complex dependent manner (Dar AA et al., 2009).

1.3.10.2. p53 family inhibition

The tumour suppressor p53 is the guardian of the genome as it detects multiple aspects of genomic instability and affects cellular survivability. In relation to the Aurora kinases, p53 regulate Aurora A in a negative manner. It promotes not only transcriptional repression of

Aurora A but also induces its degradation through the upregulation of the FbxW7 ubiquitin ligase, thus keeping Aurora A levels in check (Wu CC et al., 2012). Aurora kinases, in turn, phosphorylate and oppose p53 dependent functions by two ways. Firstly, Aurora A mediated p53 phosphorylation at Ser315 enhances its interaction with the E3 ubiquitin ligase, Mdm2, and subsequently its degradation. Aurora B also mediate similar outcome by phosphorylating Ser183, Thr211, and Ser215 in the DNA binding domain of p53. Secondly, p53 phosphorylation by both Aurora A and B lead to its inhibition of the DNA binding activity and transcription activation. Aurora A achieves this by phosphorylating Ser215 whereas Aurora B phosphorylates Ser269, Thr284 and Thr211 to elicit the same response (Katayama H et al., 2004; Gully CP et al., 2012). These effects compromise the tumour suppressive role of p53 and tunes the cell for over-riding the G1/S checkpoint towards a pro-survival pathway to malignancy.

Aurora A is also shown to phosphorylate another member of the p53 family-p73, at Ser235, which not only abrogates its transactivation function and causes cytoplasmic sequestration, but also facilitates inactivation of the spindle assembly checkpoint (SAC) and accelerated mitotic exit (Katayama H et al., 2012). These results conclusively emphasize the impact of Aurora kinases on major transcription factors in the induction of oncogenic outcomes (Figure 1.5).

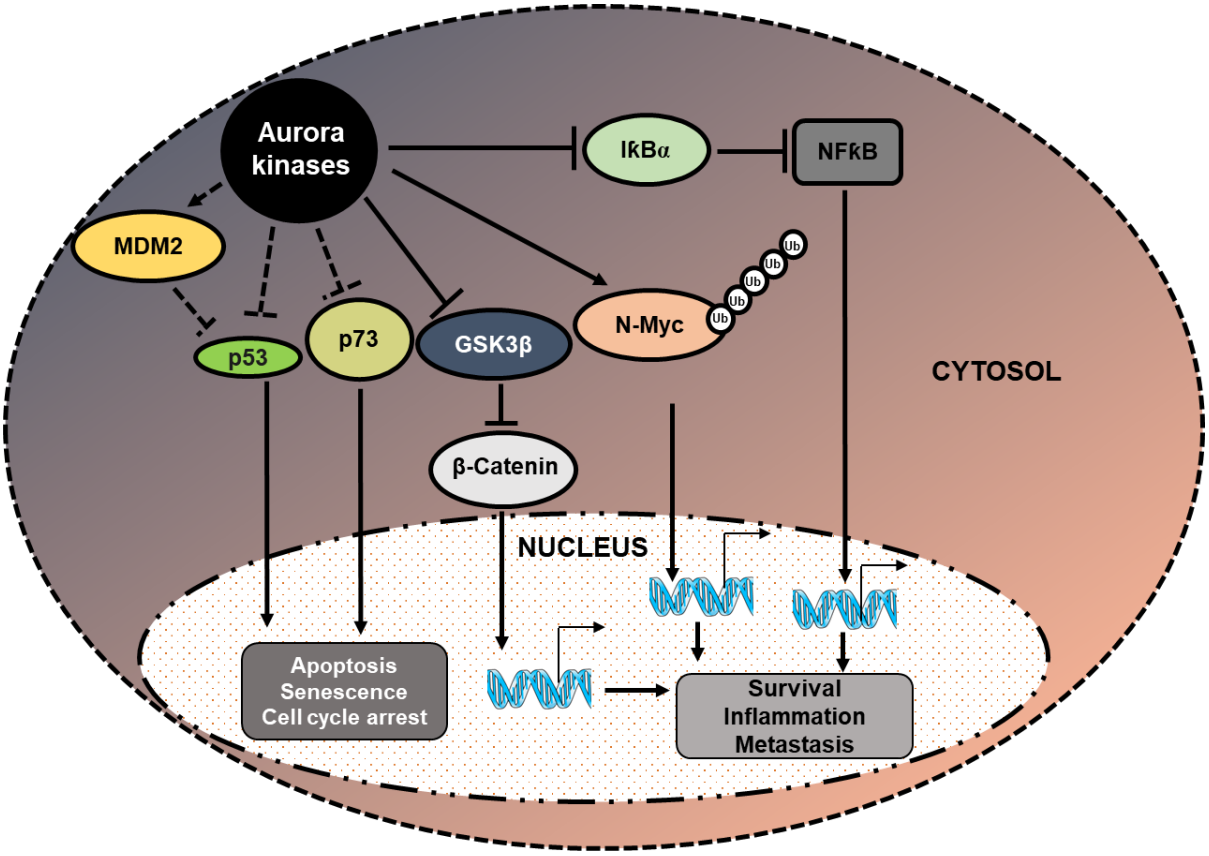

Figure 1.5: Schematic representation of regulation of transcription factors and their functions by Aurora kinases. *Aurora kinases exert their oncogenic effects through the phosphorylation of various transcription factors, or regulators of these transcription factors, only exception being N-Myc which is stabilized in a phosphorylation-independent poly-ubiquitinated form, through interaction with Aurora A, and which is competent for regulation of its downstream target genes. Solid lines represent the events occurring at the designated compartment; dashed lines represent an uncertain event which may occur either in the nucleus or the cytosol. Furthermore, Aurora kinases may themselves act in either of the compartments.*

1.4. Regulation Of Aurora Kinases By Extracellular Signalling

The activation of Aurora kinases in normal and pathophysiology is affected by two major signalling pathways, namely calcium dependent- and mitogen activated protein kinase (MAPK)-signalling cascades. Calcium signalling is reported to have a prominent and rapid impact on Aurora A activation at the centrosome (Plotnikova OV et al., 2010), and is mediated by direct Ca^{2+}-dependent calmodulin (CaM) protein binding to multiple regions on Aurora A, clustered both at the N- and C-termini. Ca2+-CaM not only mediates Aurora A activation in mitosis, by increased interaction with its partner protein, NEDD9, but also assists in Aurora A

dependent ciliary disassembly in interphase cells (Plotnikova OV et al., 2012). Aurora A, however, carries out negative feedback inhibition of Ca2+ signalling by phosphorylating a Ca2+-permeable nonselective cation channel and limiting the amplitude of Ca2+ release from the endoplasmic reticulum (ER), thereby terminating the signalling cascade (Plotnikova OV et al., 2011). Independently, it has been observed that Ca2+ deprivation inhibits Xenopus oocyte maturation by disrupting spindle elongation in meiosis I and preventing polar body emission by a mechanism independent of the MAPK signalling cascade (Sun L et al., 2008). Mechanistically, Ca2+ deprivation attenuates Aurora A protein accumulation possibly because of an inhibition of AURKA mRNA polyadenylation and thereby, the spindle elongation.

Aurora A and B kinases are affected by MAPK signalling in determining metastatic outcomes. Surprisingly, both the kinases are upregulated by the transcription factor, FOXM1, downstream of the MAPK signalling and serve as therapeutically vulnerable targets in metastatic melanoma harbouring BRAFV600E mutations (Bonet C et al., 2012; Puig-Butille JA et al., 2017). Relation between the MPK cascade and Aurora kinases is further fostered by the involvement of a protein inhibitor of the MAPK signalling cascade and a suppressor of cancer metastasis, Raf kinase inhibitory protein (RKIP), which is shown to modulate Aurora B at the kinetochores and hence, dictate outcomes of cellular cycling (Eves EM et al., 2006).

1.5. Regulation Of Aurora Kinases By Post Translational Modifications

Beyond the spatial regulation endowed by different binding proteins, Aurora kinases are subject to temporal control, for their activation and inactivation, via a plethora of post translational modification (PTM)s (Figure 1.6) which dictate its activity or sub-cellular localization. Each of these modifications are briefly described below.

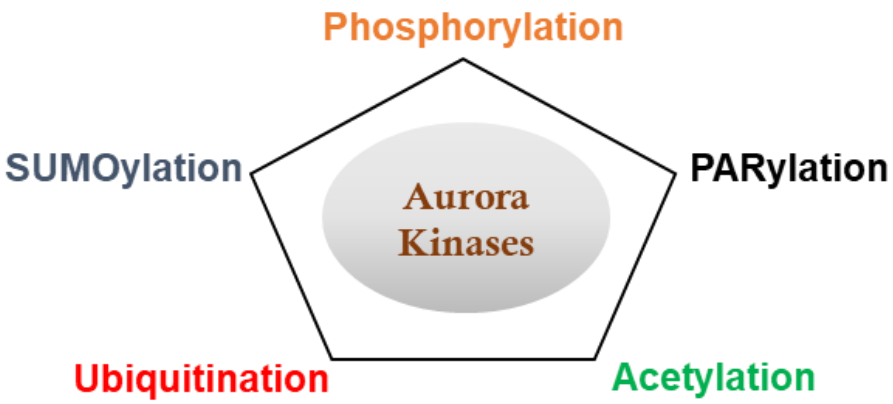

Figure 1.6: Schematic representation of the post translational modifications of Aurora kinases. *Aurora kinases are reported to undergo at least five different PTMs which modulate their activation-deactivation cycle, localization or substrate specificity.*

1.5.1. Phosphorylation

Aurora kinases are modulated by phosphorylation which affect their activity either positively or negatively, depending on the site being modified. It was first shown that okadaic acid treatment, which inhibits proteins phosphatases PP2A and PP1 (depending on the concentration used), enhances phosphorylation of a conserved Thr288 residue within the activation loop and a concomitant increase in Aurora A activity in cells. Furthermore, Thr288 falls within the consensus phosphorylation motif of cAMP-dependent protein kinase, protein kinase A (PKA), making it a likely candidate for the phosphorylation event (Walter AO et al., 2000). Thr288 is targeted by multiple other kinases, prominent amongst them being Mitogen and Stress-Activated Protein Kinase (MSK1) (Eyers PA et al., 2003) and PAK1. PAK1 is activated by p21, and exist in GIT-PIX-PAK complex. GIT is part of the pericentriolar matrix in centrosomes that recruits PIX, which in turn recruits PAK and induces its autophosphorylation and activation. PAK1 autophosphorylation catalyses gross structural alterations of its N-terminal region that otherwise masks its catalytic domain. Activated PAK1 associates and phosphorylates Aurora A at Thr288 and Ser342 in Xenopus, a phenomenon which is also

dependent on phosphorylation mediated disengagement of PAK1 from the GIT-PIX-PAK complex (Zhao ZS et al., 2005; Cotteret S et al., 2005; Ohashi S et al., 2006). In human cancer cells, Aurora A is also auto-phosphorylated at Ser51, which aids in the stabilization of the kinase by suppression of its proteasomal degradation (Kitajima S et al., 2007). The phosphorylated and active form of Aurora kinases is further maintained upon interaction with its coactivator proteins like inner centromeric protein (INCENP) as for Aurora B and Bora, Targeting Protein for Xenopus kinesin-like protein 2 (TPX2) or Positive Coactivator Protein 4 (PC4) for Aurora A (Eyers PA et al., 2003; Yasui Y et al., 2004; Dhanasekaran K et al. 2016; Dodson CA et al., 2012).

Phosphorylation, however, can also repress Aurora kinases. It was found that in Xenopus oocytes, Aurora A is phosphorylated by GSK-3β at Ser290/291 residue in the absence of progesterone and insulin signalling, which induces Aurora A mediated autophosphorylation at Ser349. This auto-phosphorylation event causes dramatic reduction in the kinase activity of Aurora A and repress substrate phosphorylation and oocyte maturation (Sarkissian M et al., 2004).

1.5.2. Poly(ADP-ribosyl)ation

Poly(ADP-ribosyl)ation [PARylation] of nuclear proteins is a widespread post translational modification that regulates a number of biological processes including chromatin reorganization, DNA damage response (DDR), transcriptional regulation, apoptosis, and mitosis (Wei H et al., 2016). Majorly, PARylation is induced by DNA strand-breaks that contributes to the survival of injured proliferating cells (D'Amours D et al., 1999). This modification is brought about by Poly(ADP-ribose) polymerases (PARPs) that constitute a large family of 18 proteins, encoded by different genes and displaying a conserved catalytic domain. PARP-1 and PARP-2 enzymes display stimulation of catalytic activities upon DNA strand-breaks and functions in repairing an interruption of the sugar phosphate backbone. PARP-1 efficiently detects the presence of a break by its N-terminal zinc-finger domain which is then translated into post translational modifications of histones H1 and H2B leading to chromatin structure relaxation and therefore to increased DNA accessibility for repair enzymes to act. Auto-PARylation of PARP-1 upon DNA damage triggers the recruitment of XRCC1, which coordinates and stimulates the repair process, to the DNA damage sites in less than 15 seconds in living cells (Okano S et al., 2003). These properties positively influence the overall

kinetics of a DNA damage signalling pathway leading rapidly to the resolution of DNA breaks. More recently, poly ADP-ribose (PAR) chains have been shown to function by acting as molecular seeds and creating phase separation (liquid droplet formation) and assembly of certain intrinsically disordered proteins DDR proteins with low-complexity domain (LCD) to facilitate dynamic, membrane-free compartments at DNA damage sites (Altmeyer M et al., 2015).

Aurora A and B kinases are shown to undergo ADP ribosylation in cells under certain physiological conditions. Aurora B is shown to undergo PARylation by PARP-1 upon H2O2 mediated DNA damage. Since Aurora B activity is necessary for mitotic progression and exit, PARylation of the kinase act to contain its kinase activity and ensure cell cycle arrest until the DNA damage is repaired (Monaco L et al., 2005). Aurora A, however, is reported to undergo the less dominant modification- mono ADP ribosylation (MARylation) by PARP10 (Zhao Y et al., 2018). MARylation of Aurora A inhibit its kinase activity. Loss of PARP10 leads to enhanced invasive and migratory capabilities of cells and downregulation of PARP10 has been observed in intrahepatic metastatic hepatocellular carcinoma (HCC). ADP ribosylation, therefore, oppose Aurora A and B kinase activities and exhibit tumor suppressive roles.

1.5.3. SUMOylation

Aurora A and B kinases possess conserved SUMOylation motif, ψ-K-X-E (ψ is a hydrophobic residue and X is any residue). SUMOylation of these kinases are shown to modulate proper localization during mitosis. Aurora A interacts with the SUMO conjugating enzyme UBC9 and is observed to co-localize with SUMO1 in the mitotic cells (Pérez de Castro I et al., 2011). SUMO deficient mutant exhibit faster kinetics at the poles with the enhanced dynamicity arising neither owing to increased degradation nor altered kinase activity, with the mechanism being presently unclear. In fact, the kinase activity was unperturbed for the K249R mutant. Phenotypically, loss of SUMOylation leads to shorter and weaker spindles and causes greater extent of H-Ras mediated co-transformation, possibly owing to the enhanced genomic instability as compared to the wild type (WT) kinase.

Aurora B, on the other hand, is SUMOylated by UBC9 through SUMO-1, 2, and 3 and at K207 residue (K202 for human) (Ban R et al., 2011; Fernández-Miranda G et al., 2010). Expression of the SUMOylation defective mutant of Aurora B (K207R) results in abnormal chromosome

segregation and cytokinesis failure possibly through mis-localization of the kinase during mitosis. Furthermore, K207R mutant is incapable of rescuing the mitotic defects that arises in Aurora B-knockout mouse embryonic fibroblasts (MEFs), while the WT kinase can. Similar to Aurora A, the SUMOylation-null mutant of Aurora B does not exhibit an altered kinase activity. However, the K207R mutant expression is accompanied by decreased phosphorylation of the Aurora-B substrate CENP-A and increased loading of the chromosome passenger complex (CPC) on chromosome arms, indicating that SUMOylation dictates Aurora B localization and fine tunes the CPC function during pro-metaphase to metaphase transition.

1.5.4. Acetylation

Acetylation has emerged as a dominant post translational modification with more than 1700 cellular proteins being acetylated at more than 3600 sites, thus unravelling the "lysine acetylome" across different cell types assessed through high-throughput, quantitative mass spectrometric studies (Choudhary C et al., 2009). Interestingly, proteins involved in a varied array of cellular functions ranging from DNA replication and repair, to nuclear hormone signalling, to vesicular trafficking, amongst many others, were found to be acetylated. Phosphorylation-dephosphorylation events are well established to have major impact on the process of mitosis. However, it was interesting to note that acetylation may also play a profound role as many cell cycle regulatory proteins are also acetylated, thus indicating to a fine tuning of the inherent mitotic regulation.

It is understood that histone deacetylase (HDAC) inhibitors alter the assembly of the kinetochores through decreased pericentromeric targeting of Aurora B and hence disrupting the cascade of the phosphorylation events necessary for mitotic spindle attachment to the kinetochore (Robbins AR et al., 2005). Furthermore, HDAC3 assists in histone H3 deacetylation during mitosis and provides a hypoacetylated H3-tail that serves as a preferred substrate for phosphorylation by Aurora B at H3S10 which in turn, is necessary for normal mitotic progression (Li Y et al., 2006). A recent report also suggests that HDAC3 deacetylates Aurora B in cells and affect its kinase activity (Fadri-Moskwik M et al., 2012). The regulation is further complicated by the association of Aurora B with class IIa histone deacetylases (HDACs 4/5/7/9) and determining their nuclear localization through a phosphorylation dependent event (Guise AJ et al., 2012). These evidences conclusively highlight the importance

of the intricate involvement of Aurora B with the HDACs in determining error-free mitotic progression.

The involvement of Tip60 as the Aurora B lysine acetyltrasferase is intriguing (Mo F et al., 2016). It was reported that Tip60 mediated acetylation of K215 of Aurora B maintains the activated form of Aurora B through the inhibition of PP2A mediated dephosphorylation. However, as the study is restricted to HeLa cells, a closer examination of the mass spectrometry results brings forth the possibility of HeLa cell specific phosphorylation of an adjacent serine residue (S222) which might assist in K215 acetylation. Moreover, Tip60 is a haploinsufficient tumor suppressor while Aurora B is an oncogene. It may be conjectured that the two proteins might play opposing functions. It is, therefore, necessary to study the relationship of Tip60 and Aurora B in a broader context involving multiple cell lines of different lineages. Finally, the involvement of other lysine acetyltransferases in acetylating Aurora B cannot be ruled out and needs further attention.

Acetylation dependent regulation of Aurora A, on the other hand, is poorly studied. A recent report shows that Aurora A is acetylated by ARID1 and acetylation is required in maintaining its kinase activity and cell proliferation and migration (Vo TTL et al., 2017). It is necessary to study Aurora A acetylation both in terms of its mitotic regulation and oncogenic function.

1.5.5. Ubiquitination

Ubiquitin-mediated destruction of Aurora kinases irreversibly inactivates Aurora kinases and is a pre-requisite for the ordered transition from mitosis to interphase. Both Aurora A and B kinases undergo targeted proteolysis after anaphase onset by the anaphase-promoting complex/cyclosome (APC/C) ubiquitin ligase. Temporal control of Aurora degradation follows differential kinetics for Aurora A and B. Aurora A degradation follow a rapid one step kinetics, while that for Aurora B happens comparatively slowly and over a broader time period. This ensures that Aurora B remains active till cytokinesis long after Aurora A activity, which is necessary for the early mitotic events, has largely been eliminated (Catherine Lindon et al., 2016). Recent evidence suggests that de-ubiquitinase, USP35, modulate the precise timing of Aurora B degradation by opposing the APC/C complex in a temporal fashion (Park J et al., 2016). Maintenance of high Aurora levels are also suitable for maintenance of transformed cells as was observed for the oncogenic gammaherpesvirus, Epstein-Barr virus (EBV),

infection. Epstein-Barr nuclear antigen 3C (EBNA3C) is a latent EBV antigen which inhibits Aurora B ubiquitination and hence help in maintaining high Aurora B levels in the cells, necessary for enhanced proliferation (Jha HC et al., 2013). Aurora A, similarly, is targeted by the tumour suppressor E3 ubiquitin ligase, von Hippel-Lindau (VHL) protein, which mono-ubiquitinates it for degradation and is necessary for the maintenance of the primary cilium (Hasanov E et al., 2017).

1.6. Impact Of DNA Damage And Repair On Aurora Kinases

DNA is susceptible to constant damage either from endogenous metabolic by-products (reactive oxygen species or reactive nitrogen species), or exogenous xenobiotic agents. DNA lesions can reach as high as 70,000 events per cell per day (Lindahl T et al., 2000). Although the majority of these lesions are single strand DNA (ssDNA) breaks, arising from oxidative damage or base hydrolysis, the conversion of these ssDNA break events to a minor fraction of double strand DNA (dsDNA) breaks can be potentially dangerous. Improper or faulty repair of DNA lesions can give rise to mutations. Germline defect in DNA repair pathway genes or inactivation of the signalling events for repair serve as toxic cocktail for accumulation of further mutations and instability of the genome. Genomic instability is, thus, a consequence of unrepaired DNA lesions arising out of defective DNA repair pathway genes to indel or point mutations or to instability of replication forks, leading to fork collapse and subsequent restricted or complex genomic translocations followed by amplifications (complicons) (Coene ED et al., 1997; Padilla-Nash HM et al., 2001; Zhu C et al., 2002).

Another aspect of genomic instability manifests itself through DNA ploidy alteration which arises due to multiple centrosomes or improper spindle kinetochore attachment and failure of spindle assembly checkpoint. Unequal chromosome segregation is a potent source of chromosomal gain or loss that may affect cellular transformation. Aurora kinases have profound impact in inducing ploidy alteration owing to their involvement in centrosomal and centromeric events. High Aurora A levels cause centrosome anomaly wherein the centrosomes undergo more than one round of duplication per cell division cycle. Presence of multiple centrosomes lead to errors in attachment to microtubules, causing mis-segregation of chromosomes and serve as a major source of aneuploidy in cells (Goepfert TM et al., 2002; Meraldi P et al., 2002; Lentini L et al., 2007). Aurora B on the other hand play pivotal role in kinetochore-microtubule attachment and formation of cytokinetic cleavage furrow. Elevated

Aurora B levels give rise to improper spindle assembly checkpoint (SAC) and faulty cytokinesis (Krenn V et al., 2015; Gurden MD et al., 2016; Shandilya J et al., 2016), in turn giving rise to aneuploid and multinucleated cell population which also cause centrosome amplification, concomitantly. Absence of a viable p53 dependent checkpoint exacerbates the effect of Aurora A and B overexpression on supernumerary centrosome formation and polyploidization (Meraldi P et al., 2002; Giet R et al., 2005). Surprisingly, the requirement of Aurora A is also highlighted in SAC, which functions through Haspin-Aurora B feedback axis (Yu F et al., 2017).

Recent discoveries underscore chromothripsis to be a potential driver of genome instability (Stephens PJ et al., 2011). It is characterized by extensive yet clustered oscillatory pattern of genomic rearrangements restricted to one or a few chromosomes, arising out of DNA double strand breaks and driven by replication-independent mechanism(s) (Zhang CZ et al., 2013). It challenges the "gradual evolution" theory of mutation in cancer and brings forth the phenomenon of generation of multiple mutations "all-at-once" within a single round of cell division. Although the broader mechanism driving chromothripsis remains unclear, it is however understood that micronuclei-based DNA damage arising in the S- and G2-phase may be a possible source of initiation of complex rearrangements (Zhang CZ et al., 2013). Under normal conditions, Aurora B suppress micronuclei formation by either phosphorylating multiple proteins like 53BP1, necessary for resolving merotelic attachments (Wang H et al., 2017) or Mis18α, necessary for suppressing chromosome misalignment, and chromosomal bridges (Lee M et al., 2017). Aurora B activity also contributes to highly localized delays in nuclear envelop formation around acentric chromosomes that allow the acentrics to merge with the late-telophase nucleus (Karg T et al. 2015). This function is achieved through the H3S10 phosphorylation of acentric chromosomes and exclusion of HP1α that would otherwise induce heterochromatin formation and association of the acentrics with nuclear lamina (Warecki B et al., 2018). However, under abnormal conditions with elevated Aurora B levels, cells exhibit increased micronuclei formation (González-Loyola A et al., 2015) possibly through the disruption of the above-mentioned pathways. It can thus be conjectured that Aurora overexpression in cancer cells may be a driving event that may positively contribute to chromothripsis. Furthermore, it would be interesting to study if Aurora B induce DNA damage in cells or more specifically, bestow DNA damage to micronuclei (as occurs in chromothripsis) or influence the choice of pathway for DNA damage repair upon overexpression.

The major pathways of repair of damaged DNA include the homologous recombination (HR) and the non-homologous end joining (NHEJ) pathways, amongst others. HR dependent repair necessitates the presence of a homologous template and is, thus, usually dependent on the S-phase and occurs through sister chromatid recombination (SCR) in somatic cells. HR/SCR is an accurate mode of repair and maintains genomic integrity. NHEJ pathway, on the other hand, does not require a corresponding template, while directly joining the broken ends and is thus more error-prone as it leads to generation of mutations at the broken end. It consists of at least two sub-pathways- a "classical" NHEJ (C-NHEJ) pathway which is dependent on the Ku heterodimer and an ''alternative'' NHEJ (A-NHEJ) pathway, which usually generates microhomology-mediated signatures at repair junctions. Cancer cells may preferentially utilize the NHEJ pathway to repair the damage and subsequently introduce mutations that can be eventually selected to provide growth advantages. Overexpression of the NHEJ pathway proteins also confer radio- and chemotherapeutic resistances to the cancer cells (Sirzén F et al., 1999; Shintani S et al., 2003; Zhang M et al., 2010). This addiction has been exploited to selectively target proteins like ligase IV, either singly or in combination with chemotherapeutic agents to kill tumours (Srivastava M et al., 2012).

Aurora A has been extensively studied in terms of DNA damage repair regulation (Katayama H et al., 2012; Wang Y et al., 2014) and it was shown that an inverse relationship exists between Aurora A/B and BRCA1/2 (Wang Y et al., 2014). Moreover, upon overexpression, Aurora A inhibits the HR pathway of DNA repair (Sourisseau T et al., 2010). Intriguingly, Aurora A inhibition de-repress the NHEJ pathway (Do TV et al., 2017), which implies that it inhibits the NHEJ pathway under normal scenario. These results indicate that Aurora A inhibits both HR and NHEJ, and must be inactivated for proper functioning of DDR to maintain stability of the genome. In line with these results, it is shown that the kinase activity of Aurora A is indeed inhibited upon DNA damage and repair induction (Krystyniak A et al., 2006). The role of Aurora B, however, is less studied. Although induction of DNA damage influences Aurora B activity (Monaco L et al., 2005; Fell VL et al., 2016), the role Aurora B might play in influencing DDR pathway choice needs further studies.

1.7. Role Of Aurora Kinases In Cellular Differentiation

Aurora kinases are increasingly being studied in physiological contexts of tissue differentiation. As most of the differentiation processes of metazoans represent an end point phenotype characterized by withdrawal from the cell cycle, the involvement of Aurora kinases in such processes further accentuate their role in extra-mitotic events.

1.7.1. Neuronal processes

1.7.1.1. Neuronal plasticity

The pioneering work on Aurora A in neurons showed that stimulation of N-methyl-D-aspartate (NMDA) receptors activate the kinase which phosphorylates CPEB, an RNA-binding protein, to steer polyadenylation-induced translation of αCaMKII (Huang YS et al., 2002). αCaMKII kinase is implicated in long term potentiation (LTP) events through regulation of signalling cascades that control synaptic strengths during neurotransmission. These results established the first link between the role of Aurora A in neuronal plasticity.

1.7.1.2. Axonal outgrowth

A potential role of Aurora B in neuronal regeneration is suggested (Jian Ming Jeremy Ng et al., 2012). This result is particularly intriguing as Aurora B is expressed robustly in mitotic cells. Upon delving into the molecular mechanism, it was observed that Aurora B was localized in the neurons in zebrafish spinal motor neurons and its activity is necessary for axonal outgrowth and regeneration following laser-mediated axotomy (Gwee SSL et al., 2018).

1.7.1.3. Neuronal polarity

RNA interference studies emphasize that Aurora A is required for neuronal polarity. Downregulation of Aurora A in hippocampal neurons disrupted axon formation and resulted in the growth of multiple neurites that were of undefined identity. Directionality of the neurons is achieved through interaction of Aurora A with Par3 and subsequent phosphorylation as was studied through the various phosphorylation mutants of Par3 (Khazaei MR et al., 2009).

1.7.1.4. Neuronal migration

Aurora A directed cytoskeletal processes in the neurons are necessary for neurite extension (Mori D. et al.,2009; Takitoh T et al., 2012). Atypical protein kinase C (aPKC) was shown to phosphorylate Aurora A at T287 and augment its interaction with its co-activator, TPX2.

Activated Aurora A phosphorylates Ndel1 and recruits it to the centrosome to spur neurite extension. Furthermore, disruption of aPKC-Aurka-Ndel1pathway specifically affected microtubule emanation from the MTOC but not the overall growth speed. Together, these findings earmark Aurora A as avital player in microtubule modulation necessary for neurite extension.

1.7.2. Skeletal muscle differentiation

Skeletal muscle differentiation represents an interesting physiologic model to study cellular cycling as differentiation induces a G1-phase block of the otherwise cycling myoblasts. Interestingly, Aurora B is found necessary for the maintenance of the differentiated state of skeletal muscles as Aurora B specific inhibitor treatment leads to the de-differentiation of myoblasts to an undifferentiated phenotype (Amabile G et al., 2009). Independently, a recent observation highlights the involvement of Aurora A in the process of differentiation as well (Karthigeyan D et al., 2018). Careful experimental designing details out the molecular pathway Aurora A prefers, to determine the timing of myoblast differentiation. Phosphorylation and inhibition of the repressive E2F family member, E2F4, by Aurora A was found to be necessary to facilitate differentiation.

1.8. Aim And Scope Of The Present Study

Aurora kinase (Aurk)s represent a group of serine/threonine kinases which are crucial regulators of mitosis. Mammals contain three paralogs of Aurora, namely Aurk A, B and C. AurkA and B are expressed ubiquitously in the somatic tissues while the expression of AurkC is restricted to the germ cells. The polar Aurora, AurkA, is necessary for centrosomal duplication and maturation. AurkB and C (the equatorial Aurks) are the members of the chromosome passenger complex and are documented well in chromosome congression, spindle bi-orientation and cytokinesis. Given the importance of these kinases, various research groups have identified novel Aurk substrates that directly play roles in the mitotic phase. With an aim to understand the reach of Aurk substrates beyond the mitotic window, an earlier effort from our laboratory led to the identification of five novel AurkA substrates (E2F4, POU6F1, PXR, MAX, and RAD23A), three of which (POU6F1, MAX, and RAD23A) are also being shared by AurkB. These set of proteins represent transcription factors (E2F4, POU6F1, MAX), proteins involved in xenobiotic sensing (PXR) or proteins involved in DNA repair (RAD23A). We observed that AurkA mediated phosphorylation of E2F4 led to an inhibition of the DNA

binding activity of the repressive E2F4 protein and an alteration of its subcellular localization. These events directly control skeletal muscle differentiation, as an inhibition of AurkA or overexpression of the phospho-deficient E2F4 mutant, exhibited retardation of C2C12 myoblast differentiation through perturbation of a network of genes directly involved in the differentiation process. *POU6F1* (also called mPOU) is also observed to be expressed in adult skeletal muscles. However, its function in the process of myogenesis is unclear. It is, therefore, necessary to study mPOU phosphorylation in the context of skeletal muscle differentiation to firstly understand the mPOU biology and secondly to elucidate the broader impact of AurkA in the differentiation process, encompassing E2F4 and mPOU.

Myc Associated factor-X (MAX) was one of the novel substrates identified in our screening. Max belongs to the basic-helix-loop-helix leucine zipper family of transcription factors and is an obligate heterodimeric partner of the critical oncogene and master transcription factor c-Myc. It functions in a non-redundant manner as its deletion in mice cannot be compensated by other members of its family and leads to early embryonic lethality. Max is shown to undergo phosphorylation by casein kinase II (CKII) in the N-terminus. It also possesses CKII consensus phosphorylation sites in its C-terminus. However, direct evidence for CKII mediated phosphorylation is lacking. Phospho-mimetic mutant of the C-terminal serine residues of Max exhibit greater extent of canonical E-box dependent DNA binding of the c-Myc/Max heterodimer complex while inhibiting the occupancy of the E-box sequence by Max/Max homodimer, as studied by *in vitro* gel shift assay. It can be conjectured that C-terminus phosphorylated Max may cause an activating effect on c-Myc/Max dependent gene transcription. However, the broader physiological impact of Max phosphorylation in the context of c-Myc/Max dependent gene transcription modulation and carcinogenesis is unclear. It is, therefore, imperative to study the consequences of phosphorylation of Max by Aurks in determining transcriptional outcomes.

The regulation of *Aurk* gene's transcription and stability of the protein are well orchestrated in a cell cycle dependent manner and tightly controlled. But this regulation is seemingly lost in cancer cells. Dysregulated expression of Aurks, stemming from genomic amplification, increased gene transcription or overexpression of its allosteric activators, is capable of initiating and sustaining malignant phenotypes and all the three Auks have been reported to be overexpressed in both solid and haematological malignancies, with the elevated expression in patients being correlated with poor prognosis and overall survival. AurkA is known to inhibit tumor suppressor pathways while assisting in proliferative and inflammatory signalling in a

phosphorylation dependent or independent manner. The role of AurkB, however, is less clear. Although AurkB is reported to inhibit tumor suppressors like p53 and GSK3β, the broader functions of this kinase toward oncogenicity need further attention. Moreover, whether the oncogenic activity of AurkB is capable of affecting genomic stability, awaits elucidation.

Aurks are known to undergo a multitude of post-translational modifications (PTMs)which influence their localization in cells or affect the kinase activity. Acetylation is a recent event which has gained significance in Aurora biology. AurkA is shown to be acetylated by ARID1, which maintains its kinase activity and assists in AurkA dependent metastatic properties. Recent evidences also indicate an intricate regulation of AurkB through reversible acetylation-deacetylation pathways. Although histone deacetylase 3 (HDAC3) was reported to be the specific deacetylase for AurkB, the lysine acetyltransferase (KAT)responsible for mediating acetylation was not unveiled. It is, therefore, important to study the KAT(s) that might regulate Aurks A and B, as this will not only broaden our understanding of the Aurora kinase biology but may also define the prospects to contain its oncogenicity.

1.9. Thesis Objectives and Objective-Specific Relevance

Considering the above stated background knowledge, we laid down the objectives of the present thesis as follows:

1.9.1. Implications of Aurora kinase mediated phosphorylation of Myc associated factor-X on c-Myc/Max (in)dependent gene expression in breast cancer

Using specific Aurk inhibitors we identified that AurkB, but not AurkA, is the major kinase for Max in cells as was analysed by mass spectrometry of Max purified from cells. We generated phosphorylation deficient mutants of the in vivo identified Max sites and found that S132, S133 and S135 residues are the major sites for the phosphorylation by AurkB in vitro. Notably, these residues lie proximal to the nuclear localization signal of Max. We asked if mutation may affect the subcellular localization of the Max proteins. Max is a nuclear protein and nuclear localization was observed for both the mutants and the wild type (WT) proteins. However, the phospho-deficient mutant exhibited two-fold higher extent of cytoplasmic distribution as compared to the WT or the phospho-mimetic mutant. This result indicates that a phosphorylation driven event is responsible for greater nuclear accumulation of Max and

hence may affect its transcription factor activity. Additionally, an earlier report which showed that the C-terminal phospho-deficient mutant of Max led to a greater extent of DNA binding of the Max/Max homodimer and a concomitant inhibition of DNA binding of the c-Myc/Max heterodimer, we conclude that AurkB mediated Max phosphorylation retains it better within the nucleus and aids in greater recruitment of c-Myc to its canonical target gene promoters.

c-Myc is a critical oncogene which affects the initiation and progression of multiple cancer types, including breast cancer. Breast cancer is extremely heterogeneous with five different subtypes (luminal A, luminal B, HER2 amplified, basal-like/ triple negative (TN) and normal-like), categorised on the basis of classical immunohistochemistry-based detection of three proteins- estrogen receptor (ER), progesterone receptor (PR) and human epidermal growth factor receptor 2 (HER2). Each of the subtypes can be sub-divided further depending on gene expression patterns. It has been shown by earlier reports that the c-Myc dependent signalling is activated and is necessary for the TN tumours. Interestingly, upon analysis of a TCGA breast cancer data-set, we observed that AurkB is elevated in all the breast cancer subtypes but luminal A, with the TN tumours exhibiting significantly higher AurkB expression as compared to the other subtypes. In order to understand if AurkB mediated Max phosphorylation truly affects c-Myc/Max dependent target gene expression, we resorted to siRNA mediated knockdown of Aurora B in a TNBC cell line, MDA-MB-231 and observed that direct c-Myc/MAX dependent genes were partially affected. The major response was seen for the differentiation related genes and tumor suppressors. An enhanced response was observed for AurkB inhibition by small molecule inhibitors in MDA-MB-231, possibly due to the higher extent of inhibition of the overall AurkB activity and hence, Max phosphorylation.

Our data primarily suggests the effect of AurkB in modulation of direct c-Myc/Max target genes. Furthermore, AurkB perturbation generates a Max-independent c-Myc activity switch to a tumour suppressive mode, as the de-repression of the differentiation related genes was observed to be enhanced upon AurkB knockdown. These results highlight the effects AurkB endow on cellular differentiation and transformation, possibly through the modulation of Max phosphorylation.

1.9.2. Acetylation dependent regulation of AurkB and a probable role of the dysregulated kinase in dictating the outcome of DNA damage repair pathway choice

As we observed that AurkB is overexpressed in breast cancer patient samples and affect the transcription of the downstream target genes of the oncogene c-Myc, we asked if AurkB can modulate another important aspect of carcinogenesis- genome stability. Cell based assays showed that high AurkB levels correlated positively with a DNA damage marker, γH2AX (phosphorylated H2AX) levels. In order to understand the probable mechanism of γH2AX accumulation in cells by AurkB, we hypothesised the possibility of two independent events. Firstly, being a kinase, AurkB may directly phosphorylate H2AX in cells. Secondly, AurkB may directly affect some other factor(s) which are directly involved in regulating γH2AX in cells, thus bringing about an indirect regulation. While the possibility of the former event cannot be ruled out, we observed that high AurkB levels inhibited Tip60 gene transcription which possibly blocks the Tip60 mediated γH2AX dynamics at the chromatin, thus leading to its accumulation even under basal conditions.

The acetyltransferase Tip60 acts as a transcriptional co-activator for many transcription factors like c-Myc, p53, E2F1, NFκB and STAT3. Its role in DNA damage response is well studied. Recent evidence also suggests its direct involvement in guiding homologous recombination (HR) dependent repair while negatively regulating the non-homologous end joining (NHEJ) pathway. HR mediated repair is an accurate mode of maintaining genomic stability by inhibiting the accumulation of mutations. NHEJ, on the other hand, follows a faster repair kinetics and cancer cells rely on it owing to its error-prone nature. Tip60 is downregulated in different cancer types, mostly through transcriptional inhibition and reduced Tip60 levels may shift the balance of DNA damage repair more toward the NHEJ pathway leading to enhanced genomic instability. Concordantly, we found that AurkB overexpression inhibit homologous recombination (HR)-dependent repair while assisting non-homologous end joining (NHEJ) in cells, a phenomenon which is in complete agreement to that observed for Tip60 downregulation.

We also aimed to unveil if Tip60 regulates AurkB in a feedback fashion. We observed that Tip60 impinges AurkB protein destabilization and inhibition of kinase activity through acetylation of two conserved lysine residues within the kinase domain of AurkB. Our results conclusively highlight the significance of a dual negative feedback loop operating between an

oncogenic kinase-AurkB and a tumor suppressor lysine acetyltransferase-Tip60, frailty of which may assist in genomic instability and cancer.

1.9.3. Reciprocal regulation of skeletal muscle differentiation by Aurora A kinase and POU6F1

Experiments carried out in our laboratory identified Ser-197 to be the major AurkA mediated phosphorylation site for mPOU *in vitro*. We extended this observation and detected S197 to indeed exist as a phosphorylated residue in cells. Ser-197 resides in the DNA binding domain of mPOU and makes critical contacts with the sugar-phosphate backbone of DNA. Consistently, we observed that AurkA phosphorylation of mPOU inhibited its canonical DNA binding, which can be explained through the electrostatic repulsion of negatively charged phosphate groups on the sugar-phosphate backbone of DNA and the phosphorylated Ser-197 residue. We also found that AurkA and mPOU exhibit an inverse relationship toward skeletal muscle differentiation. AurkA inhibition retarded differentiation while the same effect was observed for mPOU overexpression. These results indicate that AurkA mediated phosphorylation may serve as an important link toward mPOU mediated differentiation inhibition.

CHAPTER 2: MATERIALS AND METHODS

Chapter outline

2.1. General Methods

2.1.1. Agarose Gel Electrophoresis

Electrophoresis was performed for detection, analysis and purification of DNA/RNA by using 0.8-1% agarose (Sigma) gel in 1X TBE (0.09 M Tris borate and 0.002 M EDTA) electrolyte. Samples were mixed with 6X loading buffer to make final concentration as 1X (for 1X- 0.25% Bromophenol Blue, 0.25% Xylene cyanol in 40% Sucrose), loaded on the gel, electrophoresed at 150V in 1X TBE and stained in ethidium bromide solution (10µg/100 ml water) for 20 min. The stained nucleic acids were then visualized in the long wavelength UV lamp (Biorad), after destaining them with distilled water.

2.1.2. SDS-polyacrylamide gel electrophoresis (SDS-PAGE)

Purified Proteins and lysates were resolved according to their molecular weights in an SDS-PAGE. The resolving gels were made with either, 12 or 15% of acrylamide based on the resolution required in 0.375 M Tris-Cl (pH8.8), 0.1% SDS, 0.1% APS and 8% TEMED. The stacking gel composed of 5% acrylamide 0.375 M Tris-Cl (pH6.8), 0.1% SDS, 0.1% APS and 8% TEMED was layered on top of the resolving gel. Protein samples were prepared with 5X SDS sample buffer (for 1X- 50 mM Tris-HCl pH 6.8, 100 mM DTT, 0.1% Bromophenol blue, 10% Glycerol), and electrophoresed in Tris-glycine- electrophoresis buffer (25 mM Tris, 250 mM Glycine pH8.3, 0.1% SDS) after heating at 90°C for 5mins. To visualize the protein gel was stained with Coomassie Brilliant Blue (CBB) (45% MeOH, 10% glacial CH3COOH, 0.25% CBB), followed by destaining in Destaining solution (30% MeOH, 10% glacial CH3COOH).

2.1.3. Western Blot analysis

The purified proteins or whole cell lysates were resolved by SDS-PAGE (denaturing PAGE) and equilibrated for 5mins in transfer buffer (25mM tris, 192mM glycine, 0.038% SDS and 20% MeOH) along with the methanol activated PVDF membrane (Millipore). Using a semidry western transfer apparatus (Biorad) the resolved proteins were transferred on to the PVDF membrane at 25 V, for 20-40 mins depending upon the molecular weight of the protein. After blocking the PVDF blots with either 5% skimmed milk solution or 2% BSA in PBS overnight at 4°C or at room temperature for 1 hr the blots were probed with primary antibody diluted in 2.5% milk solution or

3% BSA according to the dilutions standardized for each protein in cell lysates, for a period of 8-12 hrs at 4°C depending on the affinity of the antibody. Further, after subjecting to washing with 1X PBS or PBST (PBS with 0.1% Tween 20), appropriate HRP conjugated secondary antibody solution was added and incubated for 1hr at room temperature, after which the blots were washed once again as mentioned earlier. The signal from expected protein of interest was developed using the Biorad Clarity chemiluminescence kit, as per the manufacturer's protocol. The blots were exposed in TMS (Kodak X-Ray films), for different time points and developed using GBX-Developer-Fixer Kit (Premiere Kodak reagents).

2.1.4. Silver staining

Protein samples resolved in an SDS-PAGE was fixed in a fixative solution of 40% Methanol and 10% Acetic acid for at least 2 hours with frequent changes. The gel was then thoroughly washed with 50% ethanol. The gel was then incubated in 0.02% sodium thiosulphate solution to sensitize the gel. After rinsing the gel in water, it is then incubated with 0.1% $AgNO_3$ (silver nitrate) solution for 20mins. After washing the gel thoroughly with double distilled water, the gel was then developed in a developing solution (0.04% formalin, 2% sodium carbonate). To stop the developing reaction, destaining solution made of 1% acetic acid is used. The gel is stored in a 1% acetic acid solution.

2.2. Cloning

2.2.1. Sub-cloning

For sub-cloning into bacterial and mammalian expression vectors, specific primers were used to amplify the various ORFs from the validated *E. coli* expression clones. Amplicons were purified by agarose gel extraction procedure and then the extracted DNA (2µg) was digested with the appropriate restriction enzymes (NEB) in their recommended compatible buffers. Similarly, the vector (2µg) was also digested under same conditions as the amplicons. The digested products were gel purified by agarose gel electrophoresis. Subsequently 1:3 or 1:5 molar ratio of vector to insert and maintaining 100-200ng total digested vector DNA was ligated at room temperature for 10-12 hrs using T4 DNA ligase (NEB). After ligation the total reaction mixture was transformed into *E. coli* (DH5α) and plated onto LB-agar containing the prescribed amount of the suitable

antibiotic based on the selection marker gene present in the cloned vector. Individual colonies were amplified in LB broth and plasmid was isolated. Prior to expression these clones were verified by restriction digestion (Figure 2.2.1) to release the inserts of expected length and further corroborated by sequencing these clones individually.

The list of different primers used for various sub-cloning has been enlisted in Table 2.2.2.1.

Sl. No.	**Sub-cloned construct**	**Forward primer (5'-3')**	**Reverse primer (5'-3')**
1	His_6 Max-NTD	GGAATTCCATATGATGAGCGATAACGATGAC	CCGCTCGAGGTGGTTTTTCCTTCG
2	His_6 Max-CTD	GGAATTCCATATGCACCAGCAAGATATTGAC	CCGCTCGAGGCTGGCCTCCATCCG
3	Flag-Max	ATAAGAATGCGGCCGCATGAGCGATAACGATGAC	CGCGGATCCTTAGCTGGCCTCCATCC

Table 2.2.2.1: *List of the primer sequences used for sub-cloning.*

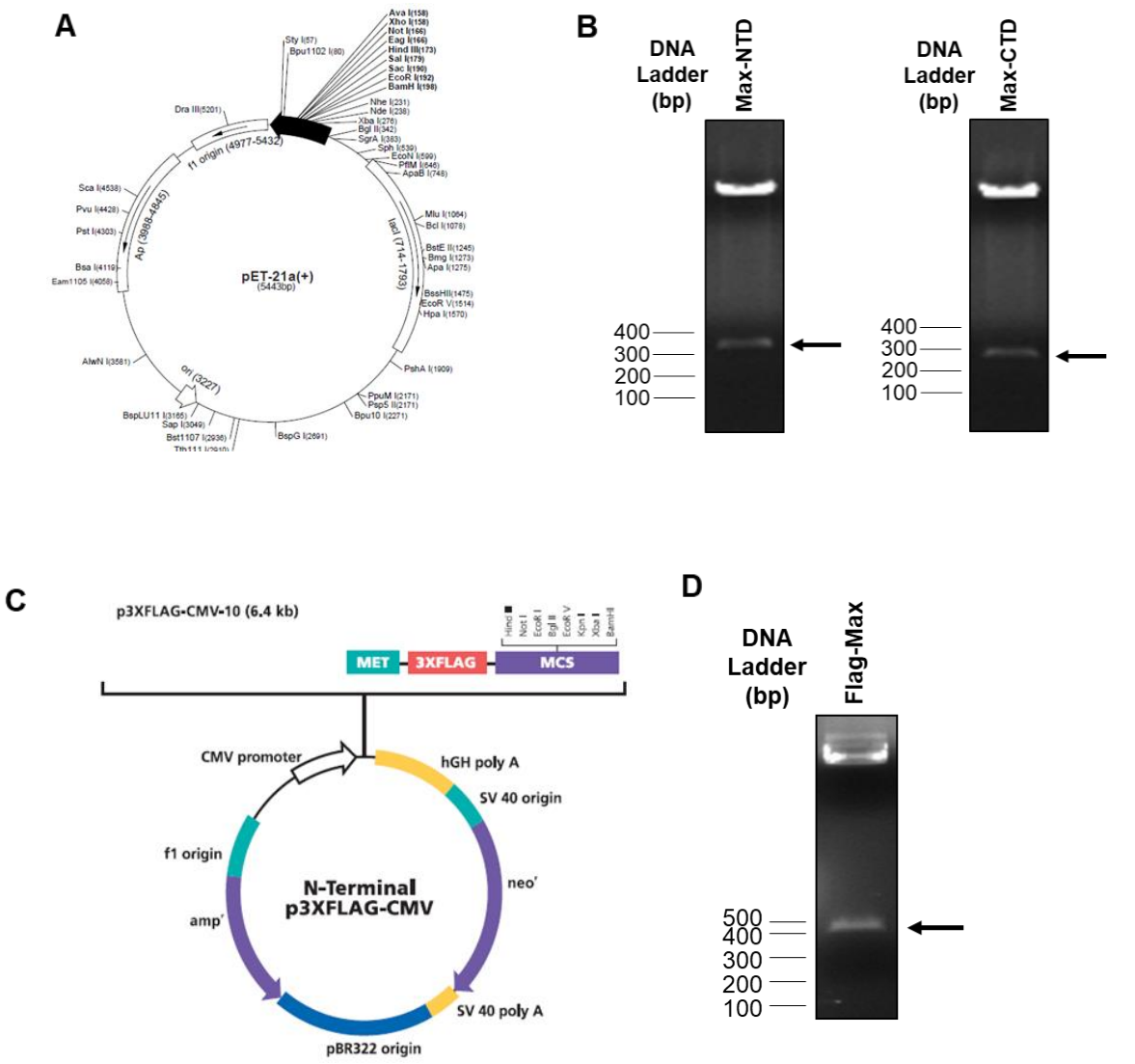

Figure 2.2.1: *Clone confirmation of Max domains (NTD and CTD) and Flag-Max.* ***A.*** *Vector map of pET21b used for cloning of N- and C-terminal domains Max bacterial expression constructs.* ***B.*** *Confirmation of the respective clones of NTD and CTD by double digestion with the respective restriction endonucleases. The cloned insert has been represented by the black arrow.* ***C.*** *Vector map of p3XFlag-CMV10 used for cloning of Flag- Max mammalian expression construct.* ***D.*** *Confirmation of the respective clone of Flag-Max by double digestion of the clones with the respective restriction endonucleases. The cloned insert has been represented by the black arrow.*

2.2.2. Site directed mutagenesis

To create various point mutants, primers were designed spanning the nucleotide coding for the desired residue to be mutated using the QuikChange Primer Design tool (Agilent), as per manufacturer's instructions. Briefly, the chosen expression plasmid containing the ORF was taken as template (50ng) and amplified using Pfu polymerase supplied with QuickChange II XL site directed mutagenesis kit (Agilent). The PCR product was incubated with Dpn1 for 2hrs at 37°C to digest the methylated template DNA and the digested product was then transformed into *E. coli* (XL10 Gold). Screening of the desired mutation was confirmed by sequencing (Figure 2.2.2).

The list of the different primers used for the present study has been enlisted in Table 2.2.2.2.

Sl. No.	Mutant generated	Forward Primer (5'-3')	Reverse Primer (5'-3')
1	POU6F1 S197D	GGCTTTAGCTTCTGGGCATC CTTGGGTGTGATGTCTAG	CTAGACATCACACCCAAGGAT GCCCAGAAGCTAAAGCC
2	AURKB K85R-K87R	ACACGTTTCCAAACCTGCCT CTGCCCAGAGGACGC	GCGTCCTCTGGGCAGAGGCA GGTTTGGAAACGTGT
3	AURKB K85Q-K87Q	GGGCGTCCTCTGGGCCAGG GCCAGTTTGGAAACGTGTA	TACACGTTTCCAAACTGGCCC TGGCCCAGAGGACGCCC
4	AURKB K110R	CCTTCTCTATCTGGGACCTG AAGAGGACCTTGAGC	GCTCAAGGTCCTCTTCAGGTC CCAGATAGAGAAGG
5	AURKB K194R	CTCTGTGAATCACCTTCCTC CCATGGCAGTACATT	AATGTACTGCCATGGGAGGA AGGTGATTCACAGAG
6	MAX S33A	CCCGCAAACTGTGAAAGGC GTCTTTGATGTGGTCCC	GGGACCACATCAAAGACGCC TTTCACAGTTTGCGGG

7	MAX S40A	CACAGTTTGCGGGACGCAGT CCCATCACTCC	GGAGTGATGGGACTGCGTCCC GCAAACTGTG
8	MAX S50A	GGGCCCGGGCTGCCTTCTCT CCTTGGA	TCCAAGGAGAGAAGGCAGCC CGGGCCC
9	MAX T59A	CATATACTGGATATATTCTG CGGCTTTGTCTAGGATTTGG G	CCCAAATCCTAGACAAAGCC GCAGAATATATCCAGTATATG
10	MAX S98A	CAGTTGGGCACTTGCCCTCG CCTTCTCCA	TGGAGAAGGCGAGGGCAAGT GCCCAACTG
11	MAX S99A	GCAGTTGGGCAGCTGACCTC GCCTTCTCCAGTG	CACTGGAGAAGGCGAGGTCA GCTGCCCAACTGC
12	MAX S108A	GGCTGTTGTCTGAGGCGGGG TAGTTGGTCTG	CAGACCAACTACCCCGCCTCA GACAACAGCC
13	MAX S109A	GAGGCTGTTGTCTGCGGAGG GGTAGTTGG	CCAACTACCCCTCCGCAGACA ACAGCCTC
14	MAX S132A-S133A-S135A	CTCTTCAGGCTCAGCCTCCG CGGCGGAGTCCGAGCCCC	GGGGCTCGGACTCCGCCGCG GAGGCTGAGCCTGAAGAG
15	MAX S132D-S133D-S135D	GCTTTGGGGCTCTTCAGGCT CATCCTCATCGTCGGAGTCC GAGCCCCCATCGAAG	CTTCGATGGGGGCTCGGACTC CGACGATGAGGATGAGCCTG AAGAGCCCCAAAGC

Table 2.2.2.2: *List of primer sequences used for site-directed mutagenesis.*

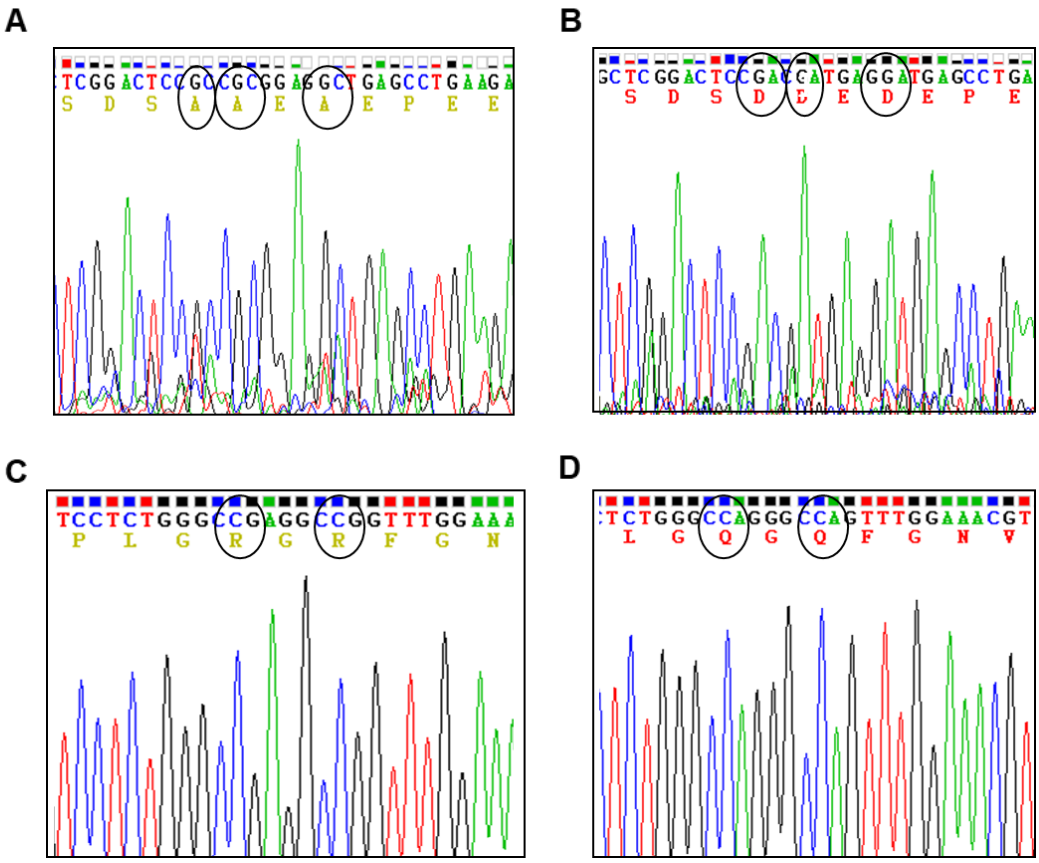

Figure 2.2.2: *Chromatogram highlighting the different point mutants generated for-* ***A.*** *Max S132A-S133A-S135A;* ***B.*** *Max S132D-S133D-S135D;* ***C.*** *Aurora kinase B K85R-K87R;* ***D.*** *Aurora kinase B K85Q-K87Q. The mutated residues are circled.*

2.3. Cell culture

2.3.1. Mammalian Cell culture

All mammalian cell lines (Figure 2.3.1), mentioned in the subsequent chapters, were procured from ATCC collection and grown as per the recommendations provided by ATCC guidelines. Briefly, the adherent cells were rinsed once with Dulbecco's phosphate buffered saline (Himedia) and then trypsinized with the prescribed amount of trypsin (Himedia) until the cells detach from the monolayer. Harvested cells were then resuspended in fresh media containing foetal bovine serum (FBS) and then dispensed into the cell culture dishes. These cell lines were grown at 37˚C with 5% CO2 till appropriate confluency is reached. Cells were then treated with various small molecule modulators mentioned in the appropriate text according to the nature of experiment done

before harvesting them for further analysis. The culture conditions for each of the cell lines is mentioned in Table 2.3.1.

Serial No.	***Cell line***	***Media and growth factor requirements***
1	HEK293	DMEM (High glucose) + 10% FBS
2	MDA-MB-231	DMEM (High glucose) + 10% FBS
3	MDA-MB-453	DMEM (High glucose) + 10% FBS
4	MCF7	DMEM (High glucose) + 10% FBS
5	BT-549	RPMI-1640 + 10%FBS + 0.023 IU/ml insulin
6	T47D	DMEM (High glucose) + 10% FBS
7	MCF10A	MEBM + 100 ng/ml cholera toxin
8	HCC70	RPMI-1640 + 10%FBS
9	C2C12	DMEM (High glucose) + 20% FBS

Table 2.3.1: *Base media and supplement requirements for various cell lines.*

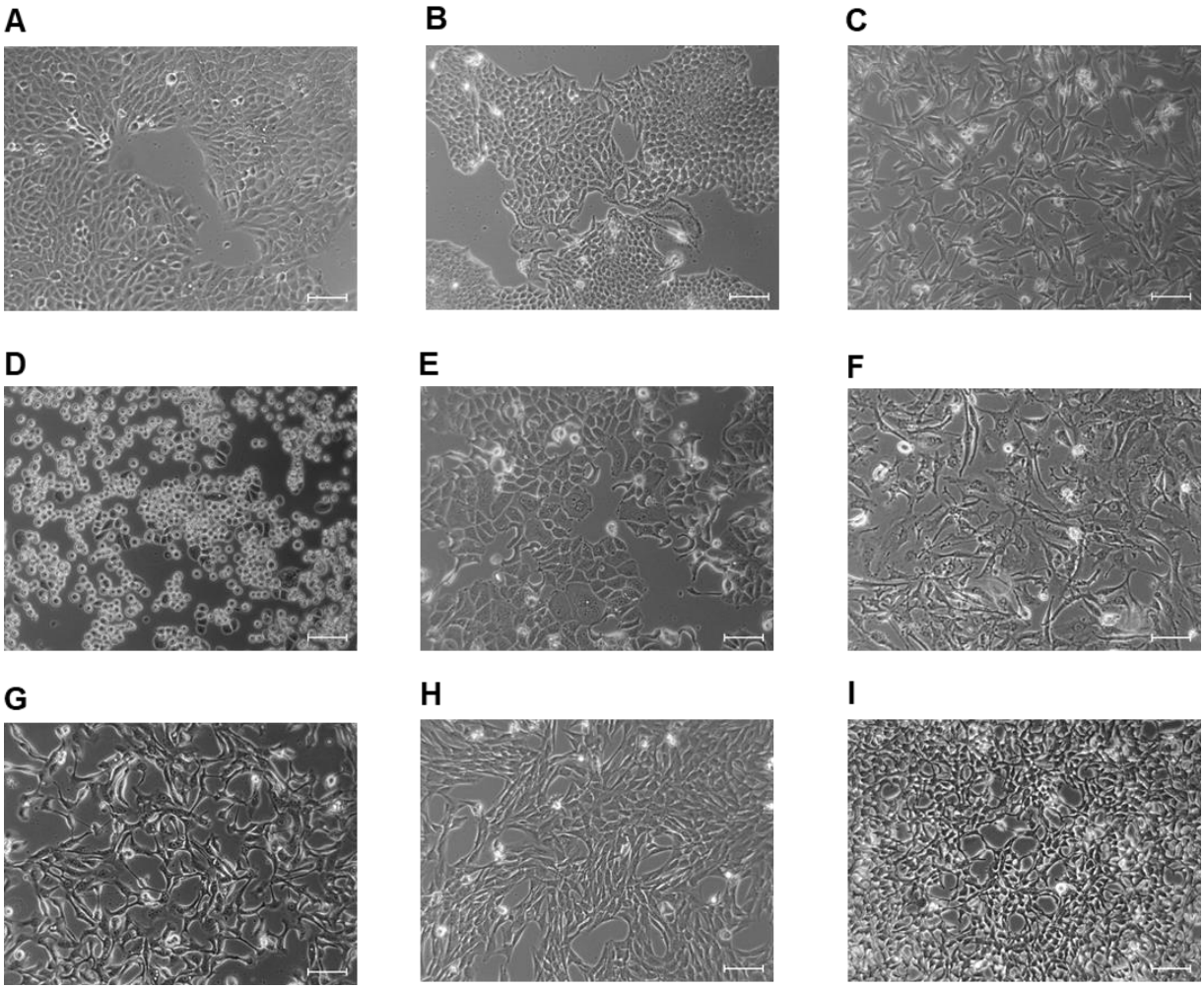

Figure 2.3.1: *Morphological features of the mammalian cells, grown in a monolayer-* ***A.*** *MCF10A;* ***B.*** *MCF7;* ***C.*** *MDA-MB-231;* ***D.*** *MDA-MB-453;* ***E.*** *T47D;* ***F.*** *BT549;* ***G.*** *HCC70;* ***H.*** *C2C12;* ***I.*** *HEK293. Scale bar represents 100µm.*

2.3.2. Insect Cell Culture

The insect ovarian cell line Sf21 from *Spodoptera frugiperda* (Figure 2.3.2) was procured from Invitrogen. The frozen stock vial was thawed on 37ºC water bath and was diluted ten times with pre-warmed Grace's insect medium (Gibco) supplemented with 0.1% Pluronic acid solution (Invitrogen # F-68), 0.1% yeastolate (Invitrogen), 10µg/ml gentamycin (Invitrogen), 10%FBS and antibiotic (penicillin, streptomycin and amphotericin B) mixture. The cells were seeded in a T25 flask and allowed to adhere to the flask for 45minutes, following which the media was changed to

completely remove the DMSO from the cryo-preservation media. The cell further allowed to grow at 27ºC BOD incubator till 70-80% confluence. The spent media was then discarded and 5ml of fresh Grace's complete media, with all the supplements, was added to the flask. The adhered cells were scraped and sub-cultured at 1:3 ratio. The cells were counted using a haemocytometer (Neubauer's Chamber) and seeded in appropriate numbers for infection, as required.

For cryopreservation, the cells were harvested after scraping, pelleted down upon centrifuging at 1000 rpm for 3mins, resuspended in freezing mixture (40% Grace's medium, 50% FBS and 10% DMSO) and transferred to cryo-vials (Corning), which were finally frozen slowly inside a cryo-cooler containing isopropanol, at -80ºC for 24hrs, following which the vials were transferred to liquid nitrogen cylinders.

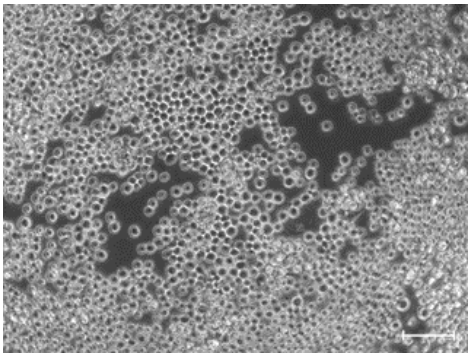

Figure 2.3.2: *Morphological features of Sf21 cells, grown in a monolayer. Scale bar represents 100µm.*

2.3.3. Culture and differentiation of C2C12 myoblasts

C2C12 myoblasts (Figure 2.3.1.H) were maintained in DMEM containing 20% FBS. Differentiation was induced by removing the maintenance media, rinsing the cells with warm 1XPBS and addition of DMEM containing 2% horse serum. Differentiation of the myoblasts can be witnessed by the appearance of myofiber with branched morphology which are the outcome of myoblast fusion, as the period of differentiation progresses.

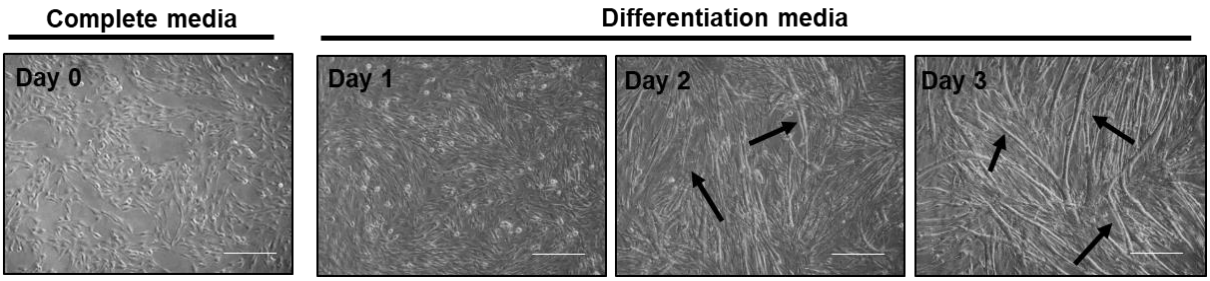

Figure 2.3.3: *Morphological features of C2C12 myoblasts upon the onset of differentiation. Day0 represent the undifferentiated cells while Day1, 2 or 3 represent the myoblasts which have initiated the differentiation program for 24, 48 or 72hrs post induction with 2% horse serum. Filled arrowheads indicate the myofibers emanating from myoblast fusion. Scale bar represents 100µm.*

2.3.3. Mammalian cell Transfection

2.3.3.1. Transfection of plasmid DNA

Plasmid vectors, competent for expression of various Flag- or hemagglutinin (HA)-tagged proteins in mammalian cells, were transfected by using either lipofectamine 2000 Plus (Invitrogen) or Gene Juice Transfection Reagent (Merck-Millipore). Briefly, the cells were seeded in culture dishes as per the manufacturer's recommendations and allowed to grow till 50-60% confluence. Recommended amount of DNA and the prescribed volume of Lipofectamine 2000/ Gene Juice Transfection Reagent was added to individual microfuge tubes and incubated at room temperature in appropriate volume of the media without serum and antibiotic. After the end of the initial mixture, DNA and Lipofectamine containing media were mixed and allowed to form complexes at room temperature for 5-10mins, following which the mixture was added over the monolayer and mixed uniformly by gentle shaking of the culture dishes. 4-6hrs post transfection, the transfected media was discarded and fresh complete media was supplemented to the cells. Cells were harvested at appropriate times post transfection and analysed for various assays by means of western blot analysis or indirect immunofluorescence. Standard amount of DNA for the corresponding cell culture dishes are mentioned in Table 2.3.2 and the transfection reagents used for the different cell lines are detailed in Table 2.3.3.

Diameter of the Culture Dish	Amount of DNA transfected
35mm dish/ 6-well plate	2µg
60mm dish	4µg
100mm dish	10µg

Table 2.3.2: *Standard DNA amounts transfected for different culture dishes.*

The following conditions were maintained for transfection of different cell lines:

Cell Line	DNA: Transfection Reagent (µg: µl)
HEK293	1:2 (DNA: Lipofectamine)
MCF7	1:2 (DNA: Lipofectamine)
MDA-MB-231	1:1.5 (DNA: Lipofectamine)
HeLa	1:3 (DNA: Gene Juice)

Table 2.3.3: *Standard DNA: transfection reagents used for different cell lines.*

2.3.3.2. Transfection of siRNA

MDA-MB-231 cells were transfected with either control siRNA (Silencer™ Negative Control No. 1 siRNA; Invitrogen # AM4611) or a mixture pool of four siRNAs targeting Aurora kinase B (ON-TARGET plus SMART pool; Dharmacon #003326-00-0005). Briefly, MDA-MB-231 cells were seeded in a 6-well plate format as per the manufacturer's recommendations and allowed to grow till 30% confluence. 100pmol of either the control siRNA or the siRNA pool targeting Aurora kinase B were added to individual microfuge tubes and incubated at room temperature in 250µl of DMEM without serum and antibiotic. 5µl of Lipofectamine RNAiMAX Reagent was incubated at room temperature in 250µl of DMEM without serum and antibiotic. After the end of the initial mixture of 5mins, siRNAs and transfection reagent containing media were mixed and allowed to

form complexes at room temperature for 20mins, following which the 500µl mixture was added over the monolayer and mixed uniformly by gentle shaking of the culture dishes. 1.5-2ml of DMEM containing 10%FBS was also added to each well. 6hrs post transfection, the transfected media was discarded and fresh complete media was supplemented to the cells. Cells were harvested after 48hrs post transfection and analysed for various assays.

2.3.4. Generation of stable cell lines

2.3.4.1. Stable knockdown of Tip60

Four different Tip60 specific shRNA constructs cloned into pGIPZ vector (Figure 2.3.3A), were purchased from Dharmacon. Potency of each of these shRNAs was first checked by western blot analysis of the whole cell lysate of HEK293 cells co-transfected with HA-Tip60 and individual shRNAs for 48hrs (Figure 2.3.3B).

For generating stable Tip60 knockdown and non-silencing control cell lines, 10µg of pGIPZ-shNS and pGIPZ-sh2 vectors were transfected into HEK293T cells along with appropriate amount of viral gene containing plasmids psPAX2 (5µg), pRSV-Rev (1.5µg) and pCMV-VSV-G (3.5µg) to package the mammalian clone into the viral particles. 48 hours post transfection, the viral particles in the culture supernatant are collected and used to infect HEK293 cells for 6hrs with 50µg/ml of DEAE-dextran. The infected cells were sorted using FACS Aria III on the basis of GFP expression (Figure 2.3.3C) and characterized on the basis of downregulation of HA-Tip60 expression, transiently transfected in these cells using 2N3T-Tip60 mammalian expression vector (Figure 2.3.3D).

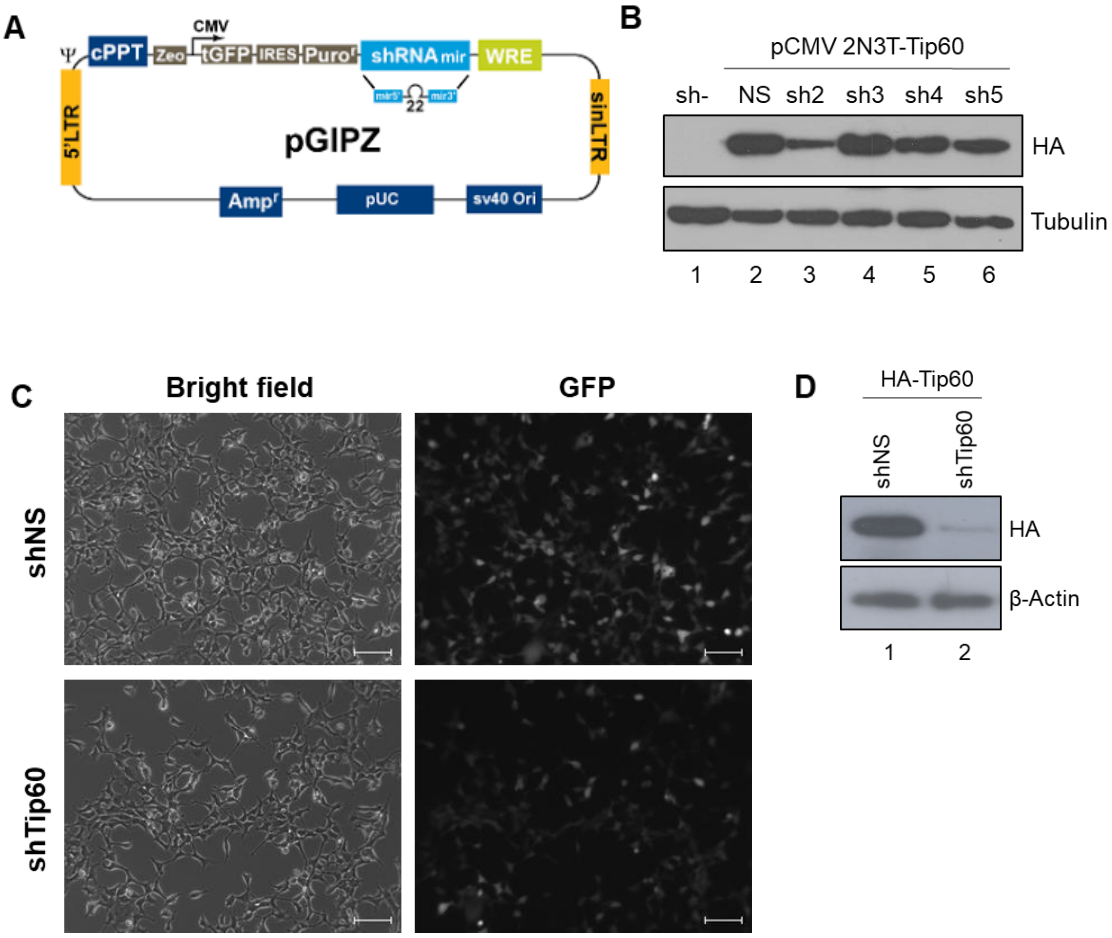

Figure 2.3.3: Generation of Tip60 stable knockdown cell line in HEK293 cells. A. *Vector map of pGIPZ vector obtained from Dharmacon.* ***B.*** *Screening for the most potent shRNA against Tip60 (sh2, sh3, sh4, and sh5) against non-silencing (shNS) control.* ***C.*** *pGIPZ-shTip60 (sh2) and shNS vectors were used to generate the corresponding lentiviral particles, which were used to infect HEK293 cells. GFP expressing HEK293 cells were sorted on the basis of GFP expression. Scale bar represents 100µm.* ***D.*** *Western blot representation for the characterization of Tip60 stable knockdown HEK293 cells. 2µg of pCMV 2N3T-Tip60 was transiently transfected into either shNS or shTip60-HEK293 cells for 48hrs and probed for the indicated proteins.*

2.3.4.1. Stable knockdown of Aurora kinase B

Six different Aurora kinase B specific shRNA constructs (doxycycline inducible) cloned into pTRIPZ vector (Figure 2.3.4A), were purchased from Dharmacon. Transient transfection of each of these shRNAs into HEK293 cells and treatment with 2µg/ml of doxycycline could not lead to the downregulation of Aurora kinase B at the protein level (Figure 2.3.4B). In order to study the potency, each of these shRNAs and the control pTRIPZ empty vector, were separately transfected into HeLa cells and treated with 0.5µg/ml of puromycin until selected for visible colony clusters. The cells were trypsinized and expanded for RFP^+ sorting, post induction with 2µg/ml of doxycycline using FACS Aria III. The sorted cells were further expanded and studied for the best shRNA at two different time points (29hrs and 49hrs), post doxycycline treatment by western blotting analysis (Figure 2.3.4C).

For generating stable Aurora kinase B knockdown and empty vector control cell lines in MDA-MB-231 breast cancer cells, 10µg of pTRIPZ-EV and 1-F10 vectors were transfected into HEK293T cells along with appropriate amount of viral gene containing plasmids psPAX2 (5µg), pRSV-Rev (1.5µg) and pCMV-VSV-G (3.5µg) to package the mammalian clone into the viral particles. 48 hours post transfection, the viral particles in the culture supernatant are collected and used to infect MDA-MB-231 cells for 6hrs with 50µg/ml of DEAE-dextran. The infected cells were sorted using FACS Aria III on the basis of RFP expression (Figure 2.3.3C) and characterized on the basis of downregulation of endogenous Aurora kinase B expression (Figure 2.3.4D).

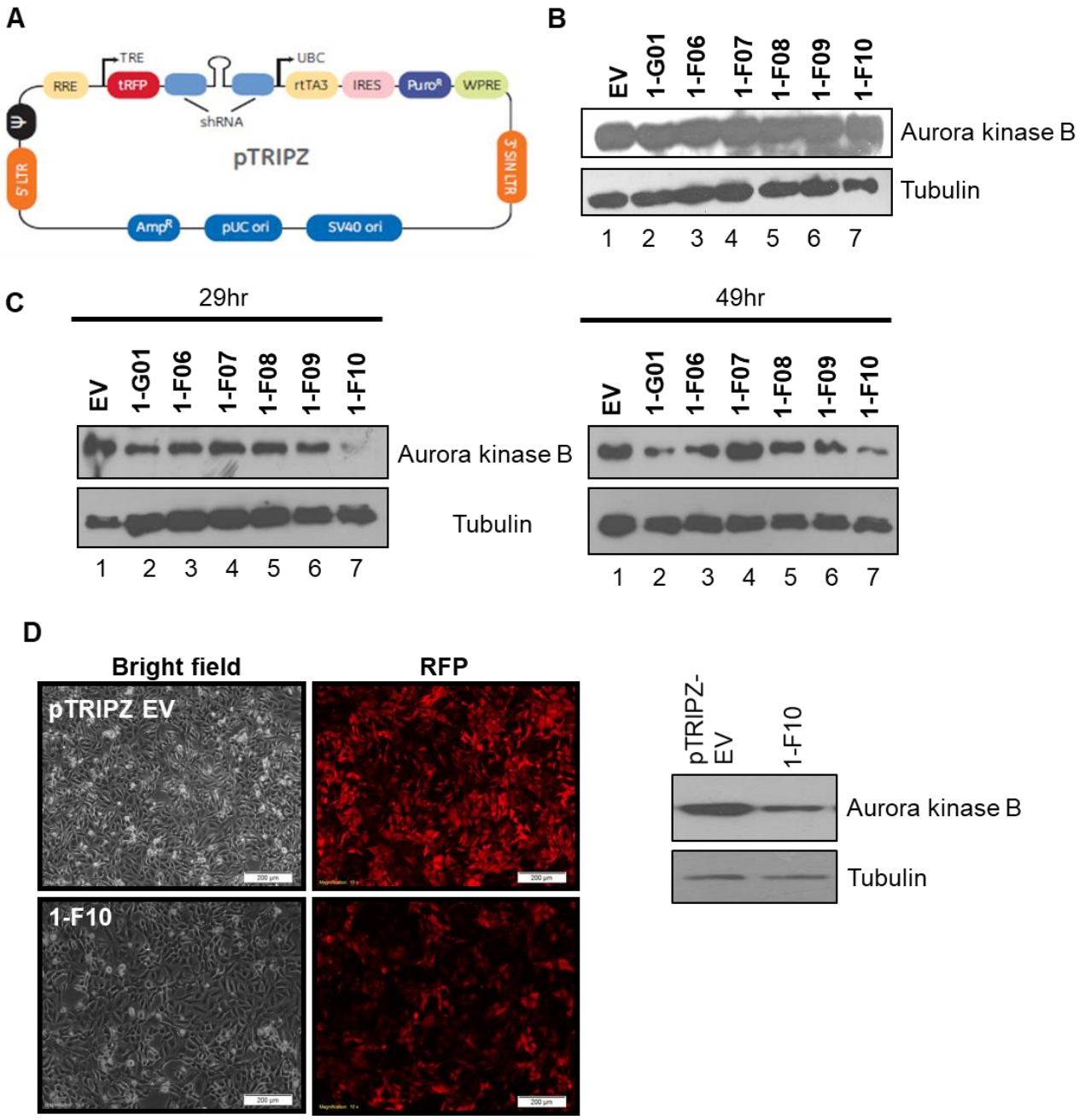

Figure 2.3.4: Generation of Aurora kinase B stable knockdown cell line. A. *Vector map of pTRIPZ vector obtained from Dharmacon.* ***B.*** *Screening for the most potent shRNA against Aurora kinase B (1-G01, 1-F06, 1-F07, 1-F08, 1-F09, and 1-F10) in HEK293 cells upon transient transfection using Lipofectamine 2000 plus. 24hrs post transfection, the cells were treated with 2µg/ml of doxycycline for 48hrs. EV represents pTRIPZ empty vector control cells.* ***C.*** *Representative western blot for the screening of the potency of different shRNAs stably expressing*

in HeLa cell upon treatment with 2µg/ml of doxycycline for either 29hrs or 49hrs. ***D.*** *Representative microscopic image of stable pTRIPZ EV and 1-F10 MDA-MB-231 cells, transduced with lentiviral particles and sorted on the basis of RFP expression. Scale bar represents 200µm. Corresponding western blot representation for the characterization of Aurora kinase B knockdown upon treatment with 2µg/ml of doxycycline for 48hrs.*

2.3.5. Indirect Immunocytochemistry

Mammalian cells were cultured on 0.1% gelatin coated coverslips in sterilized culture dishes and transfected with the various mammalian expression constructs (as mentioned in the following sections) and allowed to grow further till the point of collection as per the experimental requirements. At the end point, cells on the coverslips were rinsed with 1X PBS and fixed in 2-4% paraformaldehyde for 15 minutes. Subsequently the monolayer was washed thrice with 1X PBS and permeabilized with 0.1% Triton X-100 for 5 minutes. Once permeabilised, cells were blocked with 5% FBS at 37ºC for 30 mins, after which the cells were incubated with the primary antibody for 1hr under constant mixing conditions on a gel rocker. The cells were then washed thrice with 1X PBS and appropriate Alexa Fluor conjugated secondary antibodies were added in 1% FBS solution in 1:500-1:1000 dilution and incubated for 30 min in dark. The cells were then washed thrice with 1X PBS and stained with Hoechst dye (4µg/ml in 1X PBS) for 20 minutes to visualize the DNA. The coverslips were then mounted over grease free glass slides using 70% glycerol. Confocal microscopic images of immuno-stained cells were captured using Zeiss LSM Meta 510.

2.3.6. Cell Synchronization for mass spectrometry mediated identification of Aurora kinase B acetylation sites

2.3.6.1. G0/G1 block: pCDH-Flag Aurora B kinase overexpressing cells or the corresponding pCDH-empty vector control cells, maintained in DMEM containing 10% FBS, were synchronised at the G0/G1 boundary by serum deprivation for 72hrs at a confluence of 60-70% (Figure 2.3.4A).

2.3.6.2. G1/S block: Double thymidine block was carried out for synchronization of cells at the G1/S boundary. Briefly, 30-40% confluent pCDH-Flag Aurora B kinase overexpressing cells or the corresponding pCDH-empty vector control cells were treated with 2mM Thymidine for 18 hrs (first block). The cells were then released from the block by washing twice with warm 1X PBS

and then by addition of DMEM containing 10% FBS. 9hrs post release in complete media, 2mM thymidine was again added to the cells and harvested 17hrs later (Figure 2.3.4B).

2.3.6.3. G2/M block: Mitotic block was performed by addition of 2mM thymidine for 24 hrs, followed by washing twice with 1X PBS and releasing in DMEM containing 10%FBS for 3hrs. 100ng/ml of nocodazole was finally added for 12 hrs to block the cells in prometaphase following which they were harvested (Figure 2.3.4C).

Cells were harvested at the end of each synchronization cycles; cell pellets were washed once with 1X PBS and lysed by adding 1ml of chilled lysis buffer (50 mM Tris-HCl, pH 7.4; 150 mM NaCl; 5 mM EDTA; 1% tritonX-100; 1X-Complete protease inhibitor). Cells were incubated at 4ºC for 1hr with constant mixing. Lysate was clarified by centrifuging at 13,000 rpm at 4°C for 10 mins and incubated with 30µl of anti-Flag M2 agarose beads (pre-washed and equilibrated in lysis buffer; Sigma # F2426) for 3hrs at 4ºC with uniform mixing.

The beads were collected by centrifugation for 3mins at 2,000 rpm at 4ºC and the supernatants were removed by aspiration. The pellets were washed once with 1 ml of cold lysis buffer, twice with tris buffered saline (TBS; 50 mM tris-HCl, pH 7.4; 150 mM NaCl) and eluted in 30µl of 500ng/µl of 3X-FLAG peptide (Sigma#F4799) in TBS buffer. The immunoprecipitated samples were then divided into two fractions; one of the fractions was resolved in a 12% SDS-PAGE and immunoblot analysis was done for verifying the pulldown protein and their interacting partners, while the other fraction was similarly resolved in a 12% SDS-PAGE, but stained with CBB for processing for mass spectrometric analysis of *in vivo* acetylation sites (Figure 2.3.4D).

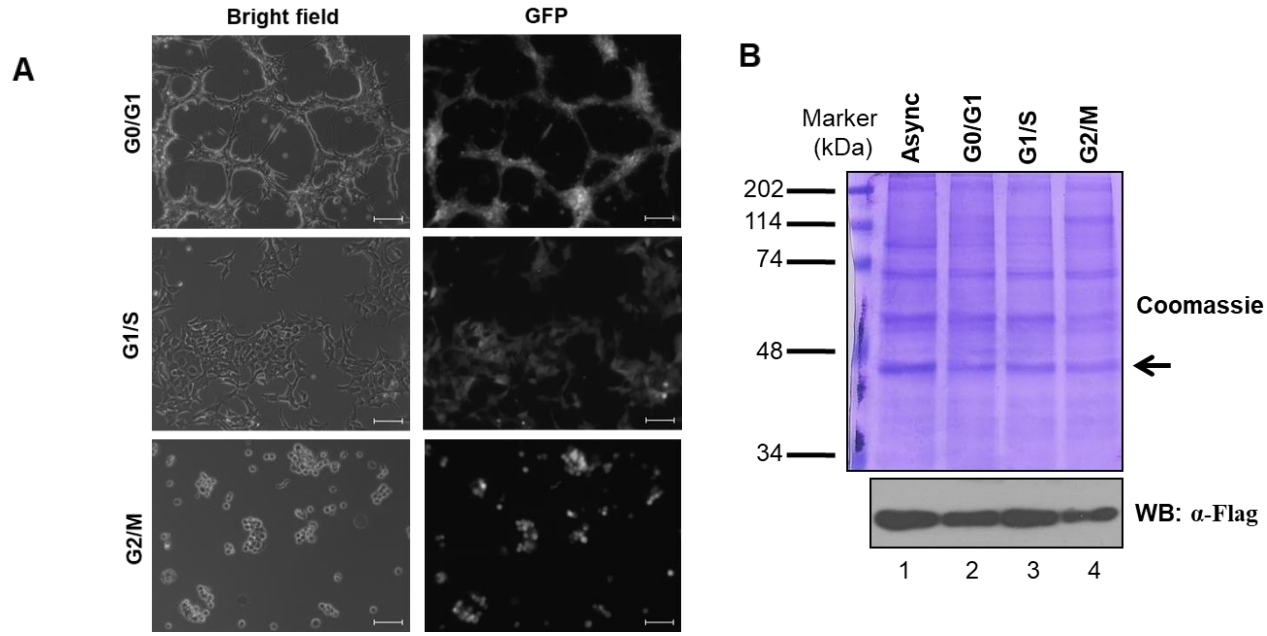

Figure 2.3.4: Synchronization of stably overexpressing Flag-AurkB HEK293 cells. *Cellular morphology upon G0/G1 block* ***(A)****, G1/S block* ***(B)*** *or G2/M synchronization* ***(C)****.* ***D.*** *Immunoprecipitation of Flag-Aurora B kinase from asynchronous or synchronised (as indicated) Flag-Aurora B kinase stable cells were carried out with anti-Flag M2 agarose beads. 40% of the immunoprecipitated fraction was loaded on a 12% SDS PAGE for coomassie staining, while 30% of the fraction was loaded on the other side of the protein marker for carrying out western blotting with anti-Flag antibody. The coomassie gel was overlaid over the western blot autoradiogram and the desired band, as has been marked by the arrow, was excised, collected in a microfuge tube and dried in absolute ethanol for 10 minutes. Ethanol was aspirated and the tubes, containing the gel pieces, were dried in a speed vacuum rotor at 60ºC until the samples were dried.*

2.4. Protein purification

2.4.1. Purification of recombinant proteins from baculovirus-infected Sf21 cells

Aurora A and Aurora B enzymes were expressed as C-terminal His_6-tagged proteins and purified using Ni-NTA (Novagen) affinity purification from the respective, recombinant baculovirus infected Sf21 cells. Briefly, Sf21 cells were cultured in five 150mm dishes till 100% confluent after which fresh complete TC100 media (Himedia) with 10% FBS was added and then scrapped to detach the monolayer following which the cells were counted and 9 million cells transferred to

fresh culture dishes, just before infection. The cells were kept in suspension during infection, and 200 µl of the viral particles containing culture supernatant were added drop wise over the surface of the culture dishes at room temperature. Following infection, they were further incubated at 27˚C. The infected cells are checked for the viral expression based on the change in morphology [cubical, spindle, or capsule shaped etc]. 70hrs post infection (prior to rupture and release of the viral particles into the culture supernatant cells were harvested by scrapping and pelleting at 1000 rpm for 10 min. Cell pellet was washed once with 1X PBS and then lysed in cold lysis buffer (homogenization buffer) containing 10mM tris-HCl pH 7.5, 10% Glycerol, 0.1% NP0, 2mM β Mercaptoethanol, 0.2mM PMSF, 500mM NaCl, 15mM Imidazole and 1X protease inhibitory cocktail (Sigma) using a Dounce homogenizer (5 strokes- 4 times with 3 min interval). After lysis, the lysate was centrifuged at 16,000rpm for 30 min and the supernatant was collected and 200µl of Ni-NTA beads, pre-washed and equilibrated with the homogenization buffer, were added and allowed to bind for 3hrs at 4°C on an end-to-end rotor. The beads were washed 7-8 times in wash buffer containing 10mM tris-HCl pH 7.5, 10% Glycerol, 0.2%NP40, 2mM β-Mercaptoethanol, 2mM PMSF, 300mM NaCl and 15mM Imidazole for poly-His tag proteins. After binding, the proteins were eluted using elution buffer containing 10mM tris-HCl, pH-7.5, 10% Glycerol, 0.1% NP0, 2mM β- Mercaptoethanol, 0.2mM PMSF, 200mM NaCl, 250mM Imidazole and 1X protease inhibitory cocktail. The protein was checked in 12% SDS-PAGE (Figure 2.4.1) and then stored at - 80°C after snap freezing them in small aliquots.

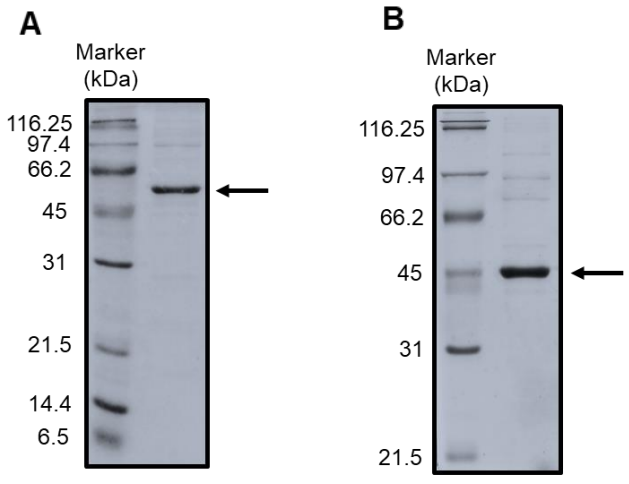

Figure 2.4.1: *Purification of Aurora A and B kinases from Sf21 cells. Representative purification profiles of His_6-Aurora A and His_6-Aurora B resolved on a 12% SDS-PAGE and stained with CBB.*

2.4.2. His_6-tag fusion protein purification

2.4.2.1. Purification of recombinant His_6-tag fusion proteins from soluble fraction of *E. coli* lysate

pET21b expression vector harbouring the clone of choice is transformed into *E. coli (DE3)*. Single colony was inoculated into 100ml of LB containing appropriate antibiotic and grown overnight in 37°C shaker incubator. These cultures were further scaled to 1l and grown till OD_{600nm} reaches 0.5 after which they were induced to express the protein of interest with 0.5mM IPTG for the next 3 hours. Subsequently, cells were harvested and then resuspended in cold homogenization buffer (10mM tris-HCl pH-7.5, 10% Glycerol, 0.1% NP40, 2mM β-Mercaptoethanol, 0.2mM PMSF, 500mM NaCl, 15mM Imidazole and 1X protease inhibitory cocktail). Cell suspension was sonicated to lyse and then centrifuged at 16,000 rpm for 30mins at 4°C. The supernatant was bound to Ni-NTA agarose (Novagen) beads for 3hrs at 4°C in an end-to-end shaker. The beads were subsequently washed 7-8 times in wash buffer (10mM tris-HCl pH-7.5, 10% Glycerol, 0.2% NP40, 2mM β-Mercaptoethanol, 2mM PMSF, 300mM NaCl, 15mM Imidazole) and eluted with the elution buffer (10mM tris-HCl pH-7.5, 10% Glycerol, 0.1% NP0, 2mM β-Mercaptoethanol, 0.2mM PMSF, 200 mM NaCl, 250mM Imidazole and 1X protease inhibitory cocktail). The purity and yield were checked in a 12% SDS PAGE followed by CBB staining.

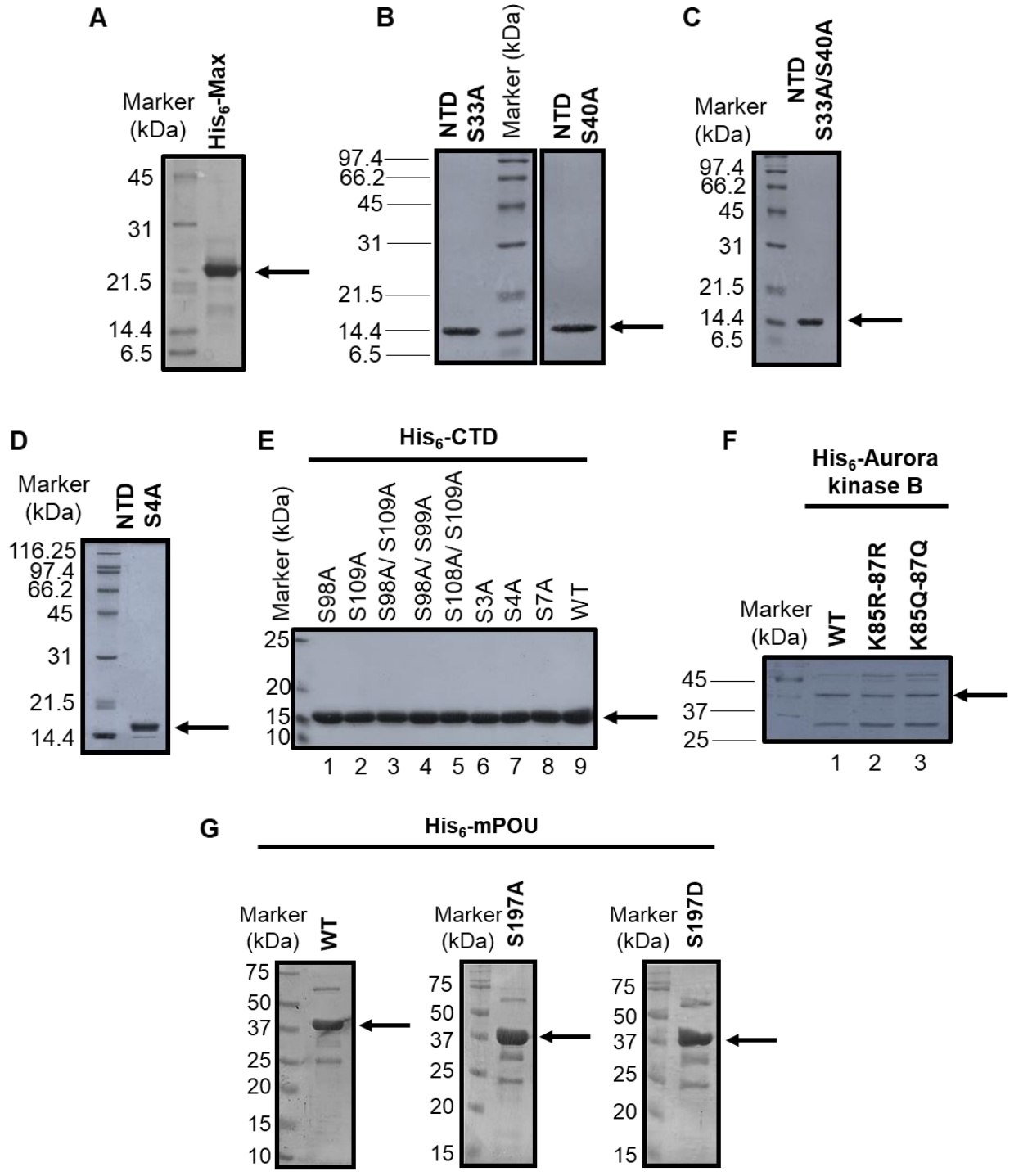

Figure 2.4.2: *Purification profiles of full length His6-Max* ***(A)****, His6-Max NTD S33A (left panel) and His6-Max NTD S40A (right panel)* ***(B)****, His6-Max NTD S33A/S40A double point mutant* ***(C)****, His6-Max NTD S33A/S40A/S50A/S59A [referred to as NTD-S4A (tetra S/T site point mutant)]* ***(D)****, His6-Max CTD WT and mutants mentioned [CTD-S3A (S132A-S133A-S135A) CTD-S4A (S98A-*

S99A-S108A-S109A) and CTD-S7A (S98A-S99A-S108A-S109A- S132A-S133A-S135A)] ***(E)****, His_6-Aurora kinase B WT and mutants mentioned* ***(F)*** *and His_6-mPOU WT and mutants mentioned* ***(G)*** *resolved on a 12% SDS PAGE and visualized by CBB staining. Filled arrowhead represent the desired protein band.*

2.4.2.1. Purification of recombinant His_6-Myc fusion proteins from inclusion bodies of *E. coli*

pRSET-His_6-Myc expression vector (Figure 2.4.3A) was transformed into *E. coli* (Rosetta pLys-S) competent cells. A single colony was grown in LB broth containing 100 µg/ml ampicillin at 30 °C and protein expression was induced with 0.5 mM IPTG at 0.3–0.4 OD_{600} nm. Induction was performed for 3hr at 30°C. Bacteria were collected and washed with cold washing buffer (10 mM Tris–HCl, pH 7.9, at 4°C, 100 mM NaCl, and 1 mM EDTA), and cell pellet was resuspended in 15ml cold lysis buffer (20mM Hepes, pH 7.9, 500mM NaCl, 10% v/v glycerol, 0.1% v/v NP-40, 10mM β-mercaptoethanol and 1mM PMSF) and sonicated on ice. Centrifugation was carried out at 12,500rpm at 4°C for 15mins (SS34 Sorval rotor); the pellet was used to purify insoluble His6-Myc. The pellet was resuspended with 10ml of E-buffer (50mM Hepes, pH 7.9, 5% v/v glycerol, 0.05% w/v of sodium deoxycholate, 0.5mM β-mercaptoethanol, 0.1% NP-40 and 1mM PMSF) and homogenized with a Dounce homogenizer. The inclusion bodies were then recovered by centrifugation at 14,000rpm for 15mins at 4C. The supernatant was discarded and to the pellet 1ml of DMSO was added. After 1hr, the pellet was solubilized in 10ml of S-buffer (10mM Hepes, pH 7.9, 6M guanidine-hydrochloride, and 5mM of β-mercaptoethanol) on a shaker at room temperature for 3 hrs. The denatured His6-Myc protein in S-buffer was adjusted to 5mM imidazole and bound with 75µl of Talon resin (Clontech) on a rotor for 2-4 hrs at room temperature. The resin was then washed thrice with 5ml each of S-buffer containing 5mM imidazole, thrice with 1ml BC500 containing 7M urea and 5mM imidazole, once with 1ml of BC100 containing 7M urea and 15mM imidazole and once with 1ml of BC100 containing 7M urea and 30mM imidazole. Recombinant His6-Myc was eluted from the resin with BC100 containing 300mM imidazole and 7M urea. The purity and yield were checked in a 12% SDS PAGE followed by CBB staining (Figure 2.4.3B).

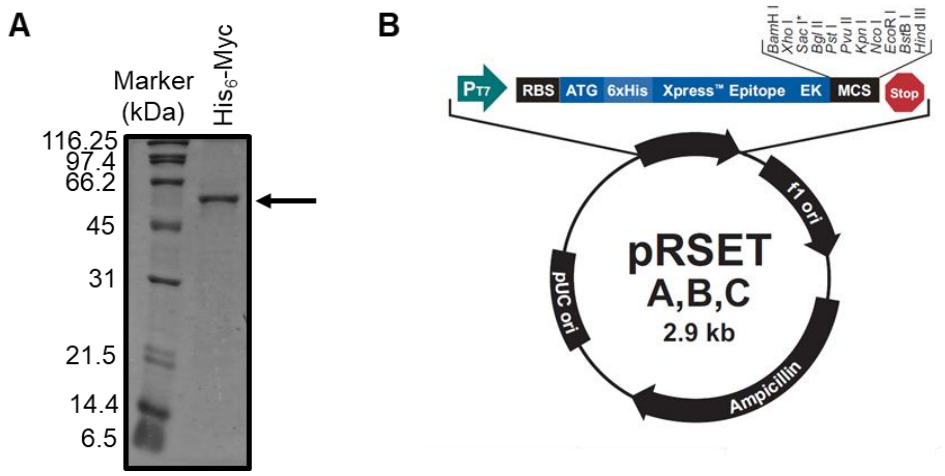

Figure 2.4.3: *Purification profile of full length His_6-Myc* ***(A)*** *expressed and purified from E. coli (Rosetta pLys-S) strain using full length His_6-Myc open reading frame cloned in pRSET vector, whose vector map is outlined* ***(B)***.

2.4.3. Flag-tag fusion protein purification

2.4.3.1. For mass spectrometric analysis

Flag-mPOU, or Flag-Max plasmid constructs, transiently transfected into HeLa cells or Flag-Aurora kinase B (stably integrated pCDH-Aurora kinase B) overexpressing HEK293 cells synchronized at various phases of the cell cycle, were harvested at various time intervals post transfection or treatment, washed once with 1X PBS and lysed by adding 300 µl of lysis solution [50mM tris-HCl pH7.4, 150mM NaCl, 1mM EDTA, 1% NP-40, 0.1% SDS, 0.5% sodium deoxycholate, 1X-Complete protease inhibitor (Merck#4693159001), 1X-PhosStop (Merck #04906837001)] and sonicated for 15 sec, twice in a Bioruptor. The lysis mix was centrifuged at 15000 rpm for 10 mins at 4ºC and the lysate was incubated with 10µl of anti-Flag M2 Magnetic Beads (pre-washed and equilibrated in lysis buffer; Merck #M8823) for 1.5 hrs at 4ºC with uniform mixing. The beads were washed one with the lysis buffer containing the inhibitors (1X-Complete protease inhibitor, and 1X-PhosStop) and thrice with lysis buffer without the inhibitors. Elution of the fusion proteins were carried out twice using 10µl of 500ng/µl of 3X flag peptide and pooled into a microfuge tube. The immunoprecipitated samples were then resolved in a 5-20% SDS-

PAGE and stained with Coomassie brilliant blue (CBB) for visualization and band excision for mass spectrometric analysis.

2.4.3.2. For studying the interactions with other protein partners

To study the association of Flag-Aurora B with either HA-Tip60 or HA-His-Myc in cells, the individual HA fusion constructs were transiently over-expressed into pCDH-Flag Aurora kinase B or pCDH-empty vector overexpressing HEK293 cells for 48 hrs, harvested and washed once with 1X PBS and lysed by adding 1ml of chilled lysis buffer (50 mM Tris-HCl, pH 7.4; 150 mM NaCl; 5 mM EDTA; 1% triton X-100; 1X-Complete protease inhibitor). Cells were incubated at 4ºC for 1hr with constant mixing. Lysate was clarified by centrifuging at 13,000 rpm at 4°C for 10 mins and incubated with 30µl of anti-Flag M2 agarose beads (pre-washed and equilibrated in lysis buffer; Sigma # F2426) for 3hrs at 4ºC with uniform mixing.

The beads were collected by centrifugation for 3mins at 2,000 rpm at 4ºC and the supernatants were removed by aspiration. The pellets were washed once with 1 ml of cold lysis buffer, twice with tris buffered saline (TBS; 50 mM tris-HCl, pH 7.4; 150 mM NaCl) and eluted in 30µl of 500ng/µl of 3X-FLAG peptide (Sigma#F4799) in TBS buffer. The immunoprecipitated samples were then resolved in a 12% SDS-PAGE and immunoblot analysis was done for verifying the pulldown protein and their interacting partners.

2.5. *In vitro* Assays

2.5.1. Kinase assay

Various recombinant proteins (as mentioned in the Results section) were expressed in *E. coli* and incubated with either His_6-tagged Aurora kinase A (40 ng) or Aurora kinase B (40 ng), expressed in Sf21 cells, using suitable baculoviral constructs, in a 30 µl reaction mixture containing 50 mM tris-HCl, 100 mM NaCl, 0.1 mM EGTA, 10 mM $MgCl_2$, 0.2% β-mercaptoethanol and [γP^{32}] ATP (Specific Activity 3.5 Ci/mmol). The reaction mixture was incubated at 30ºC for 15 min. The reaction was inhibited over ice for 5mins, constituent proteins were denatured by the addition of gel loading dye containing SDS, heated at 90ºC for 5mins and resolved using 12% denaturing PAGE, followed by autoradiography using X-ray films.

2.5.2. *In vitro* mass phosphorylation of mPOU

For mass phosphorylation, 1µg each of mPOU WT or S197A mutant was incubated with either AurkA or AurkB (40ng) at 30ºC for 30 min in presence of 2X kinase buffer and 10 mM ATP. This was followed by three replenishments with the same amount of enzyme and ATP at every half hour interval. The final incubation was prolonged for 2hrs after last replenishment. As control, mock phosphorylation reactions were carried out with the same components except without the enzyme under similar conditions. The reaction mix were separated on a 12% SDS PAGE, transferred onto a PVDF membrane and incubated with anti-phospho Ser-197 antibody.

2.5.3. Histone Acetyltransferase (HAT) gel assay

HAT gel assay was performed using lysine acetyltransferases- Tip60, PCAF or p300 and either AurkA or AurkB, as substrates, in a 30µl final reaction volume. Briefly, the reaction mixture was incubated at 30°C for 30 min consisting of 50mM tris-HCl, pH 8.0, 10% (v/v) glycerol, 1mM dithiothreitol (DTT), 1mM phenyl methyl sulfonyl fluoride (PMSF), 0.1mM EDTA, pH 8.0, 10mM sodium butyrate, and 1µl of 3.3 Ci/mmol H^3-acetyl Coenzyme A (acetyl-CoA). To visualize the radiolabelled acetylated protein, the reaction products were resolved by 12% SDS-PAGE; gel was stained by CBB to ascertain the presence of protein and was later dehydrated in DMSO for 1hr. The gel was then incubated in scintillation fluid (22.5% w/v PPO solution in DMSO) for 30mins and then rehydrated in water for 2hrs. The gel was dried using a gel drier and exposed to an X-ray film for 10-12 days. The film was later developed to get intensity profiles for each of the reaction.

For various assays carried out for western blot analysis or mass spectrometry mediated acetylation site identification, 0.04mM non-radioactive acetyl-CoA was used instead of H^3-acetyl Coenzyme A, either for 30mins or 2.5 hrs (mass acetylation; replenishment of enzyme and acCoA every 30 mins, thrice) (Figure 2.5).

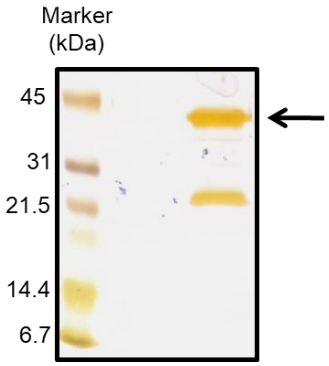

Figure 2.5: *Silver stained gel representation of mass acetylated Aurora kinase B, resolved on a 12% SDS PAGE; arrow indicates the protein band for Aurora B kinase.*

2.6. Generation of polyclonal antisera

2.6.1. Against K85-K87 acetylated peptide of Aurora kinase B in rabbit

Acetylation specific antibody against K85 and K87 di-acetylation sites was generated in rabbit. Briefly, two rabbits, each of New Zealand White strain, were injected (beneath the skin and into the muscles) with 500µg of Aurora kinase B oligopeptide, di-acetylated at K85 and K87 residues **(oligopeptide sequence:** LG**Kac**G**Kac**FGNVYLA**)**, as antigen in the form of an emulsion with Freund's complete adjuvant. 21 days post primary immunization, the rabbits were boosted four more times with 250µg of the oligopeptide, at an interval of 14 days, in the form of an emulsion with equal volume of Freund's incomplete adjuvant. 10 days post fourth booster, the crude antisera against was collected and purified by affinity purification against the antigen. Subsequently the specificity was verified by western blot analysis (Figure 2.6).

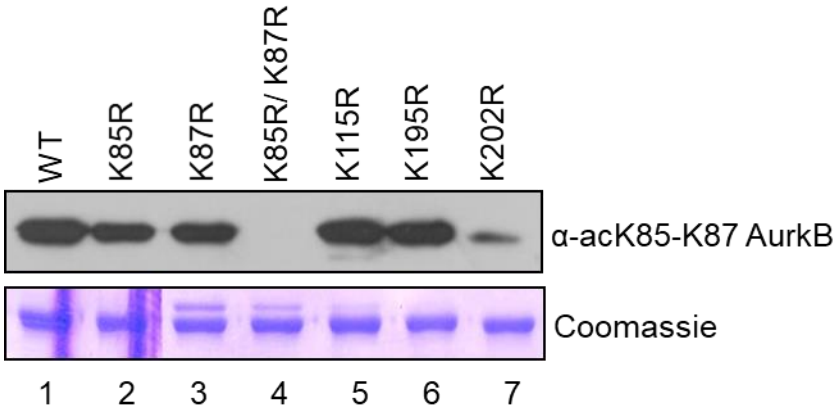

Figure 2.6: Characterization of anti-K85/K87 di-acetylation antibody. *Western blot representation of anti-K85/K87 di-acetylation antibody against Aurora kinase B. 1µg each of WT or various point mutants of Aurora kinase B were subjected to in vitro mass acetylation using Tip60 and 0.04mM acetyl-CoA. The acetylated proteins were resolved on a 12% SDS PAGE and transferred on a PVDF membrane for western blot analysis. Coomassie staining represents the amount of the different Aurora kinase B proteins used for the assay.*

2.6.2. Against phosphorylated oligopeptide of Ser-197 POU6F1 in rabbit

Phosphorylation specific antibody against Ser-197 site of mPOU was generated in rabbit. Briefly, two rabbits, each of New Zealand White strain, were injected (beneath the skin and into the muscles) with 500µg of mPOU oligopeptide, phosphorylated at Ser-197 residue **(oligopeptide sequence:** KLDITPK**Sph**AQKLKPVC**)**, as antigen in the form of an emulsion with Freund's complete adjuvant. 21 days post primary immunization, the rabbits were boosted four more times with 250µg of the oligopeptide, at an interval of 14 days, in the form of an emulsion with equal volume of Freund's incomplete adjuvant. 10 days post fourth booster, the crude antisera against was collected and purified by affinity purification against the antigen. Subsequently the specificity was verified by western blot analysis.

2.7. Mass spectrometry

2.7.1. Preparation of protein samples

2.7.1.1. *In vitro* acetylation of Aurora kinase B by Tip60

His_6-Aurora kinase B purified from *E. coli* (DE3) was subjected to *in vitro* mass acetylation with His_6-Tip60 purified from Sf21 cells using suitable baculoviral constructs. The acetylated protein was resolved on a 12% SDS PAGE, stained with CBB for visualization and processed for the determination of the sites of acetylation by mass spectrometry.

2.7.1.2. Immuno-purification of Flag-Max from HeLa cells

10µg of Flag-Max mammalian expression vector was transfected into $10X10^6$ HeLa cells seeded on a 100mm culture dish. 36hrs post transfection, the cells were harvested, and Flag-Max purified (as mentioned in 2.4.3.1.). The purified protein was resolved on a 5-20% SDS PAGE, stained with CBB for visualization and processed for the determination of the sites of acetylation by mass spectrometry.

2.7.1.3. Immuno-purification of Flag-Max from HeLa cells upon Aurora kinase inhibitor treatment

10µg of Flag-Max mammalian expression vector was transfected into $10X10^6$ HeLa cells seeded on a 100mm culture dish. 12hrs post transfection, the cells were treated with 500nM Aurora A inhibitor (MLN8237), Aurora B inhibitor (AZD1152-HQPA) or DMSO (as a control) and 24 hr post treatment with the inhibitors, the cells were harvested, and Flag-Max proteins purified (as mentioned in 2.4.3.1.). The purified proteins were resolved on a 5-20% SDS PAGE, stained with CBB for visualization and processed for the determination of the sites of acetylation by mass spectrometry.

2.7.1.4. Immuno-purification of Flag-mPOU from HeLa cells

10µg of Flag-mPOU mammalian expression vector was transfected into $10X10^6$ HeLa cells seeded on a 100mm culture dish. 36hrs post transfection, the cells were harvested, and Flag-mPOU purified (as mentioned in 2.4.3.1.). The purified protein was resolved on a 5-20% SDS PAGE, stained with CBB for visualization and processed for the determination of the sites of acetylation by mass spectrometry.

2.7.2. Processing of the purified protein bands for LC-MS/MS analysis

CBB stained protein bands were excised from the reducing PAGE gel using a sharp operating blade and chopped several times into fine pieces to make the gel block sizes of roughly $1mm^3$ in dimension. The resulting gel blocks were pooled into a microfuge tube and destained with 100-300µl of 30% acetonitrile (ACN) solution with proper mixing. The 30% ACN solution was occasionally replaced until CBB was completely removed and the gel pieces gain an amorphous whitish tinge and become transparent. Gradual dehydration was carried out firstly, by the addition of 100-300 µl of 50% acetonitrile (ACN) solution and finally using 100-300µl of 100% acetonitrile (ACN) solution with proper mixing each time for 5mins. The gel pieces were finally rendered completely dry by centrifuging at 13000rpm for 10 mins in a speed-vac connected to a vacuum pump. The dehydrated gel pieces were soaked in 50-100µl of reducing reagent [10mM dithiothreitol (Thermo Scientific #20291) in 25mM ammonium bicarbonate (ABC) solution] and incubated in dark at 56ºC for 30 mins. The reduction solution was then aspirated and replaced by 50-100µl of alkylation solution [55mM iodoacetate (Thermo Scientific #90034) in 25mM ABC solution] and incubated at 25ºC for 45mins with proper mixing, in dark. The gel blocks were then washed with 300-500µl of RNase/DNase-free MilliQ water, twice. Gradual dehydration was carried out with 100-300 µl of 30%, 50% and finally 100% ACN solution, each for 5min interval. The gel blocks dried in a speed-vac and chilled on ice. 10µl of 1ng/µl of chilled trypsin solution (in 50mM ABC) was added dropwise onto the gel blocks and kept on ice for 1hr for the gel pieces to be completely reconstituted with trypsin solution and swell up. 10-20µl of the solution was further added in case of improper reconstitution. Higher concentrations or volume for soaking of the gel blocks with the trypsin solution was, however, avoided. The mixture was incubated at 37ºC for 10-12hrs.

100µl of 75% ACN was added to the gel blocks and sonicated for 15mins and the eluent was transferred to a microfuge tube. 100µl of 75% ACN/ 1% formic acid (FA) mix was added to the

gel blocks and sonicated for 15mins. The eluent was pooled into the previous microfuge tube and the volume of the total mix was reduced by centrifuging in the speed-vac connected to a vacuum pump. Addition of 100µl of 75% ACN/ 1% formic acid mix was repeated once more and the eluents were pooled and the final volume reduced in the speed-vac to approximately 20µl, using 0.1% FA.

The mass spectra for each of the post translational modifications for different proteins are represented below:

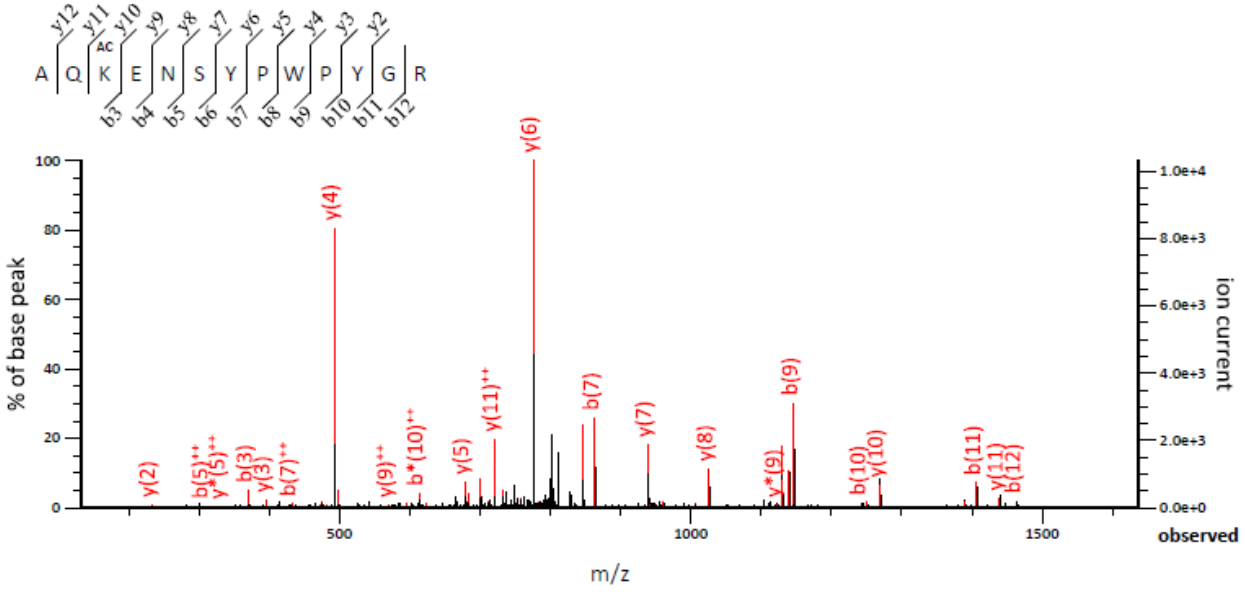

Representative mass spectra for K4 acetylation for Aurora kinase B by Tip60 in vitro.

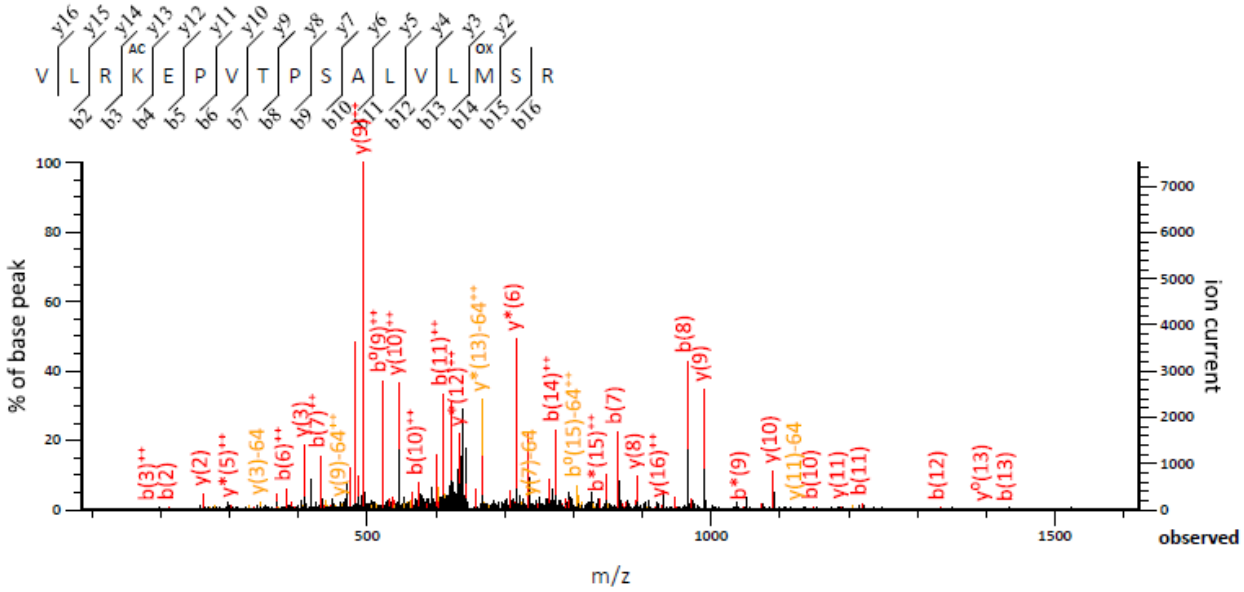

Representative mass spectra for K31 acetylation for Aurora kinase B by Tip60 in vitro.

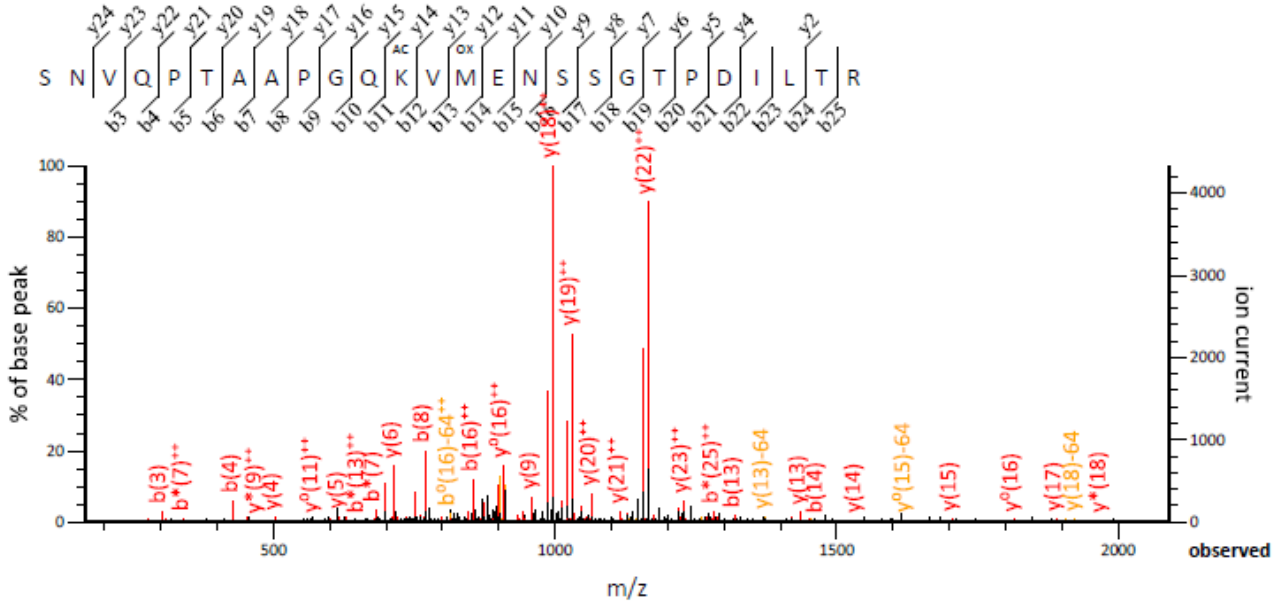

Representative mass spectra for K56 acetylation for Aurora kinase B by Tip60 in vitro.

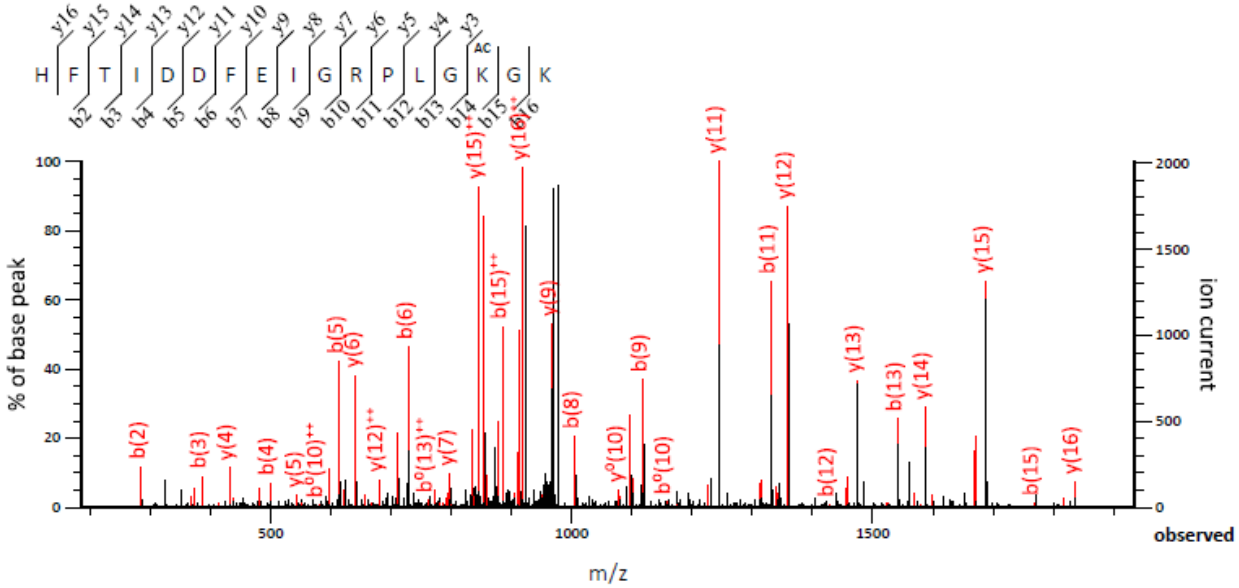

Representative mass spectra for K85 acetylation for Aurora kinase B by Tip60 in vitro.

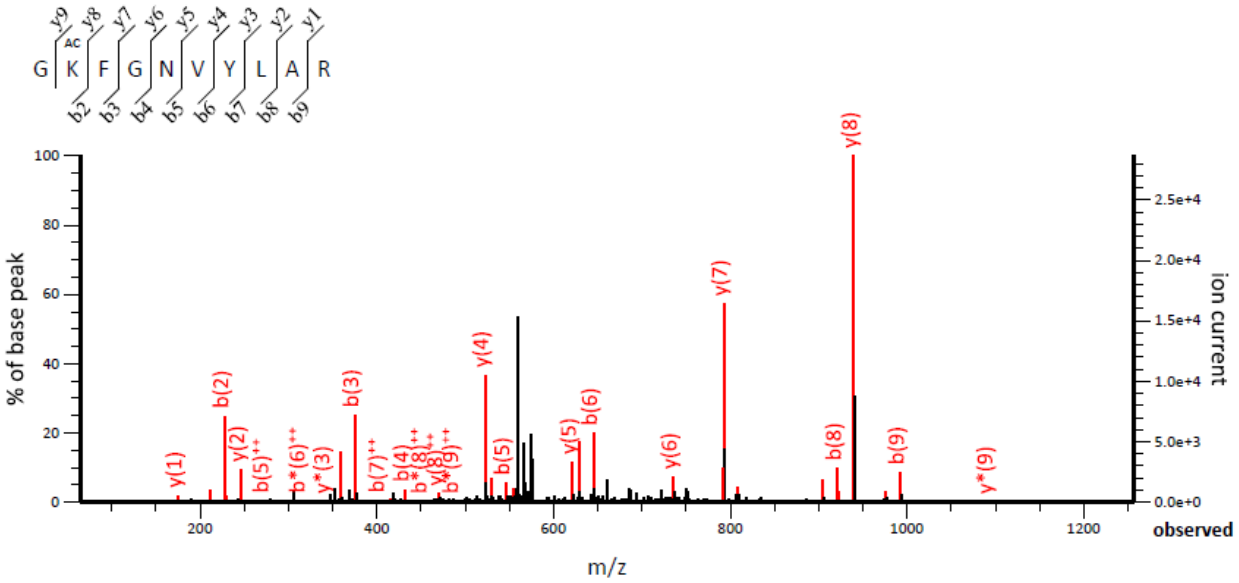

Representative mass spectra for K87 acetylation for Aurora kinase B by Tip60 in vitro.

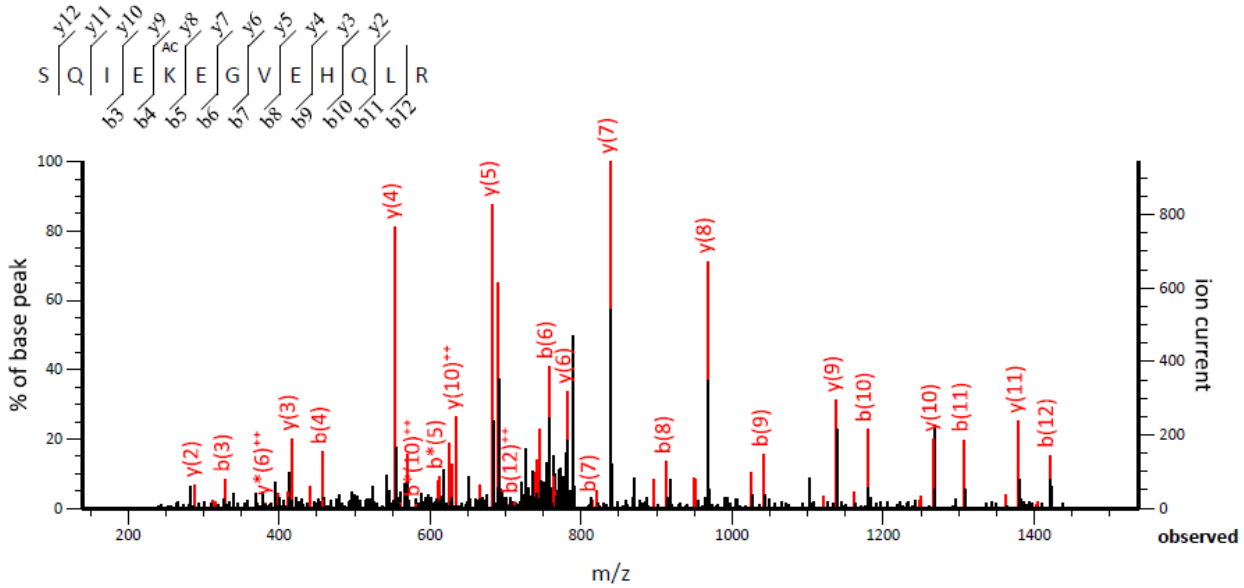

Representative mass spectra for K115 acetylation for Aurora kinase B by Tip60 in vitro.

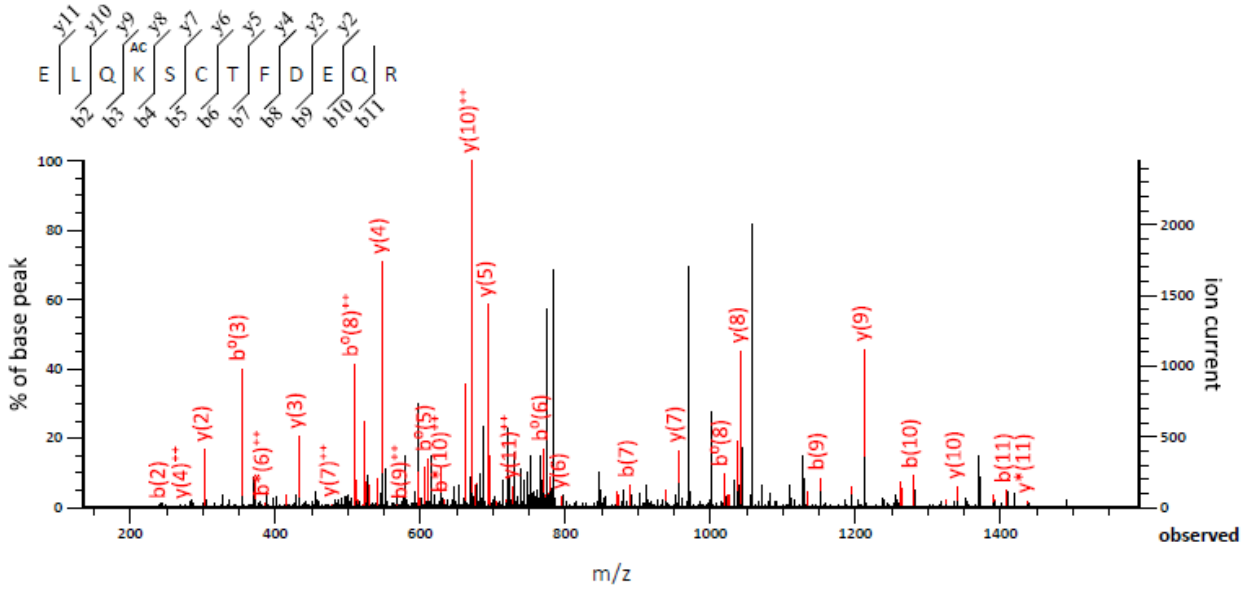

Representative mass spectra for K168 acetylation for Aurora kinase B by Tip60 in vitro.

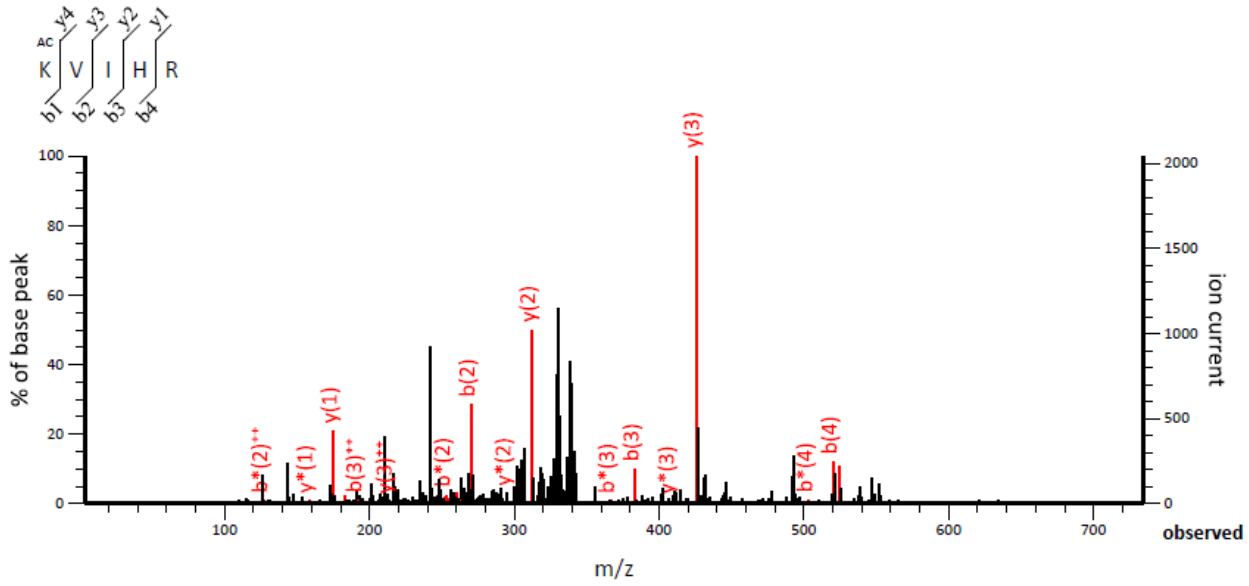

Representative mass spectra for K195 acetylation for Aurora kinase B by Tip60 in vitro.

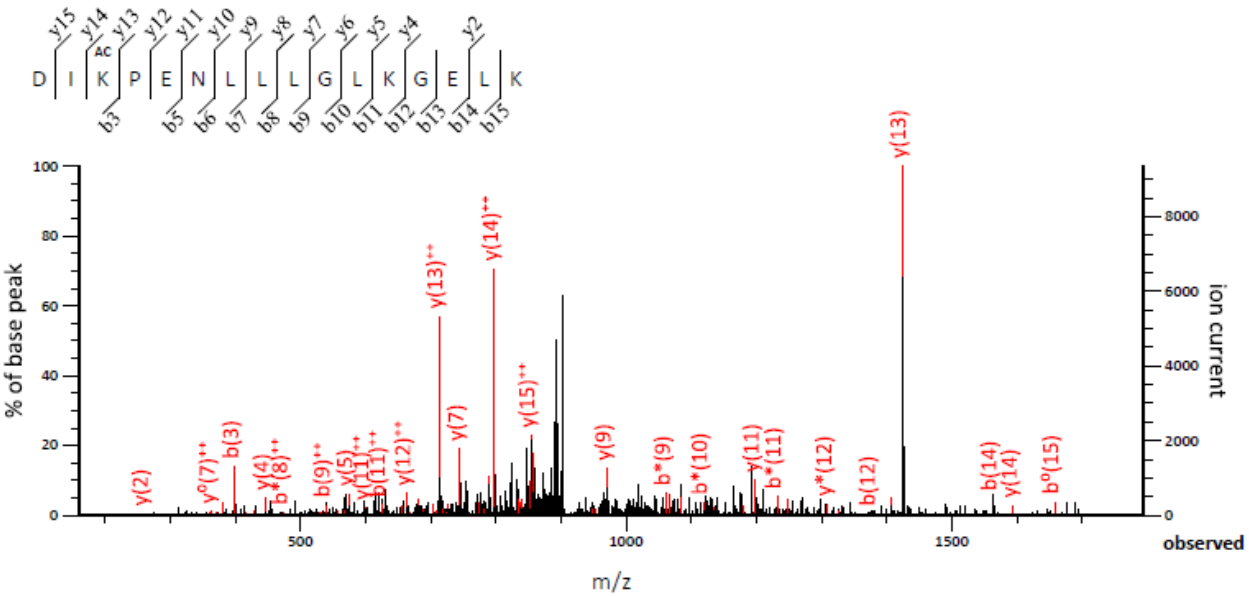

Representative mass spectra for K202 acetylation for Aurora kinase B by Tip60 in vitro.

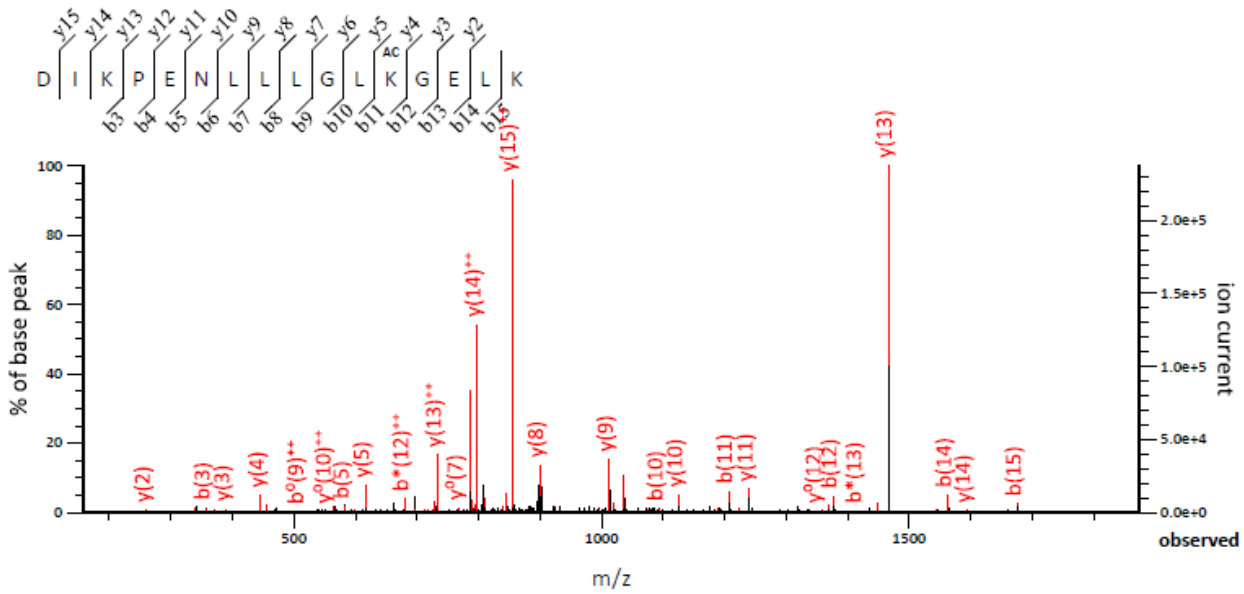

Representative mass spectra for K211 acetylation for Aurora kinase B by Tip60 in vitro.

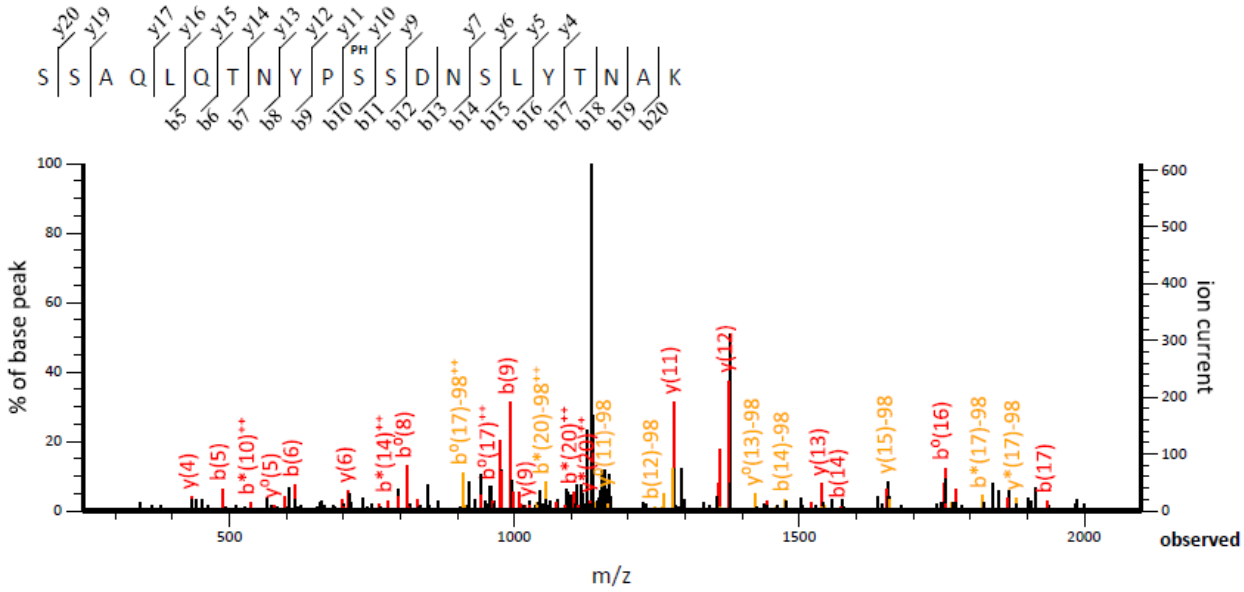

Representative mass spectra for S108 phosphorylation of Max in vivo.

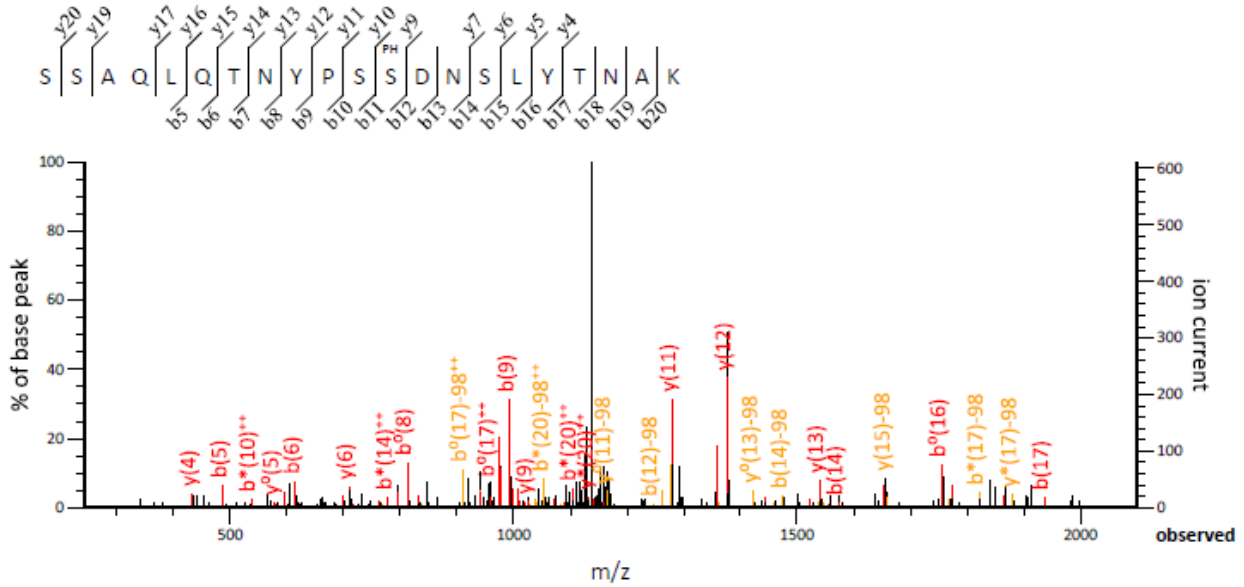

Representative mass spectra for S109 phosphorylation of Max in vivo.

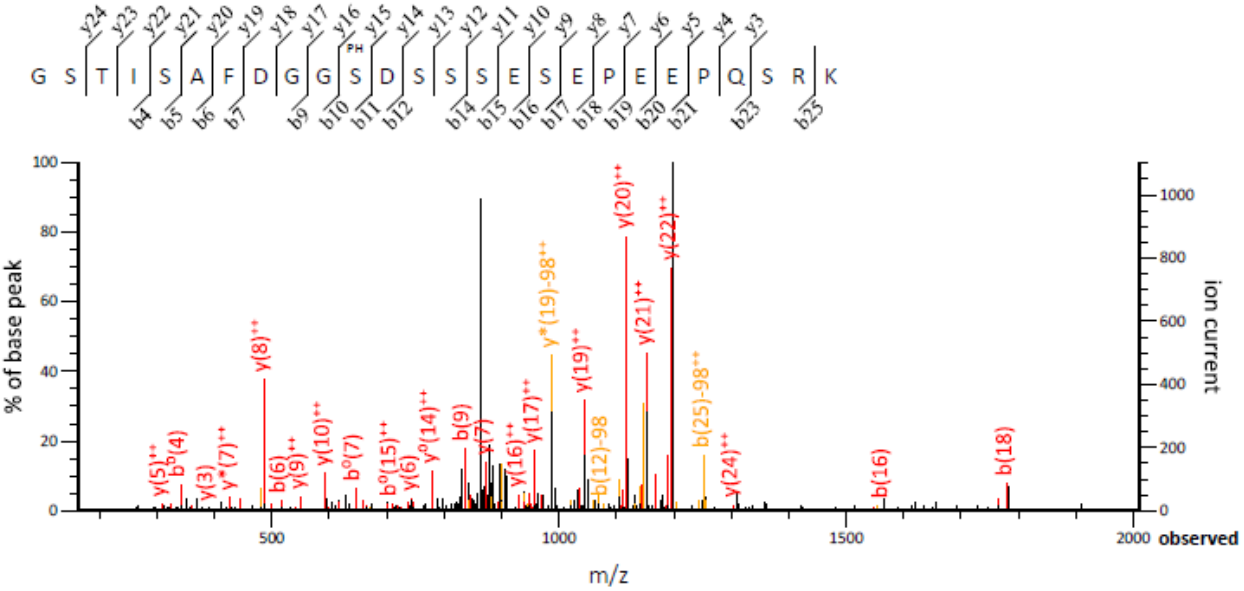

Representative mass spectra for S129 phosphorylation of Max in vivo.

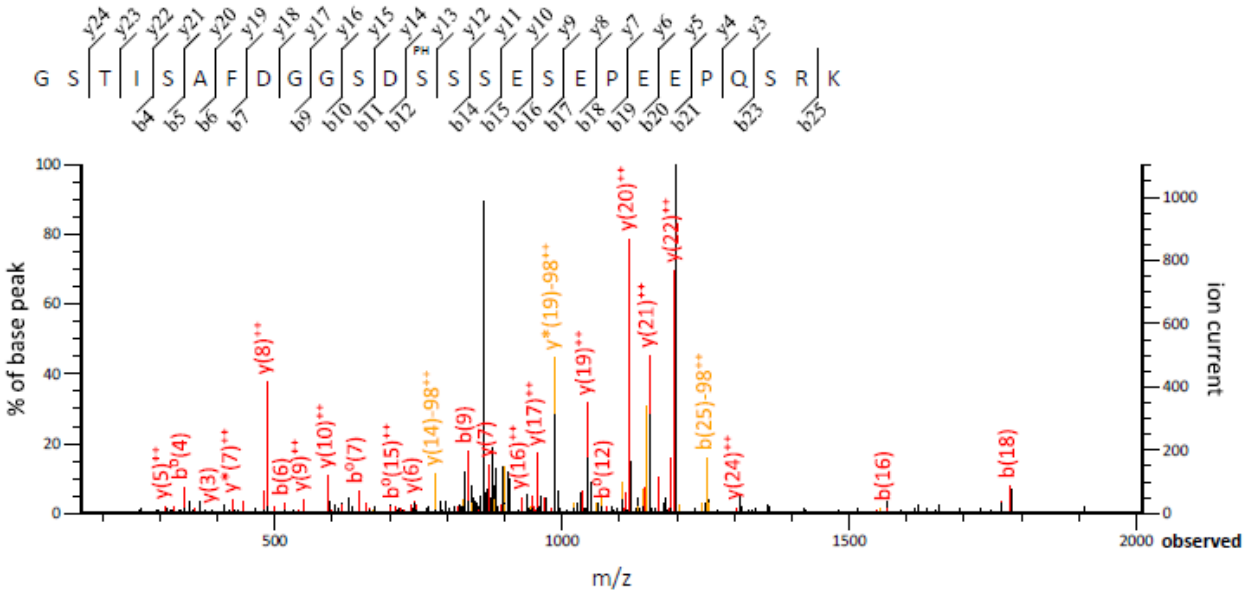

Representative mass spectra for S131 phosphorylation of Max in vivo.

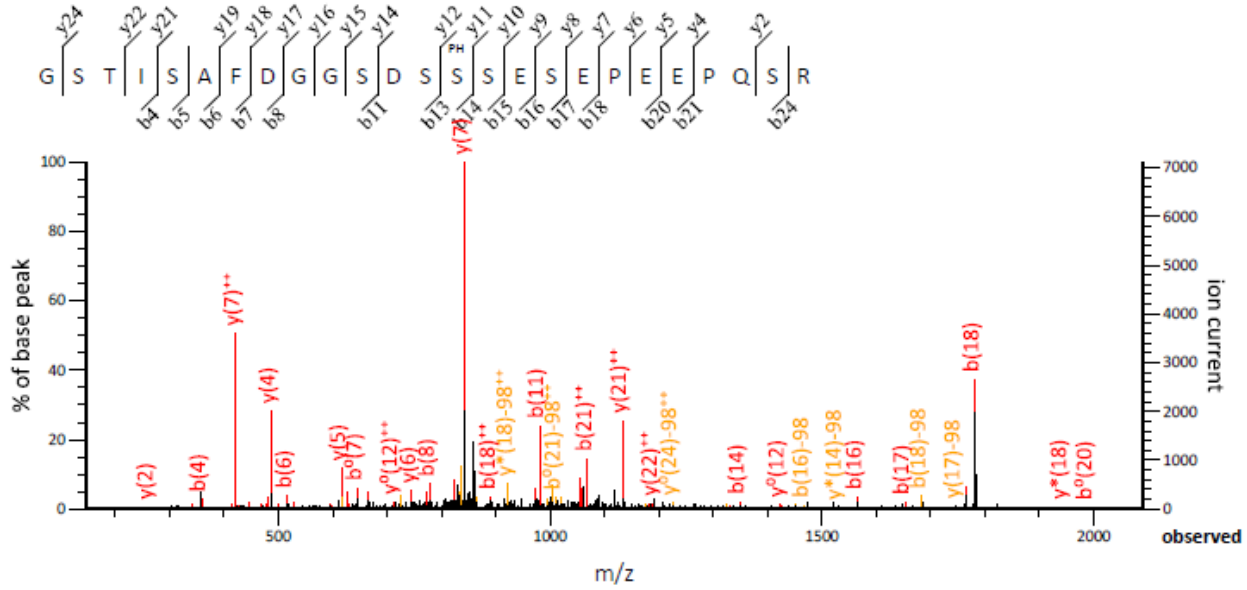

Representative mass spectra for S132 phosphorylation of Max in vivo.

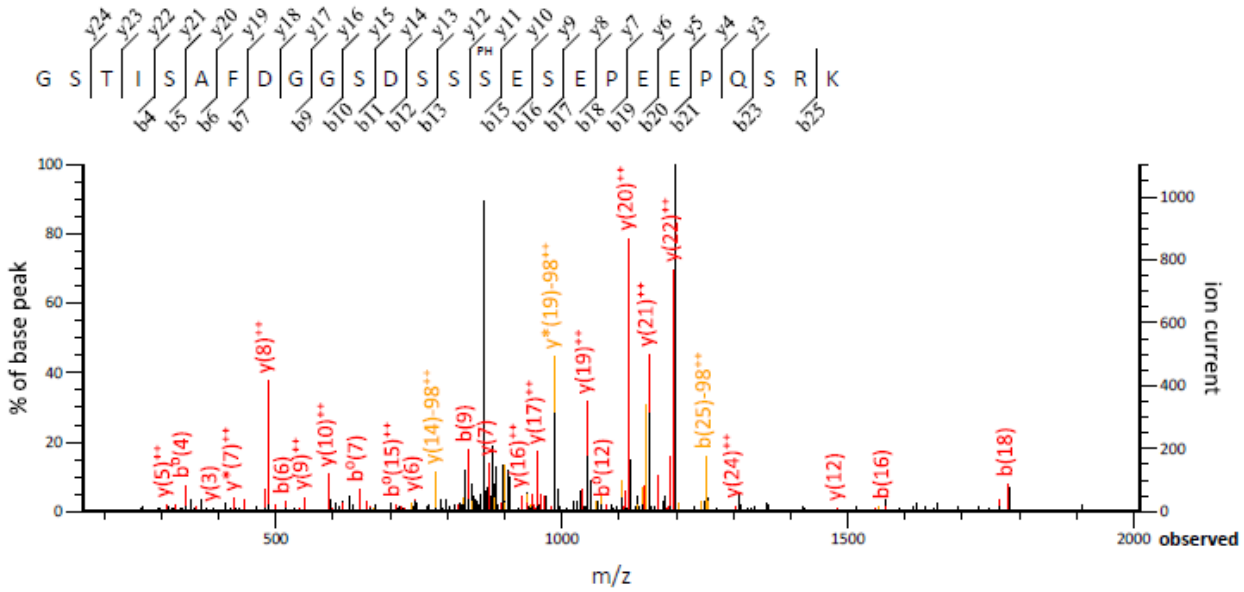

Representative mass spectra for S133 phosphorylation of Max in vivo.

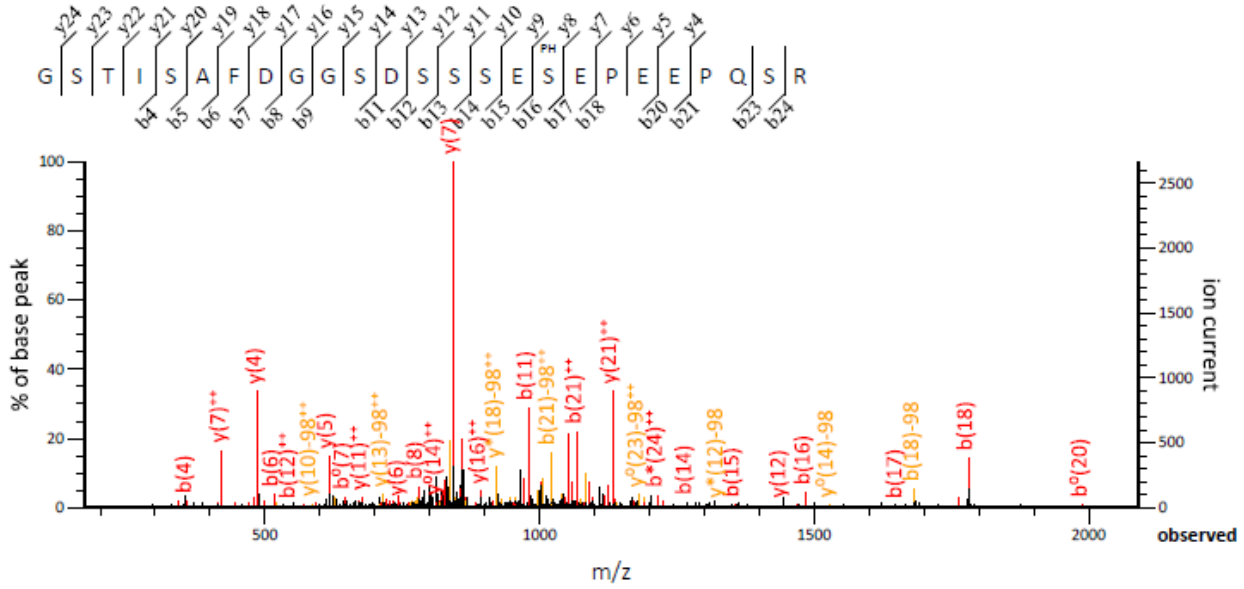

Representative mass spectra for S135 phosphorylation of Max in vivo.

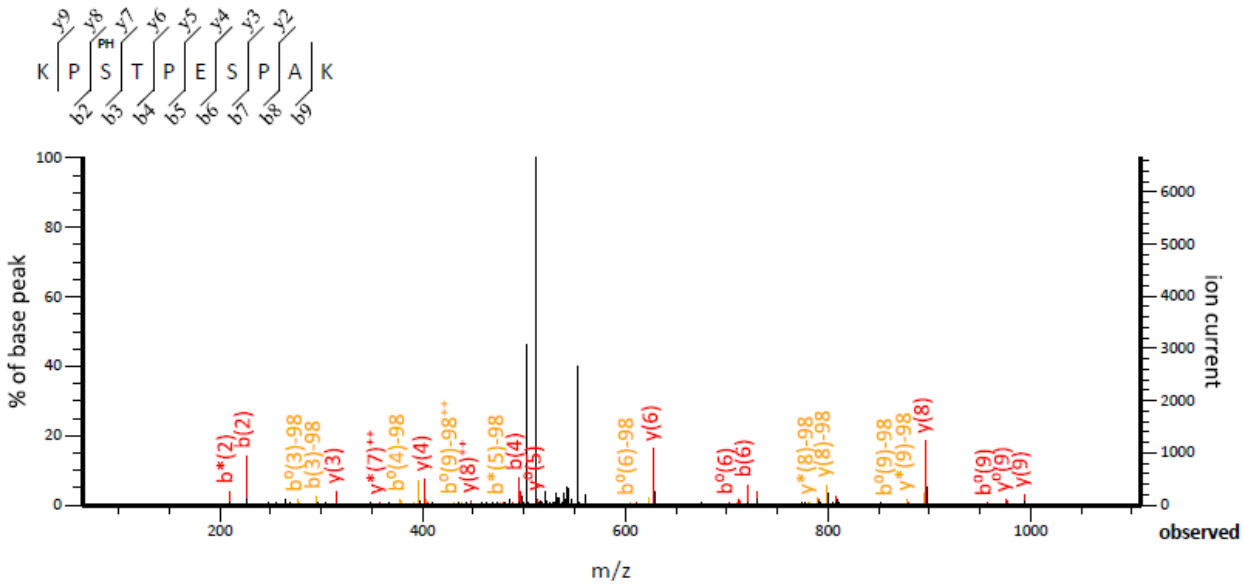

Representative mass spectra for S74 phosphorylation of mPOU in vivo.

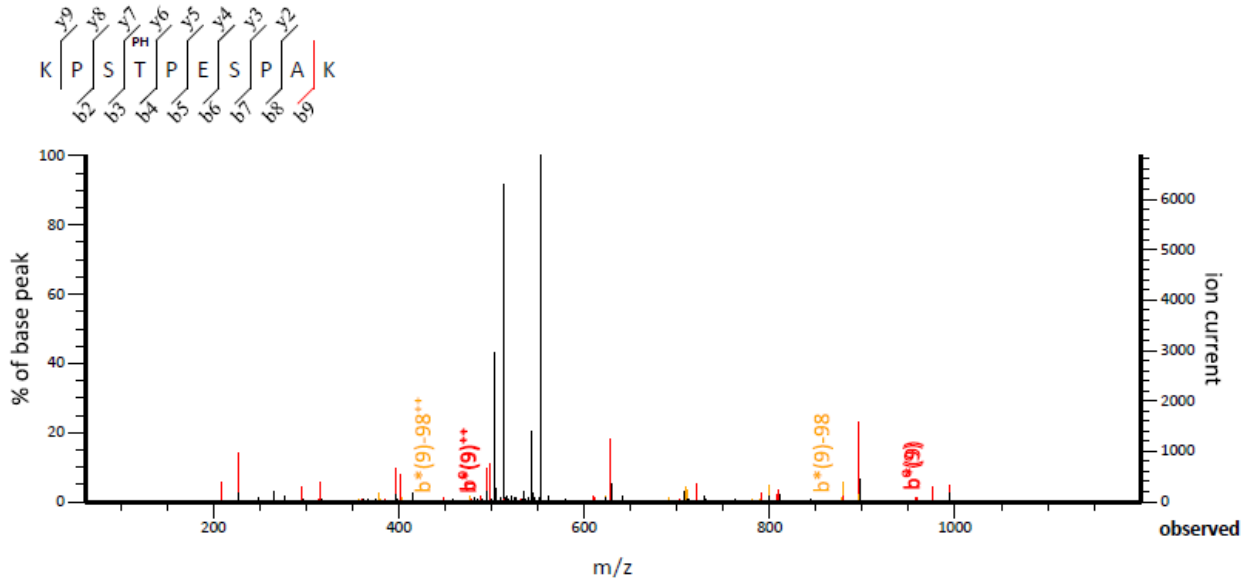

Representative mass spectra for T75 phosphorylation of mPOU in vivo.

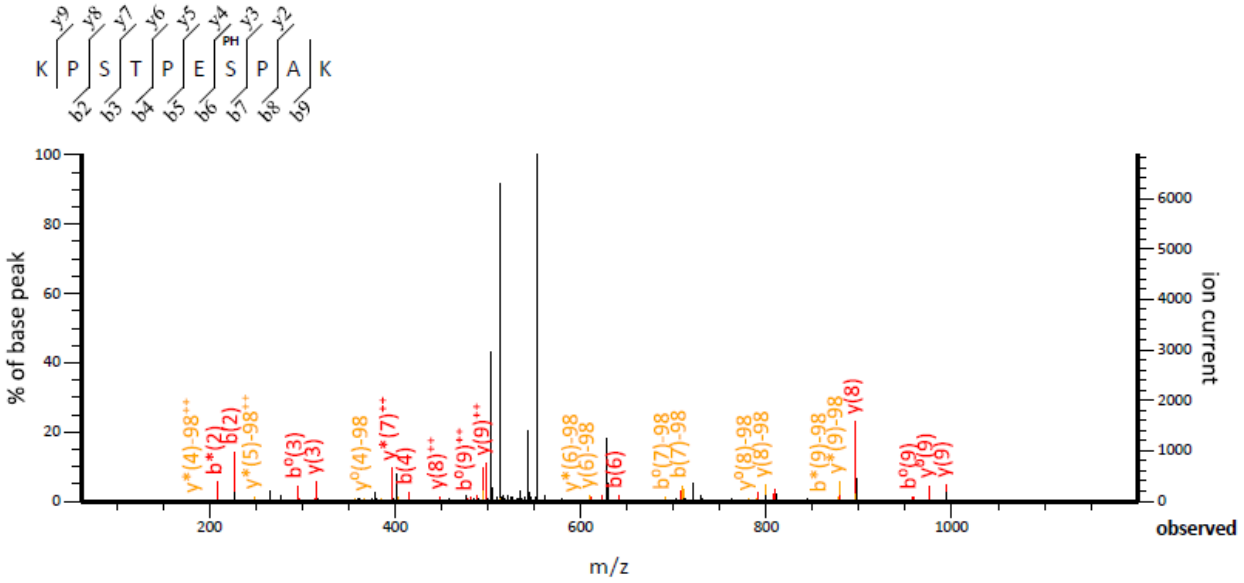

Representative mass spectra for S78 phosphorylation of mPOU in vivo.

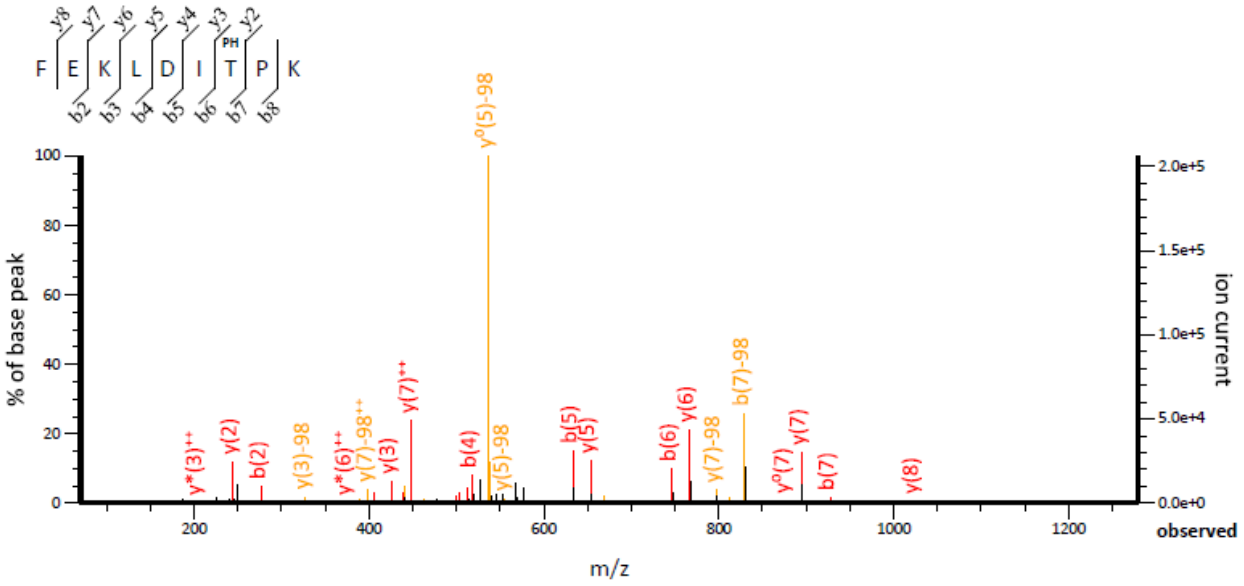

Representative mass spectra for T194 phosphorylation of mPOU in vivo.

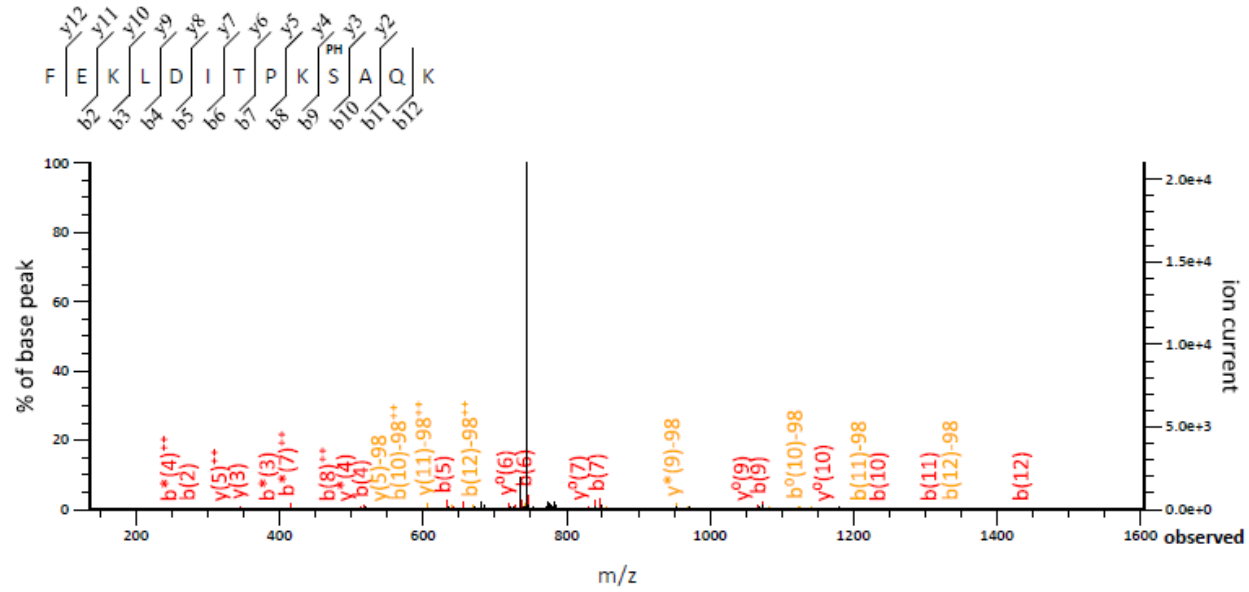

Representative mass spectra for S197 phosphorylation of mPOU in vivo.

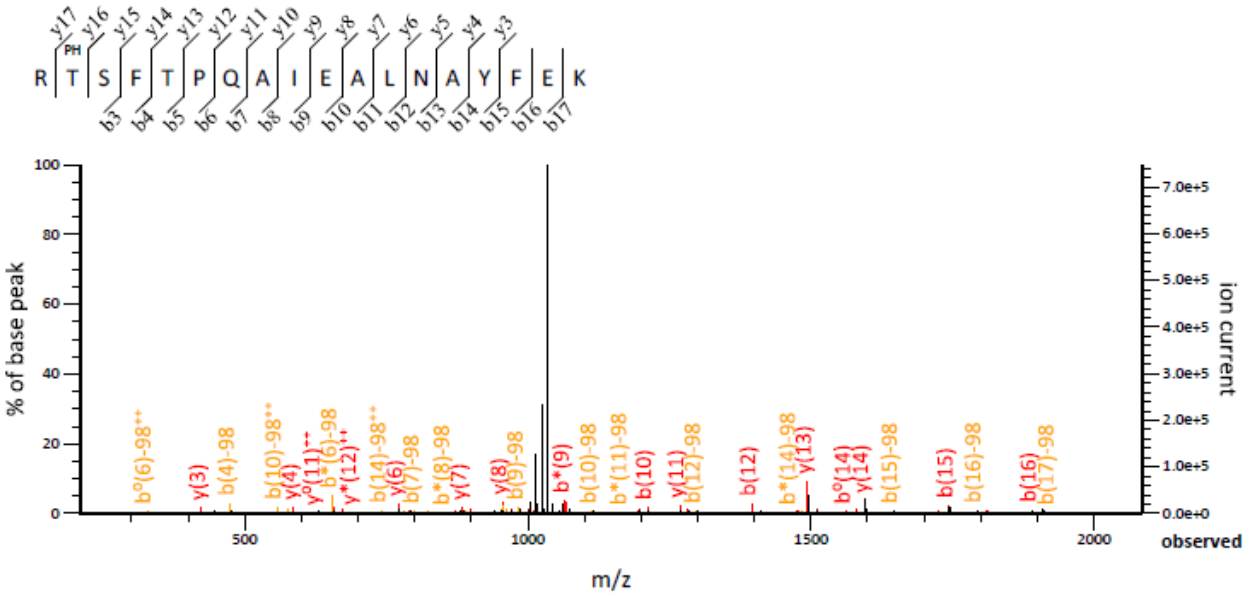

Representative mass spectra for T239 phosphorylation of mPOU in vivo.

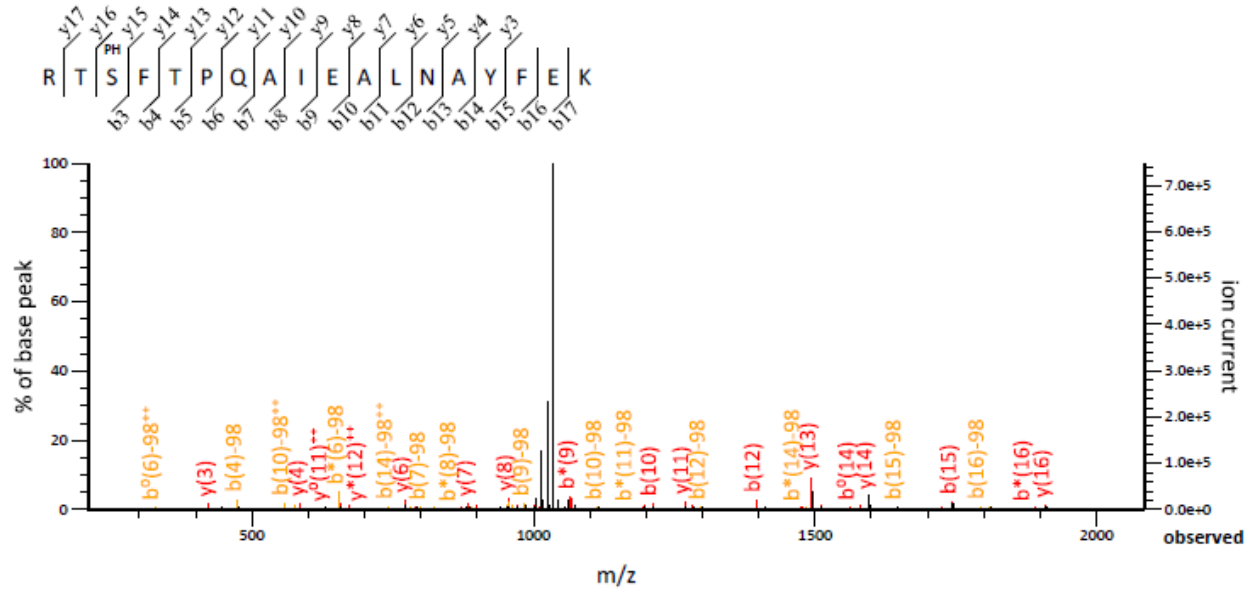

Representative mass spectra for S240 phosphorylation of mPOU in vivo.

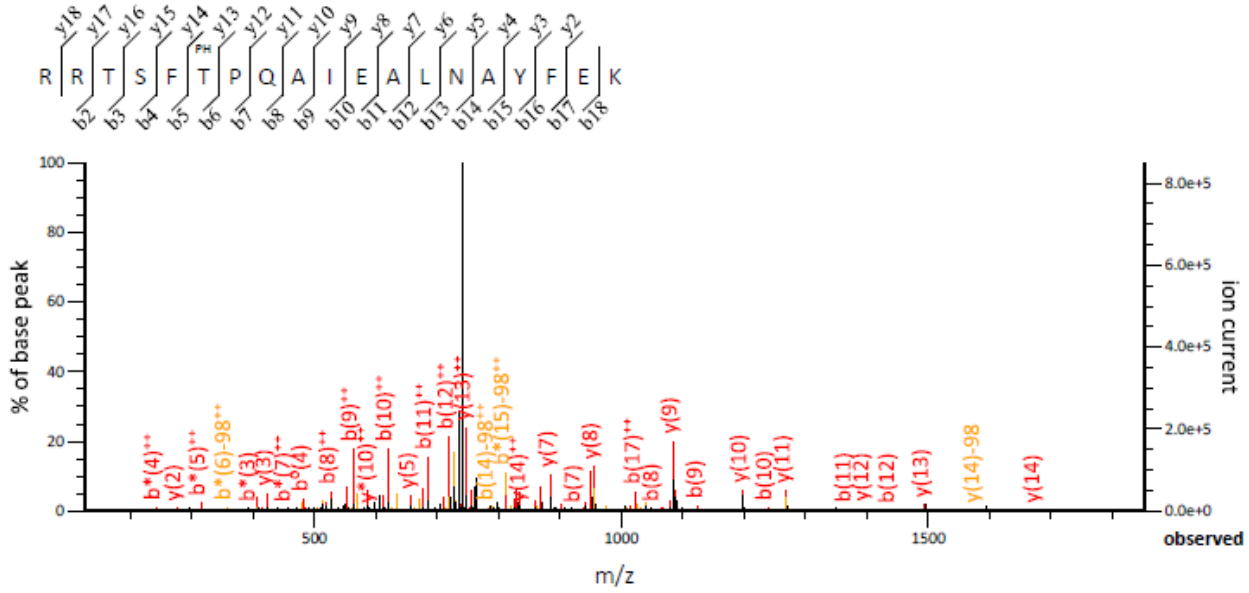

Representative mass spectra for S242 phosphorylation of mPOU in vivo.

2.8. Real time quantitative RT-PCR

Control or variously treated cells were harvested and lysed using TRIzol™ (Invitrogen™ Reagent #15596018) and total RNA isolated by phenol: chloroform extraction followed by precipitation using isopropanol. The extracted RNA was reconstituted in diethyl pyrocarbonate (DEPC) treated water, resolved on a 1.2% agarose gel to check for the integrity of the RNA (Figure 2.8), and subsequently used as template for complimentary DNA (cDNA) synthesis.

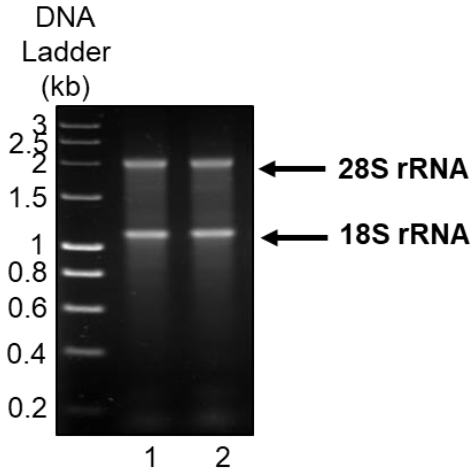

Figure 2.8: *Lanes 1 and 2 represent the profile of 1µg of total RNA extracted from cells, loaded in duplicate (technical duplicates), resolved on a 1.2% agarose gel and visualized by EtBr staining.*

The cDNA strand was prepared using oligo-dT_{23} (Sigma #O4387), M-MLV Reverse Transcriptase (Sigma #M1302) and RNaseOUT™ Recombinant Ribonuclease Inhibitor (Invitrogen™ Reagent #10777019) as per manufacturer's recommendations. This cDNA was used for real time PCR (RT-PCR) analysis using SYBR-Premix Ex Taq™ II (Tli RNaseH Plus) (Takara # RR820A) with 10pmol of specific primers (mentioned below) and different dilutions of the respective cDNAs. RT-PCR reactions were carried out in Step One Plus™ Real-Time PCR (Applied Biosystems) machine and amplification protocols were followed as indicated in the manufacturer's protocol. PCR conditions were standardized for each set of primers used. Fold expression change was calculated using ΔΔCt method using actin gene primers as internal control. Specificity and sensitivity of the primers was ascertained by melt curve analysis.

Serial No.	Gene Name	Forward Primer	Reverse Primer
1	ODC1	CTGAGGTGGTTAAAAGCTCTCCC	TCTGCACCAACTGTATTTCAGTC
2	GATA3	CAATGCCTGTGGGCTCTACT	TAAACGAGCTGTTCTTGGGG
3	β-Actin	AGATGTGGATCAGCAAGCAGGAGT	TCCTCGGCCACATTGTGAACTTTG
4	AURKB	AGAAGGAGAACTCCTACCCCT	AGTGCCGCGTTAAGATGTC
5	h-TERT	TGTCAAGGTGGATGTGACGG	GAGGAGCTCTGCTCGATGAC
6	NOP56	TCCACTCCACCTTCATTGGC	CCTCTGCCTGAACCATTGCT
7	YWHAZ	AGGAGCCCGTAGGTCATCTT	TGTGACTGATCGACAATCCCTTT
8	GATA6	GCCAACTGTCACACCACAAC	TTGCTATTACCAGAGCAAGTCT
9	RARB	TGGAGTTGGGTGGACTTTTCT	AAAAGCCCTTACATCCCTCACA
10	MAX	ATAATGCACTGGAACGAAAACG	TGGCTTTGTCTAGGATTTGGG
11	c-MYC	GTGCTCCATGAGGAGACAC	CCTCTTTTCCACAGAAACAACATC

12	HPRT1	TGCAGACTTTGCTTTCCTTG GTCAGG	CCAACACTTCGTGGGGTCCT TTTCA

Table 2: *Sequences for different qRT-PCR primers used for the genes mentioned.*

2.9. Electrophoretic mobility shift assay

2.9.1. End-labelling of oligonucleotide

40pmol of single stranded oligonucleotide was labelled at the free 5'-OH group with 20 units of T4 polynucleotide kinase (NEB # M0201) in a 50 µl reaction volume containing 1X polynucleotide kinase buffer and 30µCi γ^{32}P ATP at 37˚C for 30min. At the end of the reaction 150µl of water was added and then subjected to phenol: chloroform extraction. The extracted aqueous layer containing the labelled oligonucleotide was precipitated along with 10µg of tRNA by using ethanol and sodium acetate and then dried and dissolved in annealing buffer containing 10mM tris-HCl, and 20mM NaCl at pH 8. The sequence of the Brn5 promoter oligo nucleotides used for the assay are as follows:

5'-GATCTGCTCCTGCATGCCTAATAGG-3'

3'-CTAGACGAGGACGTACGGATTATCC-5'

2.9.2. Visualization of DNA-protein complexes

The end-labelled paired oligo was used as a probe to visualize the formation of DNA-Protein complex with the protein under investigation. To create the double stranded probe, the radiolabelled single strand was first purified by phenol: chloroform extraction and then allowed to anneal with the complementary unlabelled oligonucleotide in annealing buffer containing 10mM tris-HCl and 20mM NaCl at pH-8, by allowing the renaturation between the complementary strands to occur by first heating the mix to 95-100ºC and then allowing the temperature to gradually drop to room temperature over a long duration. The double stranded oligo is then purified by 4.5% of native-PAGE (using 4.5% Acrylamide, 0.5X TBE (0.045 M tris borate and 0.001 M EDTA), 0.1% APS and 8% TEMED) and extracted in 1X tris-EDTA (TE) buffer (10mM Tris-HCl, pH 8

and 1mM EDTA) at 37ºC. This was further purified by gel filtration using C40 packed syringe column. The probe was finally eluted in TE buffer and diluted to 5000cpm/µl and allowed to form complex with the DNA binding protein of interest in appropriate binding buffer for 20-30 min at recommended temperature (25-30ºC). The resultant complex was resolved on a native-PAGE as mentioned earlier and then subjected to autoradiography to visualize the complex and its mobility shift.

2.10. Sister chromatid recombination (SCR)/ Homologous recombination (HR) assay

SCR18-U2OS cells (Puget N et al., 2005), which are chromosomally modified to express GFP upon I-SceI endonuclease expression (Figure 2.10), were transfected with either Flag-AurkB mammalian expression construct or FANCJ shRNA plasmid or control pcDNA3β vector. 24hrs post transfection, $2X10^6$ cells were further transfected with 24µg of I-SceI expression plasmid. After 24hrs, GFP^+ cells were scored by FACS analysis using BD biosciences Verse flow cytometer. In each experiment, the percentage of GFP^+ cells (either I-SceI induced or uninduced) was measured, and I-SceI-transfected values were corrected for transfection efficiency. The spontaneous GFP^+ frequency was subtracted from this value to obtain the I-SceI-induced GFP^+ frequency. The total GFP^+ population provides a quantitative measurement of the overall SCR/HR in the assay system.

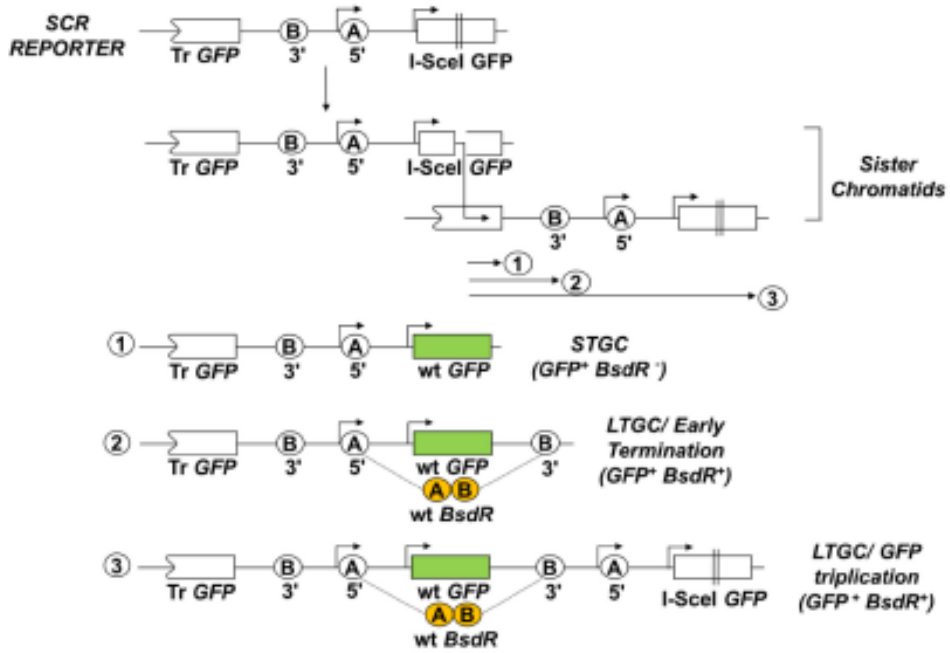

Figure 2.10: Reporter substrate for the SCR assay *[Adapted from Nath S et al., 2017].*

2.11. Non-homologous end joining assay

Alteration of NHEJ upon Aurora kinase B overexpression was studied by using an extra-chromosomal reporter assay system that permits the generation of defined DSBs and determination of accurate determination of the choice of NHEJ pathway for repair (classical or alternate- NHEJ). The reporter, pEGFP-Pem1-Ad2, consists of an engineered GFP gene which is interrupted by a 2.4 kb intron derived from the rat Pem1 gene (Figure 2.11A). An adenovirus (Ad2) exon has been introduced into the middle of this intron and it is flanked on both sides by HindIII and I-SceI restriction enzyme recognition sequences.

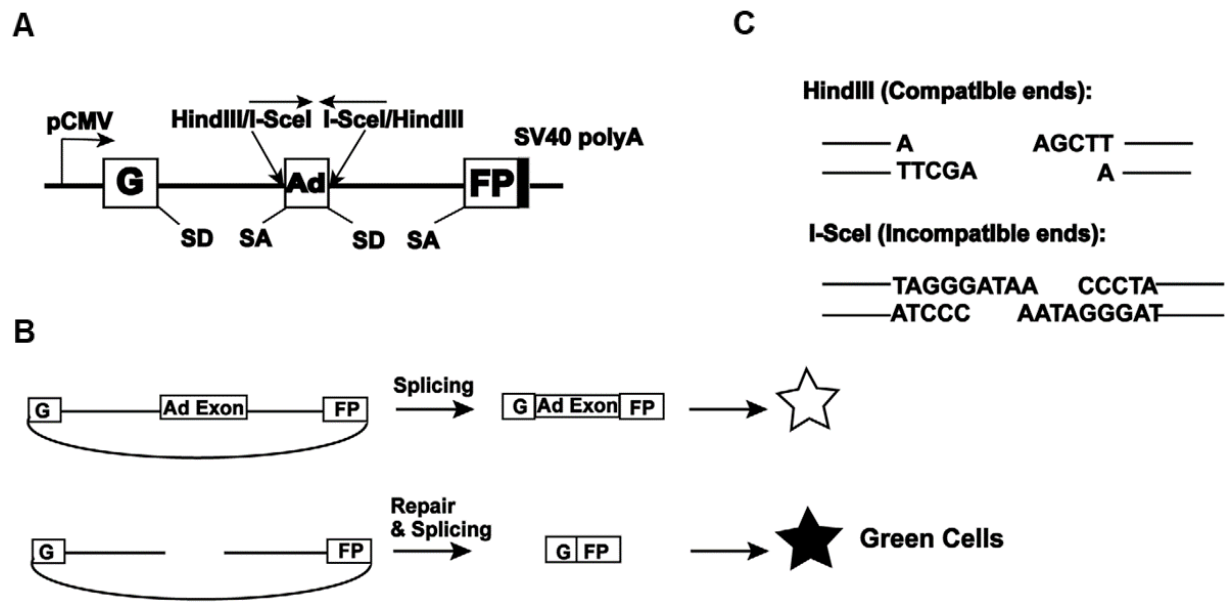

Figure 2.11: Structure of the NHEJ reporter construct. *[Adapted from Fattah F et al., 2010].*

GFP expression is hindered from the unmodified plasmid due to the interference from the Ad2 exon (Figure 2.11B). Digestion of the plasmid either with HindIII or I-SceI generates a linear plasmid lacking the adenoviral exon with either compatible 5'-overhanging cohesive ends or incompatible ends, respectively (Figure 2.11C). The HindIII sites are arranged in such a manner that cohesive 4-bp overlapping ends are generated. I-SceI sites, on the other hand, are arranged in an inverted orientation which necessitates the requirement of pre-processing before the ends can be rejoined. Undigested or partially digested plasmids generate a product that is unable to express GFP due to the retention of the Ad2 exon.

7µg of pEGFP-Pem1-Ad2 was linearized with either HindIII or I-SceI and transfected into $10X10^6$ U2OS cells. As a transfection control, cells are always co-transfected with a pCherry expression plasmid. Analysis of cherry-GFP double positive population was carried out 48hrs post transfection using BD biosciences Verse flow cytometer.

2.12. Subtype classification of breast cancer patient samples

RSEM RNA-seq data was obtained from TCGA Breast cancer invasive carcinoma dataset (Figure 2.12). Intrinsic gene centroids signature (PAM50) (Parker JS et al., 2009) was used to classify each of the available patient sample RNA sequencing data into five established intrinsic breast cancer molecular subtypes (normal-like, basal, luminal A, luminal B, and Her2 amplification) using "genefu" package (Gendoo DMA et al., 2015) with log2(TPM + 1) data matrix. The expression levels of Aurora kinase A and Aurora kinase B were then plotted as box-whisker plots.

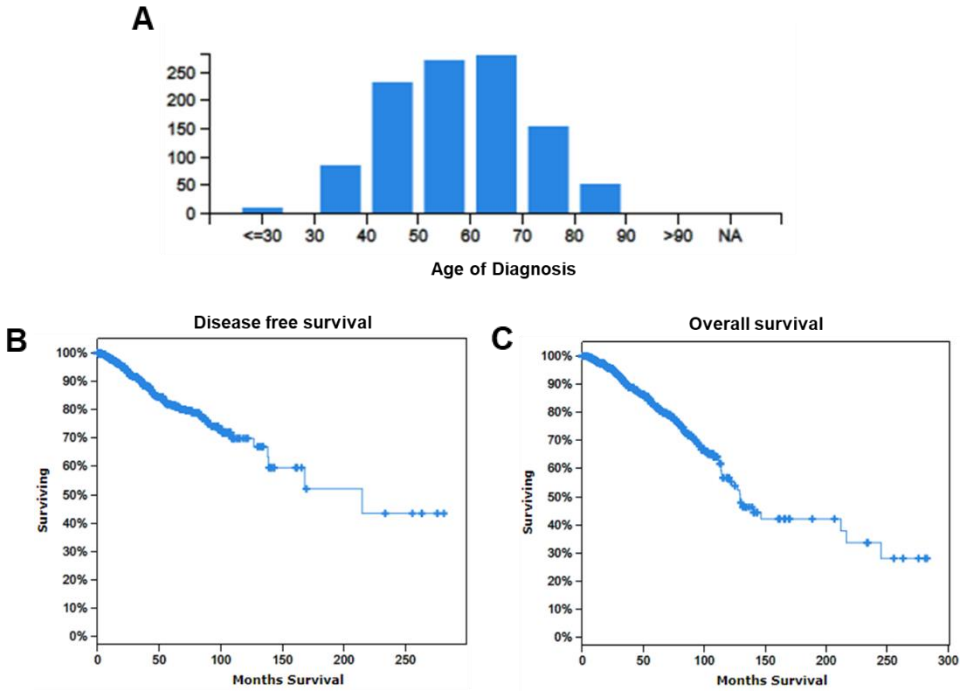

Figure 2.12: *General information about the TCGA breast cancer invasive carcinoma dataset has been depicted for the distribution of age of diagnosis of the patients* ***(A),*** *disease free survival* ***(B)*** *and overall survival* ***(C).***

CHAPTER 3: RESULTS

Chapter outline

3.1. Implication of Aurora kinase mediated phosphorylation of Myc associated factor-X on c-Myc/Max (in)dependent gene expression in breast cancer

3.2. Acetylation dependent regulation of AurkB and a probable role of the dysregulated kinase in dictating the outcome of DNA damage repair pathway choice

3.3. Reciprocal regulation of skeletal muscle differentiation by AurkA and POU6F1

3.1. Implication of Aurora kinase mediated phosphorylation of Myc associated factor-X on c-Myc/Max (in)dependent gene expression in breast cancer

General Introduction

v-Myc (viral form of cellular Myc) was initially discovered from the MC29 strain of avian tumour virus which expressed a *v-gag-myc* fusion gene, which either caused solid tumours of promyelocytic character or transformed myeloid cells to cause diffuse growths (myelocytoma). It was this unique pathology that conferred MYC its name (*my*elo*c*ytomatosis) (X. Ivanov et al., 1964; Z. Mladenov et al., 1967). The cellular form of the *myc* gene (*c-myc*) was discovered much later (B. Vennstrom et al., 1982) and together with *src*, fostered the theory of cellular basis of viral oncogenes and revolutionised cancer biology ever since.

Myc is a well-established oncogene and derives its formidable oncogenic stature through its influence on a wide range of biological functions, which places it at the juncture of cell growth and proliferation, metabolism, and genome stability (Figure 3.1). Unsurprisingly, dysregulation of the MYC network (also known as the MAX-MLX network) is responsible for causing major cancer associated deaths worldwide for both solid and haematological malignancies.

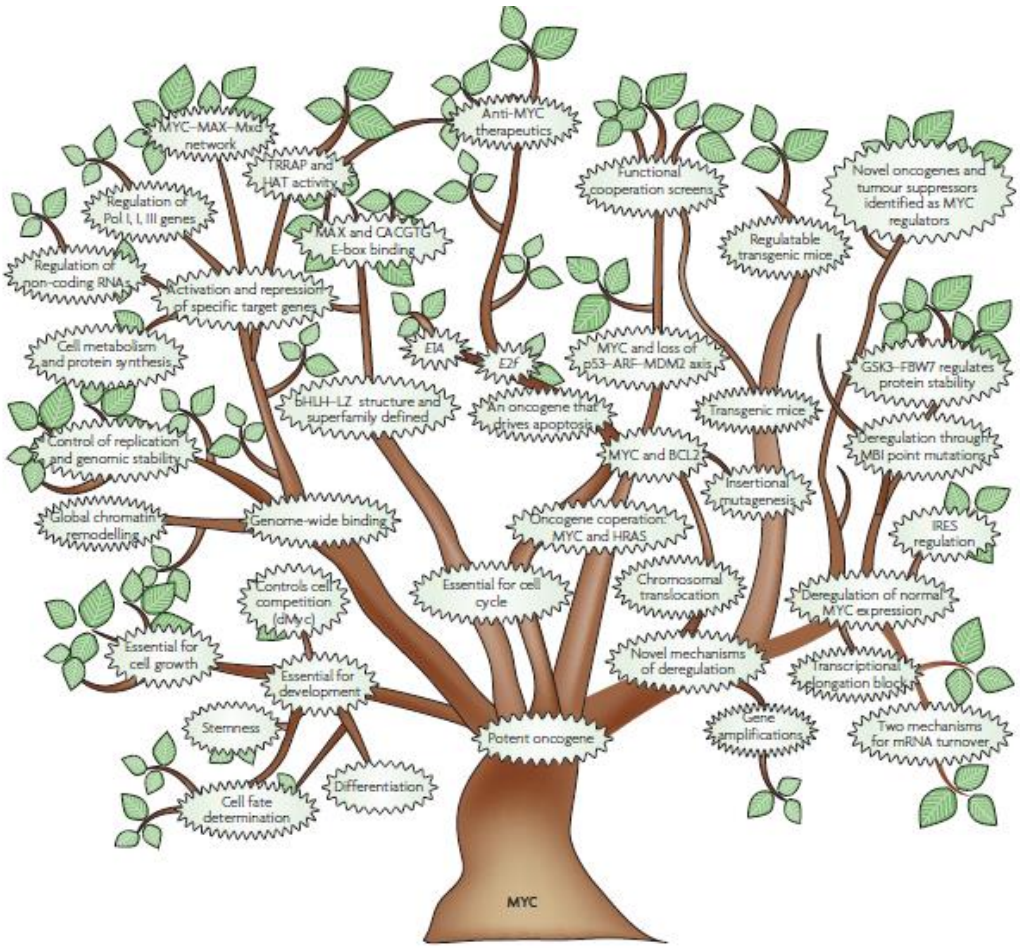

Figure 3.1: *Pictorial depiction representing various molecular, cellular and pathological activities associated with Myc [Adapted from (Meyer N et al., 2008)].*

Mammals express three different Myc proteins, namely c-Myc (cellular), N-Myc (neuronal) and L-Myc (lung) which arises from three different genes and differ both in potency of transformation and expression pattern in tissues. Each of these proteins contain four distinct domains called the Myc-boxes which are associated with functions like transactivation and apoptosis. They also contain a basic helix-loop helix leucine zipper (bHLH-LZ) domain which aids in its DNA binding and dimerization (Figure 3.2).

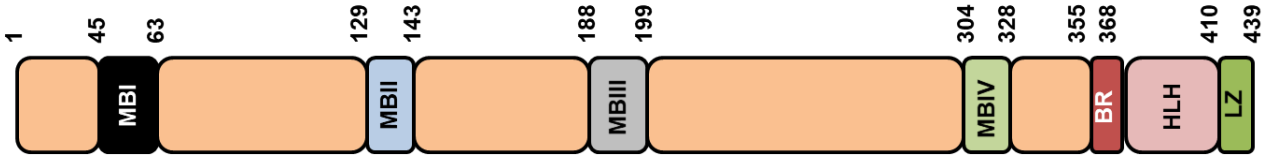

Figure 3.2: *Schematic representation of different c-Myc domains and the corresponding amino acid numbers (MB, MYC Box; BR, Basic region; HLH, Helix-loop-helix; LZ- Leucine Zipper).*

Although the domains are sufficient for transactivation, Myc lacks a prominent DNA binding by itself under physiological conditions and requires another protein, Myc Associated factor-X (Max) (Blackwood, E.M. et al., 1991). Max, therefore, is essential for Myc dependent gene transcription and the c-Myc/Max heterodimeric complex is believed to regulate the transcription of around 15-22% of the protein coding genes and can, therefore, be called a general transcription regulator (Li Z. et al., 2003; Perna D et al., 2012).

Like Myc, Max also belongs to the bHLH-LZ family (Figure 3.3). It performs a non-redundant function in development as Max knockout causes early embryonic lethality in mouse and cannot be compensated by other bHLH-LZ family proteins (Shen-Li H et al., 2000). Max, however, displays a biphasic nature of regulation depending on the cellular concentration of c-Myc (Prendergast GC et al., 1992).

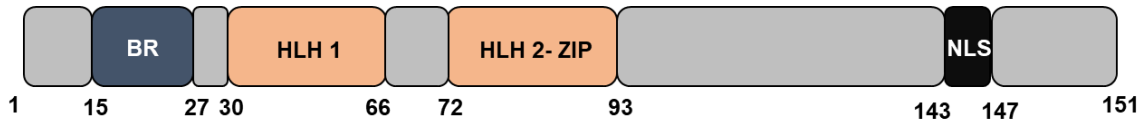

Figure 3.3: *Schematic representation of different Max domains and the corresponding amino acid numbers (BR, Basic region; HLH, Helix-loop-helix; ZIP, Leucine Zipper).*

Aurora A and B kinases (AurkA and AurkB) are critical oncogenes and like c-Myc, are reported to be dysregulated in both solid and haematological cancers. *In silico* screening in our laboratory led to the identification of Max as a substrate of Aurora kinase A (Karthigeyan D, and Kundu TK; unpublished). The following section elaborates the various biochemical, microscopic and mass

spectrometric approach that were undertaken to address a possible connection of Aurk dependent Max phosphorylation in determining the transcriptional outcome of c-Myc/Max dependent target genes in cells. We firmly believe that these findings are intriguing and will create substantial interest in the field of Myc and Aurk biology to delve deeper in the quest to contain Myc dependent cancers.

3.1.1. Aurora A and B kinases phosphorylate Max *in vitro*

Full length recombinant His_6-Max purified from *E. coli* was subjected to *in vitro* kinase assay with AurkA and B, purified from Sf21 insect cells using suitable baculoviral constructs. We observed that Max is phosphorylated by both the kinases *in vitro* (Figure 3.4).

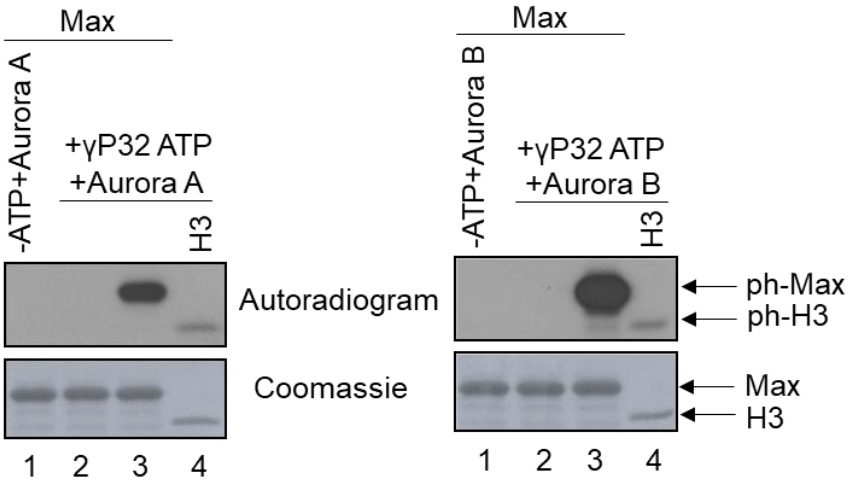

Figure 3.4: AurkA and AurkB phosphorylate Max. *In vitro kinase assay of 1µg of recombinant His_6-Max (lanes 1-3) and 500ng of histone H3 (lane 4; positive control) was performed using His_6-AurkA (left panel) and His_6-AurkB (right panel) purified from Sf21 cells. The coomassie staining for each of the lanes is shown below the autoradiogram profiles for comparing the loading levels across each lane.*

3.1.2. Determination and validation of *in vitro* phosphorylation sites of Max

In an attempt to identify the Aurora kinase mediated phosphorylation sites of Max, we carried out *in vitro* mass phosphorylation of His_6-Max with AurkB. The phosphorylated protein (ph-Max) was separated on a denaturing-polyacrylamide gel (SDS-PAGE), stained with Coomassie brilliant blue

(Figure 3.5A), and analysed by electrospray ionization-based mass spectrometry (ESI-MS/MS). We observed that the phosphorylation sites were spread over the entire length of Max protein, but mostly cluttered on the first helix region in the N-terminus (Figure 3.5B).

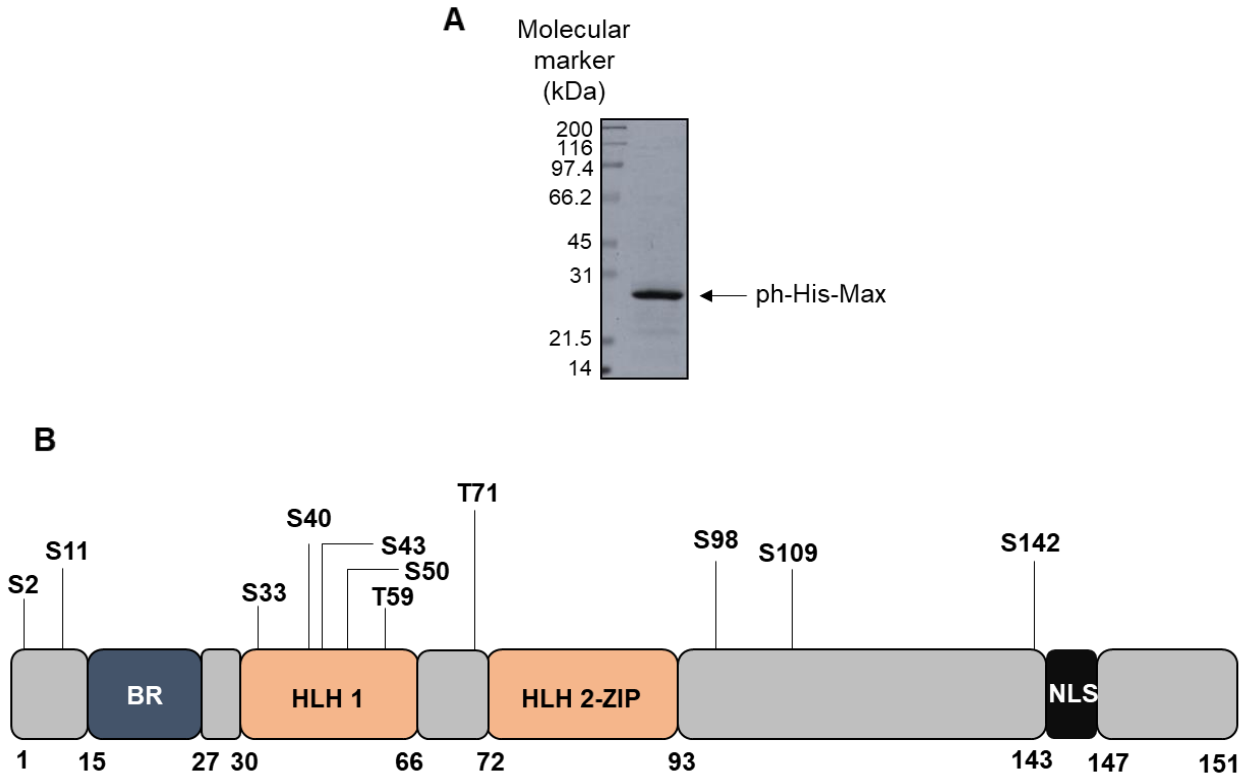

Figure 3.5: Mass spectrometric analysis of in vitro Max phosphorylation sites. A. *Coomassie stained 12% SDS-PAGE gel profile for 1µg His_6-Max protein phosphorylated in vitro by AurkB purified from Sf21 cells and which was excised for ESI-MS/MS analysis.* ***B.*** *Schematic representation of the in vitro phosphorylation sites of Max by AurkB as obtained from ESI-MS/MS analysis.*

A closer examination of the Max protein sequence revealed the presence of two serine residues, Ser-33 and Ser-40, that oblige the consensus phosphorylation motif of Ipl1 (yeast Aurk): K/R-X-T/S-I/L/V. We argued that validation of these residues as the true phosphorylation sites, by *in vitro* kinase assays using $\gamma P^{32}ATP$, may be hindered in a full-length Max context owing to phosphorylation signals emanating from the C-terminal serine residues (Ser-98, Ser-109, Ser-142). We, therefore, generated a truncated N-terminal domain of Max consisting of 1-70 amino acid (henceforth called NTD), and carried out the mutation of Ser-33 or Ser-40 in the NTD to alanine, either singly or in combination (Figure 3.6A). The mutant protein was purified from *E. coli* and

used to carry out *in vitro* kinase assay with the human, baculo-purified Aurks. However, we could not observe any reduction in the extent of phosphorylation by either AurkA (Figure 3.6B; left panel) or AurkB (Figure 3.6B; right panel). On the contrary, we observed an increase in the extent of phosphorylation upon mutation, with AurkB (Figure 3.6B; right panel). We subsequently mutated the other Ser/Thr residues that were obtained in the mass spectrometry analysis, Ser-50 and Thr-59, to alanine on the NTD-Ser-33A and Ser-40A backbone construct to generate a tetra-site mutated NTD (Ser-33A/Ser-40A/Ser-50/Thr-59), named as NTD-S4A. Unfortunately, even the NTD-S4A did not yield an abrogation of phosphorylation (Figure 3.6C).

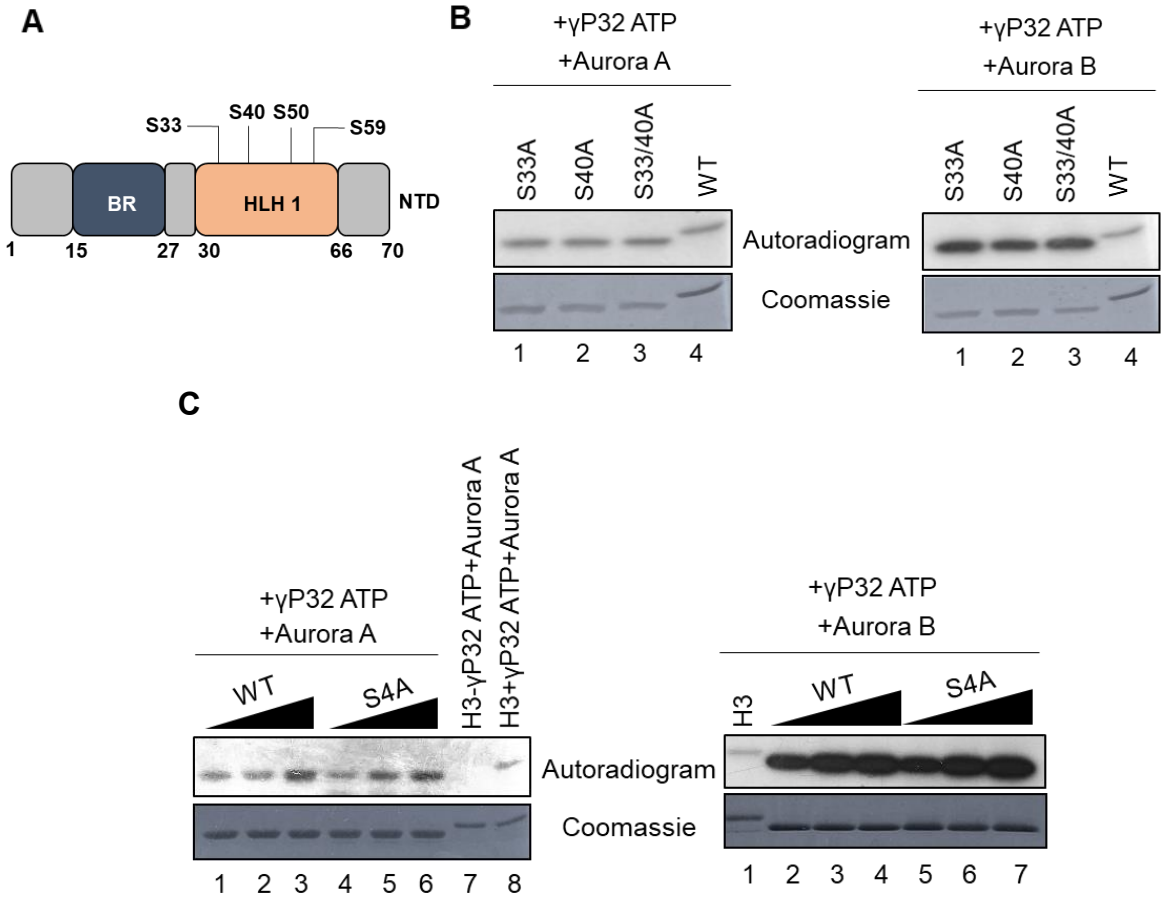

Figure 3.6: In vitro kinase assay of NTD mutants. A. *Schematic representation of the NTD of Max and the target residues, obtained from in vitro mass spectrometry of the full length His_6-Max protein, for mutation.* ***B.*** *In vitro kinase assay of 500ng recombinant His_6- NTD wild type (lane 4; positive control) and indicated point mutants (lanes 1-3) purified from E. coli, was performed using His_6-AurkA (left panel) and His_6-AurkB (right panel) purified from Sf21 cells. The coomassie staining for each of the lanes is shown below the autoradiogram profiles for comparing the loading*

levels across each lane. ***C.*** *In vitro kinase assay of 1µg His_6- NTD wild type (lanes 1-3) and NTD-Ser-33A/Ser-40A/Ser-50/Thr-59 (S4A) (lanes 4-6) was performed using increasing concentrations of His_6-AurkA (left panel) and His_6-AurkB (right panel) purified from Sf21 cells. The coomassie staining for each of the lanes is shown below the autoradiogram profiles for comparing the loading levels across each lane.*

We also carried out mutations of the serine residues that were enriched toward the C-terminal region of the protein. Since, multiple phosphorylation sites exit at the N-terminal half of the full-length protein (as discussed earlier), we argued that phosphorylation of these residues may mask any alteration that might occur owing to mutation of the C-terminal residues, in the full-length Max context. We, therefore, generated a C-terminal truncated Max fragment, encompassing 72-151 amino acids (Figure 3.7A) and carried out the mutations of Ser-98, and Ser-109 to alanine, either singly or in combination. However, similar, to the NTD mutants of Max, the CTD mutations did not yield any abrogation of phosphorylation (Figure 3.7B).

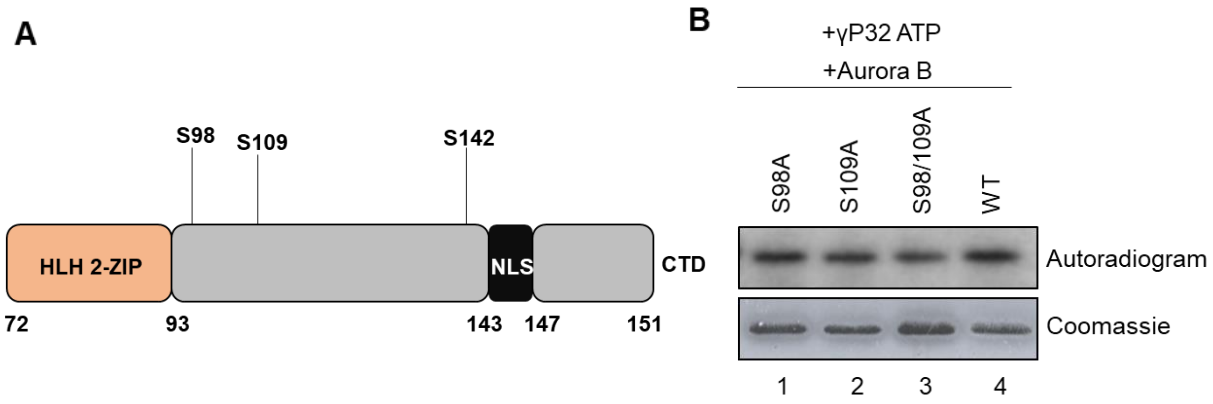

Figure 3.7: In vitro kinase assay of CTD mutants. A. *Schematic representation of the CTD of Max and the target residues for mutation that were obtained from in vitro mass spectrometry of the full length His_6-Max protein.* ***B.*** *In vitro kinase assay of His_6- CTD wild type (lane 4; positive control) and indicated point mutants (lanes 1-3) was performed using baculo-purified His_6-AurkB. The coomassie staining for each of the lanes is shown below the autoradiogram profiles for comparing the loading levels across each lane.*

3.1.3. Max harbours phosphorylated sites toward its C-terminus in cells

In order to uncover the true phosphorylated residues of Max in cells, we overexpressed full length Flag-Max fusion plasmid constructs in HeLa cells, and purified the Flag-Max protein using affinity purification (M2 agarose purification). The purified protein was separated on a denaturing-polyacrylamide gel, stained with Coomassie brilliant blue (Figure 3.8A), and analysed by liquid chromatography-based tandem mass spectrometry (LC-MS/MS). Although we could achieve 84% coverage for the Max protein in mass spectrometry (probably due to improper tryptic digestion or ionization defects), but surprisingly, unlike *in vitro* phosphorylated Max, we observed that the phosphorylation sites in HeLa cells were clustered toward the C-terminus of Max (Figure 3.8B). Intriguingly, inhibition of AurkA and B with specific inhibitors, MLN8237 and AZD1152 respectively, yielded differential and drastic results for Max phosphorylation in cell. While AurkA inhibition did not lead to any alteration in phosphorylation, inhibition of AurkB led to a complete inhibition of all the *in vivo* phosphorylated sites of Max.

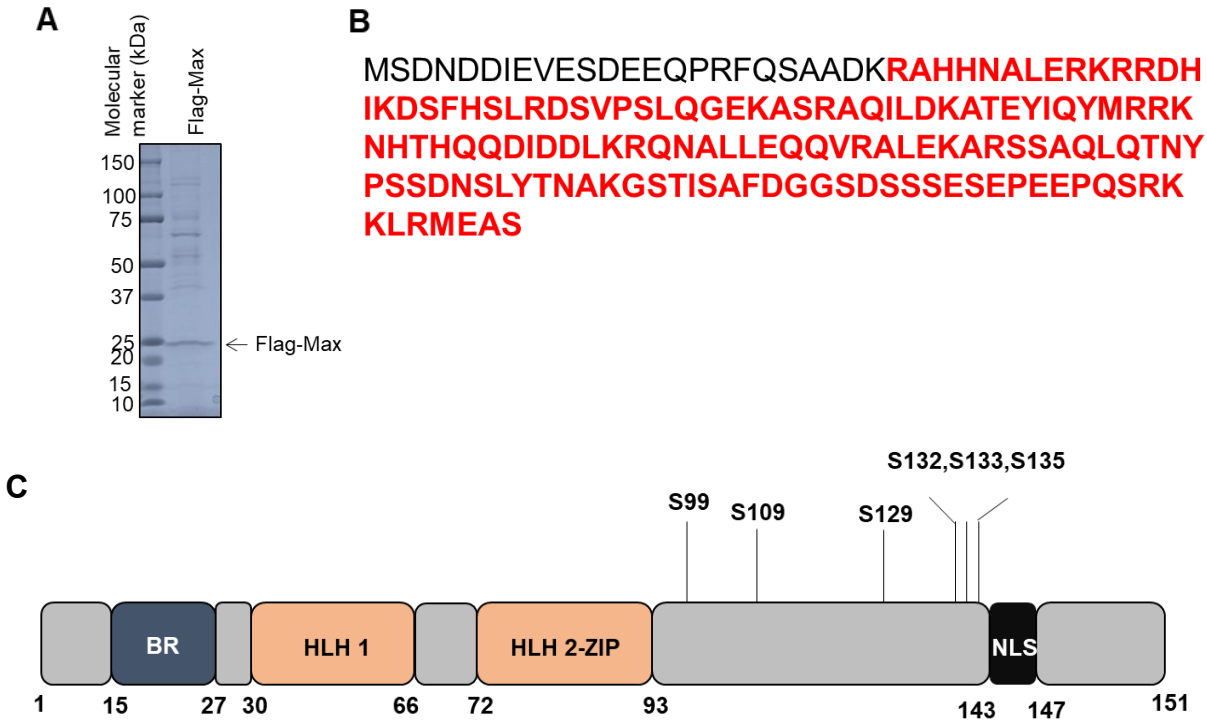

Figure 3.8: Mass spectrometric analysis of Flag-Max phosphorylation sites in HeLa. A. *Coomassie stained 5-20% gradient SDS-PAGE profile of Flag-Max fusion protein, transiently overexpressed in HeLa cells for 36 hrs and purified using M2 agarose-based affinity purification.* ***B.*** *Coverage of the amino acid residues in the LC-MS/MS based analysis of Flag-Max has been*

indicated in red. ***C.*** *Schematic representation of the in vivo phosphorylation sites of Max obtained by LC-MS/MS analysis.*

3.1.4. Mutation of a cluster of serine residues on the C-terminus of Max affects AurkB mediated phosphorylation

The drastic effect of AurkB inhibition on Max phosphorylation in cells led us to investigate the propensity of these residues as true AurkB phosphorylation sites. We made use of the truncated CTD of Max to carry out the mutations that were obtained from the cellular studies (Figure 3.9A). Simultaneous mutation of three closely spaced residues, S132, S133, and S135 to alanine (S3A) led to a substantial reduction in the extent of phosphorylation of CTD by AurkB (Figure 3.9B). We further validated this result as has been shown in (Figure 3.9C). It was, however, surprising not to find any alteration in phosphorylation of CTD-S7A, in which seven serine residues were mutated to alanine [S98A-S99A-S108A-S109A-S132A-S133A-135A (S7A)]. Although we have not studied the possibility of conformational changes of the secondary structures of CTD upon introduction of the point mutations, the likelihood of the same for the higher number of point mutations, as in S7A, cannot be ruled out. An altered conformation may, in turn bring about secondary or tertiary, non- physiological phosphorylation events.

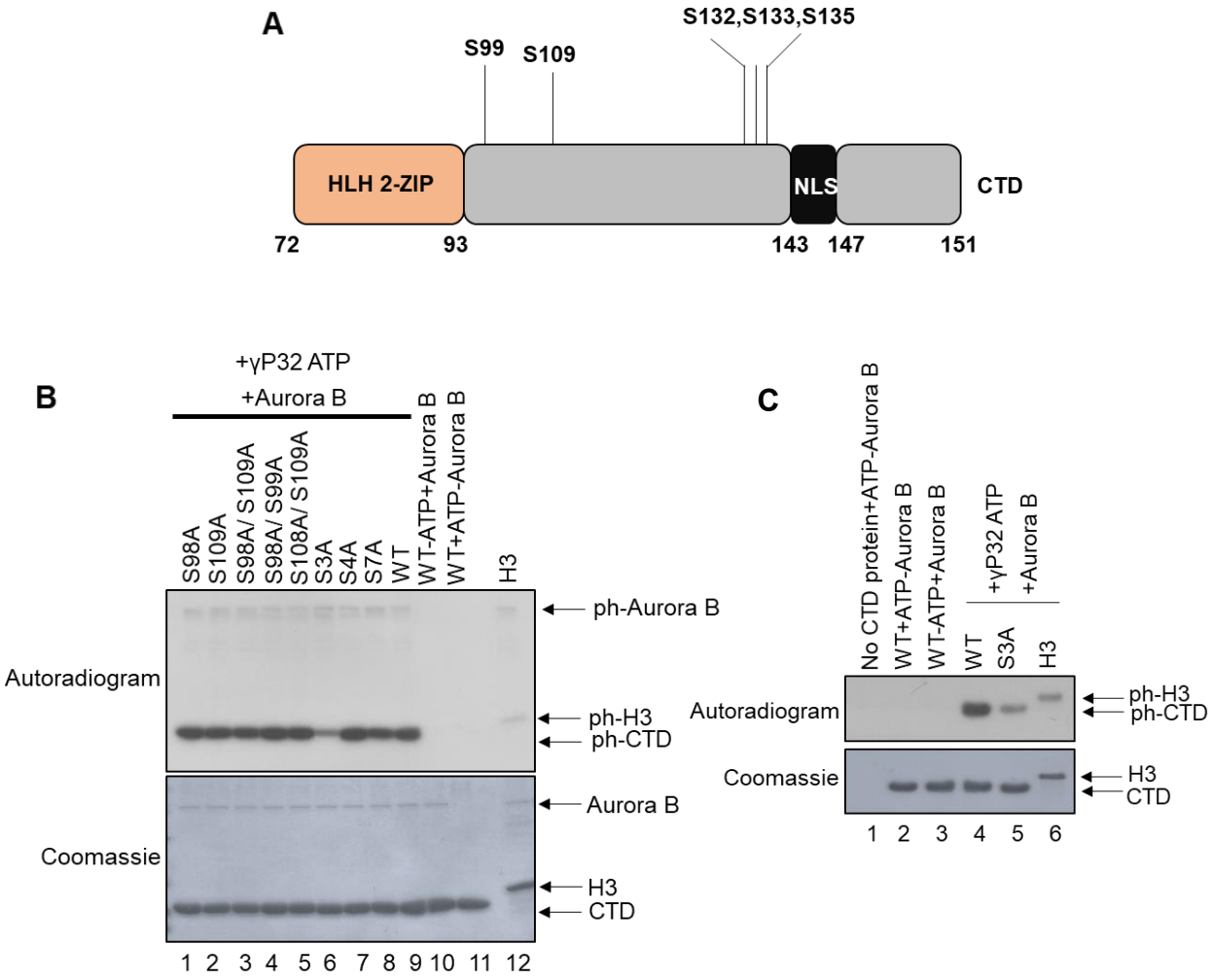

Figure 3.9: In vitro validation of Aurora kinase B mediated phosphorylation of in vivo sites of Max. A. *Schematic representation of the CTD of Max and the target residues for mutation.* ***B.*** *In vitro kinase assay performed with 1µg of CTD-WT (lane-9) and different mutant CTD proteins highlighted in each of the lanes (lanes 1-8), using His_6-AurkB purified from Sf21 cells. 500ng of histone H3 served as the positive control (lane 12). The coomassie staining for each of the lanes is shown below the autoradiogram profiles for comparing the loading levels across each lane. [S3A represents S132A-S133A-135A point mutant; S4A represents S98A-S99A-S108A-S109A point mutant and S7A represents S98A-S99A-S108A-S109A-S132A-S133A-135A point mutant].* ***C.*** *In vitro kinase assay performed with 1µg of CTD-WT (lanes 1-4) and CTD-S3A protein (lanes 5),*

using His_6-AurkB purified from Sf21 cells. 500ng of histone H3 served as the positive control (lane 6). The coomassie staining for each of the lanes is shown below the autoradiogram profiles for comparing the loading levels across each lane.

Furthermore, we carried out *in vitro* kinase assay for the wild type or the S3A mutant in the full-length Max context, but did not find a dramatic reduction of phosphorylation for the S3A mutant. As was discussed above, this result might be explained by the probable "masking" by phosphorylated sites in the N-terminus of Max in the *in vitro* assays (Figure 3.10).

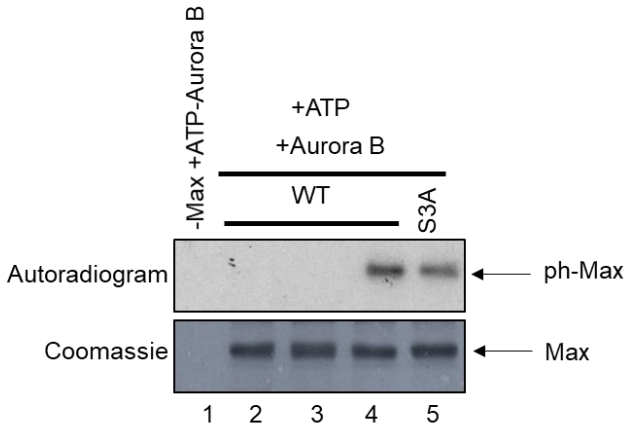

Figure 3.10: *In vitro kinase assay was performed for 1µg of His_6- Max WT (lanes 1-4) and His_6-Max S3A point mutant (lane 5) using His_6-AurkB purified from Sf21 cells. The coomassie staining for each of the lanes is shown below the autoradiogram profiles for comparing the loading levels across each lane.*

3.1.5. Study of subcellular localization alteration of Max WT and "CTD-derived" point mutant(s)

Proximity of S132, S133, and S135 to the nuclear localization signal of Max was intriguing. We wondered about the possibility of an effect on the nuclear localization of Max upon perturbation of these residues. We exploited the Flag tagged WT, S3A (phospho-deficient) as well as S3D (phospho-mimetic) mutants of full-length Max, to study the distribution of each of the Max protein constructs. Notably, all the three proteins exhibit nuclear localization. However, a closer examination revealed that the S3A mutant was approximately two-fold more likely to be present in the cytosol as well, when compared to either the WT or the S3D mutant (Figure 3.11A), and

which has been quantified (Figure 3.11B). Broadly, this result highlights that phosphorylation of S132, S133, and S135 might serve to restrict Max protein more in the nucleus, where it can serve its transcriptional activities in conjunction with Myc.

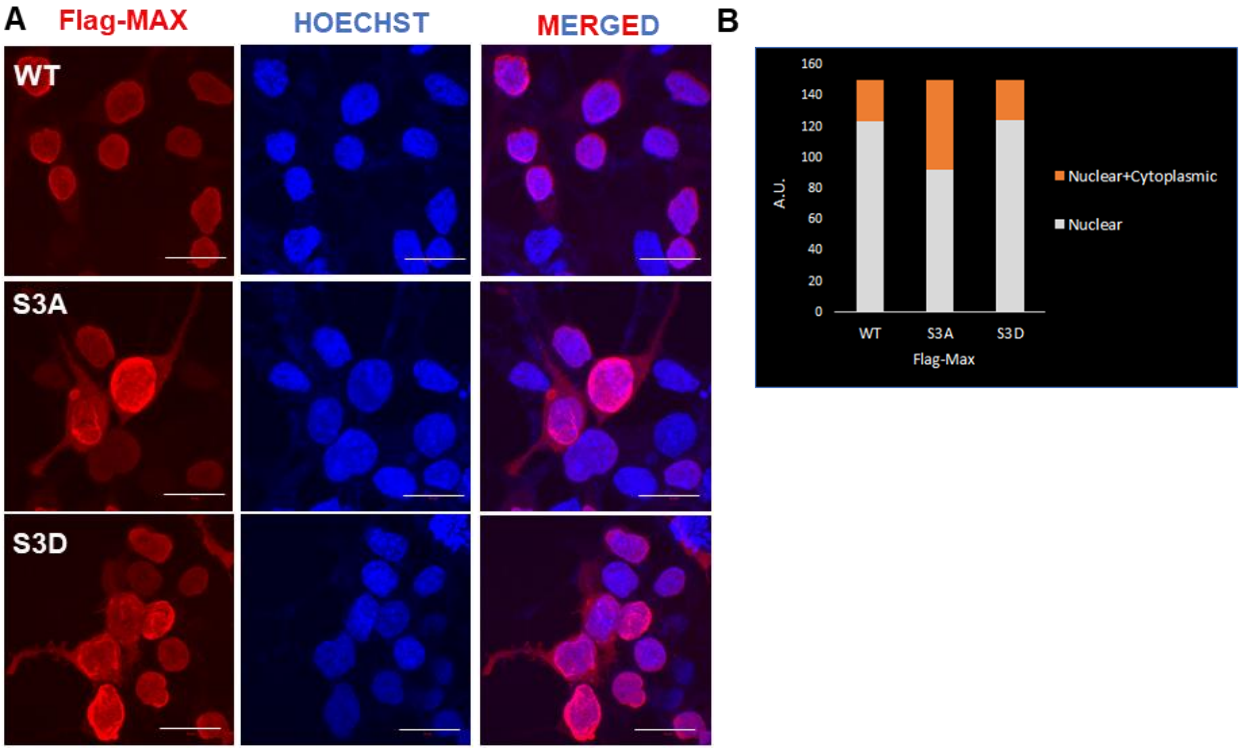

Figure 3.11: Subcellular localization of Max WT and mutants. A. *Indirect immunofluorescence of Flag-Max fusion constructs of WT, S3A or S3D mutants were transiently transfected into HEK293 cells and indirect immunofluorescence carried out against Flag tag (red) using Alexa 568 conjugated secondary antibody and the nucleus was stained with Hoechst (blue). Scale bar represent 10µm.* ***B.*** *Quantification of the localization events. 150 cells were counted for each of the constructs and plotted as bar plots.*

3.1.6. Aurora kinases exhibit subtype specific alteration in breast cancer

Breast cancer is an extremely heterogeneous disease with at least four different subtypes distinguished on the basis of classical immunohistochemistry. Further classifications have been done based on subtype-specific gene expression signatures and heterogeneity is also reflected by the subtype specific treatment regimens. A comprehensive study of Aurk dysregulation in breast cancer and molecular events associated with it is lacking. We analysed a TCGA (The Cancer

Genome Atlas) breast cancer patient cohort and in accordance with the established views, observed that both AurkA and AurkB to be significantly upregulated in the tumours as compared to the normal samples (Figure 3.12A). We further categorized the tumours into different subtypes of breast cancer and found that both the kinases exhibited upregulated expression in all the subtypes except Luminal A, which are usually slower growing tumours and pose less challenging prognosis. A comparison amongst the subtypes led to the observation that the basal-like/triple negative (TN) tumours express significantly higher levels of both these kinases as compared to either Her-2 amplified or Luminal B subtypes (Figure 3.12B).

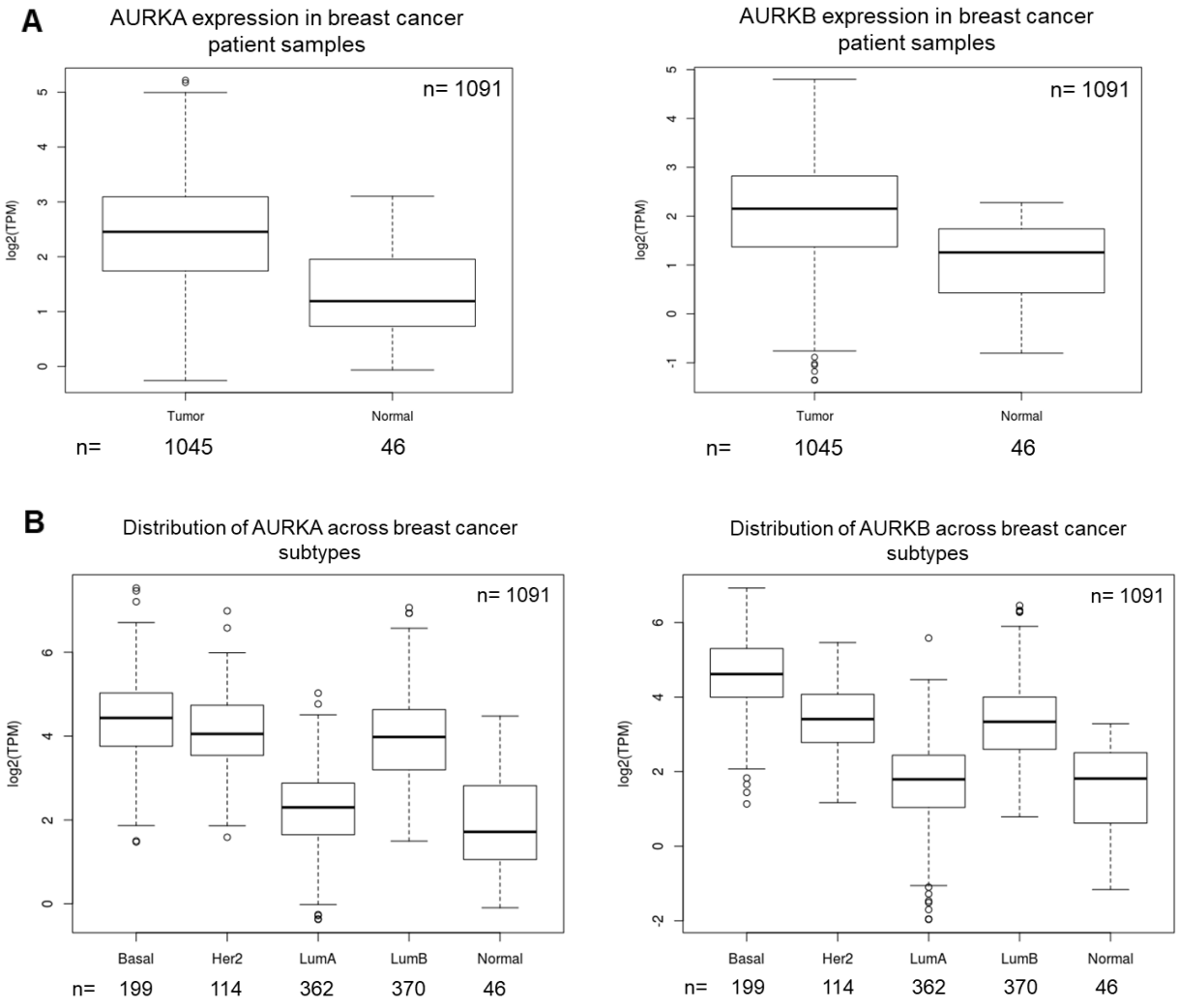

Figure 3.12: AurkA and AurkB exhibit subtype specific expression bias in breast cancer. A. *Distribution of AURKA and AURKB transcript expression in the TCGA breast cancer cohort has*

been represented as box-whisker plot, with the sample numbers mentioned below each of the sample types. Unpaired two-tailed Student's t-test has been carried out for statistical analysis of normal vs tumour expression pattern for AURKA (p= 1.515e-10 at CI = 99%) or AURKB (p= 1.236e-10 at CI = 99%). ***B.*** *mRNA expression patterns for AURKA or AURKB has been represented as box-whisker plot; sample numbers have been mentioned below each of the subtypes. Unpaired two tailed Student's t-test has been carried out for the statistical analysis of expression differences between normal vs luminal B (p= 1.484e-14); normal vs luminal A (p= 0.1313); normal vs HER2 amplified (p=5.918e-16); normal vs basal-like (p<2.2e-16); basal-like vs luminal A (p<2.2e-16); basal-like vs luminal B (p=3.206e-06); basal-like vs HER amplified (p=0.01702) at CI=99% for either AURKA* ***(left panel)*** *or between normal vs luminal B (p= 2.211e-13); normal vs luminal A (p= 0.4769); normal vs HER2 amplified (p=5.624e-14); normal vs basal-like (p<2.2e-16); basal-like vs luminal A (p<2.2e-16); basal-like vs luminal B (p<2.2e-16); basal-like vs HER amplified (p<2.2e-16) at CI=99% for AURKB* ***(right panel)***.

3.1.7. Impact of AurkB knockdown or inhibition on c-Myc/Max dependent target gene expression

Mass spectrometry data revealed that AurkB specific inhibition abrogated Max phosphorylation in cells, while biochemical and cell biology assays hinted that this phosphorylation possibly determine its nuclear localization and hence, its extent of interaction with Myc. Furthermore, we observed that AurkB was specifically enriched in the TN tumour patient samples. Interestingly, earlier reports show that the Myc pathway is activated in the basal-like/TN tumours and induce specific gene expression patterns that lead to poor physiologic and prognostic outcomes for the TNBC patients, as compared to the other subtypes. It was, therefore, pertinent to ask if AurkB perturbation affect transcription of c-Myc/Max dependent target genes in the basal-like/triple negative breast cancer (TNBC) context. Concordantly, we chose a TNBC cell line, MDA-MB-231, to study the effect of AurkB perturbation on the c-Myc dependent genes and to this end, we considered two types of gene sets for our study. The first gene pool belonged to the c-Myc/Max targets which are regulated either directly through promoter occupancy [*NOP56* (ribosome assembly protein), *h-TERT* (telomere maintenance), and *ODC1* (ornithine catabolism)], or indirectly [*YWHAZ*] through Myc dependent inhibition of a targeting *miRNA* (Su R *et al*., 2016). c-Myc/Max bind to the promoters of *NOP56* (Schlosser I *et al.* 2003), *and ODC1 (*Bello-Fernandez

C et al., 1993; Wagner A *et al*., 1993) in an E-box dependent manner and upregulate their gene transcription. The effect on *h-TERT* expression is more complex, as c-Myc exhibits repression of *h-TERT* in a chromatinized environment while activating it when the gene is naked (Zhao Y *et al.*, 2014).

The second set of gene targets we chose was more intuitive. An earlier study identified an interesting synergy between retinoic acid receptor-α (RARα) and c-Myc which comes into play upon PAK2 (a stress activated kinase) mediated phosphorylation of the C-terminal basic helix-loop-helix domain of c-Myc and subsequent dissociation from Max (Uribesalgo I *et al*., 2011). Dissociated Myc interacts with RARα and occupies the retinoic acid response elements (RAREs) and transcriptionally activate a set of pro-differentiation genes like *RAR-β* (*RARB*), *GATA6* and the *HOX* gene clusters. This causes a switch from an oncogenic to a tumour suppressive role for Myc. Since our results emphasized the impact of AurkB mediated Max phosphorylation on its nuclear localization, we hypothesized that a perturbation of the phosphorylation event, either due to AurkB knockdown or inhibition, may lead to the accumulation of a free pool of monomeric c-Myc, which may now bind to multiple other factors, one of them being RARα and affect the differentiation-related target genes in a RARE-dependent manner. Finally, we chose another differentiation-related gene, *GATA3*, for our study apart from GATA6 and RARB. *GATA3* holds prime importance in TNBC biology as it is massively downregulated in almost all the TNBC patient samples which might contribute to the poorly-differentiated phenotype observed for the TN tumour histology. *HPRT1* (Hypoxanthine-Guanine Phosphoribosyltransferase) served as the negative control in our study as the regulation of this gene is not affected by Myc.

We downregulated AurkB in MDA-MB-231 using a pool of four different siRNAs (Figure 3.13 inset for western blot validation of the knockdown) and observed that the downregulation of AurkB affected transcription from both the gene sets mentioned above (Figure 3.13). While the direct target genes like *NOP56* and *ODC1*, which are otherwise upregulated by c-Myc/Max complexes, exhibited downregulation, *h-TERT* followed the reverse pattern. *YWHAZ*, which is indirectly upregulated by c-Myc/Max, was found to be downregulated as well. Interestingly, the pro-differentiation genes, GATA6, RARB and GATA3, exhibited de-repression upon AurkB downregulation. This result fortifies our hypothesis of a possible reduction in Max phosphorylation upon AurkB knockdown leading to its dissociation from c-Myc, which first affects the direct c-Myc/max targets and secondly, frees Myc to interact with RARα and get recruited to the RAREs.

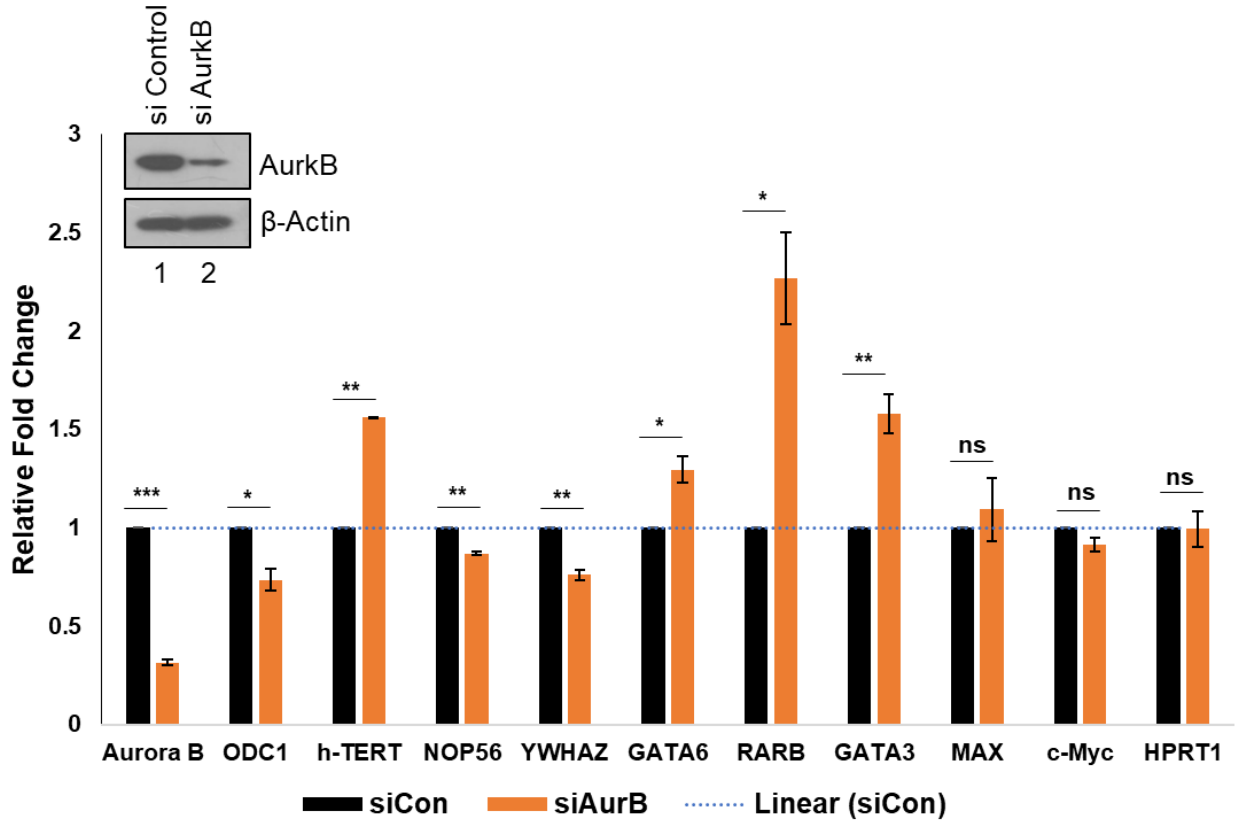

Figure 3.13: AurkB downregulation affects c-Myc/Max target gene expression. *Real time qRT-PCR analysis of the genes, represented on the x-axis, upon AurkB knockdown for 48 hrs in MDA-MB-231 cells. Actin served as the internal control. Western blot depiction of AurkB knockdown is represented in the inset. qRT-PCR data represent the mean ±SD from three independent*

*experiments with three technical replicates for each experiment. Paired two tailed Student's t-test was carried out for calculating the statistical significance of the perturbation of the indicated genes upon AurkB knockdown. *p< 0.05, **p<0.01, ***p<0.001, ns- not significant.*

We also treated MDA-MB-231 cells with a specific small molecule inhibitor of AurkB (Figure 3 .14A) and studied a subset of c-Myc/Max dependent genes. In accordance with the knockdown results, we observed that AurkB inhibition also led to similar effects on the target gene's expression (Figure 3.14B). We, however, could not observe a consistent effect of AurkB inhibition on the differentiation related genes within the time frame of the experimental conditions.

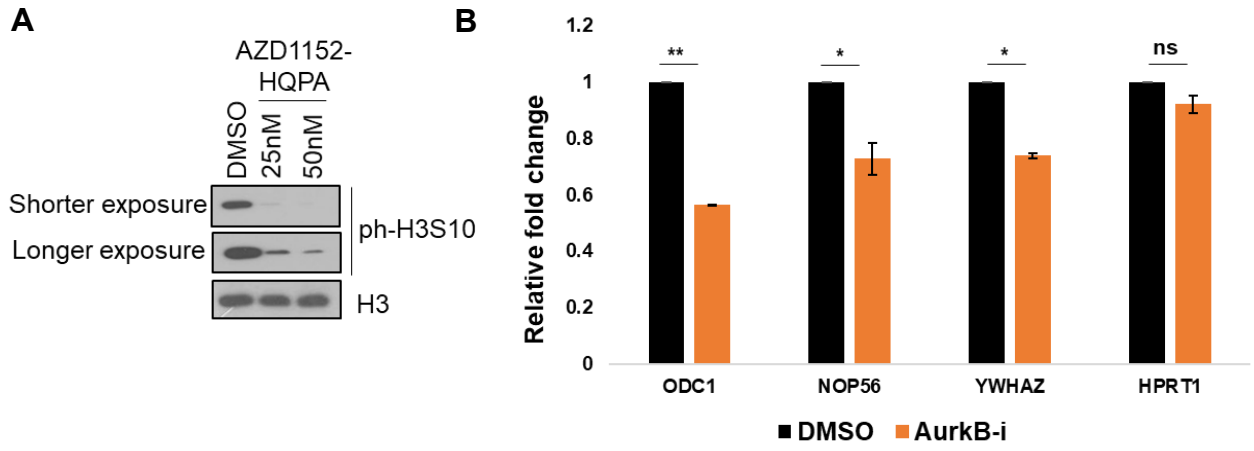

Figure 3.14: AurkB inhibition affects c-Myc/Max target gene expression. A. *Western blot representation of the indicated proteins on AurkB inhibition with 25nM or 50nM of an AurkB specific small molecule inhibitor, AZD-1152 HQPA, in MDA-MB-231 cells for 24 hrs. DMSO treated MDA-MB-231 cells served as the corresponding control and actin served as the internal control.* ***B.*** *Real time qRT-PCR analysis of the genes represented on the x-axis, upon AurkB inhibition for 24 hrs, in MDA-MB-231 cells. The data represent the mean ±SD from two independent experiments with two technical replicates for each experiment. Analysis of statistical significance was carried out using paired two tailed Student's t-test. *p< 0.05, **p<0.01, ***p<0.001, ns- not significant.*

3.2. Acetylation dependent regulation of AurkB and a probable role of the dysregulated kinase in dictating the outcome of DNA damage repair pathway choice

General Introduction

Over a decade, various research groups have linked the involvement of acetylation dependent regulatory pathways in the fine tuning of mitotic progression. The necessity of histone deacetylases (HDACs) in proper kinetochore assembly is well studied and intriguingly, it is shown that the HDAC inhibitors decrease the extent of pericentromeric targeting of Aurora B (Robbins AR et al., 2005), thus disrupting spindle attachment to the kinetochore. AurkB is also shown to physically interact with a host of HDACs, like HDAC 3, 4, 5,7 and 9, thus determining their nuclear localization during mitosis (Guise AJ et al., 2012). Moreover, HDAC 3 deacetylates AurkB at prophase to metaphase transition and drives proper chromosome congression and amphitelic attachments (Fadri-Moskwik M et al., 2012). This result signify that AurkB is acetylated in cell. However, the lysine acetyltransferase (KAT) responsible for the same had not been studied by these groups.

The following section describes the screening of various KATs of different families and the effect acetylation mediated alteration of kinase activity and protein stability of AurkB. Furthermore, we explored a possible connection between AurkB dysregulation and induction of DNA damage response.

3.2.1. Biochemical screening for the putative KAT(s) of AurkB

We chose three KATs- p300, PCAF and Tip60, belonging to three different families of lysine acetyltransferases, and used recombinant His_6-AurkB, purified from *E. coli* for an *in vitro* lysine acetyltransferase (HAT) assay. It was intriguing to find that p300 and Tip60 were capable of acetylating AurkB *in vitro*, while PCAF could not (Figure 3.15).

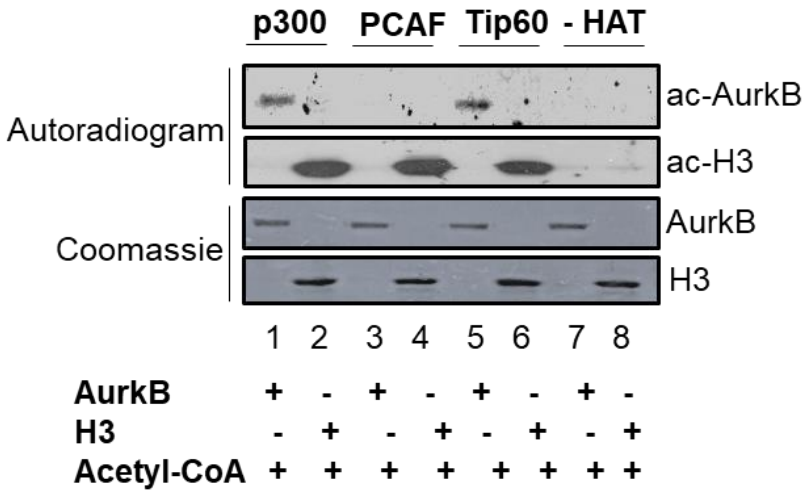

Figure 3.15: Tip60 and p300 acetylate AurkB. *In vitro lysine acetyltransferase (KAT) assay of 500ng of recombinant His_6-AurkB purified from E. coli by using His_6-p300, Flag-PCAF and His_6-Tip60 purified from Sf21 cells using suitable baculoviral constructs. The coomassie staining for each of the lanes is shown below the autoradiogram profiles for comparing the loading levels across each lane.*

3.2.2. AurkB is a substrate of Tip60

Tip60 is known to oppose oncogenic pathways. Factual downregulation of Tip60 expression in cancers and its direct involvement in DNA damage repair signalling led us to study the possibility of a Tip60 dependent regulation of AurkB. We found that Tip60 acetylated AurkB *in vitro* in a dose dependent manner (Figure 3.16). In order to identify the acetylation sites, we performed *in vitro* mass acetylation of recombinant His_6-AurkB using Tip60 purified from insect ovarian cells, Sf21, by suitable baculoviral constructs. The acetylated protein was subjected to electrospray ionisation-based mass spectrometry (ESI-MS/MS) and nine probable acetylated lysine residues were identified- K4, K31, K56, K85, K87, K115, K168, K195, and K202 [*cf*- Section 2.7.2.].

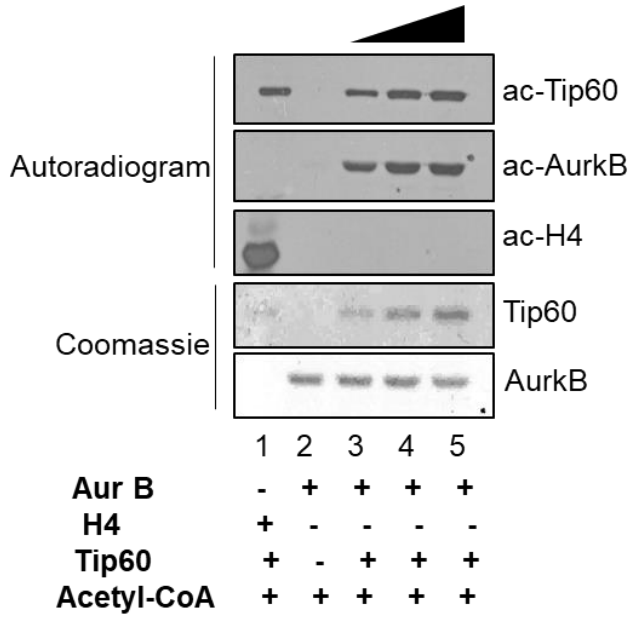

Figure 3.16: Tip60 acetylates AurkB. *In vitro KAT assay representation of the acetylation of 500ng of recombinant His_6-AurkB purified from E. coli by increasing concentrations of His_6-Tip60 purified from Sf21 cells. The coomassie staining for each of the lanes is shown below the autoradiogram profiles for comparing the loading levels across each lane.*

3.2.3. Tip60 acetylate AurkB at two highly conserved lysine residues

We observed that AurkB possesses a G-K-G-K motif, which is similar to G-K-X-G-K motif found in the well-studied Tip60 substrates- H4 and Twist (Figure 3.17A). Furthermore, similar to H4 and Twist, the probable Tip60 acetylation motif on AurkB is flanked by glycine rich amino acids. Noting the high extent of conservation of the lysine residues within the motif- K85 and K87(Figure 3.17B), we mutated these lysine residues, either singly or in combination, to arginine and the purified recombinant proteins were subjected to *in vitro* lysine acetyltransferase assay. While the K85R-K87R mutant led to a complete abrogation of Tip60 mediated acetylation, the single point mutants were only mildly affected (Figure 3.17C). The K85R-K87R mutant did not show any acetylation even for higher Tip60 concentrations (Figure 3.17D) emphasizing the importance of acetylation of both the lysine residues by Tip60.

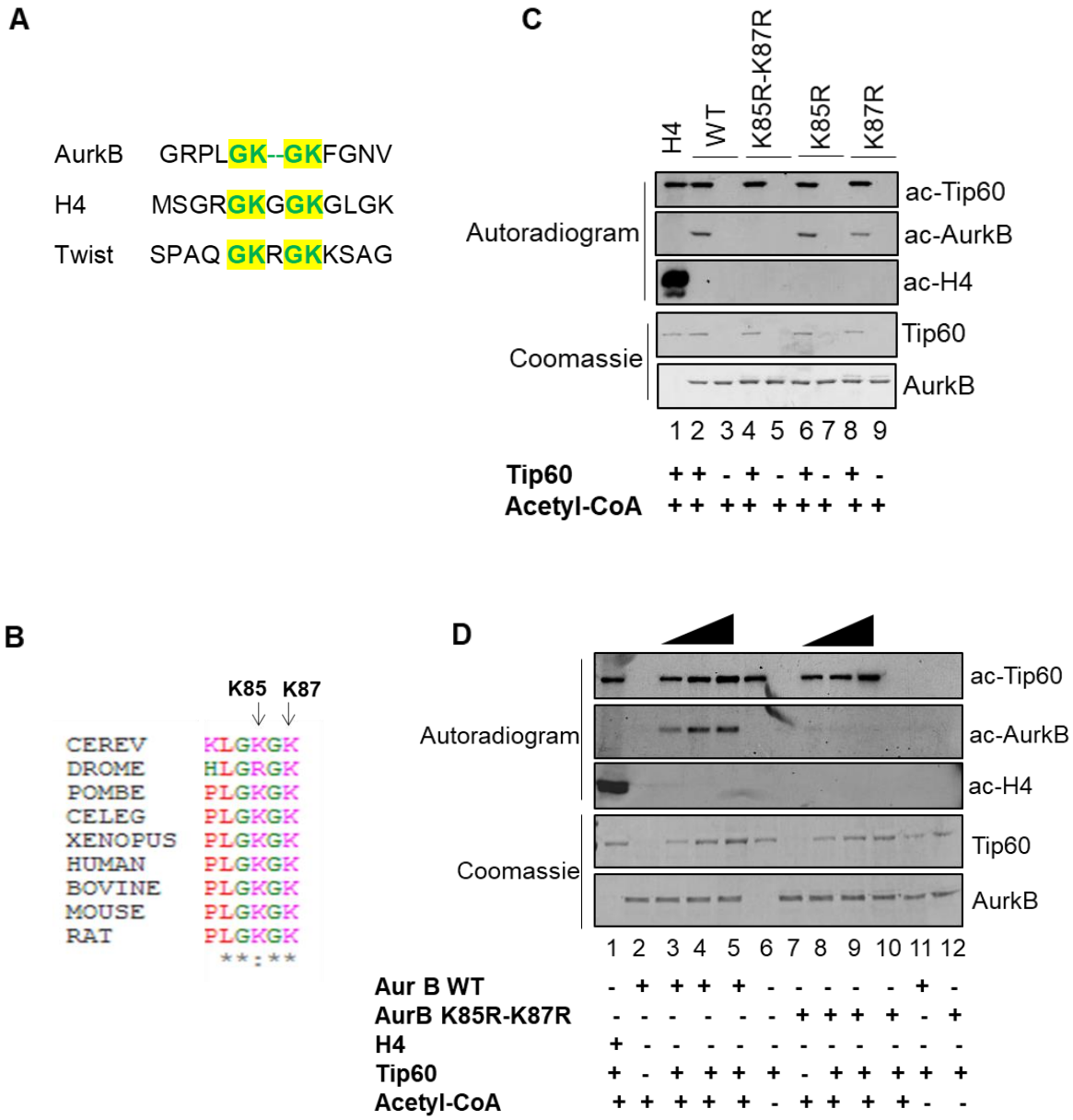

Figure 3.17: Tip60 acetylates AurkB at K85 and K87. A. *Local alignment of oligopeptide sequence displaying the similarities of putative Tip60 mediated acetylation motif on AurkB, histone H4 and Twist.* ***B.*** *Local alignment exhibiting the extent of conservation of K85 and K87 residues of AurkB in different organisms- CEREV, Saccharomyces cerevisiae; DROME, Drosophila melanogaster; POMBE, Schizosaccharomyces pombe; CELEG- Caenorhabditis elegans; XENOPUS, Xenopus laevis; HUMAN, Homo sapiens; Bovine, Bos Taurus; Mouse, Mus musculus; RAT, Rattus rattus.* ***C.*** *500ng each of His_6- AurkB WT or the indicated mutant His_6- AurkB proteins*

were used to carry out an in vitro KAT assay using His_6-Tip60 purified from Sf21 cells. ***D.*** *500ng each of His_6- AurkB WT or His_6- AurkB K85R-K87R double point mutant proteins were used to carry out an in vitro KAT assay using increasing concentrations of His_6-Tip60 purified from Sf21 cells. The coomassie staining for each of the lanes is shown below the autoradiogram profiles for comparing the loading levels across each lane.*

3.2.4. Tip60 and p300 may not possess overlapping acetylation sites on AurkB

The screening of different KATs had highlighted that p300, apart from Tip60, is also capable of acetylating AurkB *in vitro*. We subsequently studied the K85 and K87 residues of AurkB in the context of p300 mediated acetylation and observed that p300 is capable of acetylating either of the individual point mutants-K85R and K87R (Figure 3.18A), as well as the K85R-K87R double mutant (Figure 3.18B). This result emphasizes either the exclusivity of K85 and K87 residues toward Tip60 mediated acetylation or portrays the possibility of numerous p300 mediated acetylation sites on AurkB, and mutation of two (K85 and K87) amongst many, is incapable of altering the overall acetylation status of the AurkB protein. The present thesis has focussed on Tip60 mediated events and does not elucidate the role of p300 dependent AurkB acetylation and functions which, therefore, needs future efforts.

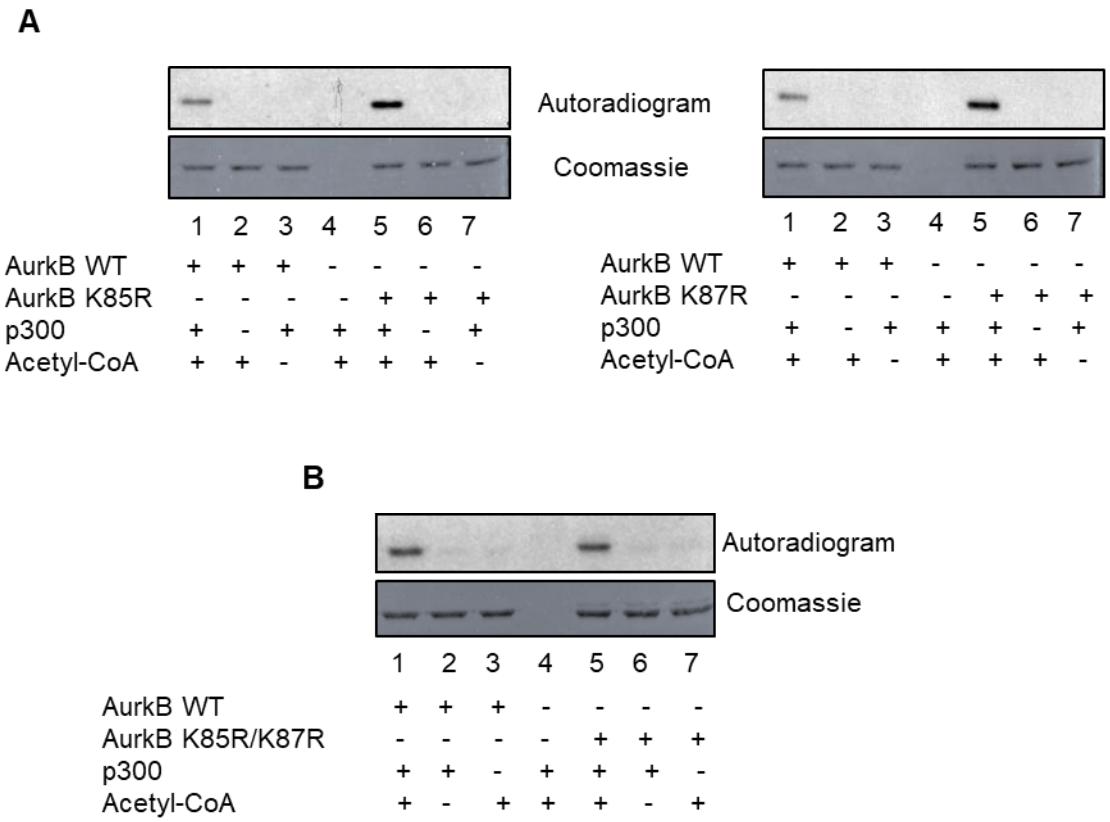

Figure 3.18: Validation of p300 mediated acetylation of AurkB for Tip60 targeted lysine residues. *500ng each of recombinant His_6-AurkB WT or the His_6-AurkB mutant proteins (single point mutants-K85R and K87R, as in panel **A**) or the double point mutant (His_6- AurkB K85R/ K87R, as in panel **B**) were used to carry out an in vitro KAT assay using His_6-Tip60 purified from Sf21 cells. The coomassie staining for each of the lanes is shown below the autoradiogram profiles for comparing the loading levels across each lane.*

3.2.5. Tip60 interacts with and acetylates AurkB in cells

In order to verify that acetylation of AurkB by Tip60 is not restricted to *in vitro* assays and indeed occur in cells, we resorted to ectopic Tip60 overexpression in HEK293 cells. We observed that the WT, but not the dominant negative HAT inactive mutant of Tip60 (ΔHAT; Q377E/G380E), led to an enhancement of acetylation of AurkB at K85 and K87 residues, as studied using a K85-K87 acetylation specific antibody (Figure 3.19A). We questioned whether this acetylation is an event that is manifested by direct interaction between the two proteins. Reciprocal co-immunoprecipitation for ectopically overexpressed HA-Tip60 in HEK293 cells stably expressing

Flag-AurkB confirmed their physical interaction (Figure 3.19B, panel-I). Furthermore, we observed that the WT and ΔHAT mutant exhibit similar extent of interaction with AurkB (Figure 3.19B, panel-II), thus arguing the increased K85-K87 acetylation of AurkB in favour of the KAT activity of Tip60. These results convincingly demonstrate that Tip60 interacts with AurkB in cells and acetylate it at K85 and K87 residues.

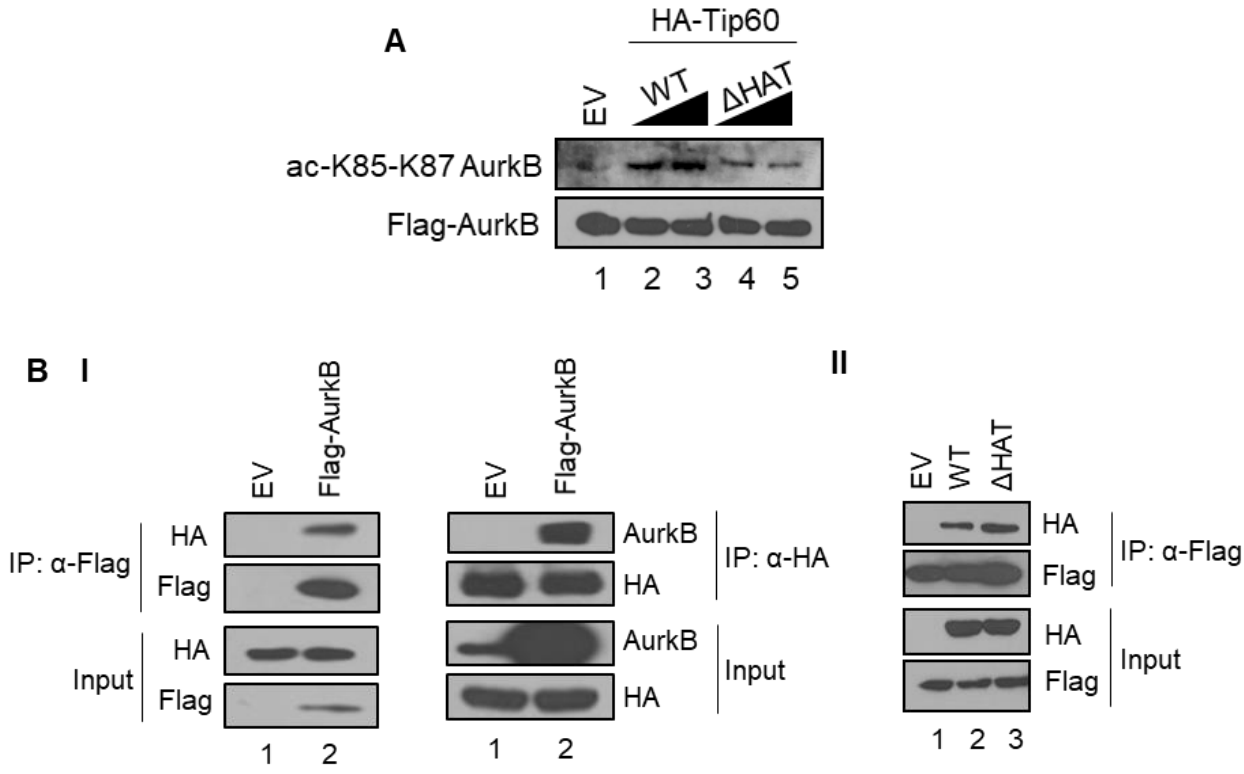

Figure 3.19: Tip60 interacts with and acetylates AurkB in cells. A. *Western blot representation of enhancement of AurkB di-acetylation at K85 and K87 residues by ectopic overexpression of HA tagged WT-Tip60, but not HAT inactive Tip60 mutant (ΔHAT), for 48 hrs in HEK293 cells stably expressing Flag-AurkB fusion protein.* ***B. Panel-I.*** *Reciprocal co-immunoprecipitation showing the interaction between HA-Tip60 (transiently overexpressed for 48hrs) and Flag-AurkB in HEK293 cells stably expressing Flag-AurkB protein.* ***Panel-II.*** *Western blot representation to show similar extent of interaction for ectopically expressed HA tagged WT Tip60 or HA tagged HAT inactive Tip60 mutant with Flag-AurkB in HEK293 cells stably expressing Flag-AurkB protein.*

3.2.6. Tip60 regulate protein levels of AurkB in cells

During the course of our study of the dual acetylation of AurkB at K85 and K87, we wanted to enrich the acetylation of these residues using broad and non-selective HDAC inhibitors like trichostatin A (TSA). TSA inhibits class I HDACs (HDAC1, 3, 4, 6, and 10) and has been shown to induce G2/M arrest, in a transcription independent manner, by targeting HDAC3 (Yun Li et al., 2006). Moreover, HDAC3 was also shown to be the one responsible for AurkB deacetylation (Fadri-Moskwik M et al., 2012).

Strikingly, treatment of HEK293 cells stably expressing Flag-AurkB with TSA led to a marked reduction of the Flag-AurkB pool (Figure 3.20A). We wondered about the likelihood of acetylation of AurkB as a trigger for its downregulation. To this end, we overexpressed HA-Tip60 in HEK293 cells and found that the endogenous AurkB levels exhibited a marked reduction, which could be rescued by simultaneous Tip60 knockdown (Figure 3.20B, panel-I). Similar rescue was also observed when Flag-AurkB was transiently overexpressed in stable Tip60 knockdown cells (Figure 3.20A, panel-II). We could faithfully reproduce these results in two other breast cancer cell lines, MDA-MB-231 and MCF7 (Figure 3.20C, panel-I and II, respectively]. We also generated point mutants corresponding to acetylation defective (K85R-K87R) or mimetic (K85Q-K87Q) conditions, on Flag-AurkB mammalian expression vector, and observed that the later exhibited reduced stability under cycloheximide chase assay conditions (Figure 3.20D). These observations collectively confirm that Tip60 mediated acetylation of AurkB at K85 and K87 residues result into its destabilization in cells.

We next asked if AurkB downregulation upon ectopic Tip60 overexpression, agrees with a physiologically relevant scenario. An earlier observation had demonstrated stabilization of Tip60 protein in cells upon UV exposure, owing to an inhibition of its degradation by MDM2. In agreement with this study, we observed that UV irradiation caused enhancement in Tip60 levels in cells and AurkB was concomitantly downregulated under such conditions (Figure 3.20E).

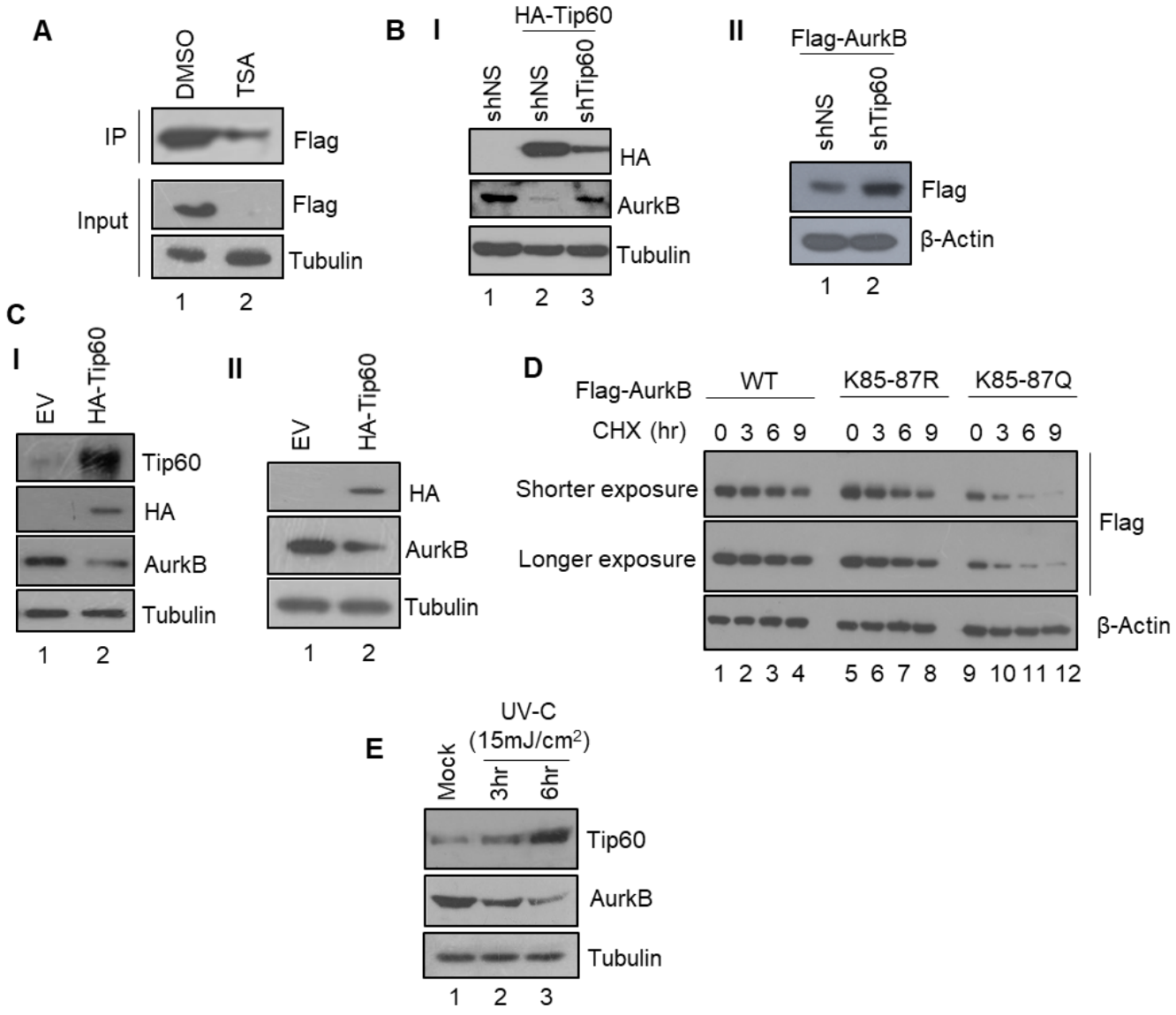

Figure 3.20: Tip60 regulates AurkB levels in cells. A. *Western blot representation of the indicated proteins upon treatment of stably overexpressing Flag-AurkB HEK293 cells with 10μM TSA or the corresponding DMSO control. IP represent the immunoprecipitated fraction from 1mg of whole cell lysate; input represent the whole cell lysate fraction.* ***B.*** *Western blot analysis showing that Tip60 overexpression reduces, while simultaneous Tip60 knockdown rescues, AurkB levels in HEK293 cells* ***(panel-I)*** *[shNS represent non-silencing shRNA control].* ***(Panel-II)*** *Transient overexpression of Flag-AurkB in stable shNS and shTip60 cell lines showing the higher levels of Flag-AurkB in the Tip60 knockdown cell line as compared to the control shNS cells.* ***C.*** *Western*

blot representation for overexpression of Tip60 in MDA-MB-231 cells ***(panel-I)*** *or MCF7 cells* ***(panel-II)*** *and study of the proteins with the indicated antibodies.* ***D.*** *Cycloheximide chase assay for WT, acetylation defective (K85R-K87R) or acetylation mimetic (K85Q-K87Q) mutants of AurkB.* ***E****. Western blot representation of HEK293 cells exposed to 15mJ/cm^2 UV-C (254 nm) and harvested at the indicated time points after irradiation for the indicated proteins.*

3.2.7. Tip60 mediated acetylation inhibit the kinase activity of AurkB

K85 and K87 residues lie within the kinase domain of AurkB. This propelled us to study if the kinase activity is affected upon acetylation by Tip60. Recombinant His_6-AurkB was acetylated *in vitro* with Tip60 and the acetylated kinase was used in an *in vitro* kinase assay with histone H3 as a substrate. We found that acetylation of AurkB lowered its kinase activity, when compared to the mock acetylated control (Figure 3.21A). We extended our study in assessing the point mutants of AurkB and observed that the acetylation mimetic K85Q-K87Q mutant exhibited reduced kinase activity as compared to either the WT or the acetylation defective K85R-K87R mutant (Figure 3.21B). The acetylation defective mutant, however, showed higher kinase activity, even as compared to the WT kinase, the cause of which is presently unclear. These results confirm that Tip60 dependent acetylation inhibit the kinase activity of AurkB.

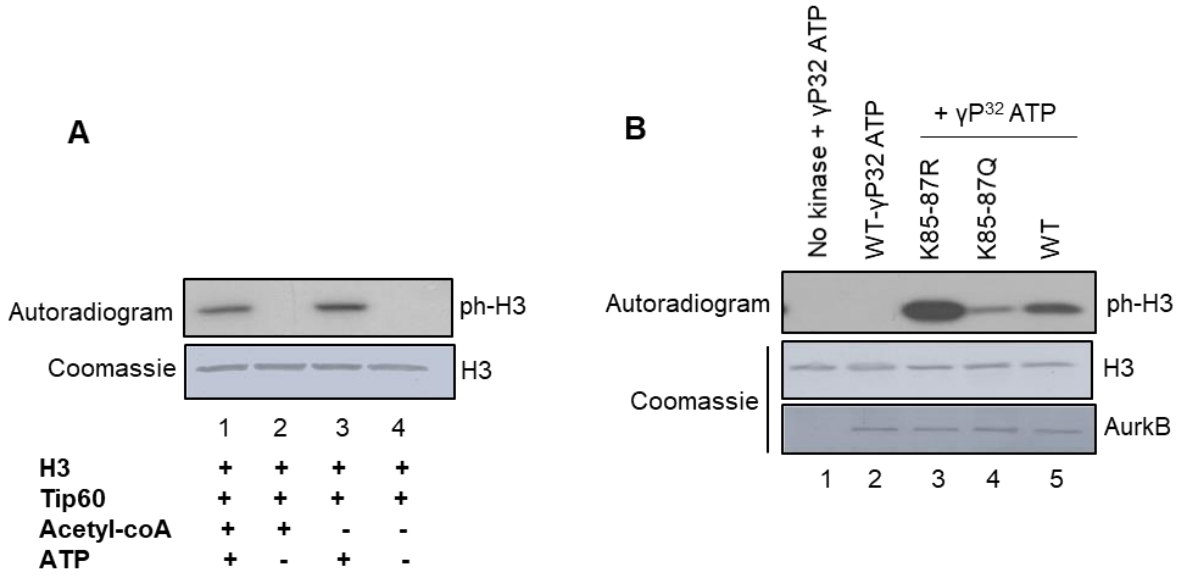

Figure 3.21: Tip60 mediated acetylation inhibits AurkB activity. A. *500ng of His_6-AurkB was either acetylated with Tip60 or mock acetylated (control) in vitro. One-tenth of the acetylation reaction was used to carry out in vitro kinase assay with 500 ng of recombinant H3. The coomassie staining for each of the lanes is shown below the autoradiogram profiles for comparing the loading levels across each lane.* ***B.*** *In vitro kinase assay was carried out using 100ng each of WT, acetylation defective mutant (K85R-K87R), or acetylation mimetic mutant (K85Q-K87Q) of AurkB using histone H3 as a substrate. Lesser extent of kinase activity was observed for the K85Q-K87Q mutant as compared to either the WT or the K85R-K87R mutant.*

3.2.8. Tip60 and AurkB follow inverse pattern of expression in breast cancer cells and modulate DNA damage response

Tip60 was observed to undergo downregulation in colorectal cancer patients (Mattera L *et al*., 2009; Sakuraba K *et al.*, 2009). Furthermore, meticulous observation unveiled Tip60 to be a haploinsufficient tumour suppressor across multiple solid and haematological cancers (Gorrini C *et al.*, 2007). The loss of heterozygosity (LOH) was linked to SNP-LOH of the Tip60 gene where the LOH for the first allele is usually not followed by epigenetic silencing of the second. However, the LOH causes cell autonomous loss of Myc induced DNA damage response (DDR), which in general, is a tumour suppressive mechanism.

We exploited breast cancer cell lines for our study and observed that Tip60 is downregulated in all these lines at the transcript level, irrespective of the subtype, when compared to the epithelial, non-malignant breast cell line, MCF10A (Figure 3.22A). Concordant to our earlier observation which suggested an acetylation-dependent regulation of AurkB levels by Tip60, we observed AurkB to be elevated in all the cell lines with reduced Tip60 levels (Figure 3.22B).

We next posed the question whether such high levels of AurkB can inflict DDR. Interestingly, we found that the γH2AX (phosphorylated H2AX; marker of DNA damage) levels correlated positively with AurkB in most of the breast cancer cell lines (Figure 3.22B). This result indicated that AurkB may be a part of an intricate network in controlling the basal DNA damage repair response. In order to understand the specificity of the relation between AurkB and γH2AX, we knocked down AurkB in one of the high AurkB expressing cell lines, MDA-MB-231, using either a doxycycline inducible shRNA against AurkB (Figure 3.22C, panel-I) or using a pool of four different siRNAs targeting AurkB (Figure 3.22C, panel-II) and found that the endogenous γH2AX levels decreased dramatically. Conversely, overexpressing AurkB in HEK293 cells enhanced the

basal γH2AX levels (Figure 3.22C, panel-III). These results indicate that AurkB regulates γH2AX levels in a cell-type and lineage independent manner.

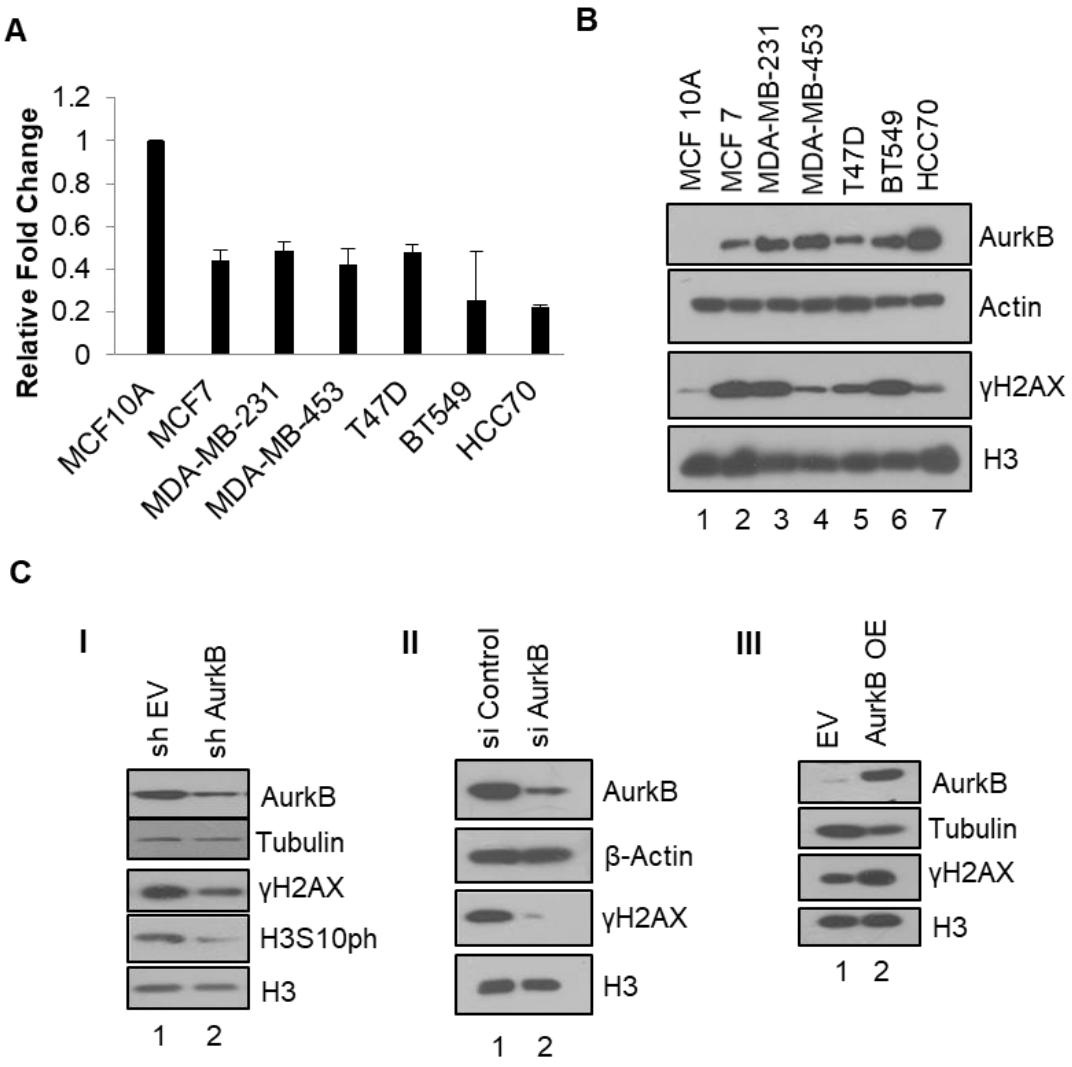

Figure 3.22: High AurkB levels elicit DDR in breast cancer cells. A. *Depiction of Tip60 transcript levels in different breast cancer cell lines as analysed by real time qRT-PCR.* ***B.*** *Representative western blot image of AurkB and γH2AX levels in different breast cancer cell lines.* ***C.*** *Western blot representation of AurkB knockdown in MDA-MB-231 {using either a shRNA* ***(panel-I)*** *or a pool of four different siRNAs* ***(panel-II)****} and overexpression in HEK293* ***(panel-III)*** *exhibiting reduced or enhanced basal γH2AX, respectively.*

3.2.9. AurkB regulates γH2AX levels by influencing Tip60 gene transcription

As γH2AX act as a signal for DNA damage, its removal is necessary to determine the completion of damage repair processes. It is known that Tip60 is not only necessary for early events in the initiation of DDR but its involvement is also necessary for the removal of γH2AX from the chromatin in an acetylation dependent manner (Ikura T et al., 2007; Ikura M et al., 2015). The later event necessitates the participation of Tip60 even for the basal levels of DNA damage, as knockdown of Tip60 leads to the accumulation of endogenous γH2AX levels.

Regulation of the endogenous pool of γH2AX by AurkB prompted us to study the likelihood of AurkB in negatively affecting Tip60 levels in cells. Intriguingly, we observed that AurkB knockdown in MDA-MB-231 cells, de-repressed Tip60 gene transcription (Figure 3.23). This observation highlights the probable axis of γH2AX accumulation in high AurkB expressing cells through inhibition of Tip60 gene transcription and also indicate that AurkB may represent one of the essential factors that inhibit Tip60 gene transcription under elevated conditions, as in cancer.

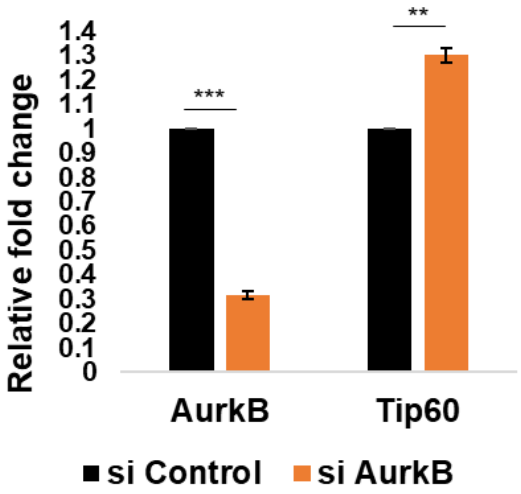

Figure 3.23: AurkB inhibit Tip60 gene transcription. *Real time qRT-PCR analysis of Tip60 gene transcription upon AurkB knockdown for 48 hrs in MDA-MB-231 cells. The data represents the mean ± SD from three independent experiments with three technical replicates for each experiment. Analysis of statistical significance was carried out using paired two tailed Student's t-test. **p<0.01, ***p<0.001.*

3.2.10. AurkB influences the choice of DNA damage repair

In order to understand the DDR foisted upon a cell by elevated AurkB levels and to study the relevance of such an event in pathobiology, we studied if AurkB affects any of the DNA damage repair pathways. Homologous recombination (HR) and non-homologous end joining (NHEJ) represent two of the major pathway choices for repairing damaged DNA, amongst others. HR is dependent on a homologous template and is an accurate, yet slower mode of repair which maintains the stability of the genome. NHEJ, on the other hand, exhibit faster repair kinetics but is highly error prone. The later mode induces mutations and translocations. A balance between these two pathways determines genomic stability.

We employed SCR18-U2OS cells to study the efficiency of sister chromatid recombination (SCR)/ HR in a cellular context (Puget N et al., 2005). These cells are genetically modified in a manner, such that GFP is expressed only upon a template dependent recombination event. The percentage of GFP positive cells, therefore, is a direct representation of the extent of SCR or HR process. We observed that AurkB overexpression led to a four-fold reduction in the overall HR mediated repair process (Figure 3.24A). Additionally, we asked if an inhibition in HR directed repair is associated with a concomitant increase of the error-prone NHEJ pathway. We made use of a suitable NHEJ reporter assay (Fattah F et al., 2010) and observed that the NHEJ pathway is indeed preferred upon AurkB upregulation (Figure 3.24B). A closer examination indicated that the “alternate” or “back-up” NHEJ (alt-NHEJ or bNHEJ) or microhomology mediated end joining (MMEJ) pathway (assessed by I-SceI digestion) exhibited a modest yet significant increase ($p=0.009$) as compared to the “canonical” or “classical” pathway of repair (mediated by HindIII digestion) upon AurkB overexpression.

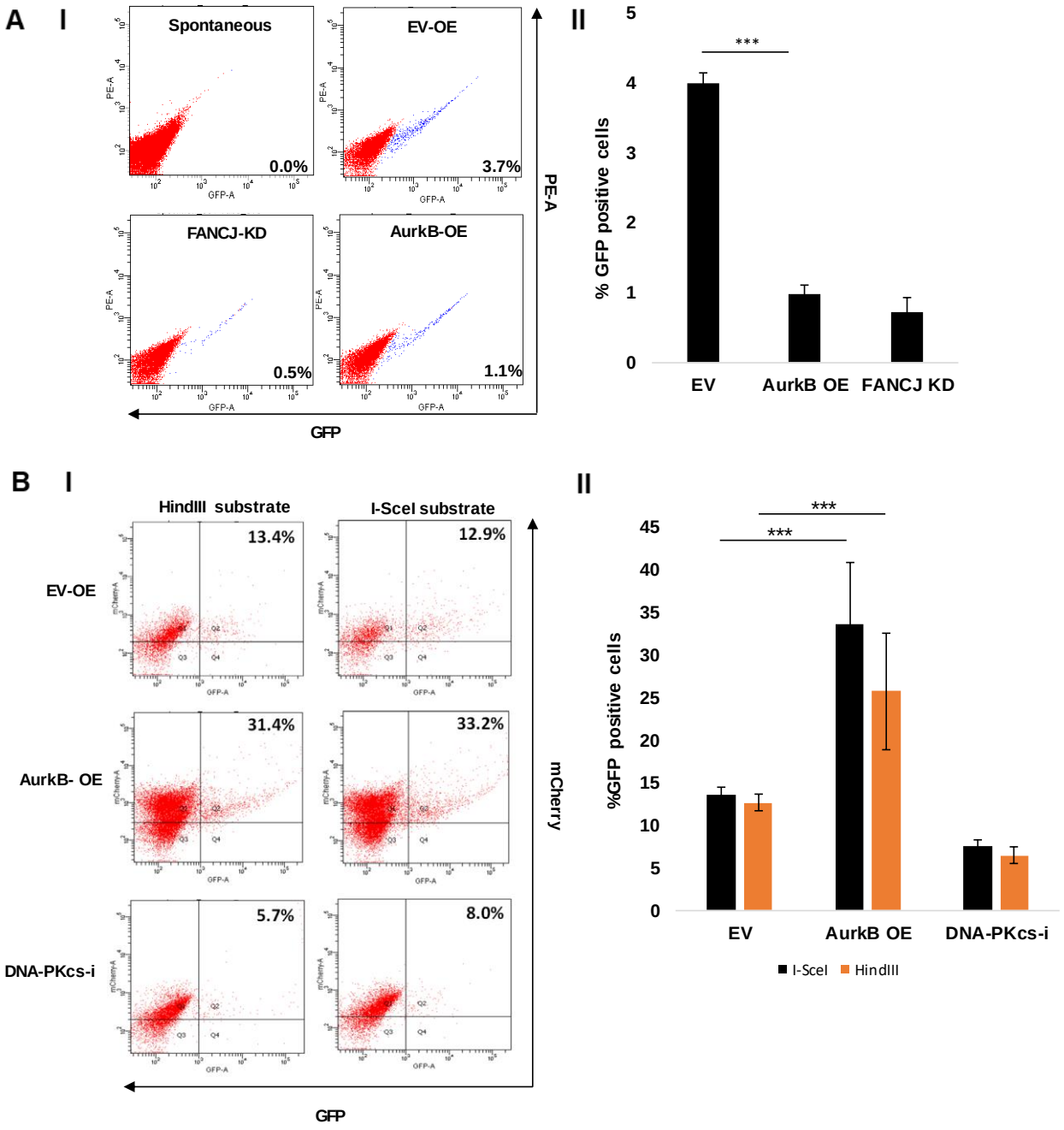

Figure 3.24: AurkB induces a compromised HR mediated repair and prefers the NHEJ pathway. A. *AurkB overexpression in SCR18-U2OS cells lead to a significant downregulation of the overall HR mediated repair while enhancing the NHEJ pathway as in* ***B****. Representative flow cytometry profiles have been shown in* ***panel-I*** *and the corresponding quantifications are represented in* ***panel-II*** *for each of HR and NHEJ assays.*

The alt-NHEJ pathway has been reported to be suppressed in growth arrested and serum starved cells (Singh SK et al., 2011; Windhofer F et al., 2007). Interestingly, AurkB expression is a representation of cellular proliferation as determined by high mitotic index. Our results, therefore, draw an interesting correlation between AurkB overexpression and de-repression of the alt-NHEJ pathway. Recent reports also suggest that the NuA4/Tip60 complex mediate a molecular discriminatory effect in preferring HR mediated repair over NHEJ (Tang J et al., 2013*;* Jacquet K *et al*., 2016). Our observations on the modulation of the overall repair pathway choice upon AurkB elevation were the exact opposite as that mediated by Tip60. This further settles our contention that AurkB mediated downregulation of Tip60 might be a guiding factor in the determination of repair pathway choice, which is being tilted more toward the error-prone NHEJ.

3.3. Reciprocal regulation of skeletal muscle differentiation by AurkA and POU6F1

General Introduction

Skeletal myogenesis is a fascinating outcome of the orchestration by different myogenic regulatory factor (MRF)s and the proteins involved in maintenance of the myogenic precursor cell (MPCs) population (satellite cells) (Figure 3.25). MRFs (Myf5, MyoD, MRF4 and myogenin) are the master regulators for the commitment of MPCs towards terminal differentiation of myoblasts. Myf5 and MyoD were earlier considered to be the commitment-related MRFs, while myogenin and MRF4 were considered to be the late or differentiation MRFs (Rudnicki MA et al., 1993; Rawls A et al., 1995; Braun T et al., 1995; Patapoutian A et al., 1995; Zhang W et al., 1995). However, later studies showed the involvement of MyoD in terminal differentiation, hinting it to a late MRF (Rawls A et al., 1998). Furthermore, MRF4 was shown to be necessary in the commitment of MPCs, suggesting that it may also play a role as an early MRF (Kassar-Duchossoy L et al., 2004). Myf5 is the earliest to be expressed chronologically and is regulated by a complex set of enhancers spanning 140kb of Myf5 regulatory region (Ott MO et al., 1991; Carvajal JJ et al., 2001).

The mouse models of MRF null mutations have served important roles in delineating the function of these MRFs *in vivo*. MyoD$^{-/-}$ mice are viable with normal physiology and morphology of skeletal muscles, with a compensatory upregulation in the expression of Myf5 (Rudnicki MA *et al.*, 1992). The skeletal muscles of Myf5$^{-/-}$ mice also appear morphologically normal and the levels of MyoD, myogenin or MRF4 do not change compared to the wild type. The Myf5 knockout mice, however, die perinataly due to the loss of distal parts of the ribs and inability to breathe. The only abnormality of skeletal muscle development in Myf5$^{-/-}$ mice is a delayed appearance of myotomal cells until MyoD is expressed (Braun T *et al.*, 1992). The absence of muscle deficiency in the MyoD$^{-/-}$ or Myf5$^{-/-}$ mice indicate a functional redundancy. Mice deficient in both MyoD and Myf5 (MyoD$^{-/-}$ Myf5$^{-/-}$) lack skeletal muscle completely (Rudnicki MA *et al.*, 1993). As myoblasts do not form in the MyoD/Myf5 double knockout, these two genes are considered as the early or commitment MRFs. Myogenin null mice also display a severe deficiency in skeletal muscle. However, they are able to form myoblasts but fail to fuse into myotubes. The myogenin null mice

die perinatally and only a few myofibers are observed at birth (Hasty P *et al.*, 1993; Venuti JM *et al.*, 1995; Nabeshima Y *et al.*, 1993). The lack of myofibers places myogenin in the later stages of differentiation and hierarchically downstream of MyoD and Myf5 (Rawls A *et al.*, 1995).

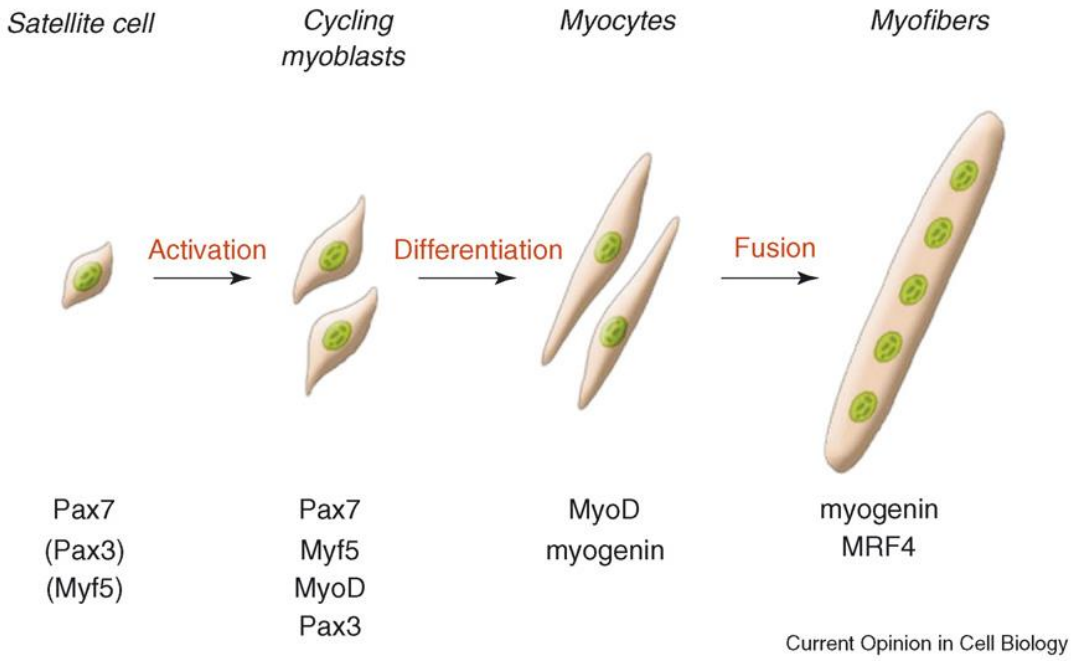

Figure 3.25: Schematic representation of adult myogenesis. *Quiescent muscle precursor cells become activated by external stimuli from the micro-environment or upon injury. The cycling skeletal myoblasts express the paired-box transcriptions factors Pax7 and Pax3, as well as the myogenic regulatory factors Myf5 and MyoD. Once committed to differentiation, myoblasts stop cycling and lose expression of Pax7, Pax3, and Myf5. Differentiating myogenin^{+ve} myocytes align and fuse to form multinucleated myofibers. MRF4 is further required for hypertrophy of the new fibers [Adapted from (Le Grand F et al., 2007)].*

The POU (*P*it l, *O*ct l, and Oct 2, *U*nc 86) domain is a bipartite DNA-binding domain, consisting of two highly conserved regions (POU-specific domain and POU homeodomain) tethered by a variable linker. The POU domain contain containing proteins are sub-divided into six broad classes and the members are heavily involved in various developmental processes (Lakich MM *et al.*,1998; Ryan AK *et al.*,1997). POU6F1, variously known as mPOU, Brn-5, or TCFβ1, is a transcription factor which is distantly related to other POU proteins that binds preferentially to a variant of the octamer motif (5'-ATGATAAT-3'). POU family members are involved in multiple processes ranging from cell fate decision of embryonic stem cells to cellular housekeeping. These family members possess two DNA-binding subdomains which have a bipartite arrangement of POU-specific (POU(S)) and POU-homeobox (POU(H)) subdomains separated by a linker region. The POU specific domain spans between 139 and 213 residues while the homeobox resides between 234 and 293 (Figure 3.26).

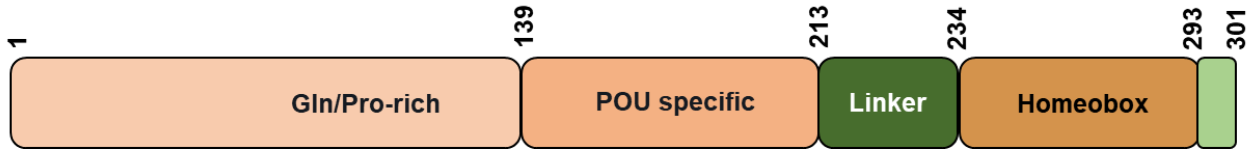

Figure 3.26: Schematic representation of various domains of mPOU. *The DNA binding domain of mPOU is a bipartite domain consisting of a POU specific and a homeobox domain linked by a flexible linker, while the N-terminal half is rich in Gln and Pro residues. The corresponding amino acid numbers are represented for each of the domains.*

The POU-family proteins play a vital role in controlling cell-fate determination and the timing of cellular events in a number of tissues (Wu R et al., 2001). Several members of the POU family have been identified as being transcription factors involved in various aspects of transcriptional regulation (Rosenfeld MG, 1991; Ruvkun G et al., 1991). The octamer element can be described as a bipartite site, with POU(S) contacting the ATGC sequence and POU(H) contacting the AAAT sequence (Laughon A et al., 1991; Verrijzer CP *et al.*, 1992). mPOU is expressed exclusively in the developing embryonic brain neocortex, whereas its expression is restricted to brain, heart, skeletal muscle and lung in the adult stages. Recent observation that the expression of TCFβ1 in both B and T cells and their ability to bind octamer and octamer-related motifs suggest that TCFβ1 has additional roles in lymphoid cell functionality. Expression of POU6F1 in the epithelial ovarian

carcinoma derived cell lines have shown the importance of mPOU in the proliferation of clear cell adenocarcinoma of the ovary.

Based on the *in-silico* screening and subsequent biochemical studies carried out in our laboratory, mPOU was identified to be a putative substrate of AurkA and Ser-197 was found to be the probable site of phosphorylation (Karthigeyan D et al., 2018). Although mPOU is reported to be expressed in a tissue specific manner in the adult stages of mice, the functional role of this transcription factor in tissue homeostasis remains unclear. The present study seeks to address the role of mPOU on one of mPOU expressing tissues systems- skeletal muscles, taking into consideration the well-established C2C12 myoblasts as a model system for the study. The following section, therefore, describes the functional outcome of AurkA and mPOU manipulations in skeletal muscle differentiation.

3.3.1. mPOU is phosphorylated at Ser-197 in cells

In order to study the existence of Ser-197 as a phospho-site in cells, we immunoprecipitated Flag-mPOU from HeLa cells (Figure 3.27) and carried out LC-MS/MS mediated analysis.

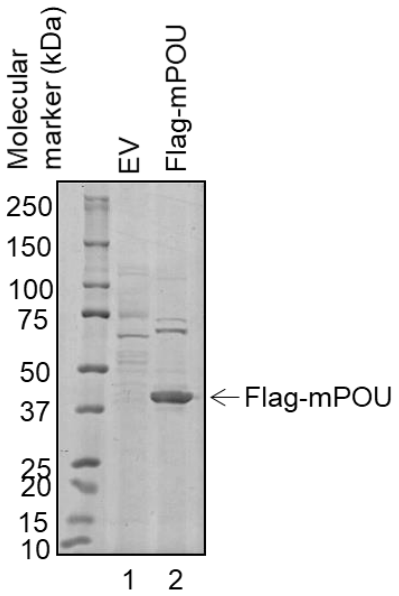

Figure 3.27: Purification of Flag fusion mPOU protein from HeLa cells. *Flag tagged mPOU fusion construct was transiently overexpressed in HeLa cells and purified using M2 agarose-based affinity purification. The purified fraction was separated on a 5-20% gradient SDS-PAGE and*

stained with coomassie brilliant blue. The profile of Flag tagged mPOU fusion protein has been represented.

Although we could achieve only 50% coverage of the entire protein in the mass spectrometry mediated peptide fragmentation (Figure 3.28A; highlighted in red), we could still find several phosphorylated sites of mPOU in cells, namely, Ser-74, Thr-75, Ser-78, Thr-194, Thr-239, Ser-240, and Thr-242. Interestingly, we could also detect Ser-197 (Figure 3.28A; highlighted in blue) as a phosphorylated site in cells, the mass spectra of which is represented in Figure 3.28B.

A

MPGISSQILTNAQGQVIGTLPWVVNSASVAAPAPAQSLQVQAVTPQLLLNAQGQVIATLA
SSPLPPPVAVR**KPSTPESPAK**SEVQPIQPTPTVPQPAVVIASPAPAAKPSASAPIPITCS
ETPTVSQLVSKPHTPSLDEDGINLEEIREFAKNFK**IRRLSLGLTQTQVGQALTATEGPAY**
SQSAICRFEKLDITPKSAQKLKPVLEKWLNEAELRNQEGQQNLMEFVGGEPSKKRK
RRTSFTPQAIEALNAYFEKNPLPTGQEITEIAKELNYDREVVRVWFCNRRQTLK**NTSKL**
NVFQIP

B

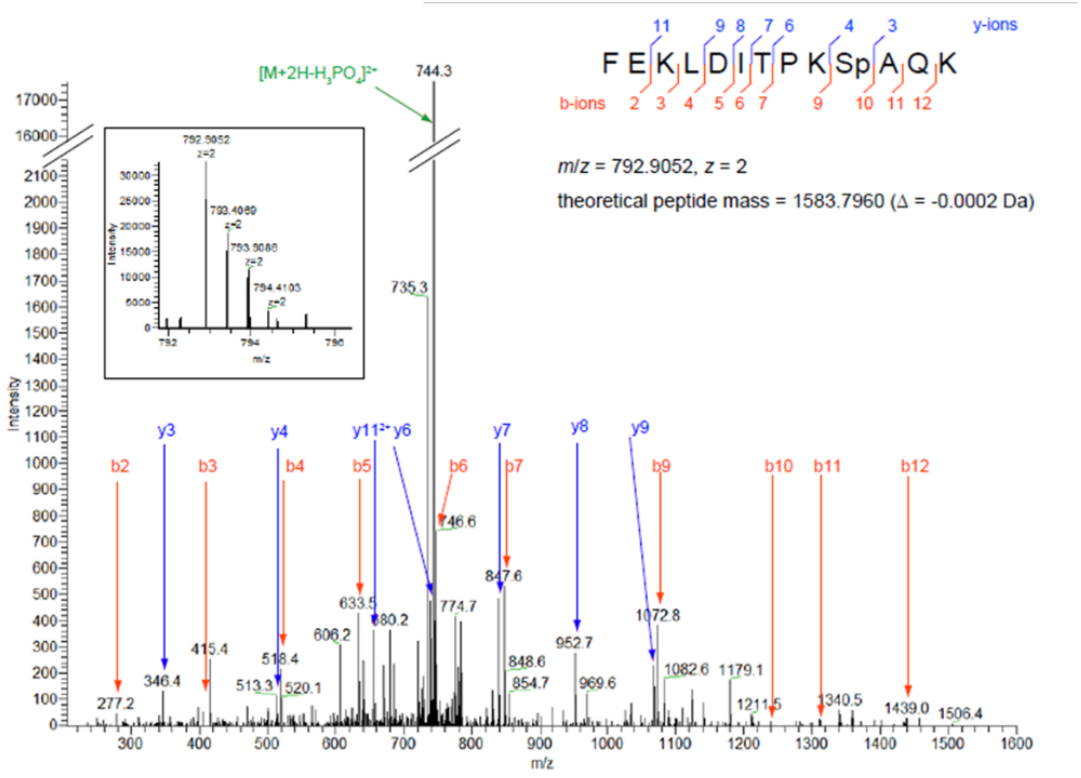

Figure 3.28: ***Mass spectrometric analysis of Flag-mPOU phosphorylation sites in HeLa cells.*** ***A.*** *Coverage of the amino acid residues in the LC-MS/MS bases analysis of Flag-mPOU has been indicated in red. Ser-197 residue has been highlighted in blue.* ***B.*** *Mass spectra for phosphorylated Ser-197.*

3.3.2. POU6F1 is phosphorylated by Aurora A kinase *in vitro* at Ser-197

We generated an anti-phosphorylated mPOU antibody specific for Ser-197 phosphorylation using phospho-oligo peptides (*cf*- Section 2.6.2.) and observed that the antibody could recognise the recombinant phosphorylated mPOU-WT protein but not the mPOU point mutant where Ser-197 is mutated to Ala (Figure 3.29). This result signifies the specificity of the antibody as well as highlights that Ser-197 is indeed phosphorylated by AurkA.

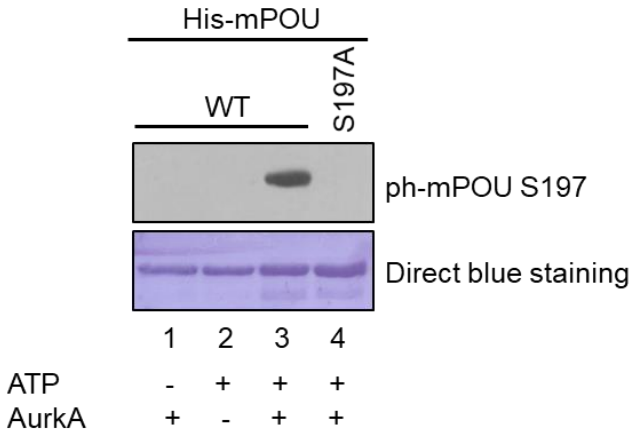

Figure 3.29: *His_6-mPOU WT or S197A point mutant were subjected to in vitro kinas assay using 5mM ATP and the corresponding wester blot representation for phospho-Ser197 antibody is shown. Direct blue staining represent that similar WT and mutant protein amounts were used for the reaction.*

3.3.3. Phosphorylation of mPOU at Ser-197 dramatically inhibits its cognate DNA binding

mPOU is a transcription factor that binds a bipartite octamer motif. We studied the effect of mPOU phosphorylation at Ser-197, on its DNA binding property. Interestingly, Ser-197 is one of the critical residues which directly contact the sugar-phosphate backbone of the consensus DNA element. This led us to hypothesise that phosphorylation of this residue might cause a partial disruption of the interaction between mPOU and its cognate DNA site. In order to validate this, we carried out gel-shift assays for recombinant His_6-WT, S197A (phospho-deficient) and S197D (phospho-mimetic)–mPOU proteins using a Brn-5 promoter oligonucleotide with the following sequence:

5’-GATCTGCTCCTGCATGCCTAATAGG-3’

3’-CTAGACGAGGACGTACGGATTATCC-5’

In agreement with our hypothesis, we observed that the phospho-mimetic (S197D) mutant exhibit a drastic and complete loss of the cognate DNA binding even at the highest protein concentrations (Figure 3.30). This result highlights the importance of Ser-197 and the possible role that AurkA mediated phosphorylation may play toward consensus DNA binding by mPOU in a physiological context.

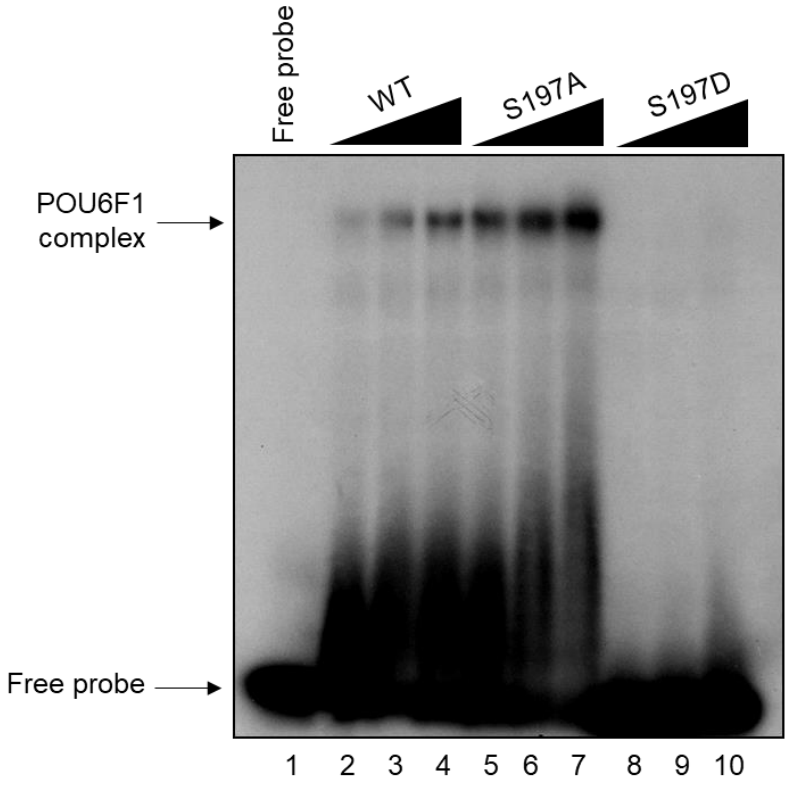

Figure 3.30: *Autoradiogram profile of a native PAGE performed using increasing amounts (100ng, 125ng and 150ng) of His_6-mPOU WT, S197A or S197D proteins purified from E. coli. The poly-histidine tagged proteins were allowed to form complexes with radiolabelled Brn5 oligonucleotide specific to POU6F1 for 30mins at 30ºC. Each of the reactions were loaded on a 4% native PAGE and subjected to electrophoresis in 0.5X tris-borate EDTA (TBE) buffer for 2hrs at 150V at 4ºC so as to ensure the integrity of the complexes. The gel was then dried and exposed against an X-ray film for 6hrs so as to visualize the complexes formed.*

3.3.4. Catalytic activity of AurkA is necessary for skeletal muscle differentiation

The function of AurkA during the transition from proliferation to differentiation of myoblasts is unknown. To study the necessity of AurkA catalytic activity and to distinguish between the roles of AurkA and AurkB in skeletal muscle differentiation, we treated C2C12 myoblasts with AurkA- or AurkB-specific inhibitors, MLN8237 or ZM447439, respectively and observed a significant decline in the expression of myogenin and myosin heavy chain levels upon MLN8237 treatment, but not for ZM447439 treatment (Figure 3.31A, compare lanes 2 vs 3 vs 4). Myf5 was found to undergo downregulation with the onset of differentiation (Figure 3.31A, lane 1 vs. 2), as reported earlier. AurkA inhibitor treatment led to a modest rescue of Myf5 levels, highlighting that the inhibitor treated myoblasts are retarded toward differentiation. These results indicate the critical role of the kinase activity during the onset of skeletal muscle differentiation. Furthermore, we observed a dramatic decline in the mitotic marker-H3S10 phosphorylation upon induction of differentiation, as the cells undergo G1 phase block upon differentiation induction (Figure 3.31B, lane 1 vs. 2), which further reduced upon inhibitor treatment (Figure 3.31B, lane 2 vs. 3 and 4). These results indicate that the myoblasts are exiting mitosis upon differentiation. Alternatively, as Aurora kinase phosphorylates histone H3 at Ser-10, a reduction in the level of the kinase upon differentiation concomitantly reduces H3 phosphorylation.

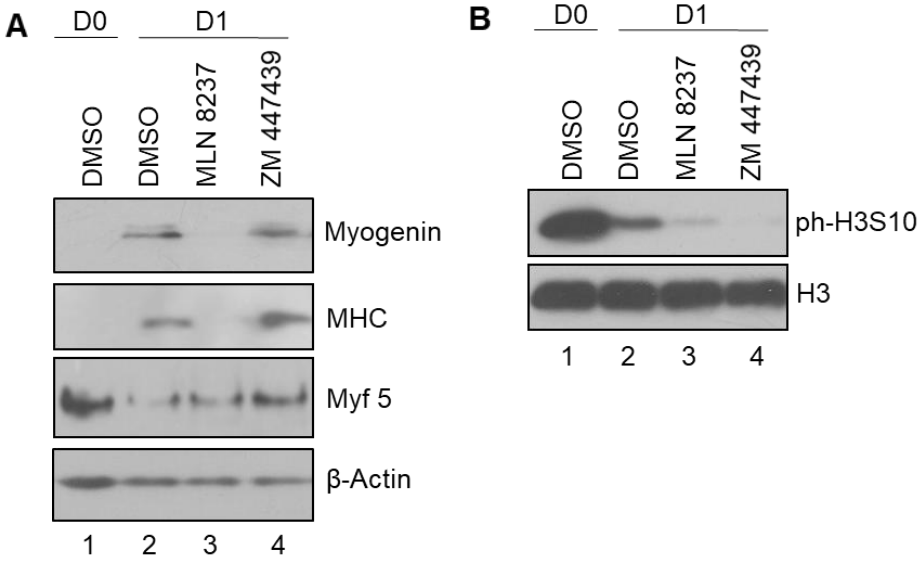

Figure 3.31: Catalytic activity of AurkA is necessary for differentiation. *Representative western blot exhibiting the altered expressions of the differentiation specific markers' levels (**A**) or H3S10 phosphorylation (**B**) on Day1 of C2C12 differentiation, using the indicated antibodies in the*

presence of MLN8237 and ZM44732 that inhibits AurkA and B, respectively. C2C12 myoblasts, maintained in proliferative media (DMEM,20%FBS), were treated with the corresponding inhibitors or DMSO for 2hrs prior to shifting them to differentiation media (DMEM,2% Horse serum). The cells were further treated with the compounds for a period of 24hrs (D1) before harvesting and lysing for analysis.

3.3.5. mPOU expression opposes skeletal muscle differentiation

We sought to understand the necessity of mPOU protein in the context of muscle differentiation. In this regard, C2C12 myoblasts were transfected with Flag tagged mPOU WT construct and the cells were induced to differentiate for 48hrs in the differentiation media. We observed a reduction in the levels of myosin heavy chain (MHC) (Figure 3.32A; right panel), a differentiation specific protein marker. Concordantly, the opposite effect was observed when C2C12 myoblasts were transfected with mPOU specific siRNA. We witnessed that the levels of MHC were increased manifold for the mPOU-siRNA treated cell population as compared to the control cells upon differentiation induction (Figure 3.32B; right panel). These results signify that mPOU may play a role which is opposite to that played by AurkA in the process of skeletal muscle differentiation.

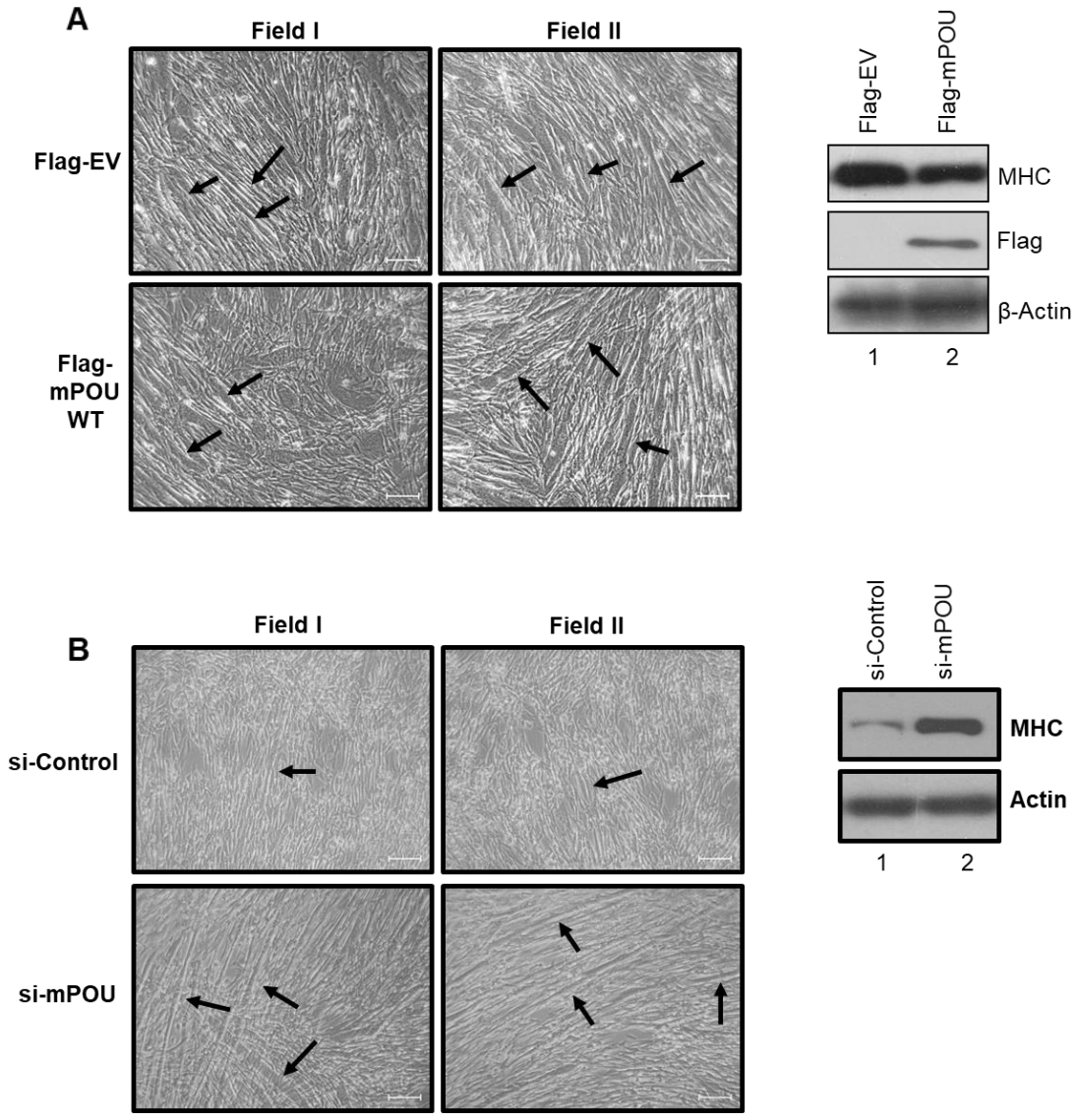

Figure 3.32: mPOU inhibits skeletal muscle differentiation. A; left panel. *Representative bright field images of two different fields of C2C12 myoblasts overexpressing either the empty vector construct (Flag-EV) or WT-mPOU (Flag-mPOU WT) construct, captured at 10X magnification 48hrs post onset of differentiation.* ***B; left panel.*** *Representative bright field images of two different fields of C2C12 myoblasts transfected with either the control siRNA (si-Control) or mPOU specific siRNA (si-mPOU), captured at 10X magnification 48hrs post onset of differentiation. The corresponding western blots for the indicated proteins extracted from mPOU overexpressed or downregulated cells, have been shown on the* ***right panels*** *for A and B respectively. Scale bar represents 100µm.*

CHAPTER 4: SUMMARY

Aurora kinases are well-studied mitotic kinases whose transcriptional roles are poorly studied. In an earlier attempt to uncover the non-mitotic functions of Aurora kinases through substrate phosphorylation, a screen for identification of novel protein targets was carried out in our laboratory (Karthigeyan D et al., 2018). The experimental strategy encompassed randomly designed oligo-peptides harbouring Ipl1 (yeast Aurora kinase) consensus phosphorylation motif flanked by different combinations of amino acid sequences. Five novel proteins factors, including Max was identified as the probable targets of Aurora kinase A (Karthigeyan D, and Kundu TK; unpublished). We observe that Max exhibits promiscuity as a substrate for both Aurora A and B kinases in its full-length protein context, as determined by *in vitro* assays. However, using specific small molecule inhibitors that display robust specificity against Aurora A or B kinases respectively, we identify Aurora kinase B as the likely kinase phosphorylating Max *in vivo* at multiple C-terminal serine residues. Interestingly, these serine clusters lie in close proximity to the nuclear localization signal of Max, which prompted us to study a probable effect on Max localization upon perturbation of these putative phosphorylation sites. Using phosphorylation-deficient or mimetic mutants, we observe that phosphorylation endows Max with a greater efficiency of nuclear localization. This result highlights the probability of an effect on Myc/Max target genes through phosphorylation dependent alteration of Max sub-cellular distribution. Concordantly, Aurora kinase B knockdown or inhibition in triple negative breast cancer (TNBC) cell line, MDA-MB-231, causes a significant alteration of gene expression of the Myc/Max direct target genes. We also observe an upregulation in the expression of genes like RARB and GATA6 upon Aurora kinase B knockdown, which might be an indirect evidence of RARα/Myc hetero-oligomer formation owing to a potential compromise in Myc and Max dimerization in the nucleus.

Apart from studying the modulation of the transcriptional outcomes of Myc through Max phosphorylation, we also address one of the potential modes of dysregulation of Aurora kinase B, through protein stabilization, in cancer. We find that Tip60 acetylate Aurora kinase B at two closely spaced lysine residues and not only inhibits its kinase activity but also its protein stability. Aurora kinase B, on the other hand, impinges upon Tip60 gene repression and therefore, dictates the choice of DNA damage repair. Elevated expression of Aurora kinase B inhibits HR and

facilitates NHEJ. We also observe that Aurora kinase B is capable of inflicting DNA Damage Response (DDR), as is evident by the alteration of basal levels of γH2AX with that of Aurora kinase B levels.

Finally, we study a potential aspect of regulation of a non-oncogenic, yet physiologically important function of Aurora kinase A in the regulation of skeletal muscle differentiation. We find that the catalytic activity of Aurora kinase A, but not Aurora kinase B, is necessary for maintaining the differentiated state of skeletal muscles. Using small molecule chemical inhibitors, we demonstrate that Aurora kinase A inhibition leads to a complete block in the differentiation process. Furthermore, overexpression of one of the novel Aurora kinase A substrates, mPOU, retards C2C12 myoblast differentiation. These results emphasize the possible operation of a negative feedback loop between Aurora kinase A and mPOU in the differentiation of skeletal muscle differentiation.

CHAPTER 5: DISCUSSION AND FUTURE PERSPECTIVES

Chapter Outline

5.1. Discussion

5.1.1. Ramifications of Aurora kinase B expression on Myc/Max target genes in cancer manifestation

5.1.2. Tip60-Aurora kinase B negative feedback loop in determining carcinogenesis

5.1.3. Aurora A-mPOU axis of action in the regulation of skeletal muscle differentiation

5.1. Discussion

Aurora kinase B is the catalytic component of the chromosomal passenger complex (CPC) and ensures proper chromosome alignment and segregation. It also assists in cleavage furrow formation and cytokinesis and hence, a reduction in its kinase activity by either small molecule chemical inhibitors or RNA interference gives rise to chromosome segregation defects and aneuploidy. Aurora kinase B overexpression in cultured cells and mouse model is reported to be tumorigenic by inhibiting p53 and p21 activity (Gully CP et al., 2012; González-Loyola A et., 2015) or by modulation of Myc dependent tumours (den Hollander J et al., 2010; Yang D et al., 2010). Furthermore, the paralogue, Aurora kinase A, has been reported to participate in varying signalling events which culminate into tumorigenesis and cancer progression (Katayama H et al., 2004; Briassouli P et al., 2007; Otto T et al., 2009; Lu L et al., 2015; Zheng F et al., 2016).

The present study contributes to the expansion of our knowledge about Aurora kinase biology from two distinct dimensions. We not only highlight the novel oncogenic roles of Aurora kinase B in cancer manifestation but also emphasize the importance of the kinase activity of Aurora A in the regulation of a basic physiological process of skeletal muscle differentiation. We could further segregate the effects of dysregulated Aurora kinase B in carcinogenesis into two definite sub-actionable modes, firstly through the modulation of transcriptional output of the enigmatic Myc oncogene through Max phosphorylation and secondly, by pitching the balance of DNA damage repair in favour of an error-prone DNA damage repair pathway on the other, thus generating a toxic cocktail for conferring malignancy to an otherwise normal cell.

5.2. Ramifications of Aurora kinase B expression on Myc/Max target genes in cancer manifestation

We identified Myc Associated factor-X (MAX) as a probable substrate of Aurora kinase A in a screen, directed to the identification of novel nuclear or nucleolar proteins whose involvement lie within the realms of transcription and DNA repair (Karthigeyan D, and Kundu TK; unpublished). Max belongs to the bHLH-LZ superfamily of proteins and plays non-redundant roles in development (Shen-Li H et al., 2000). It is an obligatory dimerization partner of Myc (Blackwood

E.M. et al., 1991) and is necessary for E-box dependent transcription and oncogenesis. Max, however, displays a biphasic nature of regulation depending on the cellular concentration of Myc (Prendergast GC et al., 1992). It usually forms a homodimer or may heterodimerize with other bHLH-LZ family proteins like Mad, Mxd, Mlx and Mnt (usually called the Max network proteins). Myc, being an immediate early response gene, exhibit growth factor dependent expression. Accumulation of high Myc levels in cells sequester Max away from the other bHLH-LZ family proteins and forms the c-Myc/Max heterodimer, which in turn affect the downstream target genes. Furthermore, post translational modifications like phosphorylation is noted to affect Max activity and subsequently affects Myc/Max dependent functions. Casein kinase II (CKII) is reported to phosphorylate Max at its N-terminal Ser-2 and Ser-11 residues which inhibit its homodimer formation (Berberich SJ et al., 1992; Prendergast GC et al., 1992). Although it is postulated that CKII might also phosphorylate multiple C-terminal serine residues of Max that obey the CKII consensus phosphorylation motif (Ser/Thr residues present within a microenvironment rich in acidic amino acids like Asp or Glu), the results do not conclusively reveal the involvement of this kinase. Interestingly, mutation of these C-terminal serine residues to the corresponding phospho-deficient mutant (S131A-S133A-S135A) hampers the DNA binding of the Myc/Max heterodimer while assisting the same for the Max homodimer (Prendergast GC et al., 1992). Moreover, recent reports indicate that Max mutations in hereditary pheochromocytoma and paraganglioma lead to the generation of the truncated or mutated protein with altered functions (Comino-Méndez I et al., 2011; Burnichon N et al., 2012). Intriguingly, Ser-133 is found to be mutated in a fraction of these patients and postulated to affect Max homodimerization and hence the repressive functions, with the disease as an outcome.

Using specific small molecule inhibitors, we found that Aurora kinase B, and not Aurora kinase A, is the dominant kinase phosphorylating Max in cells. We also ascertained that the C-terminal stretch of serine residues represent the likely target of phosphorylation which enforces nuclear distribution of Max twice more likely, when compared to the unphosphorylated counterpart, in cells. We conjecture that the nuclear enrichment of Max may serve as one of the limiting factors in its dimerization with Myc in the nucleus and in determining Myc/Max dependent transactivation of the enhancer-box (E-box; the consensus DNA element for Myc/Max heterodimer) containing target gene promoters. A reduction of Max C-terminal phosphorylation may, therefore, cause reduced Myc/Max dependent transcription.

With an aim to study the effects of Aurora kinase B phosphorylation of Max on the modulation of Myc/Max target genes, we focussed on a cancer model which displays dependence on the Myc oncogene. Breast cancer is one such archetypical examples which displays Myc pathway activation, albeit with a certain specificity. It has been shown that the gene expression signature (a subset of genes whose differential expression constitutes a hierarchical cluster and can be used as a reference to define a subtype-specific gene expression pattern) of the basal-like or the TNBC subtype is reminiscent of the core set of genes which are being modulated by Myc upon activation by growth factors (Chandriani S et al., 2009; Horiuchi D et al., 2012). Furthermore, Myc shows preferential overexpression in TNBC cells, which partially explains Myc-addiction observed for the TN tumours (Brasó-Maristany F et al., 2016; Horiuchi D et al., 2016).

We sought to study a probable synthetic lethality that may exist between the Myc network and Aurora kinase B knockdown/inhibition, which may not only address the effects of Aurora kinase B perturbation on the Myc/Max targets but also possibly unveil Aurora kinase B as a therapeutic vulnerability for Myc dependent cancers. Upon analysis of a TCGA cohort of breast cancer patient samples, we observed that Aurora A and B kinases exhibit significant upregulation at the transcript level in the tumours as compared to the normal samples. Intriguingly, we also unveil a significant preponderance for upregulation of both Aurora A and B kinases in the basal-like/triple negative (TN) tumours over the other subtypes and normal samples. We considered TNBC as a model system and employed MDA-MB-231 TNBC cells for studying the effects on Myc/Max dependent gene expression patterns. In agreement with the hypothesis of higher nuclear retention of Max by Aurora kinase B phosphorylation, we indeed observed that either downregulation or inhibition of Aurora kinase B affected the Myc/Max activated or repressed gene sets. Interestingly, we also observed a concomitant enhancement in the transcription of certain differentiation related genes like *GATA3*, *GATA6* and *RARB* in triple negative breast cancer cells upon Aurora kinase B knockdown.

An earlier attempt to study the Max independent functions of Myc led to the identification of an interesting synergy between retinoic acid receptor-α (RARα) and c-Myc which seemed to be dependent on the PAK2 kinase (a stress activated kinase). PAK2 phosphorylates the C-terminal basic helix-loop-helix domain of c-Myc which causes its dissociation from Max (Uribesalgo I et al., 2011). The phospho-mimetic mutant of c-Myc (PAK2 phosphorylated residues), when

overexpressed, was observed to interact with RARα and transcriptionally activate the pro-differentiation genes like *RAR-β* (*RARB*), *GATA6* and the *HOX* gene clusters from retinoic acid response elements (RAREs) that are present on the promoter of these genes. This causes a switch from an oncogenic to a tumour suppressive role for c-Myc. As our gene expression results display an upregulation of the RARα target genes upon Aurora kinase B downregulation, we propose that this may occur owing to the accumulation of a free pool of monomeric c-Myc, which may now bind to RARα and affect the differentiation-related target genes in a RARE-dependent manner. This result emphasizes a possible reduction of Myc and Max dimerization when Aurora kinase B is targeted in cells.

TN tumours display poorly differentiated morphology and a majority of these tumours exhibit massive downregulation of *GATA3*. *GATA3* is a marker for the breast luminal cells (Kouros-Mehr H et al., 2006) and an enforced *GATA3* expression in TNBC cells lead to a change in gene expression signature from basal-like to the luminal-like pattern (Chu IM et al., 2012). Furthermore, *GATA3* expression is tumour suppressive in nature and causes a reduction in migration and invasive properties of the TNBCs in mice (Yan W et al., 2010; Dydensborg AB et al., 2009; Chu IM et al., 2012). Our observation of *GATA3* de-repression in Aurora kinase B knockdown cells reflects a promising strategy to overcome the poor differentiation observed for TN tumours and possibly rescue the chemo- and radiotherapeutic resistances observed for these tumours. Based on our preliminary observations and speculations, we propose a model for the action of AurkB mediated regulation of Myc/Max dependent gene transcription and the probable effects that might emanate upon AurkB perturbation (Figure 5.2.1).

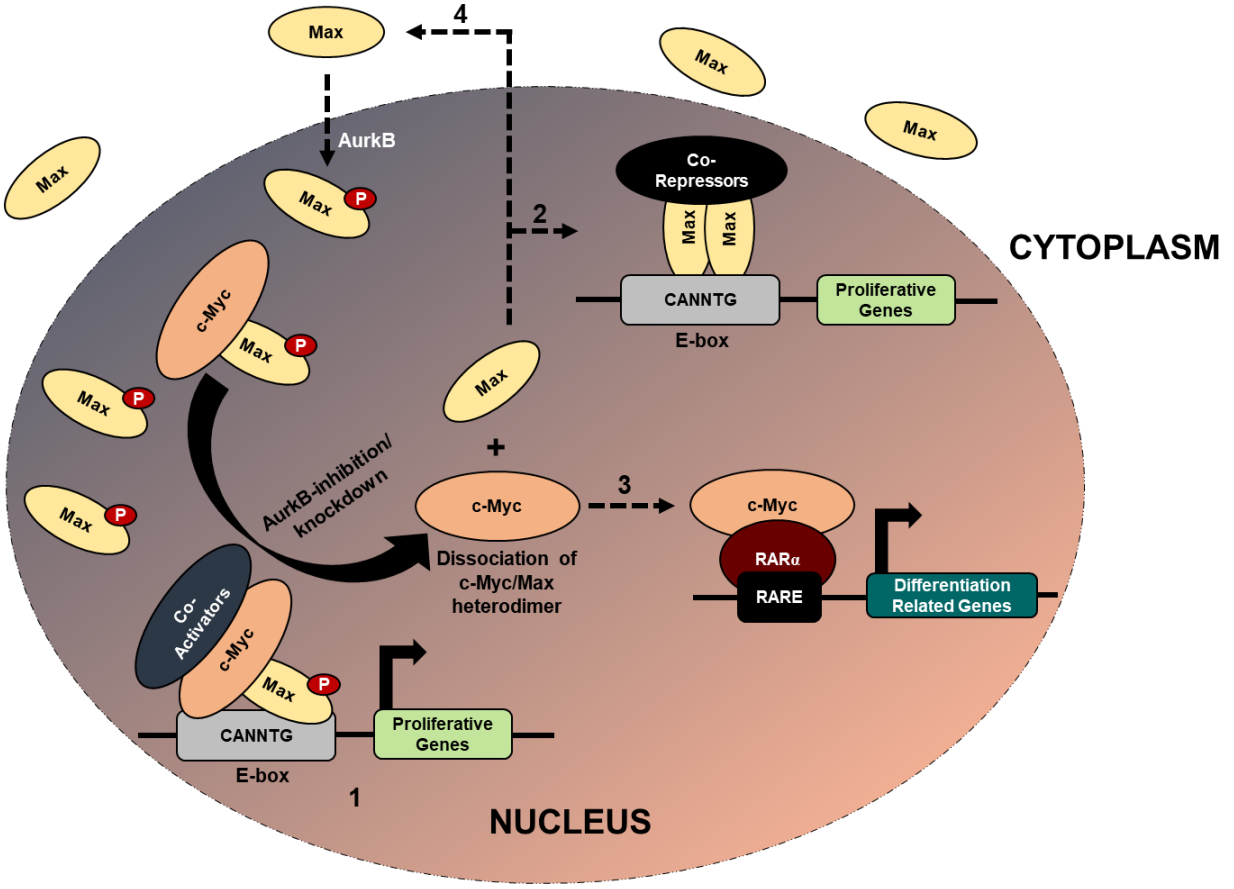

Figure 5.2.1: Proposed model highlighting the intricate regulatory mechanism for Myc/Max dependent and independent transcription by Aurora kinase B *[1- E-box engagement of Myc/Max heterodimeric complexes with co-activators like p300 or Tip60; 2- Homodimeric Max, generated upon AurkB perturbation displaces Myc and occupies the E-boxes; 3- "Free" Myc interacts with factors like RARα and is recruited to differentiation related genes; 4- Reduction in Max phosphorylation levels upon AurkB knockdown or inhibition expels it out of the nucleus, thus reducing the probability of Myc/Max heterodimerization].*

Our results on perturbation of Aurora kinase B and the subsequent effects on Myc/Max dependent gene expression is enthralling in the light of the fact that Myc is undruggable. Various efforts have been undertaken till date to identify the synthetic lethality associated with Myc. We believe that Aurora kinase B may represent one of such therapeutic vulnerabilities which can be targeted using highly potent and specific small molecule inhibitors (like the orally bio-available AZD1152-

HQPA) to contain the oncogenicity of Myc dependent cancers. As the initial observation of Myc regulating *RARB* expression in conjunction with RARα was made in HL60 (promyelocytic leukaemia) cells (Uribesalgo I et al., 2011), we speculate that Aurora kinase B perturbation for Myc dependent cancers will prove to generate feasible therapeutic options and likely to be effective across solid and haematological malignancies. However, as it is understood that Myc, not being a pioneer transcription factor (Soufi A et al., 2015), binds to genomic locations possessing active chromatin marks (Guccione E et al., 2006; Zeller KI et al., 2006), and which is further facilitated through Myc-dependent recruitment of co-activators like p300, PCAF and Tip60 (Faiola F et al., 2005; Frank SR et al., 2003; Liu X et al., 2003), we argue that the set of genes directly modulated by Myc/Max complexes would differ depending on the cell type, as the active chromatin state varies for different cell lineages. Moreover, as the mechanism of Aurora kinase B mediated Max phosphorylation seems to be a more general event which might be prevalent in probably all cells, it is also necessary to study whether the viability of normal cells get affected upon Aurora kinase B perturbation.

Our observations bring forth new avenues of studying Myc biology. We speculate that it will be important to study two aspects which might vary on the cell type under consideration. Firstly, the study of the Myc interactome upon Aurora B perturbation will reveal the protein partners that are necessary to bring about tumour suppressive functions by Myc, as carried out by RARα. Secondly, subsequent ChIP-sequencing of Myc under the same conditions may reveal the actual genomic targets that Myc engages in a Max independent manner, in association with other proteins or transcription factors, to bring about its tumour suppressive roles. These studies will, in retrospect, represent the cohort of genes that are being modulated by Aurora kinase B overexpression, through constant Max phosphorylation, to bring about Myc/Max dependent oncogenesis as opposed to tumour suppression. Although RARB re-expression, which is otherwise repressed in TNBCs, is being targeted as a pro-differentiation therapy (Merino VF et al., 2016; Bansal N at al., 2016), and our result of RARB de-repression upon Aurora kinase B knockdown is intriguing, we still believe that the reach of Max independent functions of Myc may be beyond the retinoic acid pathway and can be answered by the Myc interactome and genome wide redistribution of Myc upon Aurora kinase B perturbation.

Finally, it is important and necessary to study two more aspects which may guide a future investigation in the regulation of Myc/Max biology through Aurora kinases. Firstly, we have observed that Myc in itself undergoes phosphorylation by both Aurora A and B kinases *in vitro* (Figure 5.2.2A) and associates with Aurora kinase B in cells (Figure 5.2.2B). It would be interesting and important to unveil the Aurora mediated phosphorylation residues on Myc which will help us in understanding the supreme role of Aurora kinases in regulating the oncogenic functions of Myc, in its entirety.

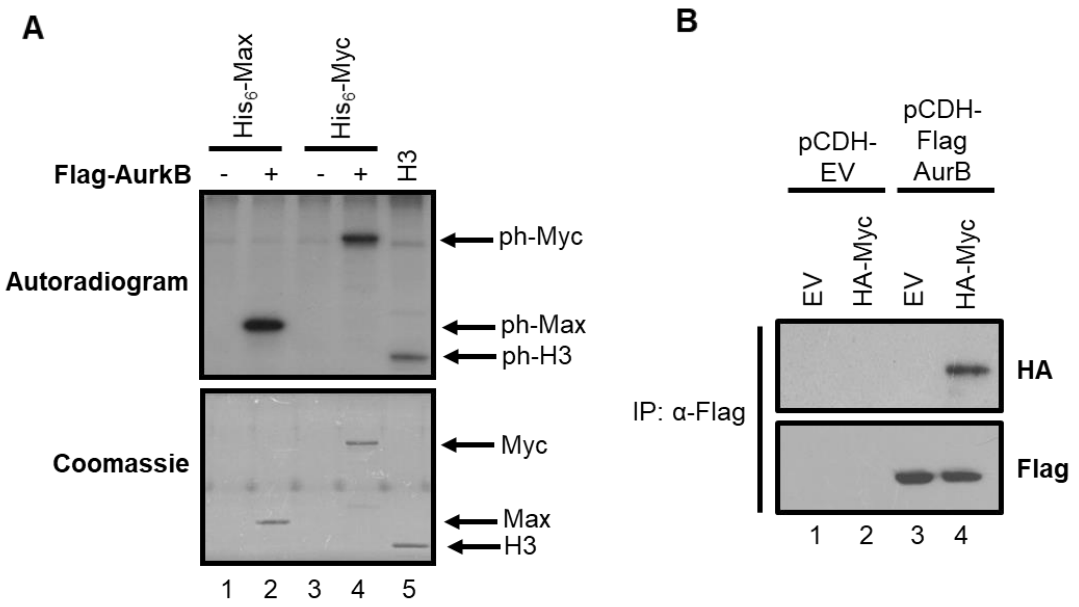

Figure 5.2.2: Aurora kinase B phosphorylates c-Myc. A. *In vitro kinase assay of 1µg each of recombinant His_6-Max (lane 2) and recombinant His_6-Myc (lane 4) or 500ng of histone H3 (lane 5; positive control) was performed using Flag-AurkB purified from HEK291 cells stably overexpressing Flag-AurkB and γP^{32} ATP. The coomassie staining for each of the lanes is shown below the autoradiogram profiles for comparing the loading levels across each lane.* ***B.*** *Western blot representation of co-immunoprecipitation showing the interaction between HA-His-Myc (transiently overexpressed for 48hrs) and Flag-AurkB in HEK293 cells stably expressing Flag-AurkB protein.*

Secondly, while studying the localization of Max phosphorylation mutants in cells, we observed that the cells harbouring the phospho-deficient mutant of Max were visibly bigger in size, possibly indicative of a G2-M arrest. Myc, in association with Max, is well known to be necessary for the

transactivation of genes that aid in G2/M progression. This result is introspective as it highlights the possibility of reduced Myc and Max association and hence reduced expression of the cell cycle progression genes. This prospect, however, needs to be quantified through DNA content analysis using flow cytometry, post transfection with either the WT or the phosphorylation mutants of Max.

5.3. Tip60-Aurora kinase B negative feedback loop in determining carcinogenesis

Post translational modification (PTM)s endow proteins with a plethora of alterative functional options and has emerged as an important regulatory strategy in higher eukaryotes. Aurora kinases are no exception and harbours numerous PTMs that dictate their spatial localization and kinase activity. Acetylation is one of the PTMs which has transpired in the fine tuning of dynamic mitotic processes (Robbins AR et al., 2005) and has bee shown to be necessary in the condensation of mitotic chromosomes by Aurora kinase B (Li Y et al., 2006). Recent observations also highlight intricate involvement of various HDACs with Aurora B at different stages of mitosis in determining error-free mitotic progression (Fadri-Moskwik M et al., 2012; Guise AJ et al., 2012).

The acetyltransferase Tip60 act as a transcriptional co-activator for many transcription factors like c-Myc ((Frank SR et al., 2003), p53 (Tang Y et al., 2006; Sykes SM et al., 2006), E2F1 (Taubert S et al., 2004; Van Den Broeck A et al., 2012), and NFκB (Briassouli P et al., 2007; Kim JW et al., 2012). It also plays interesting repressive actions toward STAT3 (Xiao H et al., 2003). More importantly, the role of Tip60 in DNA damage response is widely correlated (Squatrito M et al., 2006; Ikura T et al., 2000; Sun Y et al., 2010; Ikura T et al., 2007; Ikura M et al., 2015; Sun Y et al., 2005; Hu R et al., 2013) and recent evidences also highlight its involvement in facilitating the accurate repair of DNA damage while inhibiting the error-prone repair pathways (Tang J et al., 2013; Jacquet K et al., 2016; Clarke TL et al., 2017). Tip60 is further observed to be downregulated in different cancer types (Gorrini C et al., 2007; Mattera L et al., 2009), with reduced Tip60 levels consequently heightening mutation accumulation and genomic rearrangements (Bassi C et al., 2016), possibly due to the enhanced functioning of the error-prone pathways.

DNA is susceptible to incessant damage by endogenous and exogenous sources which pose serious threat to the stability of the genetic code. DNA lesions can reach as high as 70,000 events per cell per day (Lindahl T et al., 2000), majority of which are single strand DNA (ssDNA) breaks, arising from oxidative damage or base hydrolysis. The conversion of these ssDNA break events to a minor fraction of double strand DNA (dsDNA) breaks can be potentially lethal. Cells have evolved multiple pathways to repair these DNA lesions to maintain the stability of the genome. The major pathways of repair of damaged DNA include the homologous recombination (HR) and the non-homologous end joining (NHEJ) pathways, amongst others. HR dependent repair necessitates the presence of a homologous template and is, thus, usually dependent on the S-phase of the cell cycle and occurs through sister chromatid recombination (SCR) in somatic cells. HR/SCR is an infallible mode of repair and maintains genomic integrity. NHEJ pathway, on the other hand, does not require a corresponding template, and directly joins the broken ends with minimal or no homology. It follows a comparatively rapid kinetics and is more error-prone as it leads to generation of mutations and translocations at the broken end. NHEJ consists of at least two sub-pathways- "classical" NHEJ (C-NHEJ) pathway which is dependent on the Ku heterodimer and ''alternative'' NHEJ (A-NHEJ) pathway, which usually generates microhomology sequence-mediated end ligation. Cancer cells may preferentially utilize the NHEJ pathway to repair the damage and subsequently introduce mutations that can be eventually selected to provide growth advantages. Overexpression of the NHEJ pathway proteins also confer radio- and chemotherapeutic resistances to the cancer cells (Sirzén F et al., 1999; Shintani S et al., 2003; Zhang M et al., 2010). This addiction has been exploited to selectively target proteins like ligase IV, either singly or in combination with chemotherapeutic agents to kill tumours (Srivastava M et al., 2012). Germline defects in DNA repair pathway genes or inactivation of the signalling events for repair or enhancement of the error-prone NHEJ pathway signalling, therefore, generates a toxic milieu for accumulation of further mutations or translocation events, concomitantly causing instability of the genome.

Another aspect of genomic instability manifests itself through DNA ploidy alteration which arises due to multiple centrosomes or improper spindle kinetochore attachment and failure of spindle assembly checkpoint. Unequal chromosome segregation is a potent source of chromosomal gain or loss that may affect cellular transformation. Aurora kinases have profound impact in inducing ploidy alteration owing to their involvement in centrosomal and centromeric events. High Aurora

kinase A levels cause centrosome anomaly wherein the centrosomes undergo more than one round of duplication per cell division cycle. Presence of multiple centrosomes lead to errors in attachment to microtubules, causing mis-segregation of chromosomes and serve as a major source of aneuploidy in cells (Goepfert TM et al., 2002; Meraldi P et al., 2002; Lentini L et al., 2007). Aurora kinase B, on the other hand, play pivotal role in kinetochore-microtubule attachment and formation of cytokinetic cleavage furrow. Elevated Aurora B levels give rise to improper spindle assembly checkpoint (SAC) and faulty cytokinesis (Krenn V et al., 2015; Gurden MD et al., 2016; Shandilya J et al., 2016), thus giving rise to aneuploid and multinucleated cell population which also cause centrosome amplification, concomitantly. Absence of a viable p53 dependent checkpoint exacerbates the effect of Aurora A and B kinase overexpression on supernumerary centrosome formation and polyploidization (Meraldi P et al., 2002; Giet R et al., 2005). Surprisingly, the requirement of Aurora A is also highlighted in SAC, which functions through Haspin-Aurora B feedback axis (Yu F et al., 2017).

Aurora kinase A has been extensively studied in the context of DNA damage repair regulation (Katayama H et al., 2012; Wang Y et al., 2014), Furthermore, the existence of an inverse relationship between Aurora A and B kinases and BRCA1/2 activity has been worked out well (Wang Y et al., 2014). Moreover, the catalytic activity of Aurora kinase A has been shown to inhibit both the HR and the NHEJ pathways (Sourisseau T et al., 2010; Do TV et al., 2017), placing it at pivotal juncture in the regulation of DNA damage repair events. These results indicate Aurora A to be an inhibitory kinase which must be inactivated for proper functioning of DDR to maintain stability of the genome. In line with these results, it is observed that the kinase activity of Aurora A is inhibited upon DNA damage and repair induction (Krystyniak A et al., 2006). Although induction of DNA damage inhibits Aurora kinase B activity by multiple modes (Monaco L et al., 2005; Fell VL et al., 2016), understanding of the molecular events related to Aurora kinase B expression in influencing DDR pathway choice, however, is less clear.

We found a previously unanticipated link between Aurora kinase B and modulation of DNA damage repair pathway. We were intrigued to find that Aurora kinase B modulates the basal levels of γH2AX, a marker for DNA damage response (DDR). DDR is an anti-cancer barrier that is usually observed in pre-cancerous lesions (Bartkova J et al., 2005; Gorgoulis VG et al., 2005). This observation paves way for coining of Aurora kinase B as a potential oncogene, as an elevation

in the levels of various oncogenes like Myc, cyclin E and E2F1 inflict DDR (oncogene-induced DDR) (Bartkova J et al., 2005; Gorrini C et al., 2007; Mattera L et al., 2009). Aurora kinase B was also found to exhibit elevated expression in all the breast cancer cells we studied, as compared to a normal-like epithelial cell line, MCF10A. Surprisingly, the levels of the haploinsufficient tumour suppressor acetyltransferase Tip60, was found to be reduced in all the cells with elevated Aurora B and Tip60 gene expression was validated to be de-repressed upon Aurora kinase B knockdown. As the recent evidences bring forth the molecular discrimination that Tip60 carries out through H4 acetylation in promoting HR mediated repair and inhibiting NHEJ, our observation of Aurora kinase B repressing Tip60 posed the probability of Aurora B elevation in expression in influencing the choice of DNA damage repair pathway through Tip60 repression. We indeed observed that ectopic Aurora kinase B expression inhibited HR and facilitated NHEJ dependent repair.

Additionally, we observed that Tip60 exhibits its tumour suppressive effects by acetylation of Aurora kinase B at two highly conserved lysine residues within its kinase domain. Tip60 mediated di-acetylation leads not only to the inhibition of kinase activity of Aurora B but also enforces a reduction in its protein levels. Collectively, our observations underscore an intricate functional interplay between AurkB and Tip60, frailty of which may be an initial event in carcinogenesis.

We conjecture that under normal physiology, Tip60 mediated acetylation may serve to contain Aurora kinase B oncogenicity; elevation of AurkB levels in cancer through transcriptional dysregulation or genomic amplification impairs Tip60 gene transcription, which subsequently stabilize AurkB protein and pitches the balance in favour of faulty DNA damage repair and genomic instability (Figure 5.3.1).

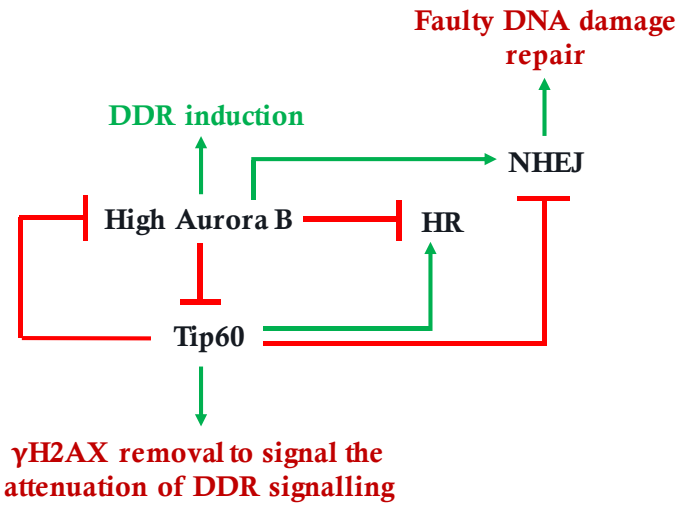

Figure 5.3.1: ***Proposed model for functional interaction of AurkB - Tip60 network in carcinogenesis.***

One of the important highlights that our study provides is about the suppression of HR mediated DNA damage repair upon AurkB overexpression. Earlier observations have emphasized that HR defective tumours are synthetic lethal for PARP1 inhibition. However, it is usually observed that the tumours develop PARP inhibitor resistance owing to multiple reasons; one such reason being the reversal of *BRCA1* or *BRCA2* mutations, which causes HR inactivation, to the WT allele. This causes restoration of HR and loss of PARP1 inhibitor sensitivity. We postulate that the AurkB overexpressing cells might be susceptible to PARP1 inhibitor mediated cell death, thus emphasizing an underlying possibility of killing AurkB overexpressing tumours with PARP1 inhibitors.

Although our assays for Aurora kinase B overexpression in cells inflicting DDR signifies the importance of Aurora kinase B as an oncogene, it is necessary to examine whether Aurora kinase B can drive DDR in cells upon Tip60 knockdown or not. This study will clarify the haplo-insufficient nature of the Tip60 tumour suppressor in the context of AurkB mediated oncogenesis.

As Aurora kinase B does not possess a DNA binding domain, the mechanistic understanding of Tip60 repression by elevated Aurora kinase B levels is presently unclear and requires future investigation. It is feasible that Aurora B engages transcriptional repressors onto the Tip60

promoter or phosphorylate oncogenic transcription factors which in turn may repress Tip60 through the recruitment of co-repressors.

5.4. Aurora A-mPOU axis of action in the regulation of skeletal muscle differentiation

Skeletal muscle differentiation represents a well-balanced act of cycling myoblasts and cell cycle phase specific block to promote the initiation of differentiation. Induction of differentiation either through stimuli from the microenvironment or adjacent fibres or muscle injury enforces a G1 arrest of the otherwise cycling myoblasts, which now migrate (to the site of injury) and fuse with adjacent myoblasts to give rise to cylindrical muscle fibres (Figure 5.4.1).

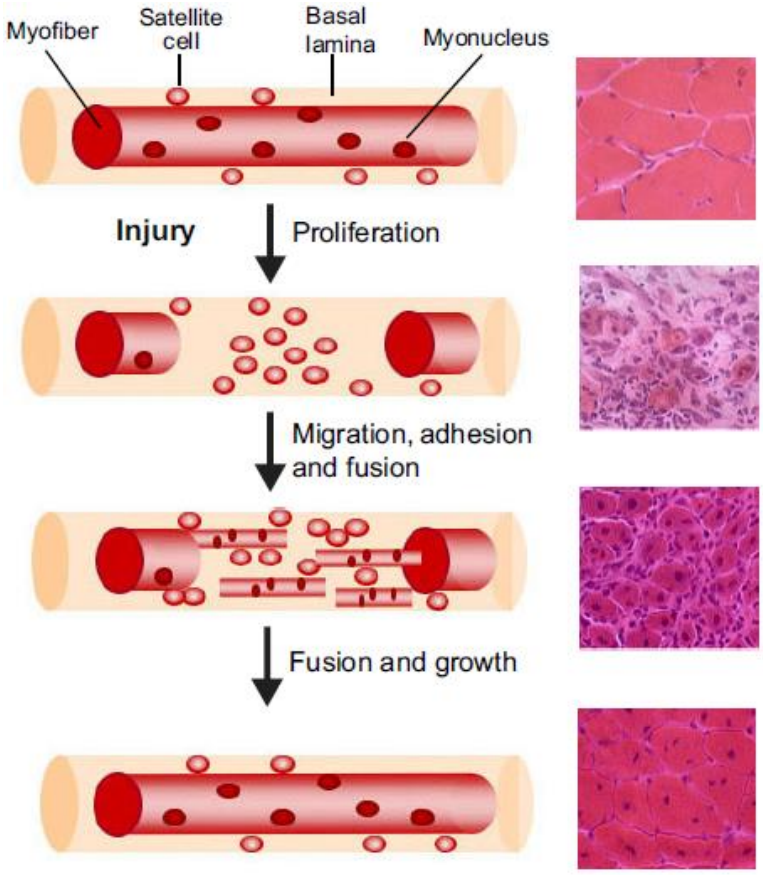

Figure 5.4.1: Muscle regeneration in adult mouse muscle. *Injury induced segmental necrosis of the myofibers activate the satellite cells which begin to proliferate and form myoblasts. The myoblasts differentiate and then migrate, adhere and fuse with one another to form multiple myotubes. Myoblasts/myotubes fuse with the already existing, uninjured myofibers to repair the*

injured myofiber. Regenerated myofibers are easily identified by the presence of centrally located nuclei. A representative mouse muscle section, stained with Haematoxylin and Eosin, is depicted in the cross-section for the corresponding schematic representation to illustrate the morphological features of the tissue [Adapted from (Abmayr SM et al., 2012)].

Interestingly, Aurora B was reported to be necessary for the maintenance of the differentiated state of skeletal muscles as Aurora kinase B specific inhibitor treatment led to the de-differentiation of myoblasts to an undifferentiated phenotype (G Amabile *et al.*, 2009). Independently, we uncovered a hitherto unappreciated role of Aurora kinase A in the process of skeletal muscle differentiation through a phosphorylation dependent regulation of the repressive E2F member, E2F4. We found that Aurora kinase A is necessary for the switch of proliferating myoblasts to differentiating myotubes by phosphorylating E2F4 and inhibiting its DNA binding. The phospho-deficient mutant of E2F4 was also found to corroborate the inhibitory actions on the expression of differentiation specific genes (Karthigeyan D et al., 2018).

We extended our investigations in the present thesis and observed the involvement of the catalytic activity of Aurora kinase A in assisting the process of differentiation as the use of Aurora A-, but not Aurora B-specific inhibitor retarded or inhibited muscle differentiation. We conjecture that the requirement of kinase activity of Aurora kinase A might be implied not only through E2F4but also through mPOU, which was previously identified in a screening in our laboratory, thus expanding the reach of Aurora A in the process of differentiation. Conversely, we also found that mPOU negatively modulate differentiation, a process which opposes Aurora A action. We hypothesize the action of a negative feedback circuit operative between Aurora A and mPOU that functions to maintain the homeostasis of muscle precursor cells and the proliferating and differentiating myoblasts.

It is necessary to study the mechanistic details through which mPOU may inhibit the differentiation process, especially in the context of satellite cell niche maintenance. It is possible that mPOU is an important regulator for the maintenance of these muscle precursors, depletion of which is facilitating differentiation, as has previously been observed for PAX7 (Zammit PS et al., 2006; Olguin HC et al., 2004). Furthermore, our observation on the DNA binding activity of mPOU upon Aurora A mediated phosphorylation implies a probable DNA binding independent role of mPOU, possibly through the interaction with other mediatory factors, for its actions. Interestingly, mPOU

possess a well conserved binding motif (RVWF) for protein phosphatase 1 (PP1) towards its C-terminus. A three-dimensional reconstruction of the structure of mPOU shows that Ser-197 residue, which is the major site for Aurora kinase A phosphorylation, lies in close proximity to the PP1 binding motif (Figure 5.4.2). This depiction increases the probability of an Aurora kinase A-mPOU-PP1 axis in determining the fate, timely cell cycle exit and differentiation entry upon injury or receipt of cues for differentiation.

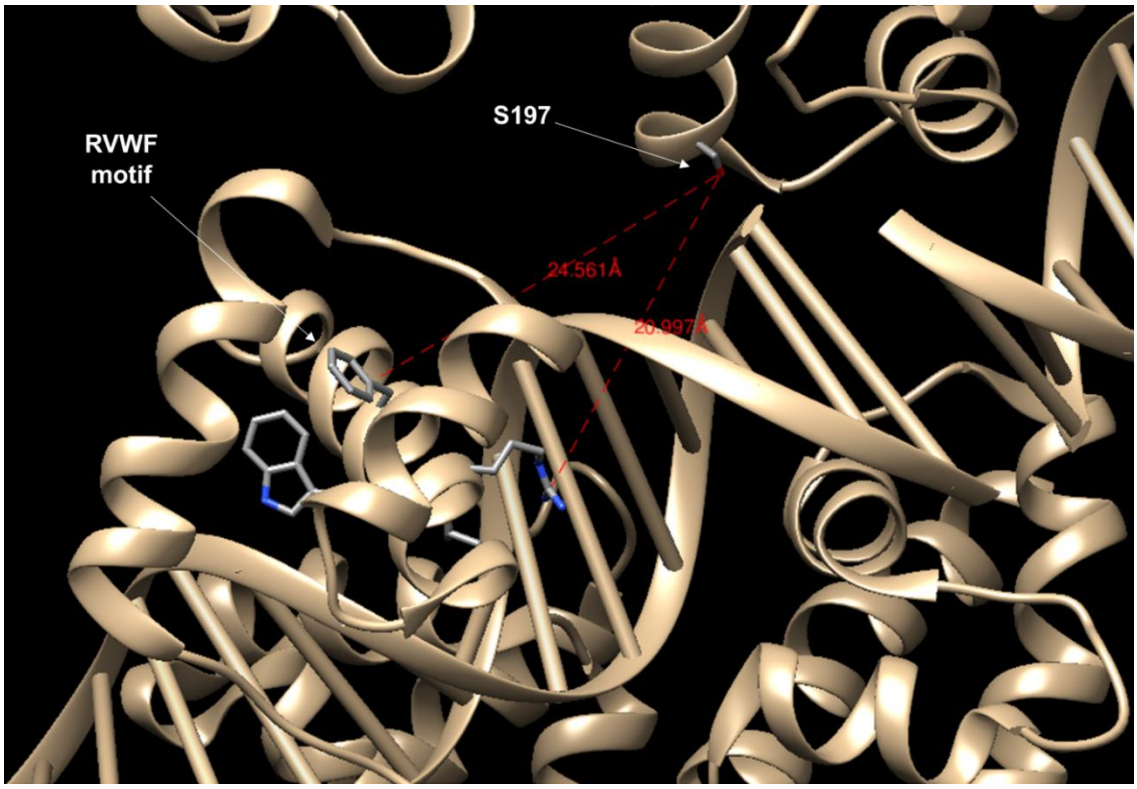

Figure 5.4.2: *A three-dimensional illustration of mPOU bound to its cognate DNA [generated using Chimera software]. Ser-197 (S197) and the PP1 binding (RVWF) motif (highlighted in white) lie within 20-25 Aº distance to each other (highlighted in red).*

Our observations imply a negative regulation of muscle differentiation by Aurora A inhibitors. Of late, many of such inhibitors are being pursued for clinical trials of both solid and haematological malignancies. Our findings highlight potentially important implications for the current approaches aimed at Aurora kinase A inhibition. One needs to exert caution as these inhibitors may lead to serious problems of differentiation of the skeletal muscles for the patients.

Finally, we screened for the probable KATs that acetylate Aurora kinase A *in vitro* and found that P/CAF to be one of them, apart from p300 (Figure 5.4.3). It would be interesting to study the function of Aurora kinase A from the perspective of P/CAF. Interestingly, P/CAF acetyltransferase has been observed to be a therapeutic vulnerability for alveolar rhabdomyosarcoma (a form of soft tissue cancer of the muscles), majority of which is being driven by PAX3-FOXO1 fusion oncogene (Bharathy N et al., 2016). This investigation may not only aid in the understanding of the function(s) of P/CAF mediated Aurora A acetylation but may also unveil therapeutic opportunities for the treatment of this paediatric disease.

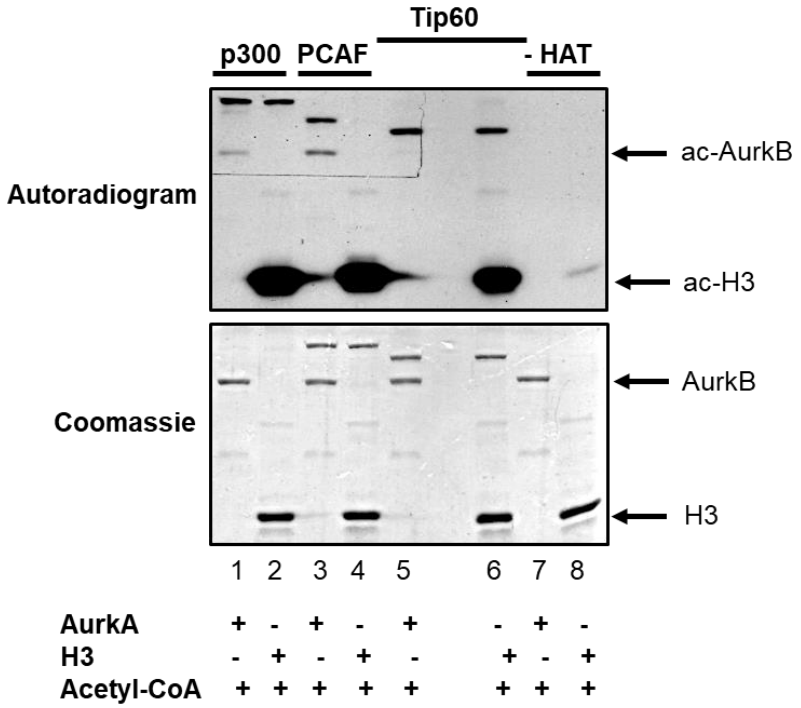

Figure 5.4.3: P/CAF and p300 acetylate AurkA. *In vitro lysine acetyltransferase (KAT) assay of 500ng of recombinant His_6-AurkA purified from E. coli by using His_6-p300, Flag-PCAF and His_6-Tip60 purified from Sf21 cells using suitable baculoviral constructs. The coomassie staining for each of the lanes is shown below the autoradiogram profiles for comparing the loading levels across each lane.*

LIST OF PUBLICATIONS

1. Dhanasekaran K, **Bose A**, Rao VJ, Boopathi R, Shankar SR, Rao VK, Swaminathan A, Vasudevan M, Taneja R, Kundu TK. **Unraveling the role of aurora A beyond centrosomes and spindle assembly: implications in muscle differentiation.** FASEB J. 2018 Jul 11:fj201800997. doi: 10.1096/fj.201800997.

2. **Bose A**, Rao VJ, Sharmi Nath, Surabhi Sudevan, Shima H, Igarashi K, Nagaraju G, Kundu TK. **Inverse regulation of DNA damage repair pathway choice by Aurora kinase B and Tip60 guides genome stability** (Manuscript under preparation).

3. **Bose A**, Rao VJ, Dhanasekaran K, Shima H, Igarashi K, Kundu TK. **Aurora kinase B regulates Max phosphorylation and mediates a switch from tumour suppressive to oncogenic functions of Myc** (Manuscript under preparation).

4. **Bose A**, Dhanasekaran K, Rao VJ, Shima H, Igarashi K, Kundu TK. **Determination of skeletal muscle differentiation by the mPOU-Aurora kinase A regulatory axis** (Manuscript under preparation).

REFERENCES

A Schulze, K Zerfass, D Spitkovsky, S Middendorp, J Bergès, K Helin, P Jansen-Dürr, and B Henglein. Cell cycle regulation of the cyclin A gene promoter is mediated by a variant E2F site. Proc Natl Acad Sci U S A. 1995 Nov 21; 92(24): 11264–11268.

A Zetterberg and O Larsson. Kinetic analysis of regulatory events in G1 leading to proliferation or quiescence of Swiss 3T3 cells. Proc Natl Acad Sci U S A. 1985 Aug; 82(16): 5365–5369.

Abmayr SM, Pavlath GK. Myoblast fusion: lessons from flies and mice. Development. 2012 Feb;139(4):641-56. doi: 10.1242/dev.068353.

Abbas T, Jha S, Sherman NE, Dutta A. Autocatalytic Phosphorylation of CDK2 at the Activating Thr160 Cell Cycle Pages 843-852

Abbas T, Sivaprasad U, Terai K, Amador V, Pagano M, Dutta A. PCNA-dependent regulation of p21 ubiquitylation and degradation via the CRL4Cdt2 ubiquitin ligase complex. Genes Dev. 2008 Sep 15;22(18):2496-506. doi: 10.1101/gad.1676108.

Adams RR, Wheatley SP, Gouldsworthy AM, Kandels-Lewis SE, Carmena M, Smythe C, Gerloff DL, Earnshaw WC. INCENP binds the Aurora-related kinase AIRK2 and is required to target it to chromosomes, the central spindle and cleavage furrow. Curr Biol. 2000 Sep 7;10(17):1075-8.

Altmeyer M, Neelsen KJ, Teloni F, Pozdnyakova I, Pellegrino S, Grøfte M, Rask MB, Streicher W, Jungmichel S, Nielsen ML, Lukas J. Liquid demixing of intrinsically disordered proteins is seeded by poly(ADP-ribose). Nat Commun. 2015 Aug 19;6:8088. doi: 10.1038/ncomms9088.

Amabile G, D'Alise AM, Iovino M, Jones P, Santaguida S, Musacchio A, Taylor S, Cortese R. The Aurora B kinase activity is required for the maintenance of the differentiated state of murine myoblasts. Cell Death Differ. 2009 Feb;16(2):321-30. doi: 10.1038/cdd.2008.156.

Andersen SS. Balanced regulation of microtubule dynamics during the cell cycle: a contemporary view. Bioessays. 1999 Jan;21(1):53-60.

Andersen SS1. Balanced regulation of microtubule dynamics during the cell cycle: a contemporary view. Bioessays. 1999 Jan;21(1):53-60.

Andrews PD, Ovechkina Y, Morrice N, Wagenbach M, Duncan K, Wordeman L, Swedlow JR. Aurora B regulates MCAK at the mitotic centromere. Dev Cell. 2004 Feb;6(2):253-68.

Auger KR, Serunian LA, Soltoff SP, Libby P, Cantley LC. PDGF-dependent tyrosine phosphorylation stimulates production of novel polyphosphoinositides in intact cells. Cell. 1989 Apr 7;57(1):167-75.

B. Vennstrom, D. Sheiness, J. Zabielski, and J. M. Bishop. Isolation and characterization of c-myc, a cellular homolog of the oncogene (v-myc) of avian myelocytomatosis virus strain 29. Journal of Virology, vol. 42, no. 3, pp. 773–779, 1982.

Bansal N, Bosch A, Leibovitch B, Pereira L, Cubedo E, Yu J, Pierzchalski K, Jones JW, Fishel M, Kane M, Zelent A, Waxman S, Farias E. Blocking the PAH2 domain of Sin3A inhibits tumorigenesis and confers retinoid sensitivity in triple negative breast cancer. Oncotarget. 2016 Jul 12;7(28):43689-43702. doi: 10.18632/oncotarget.9905.

Bahrami S, Drabløs F. Gene regulation in the immediate-early response process. Adv Biol Regul. 2016 Sep;62:37-49. doi: 10.1016/j.jbior.2016.05.001.

Ban R, Nishida T, Urano T. Mitotic kinase Aurora-B is regulated by SUMO-2/3 conjugation/deconjugation during mitosis. Genes Cells. 2011 Jun;16(6):652-69. doi: 10.1111/j.1365-2443.2011.01521.

Bartkova J, Horejsí Z, Koed K, Krämer A, Tort F, Zieger K, Guldberg P, Sehested M, Nesland JM, Lukas C, Ørntoft T, Lukas J, Bartek J. DNA damage response as a candidate anti-cancer barrier in early human tumorigenesis. Nature. 2005 Apr 14;434(7035):864-70.

Barretta ML, Spano D, D'Ambrosio C, Cervigni RI, Scaloni A, Corda D, Colanzi A. Aurora-A recruitment and centrosomal maturation are regulated by a Golgi-activated pool of Src during G2. Nat Commun. 2016 May 31;7:11727. doi: 10.1038/ncomms11727.

Bassi C, Li YT, Khu K, Mateo F, Baniasadi PS, Elia A, Mason J, Stambolic V, Pujana MA, Mak TW, Gorrini C. The acetyltransferase Tip60 contributes to mammary tumorigenesis by modulating DNA repair. Cell Death Differ. 2016 Jul;23(7):1198-208. doi: 10.1038/cdd.2015.173. Epub 2016 Feb 26.

Beardmore VA, Ahonen LJ, Gorbsky GJ, Kallio MJ. Survivin dynamics increases at centromeres during G2/M phase transition and is regulated by microtubule-attachment and Aurora B kinase activity. J Cell Sci. 2004 Aug 15;117(Pt 18):4033-42.

Bell SP, Dutta A. DNA replication in eukaryotic cells. Annu Rev Biochem. 2002;71:333-74.

Bello-Fernandez C1, Packham G, Cleveland JL. The ornithine decarboxylase gene is a transcriptional target of c-Myc. Proc Natl Acad Sci U S A. 1993 Aug 15;90(16):7804-8.

Bertoli C, Skotheim JM, de Bruin RA. Control of cell cycle transcription during G1 and S phases. Nat Rev Mol Cell Biol. 2013 Aug;14(8):518-28. doi: 10.1038/nrm3629.

Bertolin G, Bulteau AL, Alves-Guerra MC, Burel A, Lavault MT, Gavard O, Le Bras S, Gagné JP, Poirier GG, Le Borgne R, Prigent C, Tramier M. Aurora kinase A localises to mitochondria to control organelle dynamics and energy production. Elife. 2018 Aug 2;7. pii: e38111. doi: 10.7554/eLife.38111.

Berberich SJ, Cole MD. Casein kinase II inhibits the DNA-binding activity of Max homodimers but not Myc/Max heterodimers. Genes Dev. 1992 Feb;6(2):166-76.

Bharathy N, Suriyamurthy S, Rao VK, Ow JR, Lim HJ, Chakraborty P, Vasudevan M, Dhamne CA, Chang KT, Min VL, Kundu TK, Taneja R. P/CAF mediates PAX3-FOXO1-dependent oncogenesis in alveolar rhabdomyosarcoma. J Pathol. 2016 Nov;240(3):269-281. doi: 10.1002/path.4773. Epub 2016 Sep 27.

Blackwood, E.M., Eisenman, R.N. Max: a helix-loop-helix zipper protein that forms a sequence-specific DNA-binding complex with Myc. Science (1991). 251, 1211–1217.

Blas-Rus N, Bustos-Morán E, Pérez de Castro I, de Cárcer G, Borroto A, Camafeita E, Jorge I, Vázquez J, Alarcón B, Malumbres M, Martín-Cófreces NB, Sánchez-Madrid F. Aurora A drives early signalling and vesicle dynamics during T-cell activation. Nat Commun. 2016 Apr 19;7:11389. doi: 10.1038/ncomms11389.

Bonet C1, Giuliano S, Ohanna M, Bille K, Allegra M, Lacour JP, Bahadoran P, Rocchi S, Ballotti R, Bertolotto C. Aurora B is regulated by the mitogen-activated protein kinase/extracellular signal-regulated kinase (MAPK/ERK) signaling pathway and is a valuable potential target in melanoma cells. J Biol Chem. 2012 Aug 24;287(35):29887-98. doi: 10.1074/jbc.M112.371682.

Bornstein G, Bloom J, Sitry-Shevah D, Nakayama K, Pagano M, Hershko A. Role of the SCFSkp2 ubiquitin ligase in the degradation of p21Cip1 in S phase. J Biol Chem. 2003 Jul 11;278(28):25752-7.

Boveri T. Concerning the origin of malignant tumours by Theodor Boveri. Translated and annotated by Henry Harris. J Cell Sci. 2008 Jan;121 Suppl 1:1-84. doi: 10.1242/jcs.025742.

Braun T, Arnold HH. Inactivation of Myf-6 and Myf-5 genes in mice leads to alterations in skeletal muscle development. EMBO J 1995; 14:1176-86.

Braun T, Rudnicki MA, Arnold HH, Jaenisch R. Targeted inactivation of the muscle regulatory gene Myf-5 results in abnormal rib development and perinatal death. Cell 1992; 71:369-82.

Brasó-Maristany F, Filosto S, Catchpole S, Marlow R, Quist J, Francesch-Domenech E, Plumb DA, Zakka L, Gazinska P, Liccardi G, Meier P, Gris-Oliver A, Cheang MC, Perdrix-Rosell A, Shafat M, Noël E, Patel N, McEachern K, Scaltriti M, Castel P, Noor F, Buus R, Mathew S1, Watkins J, Serra V, Marra P, Grigoriadis A, Tutt AN. PIM1 kinase regulates cell death, tumor growth and chemotherapy response in triple-negative breast cancer. Nat Med. 2016 Nov;22(11):1303-1313. doi: 10.1038/nm.4198. Epub 2016 Oct 24.

Briassouli P, Chan F, Savage K, Reis-Filho JS, Linardopoulos S. Aurora-A regulation of nuclear factor-kappaB signaling by phosphorylation of IkappaBalpha. Cancer Res. 2007 Feb 15;67(4):1689-95.

Brockmann M, Poon E, Berry T, Carstensen A, Deubzer HE, Rycak L, Jamin Y, Thway K, Robinson SP, Roels F, Witt O, Fischer M, Chesler L, Eilers M. Small Molecule Inhibitors of Aurora-A Induce Proteasomal Degradation of N-Myc in Childhood Neuroblastoma. Cancer Cell. 2016 Aug 8;30(2):357-358. doi: 10.1016/j.ccell.2016.07.002.

Büchel G, Carstensen A, Mak KY, Roeschert I, Leen E, Sumara O, Hofstetter J, Herold S, Kalb J, Baluapuri A, Poon E, Kwok C, Chesler L, Maric HM, Rickman DS, Wolf E, Bayliss R, Walz S, Eilers M. Association with Aurora-A Controls N-MYC-Dependent Promoter Escape and Pause Release of RNA Polymerase II during the Cell Cycle. Cell Rep. 2017 Dec 19;21(12):3483-3497. doi: 10.1016/j.celrep.2017.11.090.

Burnichon N, Cascón A, Schiavi F, Morales NP, Comino-Méndez I, Abermil N, Inglada-Pérez L, de Cubas AA, Amar L, Barontini M, de Quirós SB, Bertherat J, Bignon YJ, Blok MJ, Bobisse S, Borrego S, Castellano M, Chanson P, Chiara MD, Corssmit EP, Giacchè M, de Krijger RR, Ercolino T, Girerd X, Gómez-García EB, Gómez-Graña A, Guilhem I, Hes FJ, Honrado E, Korpershoek E, Lenders JW, Letón R, Mensenkamp AR, Merlo A, Mori L, Murat A, Pierre P, Plouin PF, Prodanov T, Quesada-Charneco M, Qin N, Rapizzi E, Raymond V, Reisch N, Roncador G, Ruiz-Ferrer M, Schillo F, Stegmann AP, Suarez C, Taschin E, Timmers HJ, Tops CM, Urioste M, Beuschlein F, Pacak K, Mannelli M, Dahia PL, Opocher G, Eisenhofer G, Gimenez-Roqueplo AP, Robledo M. MAX mutations cause hereditary and sporadic pheochromocytoma and paraganglioma. Clin Cancer Res. 2012 May 15;18(10):2828-37. doi: 10.1158/1078-0432.CCR-12-0160. Epub 2012 Mar 27.

Carbone M, Rossi MN, Cavaldesi M, Notari A, Amati P, Maione R. Poly(ADP-ribosyl)ation is implicated in the G0-G1 transition of resting cells. Oncogene. 2008 Oct 16;27(47):6083-92. doi: 10.1038/onc.2008.221.

Carmena M, Earnshaw WC. The cellular geography of aurora kinases. Nat Rev Mol Cell Biol. 2003 Nov;4(11):842-54.

Catherine Lindon,1,* Rhys Grant,1 and Mingwei Min2 Ubiquitin-Mediated Degradation of Aurora Kinases Front Oncol. 2016 Jan 18;5:307. doi: 10.3389/fonc.2015.00307.

Cazales M, Schmitt E, Montembault E, Dozier C, Prigent C, Ducommun B. CDC25B phosphorylation by Aurora-A occurs at the G2/M transition and is inhibited by DNAdamage. Cell Cycle. 2005 Sep;4(9):1233-8.

Chakraborty AK, Weiss A. Insights into the initiation of TCR signaling. Nat Immunol. 2014 Sep;15(9):798-807. doi: 10.1038/ni.2940.

Chandriani S, Frengen E, Cowling VH, Pendergrass SA, Perou CM, Whitfield ML, Cole MD. A core MYC gene expression signature is prominent in basal-like breast cancer but only partially overlaps the core serum response. PLoS One. 2009 Aug 19;4(8):e6693. doi: 10.1371/journal.pone.0006693.

Chan FL, Vinod B, Novy K, Schittenhelm RB, Huang C, Udugama M, Nunez-Iglesias J, Lin JI, Hii L, Chan J, Pickett HA, Daly RJ, Wong LH. Aurora Kinase B, a novel regulator of TERF1 binding and telomeric integrity. Nucleic Acids Res. 2017 Dec 1;45(21):12340-12353. doi: 10.1093/nar/gkx904.

Charles JF, Jaspersen SL, Tinker-Kulberg RL, Hwang L, Szidon A, Morgan DO. The Polo-related kinase Cdc5 activates and is destroyed by the mitotic cyclin destruction machinery in S. cerevisiae. Curr Biol. 1998 Apr 23;8(9):497-507.

Cheeseman IM, Chappie JS, Wilson-Kubalek EM, Desai A. The conserved KMN network constitutes the core microtubule-binding site of the kinetochore. Cell. 2006 Dec 1;127(5):983-97.

Cheung P, Allis CD, Sassone-Corsi P. Signaling to chromatin through histone modifications. Cell. 2000 Oct 13;103(2):263-71.

Choudhary C, Kumar C, Gnad F, Nielsen ML, Rehman M, Walther TC, Olsen JV, Mann M. Lysine acetylation targets protein complexes and co-regulates major cellular functions. Science. 2009 Aug 14;325(5942):834-40. doi: 10.1126/science.1175371.

Chow JP, Siu WY, Ho HT, Ma KH, Ho CC, Poon RY. Differential contribution of inhibitory phosphorylation of CDC2 and CDK2 for unperturbed cell cycle control and DNA integrity checkpoints. J Biol Chem. 2003 Oct 17;278(42):40815-28.

Chu IM, Lai WC, Aprelikova O, El Touny LH, Kouros-Mehr H, Green JE. Expression of GATA3 in MDA-MB-231 triple-negative breast cancer cells induces a growth inhibitory response to TGFß. PLoS One. 2013;8(4):e61125. doi: 10.1371/journal.pone.0061125. Epub 2013 Apr 8.

Chu IM, Michalowski AM, Hoenerhoff M, Szauter KM, Luger D, Sato M, Flanders K, Oshima A, Csiszar K, Green JE. GATA3 inhibits lysyl oxidase-mediated metastases of human basal triple-negative breast cancer cells. Oncogene. 2012 Apr 19;31(16):2017-27. doi: 10.1038/onc.2011.382. Epub 2011 Sep 5.

Coene ED, Schelfhout V, Winkler RA, Schelfhout AM, Van Roy N, Grooteclaes M, Speleman F, De Potter CR. Amplification units and translocation at chromosome 17q and c-erbB-2 overexpression in the pathogenesis of breast cancer. Virchows Arch. 1997 May;430(5):365-72.

Clarke TL, Sanchez-Bailon MP, Chiang K, Reynolds JJ, Herrero-Ruiz J, Bandeiras TM, Matias PM, Maslen SL, Skehel JM, Stewart GS, Davies CC. PRMT5-Dependent Methylation of the

TIP60 Coactivator RUVBL1 Is a Key Regulator of Homologous Recombination. Mol Cell. 2017 Mar 2;65(5):900-916.e7. doi: 10.1016/j.molcel.2017.01.019. Epub 2017 Feb 23.

Comino-Méndez I, Gracia-Aznárez FJ, Schiavi F, Landa I, Leandro-García LJ, Letón R, Honrado E, Ramos-Medina R, Caronia D, Pita G, Gómez-Graña A, de Cubas AA, Inglada-Pérez L, Maliszewska A, Taschin E, Bobisse S, Pica G, Loli P, Hernández-Lavado R, Díaz JA, Gómez-Morales M, González-Neira A, Roncador G, Rodríguez-Antona C, Benítez J, Mannelli M, Opocher G, Robledo M, Cascón A. Exome sequencing identifies MAX mutations as a cause of hereditary pheochromocytoma. Nat Genet. 2011 Jun 19;43(7):663-7. doi: 10.1038/ng.861.

Conduit PT, Feng Z, Richens JH, Baumbach J, Wainman A, Bakshi SD, Dobbelaere J, Johnson S, Lea SM, Raff JW. The centrosome-specific phosphorylation of Cnn by Polo/Plk1 drives Cnn scaffold assembly and centrosome maturation. Dev Cell. 2014 Mar 31;28(6):659-69. doi: 10.1016/j.devcel.2014.02.013.

Cotteret S, Chernoff J. Pak GITs to Aurora-A. Dev Cell. 2005 Nov;9(5):573-4.

Coverley D, Laman H, Laskey RA. Distinct roles for cyclins E and A during DNA replication complex assembly and activation. Nat Cell Biol. 2002 Jul;4(7):523-8.

Crawford HC, Fingleton BM, Rudolph-Owen LA, Goss KJ, Rubinfeld B, Polakis P, Matrisian LM. The metalloproteinase matrilysin is a target of beta-catenin transactivation in intestinal tumors. Oncogene. 1999 May 6;18(18):2883-91.

Crosio C, Fimia GM, Loury R, Kimura M, Okano Y, Zhou H, Sen S, Allis CD, Sassone-Corsi P. Mitotic phosphorylation of histone H3: spatio-temporal regulation by mammalian Aurora kinases. Mol Cell Biol. 2002 Feb;22(3):874-85.

D'Amours D, Desnoyers S, D'Silva I, Poirier GG. Poly(ADP-ribosyl)ation reactions in the regulation of nuclear functions. Biochem J. 1999 Sep 1;342 (Pt 2):249-68.

Dar AA, Belkhiri A, El-Rifai W. The aurora kinase A regulates GSK-3beta in gastric cancer cells. Oncogene. 2009 Feb 12;28(6):866-75. doi: 10.1038/onc.2008.434.

Dauch D, Rudalska R, Cossa G, Nault JC, Kang TW, Wuestefeld T, Hohmeyer A, Imbeaud S, Yevsa T, Hoenicke L, Pantsar T, Bozko P, Malek NP, Longerich T, Laufer S, Poso A, Zucman-Rossi J, Eilers M, Zender L. A MYC-aurora kinase A protein complex represents an actionable drug target in p53-altered liver cancer. Nat Med. 2016 Jul;22(7):744-53. doi: 10.1038/nm.4107.

Davie JR, Drobic B, Perez-Cadahia B, He S, Espino PS, Sun JM, Chen HY, Dunn KL, Wark L, Mai S, Khan DH, Davie SN, Lu S, Peltier CP, Delcuve GP. Nucleosomal response, immediate-early gene expression and cell transformation. Adv Enzyme Regul. 2010;50(1):135-45. doi: 10.1016/j.advenzreg.2009.10.008.

De Souza CP, Osmani AH, Wu LP, Spotts JL, Osmani SA. Mitotic histone H3 phosphorylation by the NIMA kinase in Aspergillus nidulans. Cell. 2000 Aug 4;102(3):293-302.

DeGregori J, Leone G, Ohtani K, Miron A, Nevins JR. E2F-1 accumulation bypasses a G1 arrest resulting from the inhibition of G1 cyclin-dependent kinase activity. Genes Dev. 1995 Dec 1;9(23):2873-87.

DeLuca JG, Gall WE, Ciferri C, Cimini D, Musacchio A, Salmon ED. Kinetochore microtubule dynamics and attachment stability are regulated by Hec1. Cell. 2006 Dec 1;127(5):969-82.

den Hollander J, Rimpi S, Doherty JR, Rudelius M, Buck A, Hoellein A, Kremer M, Graf N, Scheerer M, Hall MA, Goga A, von Bubnoff N, Duyster J, Peschel C, Cleveland JL, Nilsson JA, Keller U. Aurora kinases A and B are up-regulated by Myc and are essential for maintenance of the malignant state. Blood. 2010 Sep 2;116(9):1498-505. doi: 10.1182/blood-2009-11-251074.

Denu RA, Zasadil LM, Kanugh C, Laffin J, Weaver BA, Burkard ME. Centrosome amplification induces high grade features and is prognostic of worse outcomes in breast cancer. BMC Cancer. 2016 Jan 29;16:47. doi: 10.1186/s12885-016-2083-x.

Dhanasekaran K, Bose A, Rao VJ, Boopathi R, Shankar SR, Rao VK, Swaminathan A, Vasudevan M, Taneja R, Kundu TK. Unraveling the role of aurora A beyond centrosomes and spindle assembly: implications in muscle differentiation. FASEB J. 2018 Jul 11:fj201800997. doi: 10.1096/fj.201800997.

Dhanasekaran K, Kumari S, Boopathi R, Shima H, Swaminathan A, Bachu M, Ranga U, Igarashi K, Kundu TK. Multifunctional human transcriptional coactivator protein PC4 is a substrate of Aurora kinasesand activates the Aurora enzymes. FEBS J. 2016 Mar;283(6):968-85. doi: 10.1111/febs.13653.

Ditchfield C, Johnson VL, Tighe A, Ellston R, Haworth C, Johnson T, Mortlock A, Keen N, Taylor SS. Aurora B couples chromosome alignment with anaphase by targeting BubR1, Mad2, and Cenp-Eto kinetochores. J Cell Biol. 2003 Apr 28;161(2):267-80.

Do TV, Hirst J, Hyter S, Roby KF, Godwin AK. Aurora A kinase regulates non-homologous end-joining and poly(ADP-ribose) polymerase function in ovarian carcinoma cells. Oncotarget. 2017 Jul 5;8(31):50376-50392. doi: 10.18632/oncotarget.18970.

Dodson CA1, Bayliss R. Activation of Aurora-A kinase by protein partner binding and phosphorylation are independentand synergistic. J Biol Chem. 2012 Jan 6;287(2):1150-7. doi: 10.1074/jbc.M111.312090.

Donnella HJ, Webber JT, Levin RS, Camarda R, Momcilovic O, Bayani N, Shah KN, Korkola JE, Shokat KM, Goga A, Gordan JD, Bandyopadhyay S. Kinome rewiring reveals AURKA limits

PI3K-pathway inhibitor efficacy in breast cancer. Nat Chem Biol. 2018 Aug;14(8):768-777. doi: 10.1038/s41589-018-0081-9.

Dustin ML. What counts in the immunological synapse? Mol Cell. 2014 Apr 24;54(2):255-62. doi: 10.1016/j.molcel.2014.04.001.

Dydensborg AB, Rose AA, Wilson BJ, Grote D, Paquet M, Giguère V, Siegel PM, Bouchard M. GATA3 inhibits breast cancer growth and pulmonary breast cancer metastasis. Oncogene. 2009 Jul 23;28(29):2634-42. doi: 10.1038/onc.2009.126. Epub 2009 Jun 1.

Emanuele MJ, Lan W, Jwa M, Miller SA, Chan CS, Stukenberg PT. Aurora B kinase and protein phosphatase 1 have opposing roles in modulating kinetochore assembly. J Cell Biol. 2008 Apr 21;181(2):241-54. doi: 10.1083/jcb.200710019.

Eves EM1, Shapiro P, Naik K, Klein UR, Trakul N, Rosner MR. Raf kinase inhibitory protein regulates aurora B kinase and the spindle checkpoint. Mol Cell. 2006 Aug;23(4):561-74.

Ewen ME, Sluss HK, Sherr CJ, Matsushime H, Kato J, Livingston DM. Functional interactions of the retinoblastoma protein with mammalian D-type cyclins. Cell. 1993 May 7;73(3):487-97.

Ewen ME, Sluss HK, Whitehouse LL, Livingston DM. TGF beta inhibition of Cdk4 synthesis is linked to cell cycle arrest. Cell. 1993 Sep 24;74(6):1009-20.

Eyers PA1, Erikson E, Chen LG, Maller JL. A novel mechanism for activation of the protein kinase Aurora A. Curr Biol. 2003 Apr 15;13(8):691-7.

Fadri-Moskwik M1, Weiderhold KN, Deeraksa A, Chuang C, Pan J, Lin SH, Yu-Lee LY. Aurora B is regulated by acetylation/deacetylation during mitosis in prostate cancer cells. FASEB J. 2012 Oct;26(10):4057-67. doi: 10.1096/fj.12-206656.

Fang G, Yu H, Kirschner MW. Direct binding of CDC20 protein family members activates the anaphase-promoting complex in mitosis and G1. Mol Cell. 1998 Aug;2(2):163-71.

Fattah F, Lee EH, Weisensel N, Wang Y, Lichter N, Hendrickson EA. Ku regulates the non-homologous end joining pathway choice of DNA double-strand break repair in human somatic cells. PLoS Genet. 2010 Feb 26;6(2):e1000855. doi: 10.1371/journal.pgen.1000855.

Fell VL, Walden EA, Hoffer SM, Rogers SR, Aitken AS, Salemi LM, Schild-Poulter C. Ku70 Serine 155 mediates Aurora B inhibition and activation of the DNA damage response. Sci Rep. 2016 Nov 16;6:37194. doi: 10.1038/srep37194.

Fernández-Miranda G1, Pérez de Castro I, Carmena M, Aguirre-Portolés C, Ruchaud S, Fant X, Montoya G, Earnshaw WC, Malumbres M. SUMOylation modulates the function of Aurora-B kinase. J Cell Sci. 2010 Aug 15;123(Pt 16):2823-33. doi: 10.1242/jcs.065565.

Faiola F, Liu X, Lo S, Pan S, Zhang K, Lymar E, Farina A, Martinez E. Dual regulation of c-Myc by p300 via acetylation-dependent control of Myc protein turnover and coactivation of Myc-induced transcription. Mol Cell Biol. 2005 Dec;25(23):10220-34.

Frangini A, Sjöberg M, Roman-Trufero M, Dharmalingam G, Haberle V, Bartke T, Lenhard B, Malumbres M, Vidal M, Dillon N. The aurora B kinase and the polycomb protein ring1B combine to regulate active promoters in quiescent lymphocytes. Mol Cell. 2013 Sep 12;51(5):647-61. doi: 10.1016/j.molcel.2013.08.022.

Frank SR, Parisi T, Taubert S, Fernandez P, Fuchs M, Chan HM, Livingston DM, Amati B. MYC recruits the TIP60 histone acetyltransferase complex to chromatin. EMBO Rep. 2003 Jun;4(6):575-80.

Friend SH, Bernards R, Rogelj S, Weinberg RA, Rapaport JM, Albert DM, Dryja TP. A human DNA segment with properties of the gene that predisposes to retinoblastoma and osteosarcoma. Nature. 1986 Oct 16-22;323(6089):643-6.

Fry AM, Mayor T, Meraldi P, Stierhof YD, Tanaka K, Nigg EA. C-Nap1, a novel centrosomal coiled-coil protein and candidate substrate of the cell cycle-regulated protein kinase Nek2. J Cell Biol. 1998 Jun 29;141(7):1563-74.

Fung YK, Murphree AL, T'Ang A, Qian J, Hinrichs SH, Benedict WF. Structural evidence for the authenticity of the human retinoblastoma gene. Science. 1987 Jun 26;236(4809):1657-61.

Gabrielli BG, Lee MS, Walker DH, Piwnica-Worms H, Maller JL. Cdc25 regulates the phosphorylation and activity of the Xenopus cdk2 protein kinase complex. J Biol Chem. 1992 Sep 5;267(25):18040-6.

Gendoo DMA, Ratansirigulchai N, Schröder MS., Paré L, Parker JS, Prat A, and Haibe-Kains B. Genefu: an R/Bioconductor package for computation of gene expression-based signatures in breast cancer. Bioinformatics. 2016 Apr 1; 32(7):1097-1099. doi:10.1093/bioinformatics/btv693

Gestaut DR, Graczyk B, Cooper J, Widlund PO, Zelter A, Wordeman L, Asbury CL, Davis TN. Phosphoregulation and depolymerization-driven movement of the Dam1 complex do not require ring formation. Nat Cell Biol. 2008 Apr;10(4):407-14. doi: 10.1038/ncb1702.

Giet R1, Petretti C, Prigent C. Aurora kinases, aneuploidy and cancer, a coincidence or a real link? Trends Cell Biol. 2005 May;15(5):241-50.

Giles RH, van Es JH, Clevers H. Caught up in a Wnt storm: Wnt signaling in cancer. Biochim Biophys Acta. 2003 Jun 5;1653(1):1-24.

Goepfert TM1, Adigun YE, Zhong L, Gay J, Medina D, Brinkley WR. Centrosome amplification and overexpression of aurora A are early events in rat mammarycarcinogenesis. Cancer Res. 2002 Jul 15;62(14):4115-22.

González-Loyola A, Fernández-Miranda G, Trakala M, Partida D, Samejima K, Ogawa H, Cañamero M, de Martino A, Martínez-Ramírez Á, de Cárcer G, Pérez de Castro I, Earnshaw WC, Malumbres M. Aurora B Overexpression Causes Aneuploidy and p21Cip1 Repression during Tumor Development. Mol Cell Biol. 2015 Oct;35(20):3566-78. doi: 10.1128/MCB.01286-14.

González-Loyola A, Fernández-Miranda G, Trakala M, Partida D, Samejima K, Ogawa H, Cañamero M, de Martino A, Martínez-Ramírez Á, de Cárcer G, Pérez de Castro I, Earnshaw WC, Malumbres M.

Gordon F, Luger K, Hansen JC. The core histone N-terminal tail domains function independently and additively during salt-dependent oligomerization of nucleosomal arrays. J Biol Chem. 2005 Oct 7;280(40):33701-6.

Gorgoulis VG, Vassiliou LV, Karakaidos P, Zacharatos P, Kotsinas A, Liloglou T, Venere M, Ditullio RA Jr, Kastrinakis NG, Levy B, Kletsas D, Yoneta A, Herlyn M, Kittas C, Halazonetis TD. Activation of the DNA damage checkpoint and genomic instability in human precancerous lesions. Nature. 2005 Apr 14;434(7035):907-13.

Gorrini C, Squatrito M, Luise C, Syed N, Perna D, Wark L, Martinato F, Sardella D, Verrecchia A, Bennett S, Confalonieri S, Cesaroni M, Marchesi F, Gasco M, Scanziani E, Capra M, Mai S, Nuciforo P, Crook T, Lough J, Amati B. Tip60 is a haplo-insufficient tumour suppressor required for an oncogene-induced DNA damage response. Nature. 2007 Aug 30;448(7157):1063-7.

Goto H, Kiyono T, Tomono Y, Kawajiri A, Urano T, Furukawa K, Nigg EA, Inagaki M. Complex formation of Plk1 and INCENP required for metaphase-anaphase transition. Nat Cell Biol. 2006 Feb;8(2):180-7.

Goto H, Tomono Y, Ajiro K, Kosako H, Fujita M, Sakurai M, Okawa K, Iwamatsu A, Okigaki T, Takahashi T, Inagaki M. Identification of a novel phosphorylation site on histone H3 coupled with mitotic chromosome condensation. J Biol Chem. 1999 Sep 3;274(36):25543-9.

Grant R, Abdelbaki A, Bertoldi A, Gavilan MP, Mansfeld J, Glover DM, Lindon C. Constitutive regulation of mitochondrial morphology by Aurora A kinase depends on a predicted cryptic targeting sequence at the N-terminus. Open Biol. 2018 Jun;8(6). pii: 170272. doi: 10.1098/rsob.170272.

Gu Y, Rosenblatt J, Morgan DO. Cell cycle regulation of CDK2 activity by phosphorylation of Thr160 and Tyr15. EMBO J. 1992 Nov;11(11):3995-4005.

Guccione E, Martinato F, Finocchiaro G, Luzi L, Tizzoni L, Dall' Olio V, Zardo G, Nervi C, Bernard L, Amati B. Myc-binding-site recognition in the human genome is determined by chromatin context. Nat Cell Biol. 2006 Jul;8(7):764-70. Epub 2006 Jun 11.

Guise AJ1, Greco TM, Zhang IY, Yu F, Cristea IM. Aurora B-dependent regulation of class IIa histone deacetylases by mitotic nuclear localization signal phosphorylation. Mol Cell Proteomics. 2012 Nov;11(11):1220-9. doi: 10.1074/mcp.M112.021030.

Gully CP, Velazquez-Torres G, Shin JH, Fuentes-Mattei E, Wang E, Carlock C, Chen J, Rothenberg D, Adams HP, Choi HH, Guma S, Phan L, Chou PC, Su CH, Zhang F, Chen JS, Yang TY, Yeung SC, Lee MH. Aurora B kinase phosphorylates and instigates degradation of p53. Proc Natl Acad Sci U S A. 2012 Jun 12;109(24):E1513-22. doi: 10.1073/pnas.1110287109.

Gurden MD, Anderhub SJ, Faisal A, Linardopoulos S. Aurora B prevents premature removal of spindle assembly checkpoint proteins from the kinetochore: A key role for Aurora B in mitosis. Oncotarget. 2016 Jul 18;9(28):19525-19542. doi: 10.18632/oncotarget.10657.

Gurden MD1, Anderhub SJ2,3, Faisal A2,4, Linardopoulos S1,2. Aurora B prevents premature removal of spindle assembly checkpoint proteins from the kinetochore: A key role for Aurora B in mitosis. Oncotarget. 2016 Jul 18;9(28):19525-19542. doi: 10.18632/oncotarget.10657.

Gurley LR, Walters RA, Tobey RA. Sequential phsophorylation of histone subfractions in the Chinese hamster cell cycle. J Biol Chem. 1975 May 25;250(10):3936-44.

Gustafson WC, Meyerowitz JG, Nekritz EA, Chen J, Benes C, Charron E, Simonds EF, Seeger R, Matthay KK, Hertz NT, Eilers M, Shokat KM, Weiss WA. Drugging MYCN through an allosteric transition in Aurora kinase A. Cancer Cell. 2014 Sep 8;26(3):414-427. doi: 10.1016/j.ccr.2014.07.015.

Gwee SSL, Radford RAW, Chow S, Syal MD, Morsch M, Formella I, Lee A, Don EK, Badrock AP, Cole NJ, West AK, Cheung SNS, Chung RS. Aurora kinase B regulates axonal outgrowth and regeneration in the spinal motor neurons of developing zebrafish. Cell Mol Life Sci. 2018 Feb 21. doi: 10.1007/s00018-018-2780-5.

Hasanov E1,2, Chen G1, Chowdhury P1,3, Weldon J1, Ding Z4, Jonasch E5, Sen S6, Walker CL1,3, Dere R1,3. Ubiquitination and regulation of AURKA identifies a hypoxia-independent E3 ligase activity of VHL. Oncogene. 2017 Jun 15;36(24):3450-3463. doi: 10.1038/onc.2016.495.

Hasty P, Bradley A, Morris JH, Edmondson DG, Venuti JM, Olson EN, et al. Muscle deficiency and neonatal death in mice with targeted mutation in the myogenin gene. Nature 1993; 364:501-6.

He TC, Sparks AB, Rago C, Hermeking H, Zawel L, da Costa LT, Morin PJ, Vogelstein B, Kinzler KW. Identification of c-MYC as a target of the APC pathway. Science. 1998 Sep 4;281(5382):1509-12.

Heinlein CA, Chang C. Androgen receptor in prostate cancer. Endocr Rev. 2004 Apr;25(2):276-308.

Honda K, Mihara H, Kato Y, Yamaguchi A, Tanaka H, Yasuda H, Furukawa K, Urano T. Degradation of human Aurora2 protein kinase by the anaphase-promoting complex-ubiquitin-proteasome pathway. Oncogene. 2000 Jun 1;19(24):2812-9.

Horiuchi D, Kusdra L, Huskey NE, Chandriani S, Lenburg ME, Gonzalez-Angulo AM, Creasman KJ, Bazarov AV, Smyth JW, Davis SE, Yaswen P, Mills GB, Esserman LJ, Goga A. MYC pathway activation in triple-negative breast cancer is synthetic lethal with CDK inhibition. J Exp Med. 2012 Apr 9;209(4):679-96. doi: 10.1084/jem.20111512. Epub 2012 Mar 19.Hsu JY, Sun ZW, Li X, Reuben M, Tatchell K, Bishop DK, Grushcow JM, Brame CJ, Caldwell JA, Hunt DF, Lin R, Smith MM, Allis CD. Mitotic phosphorylation of histone H3 is governed by Ipl1/aurora kinase and Glc7/PP1 phosphatase in budding yeast and nematodes. Cell. 2000 Aug 4;102(3):279-91.

Horiuchi D, Camarda R, Zhou AY, Yau C, Momcilovic O, Balakrishnan S, Corella AN, Eyob H, Kessenbrock K, Lawson DA, Marsh LA, Anderton BN, Rohrberg J, Kunder R, Bazarov AV, Yaswen P, McManus MT, Rugo HS, Werb Z, Goga A. PIM1 kinase inhibition as a targeted therapy against triple-negative breast tumors with elevated MYC expression. Nat Med. 2016 Nov;22(11):1321-1329. doi: 10.1038/nm.4213. Epub 2016 Oct 24.

Hu R, Wang E, Peng G, Dai H, Lin SY. Zinc finger protein 668 interacts with Tip60 to promote H2AX acetylation after DNA damage. Cell Cycle. 2013 Jul 1;12(13):2033-41. doi: 10.4161/cc.25064. Epub 2013 Jun 6.

Huang H, Feng J, Famulski J, Rattner JB, Liu ST, Kao GD, Muschel R, Chan GK, Yen TJ. Tripin/hSgo2 recruits MCAK to the inner centromere to correct defective kinetochore attachments. J Cell Biol. 2007 May 7;177(3):413-24.

Huang YS, Jung MY, Sarkissian M, Richter JD. N-methyl-D-aspartate receptor signaling results in Aurora kinase-catalyzed CPEB phosphorylation and alpha CaMKII mRNA polyadenylation at synapses. EMBO J. 2002 May 1;21(9):2139-48.

Ida Blomberg and Ingrid Hoffmann. Ectopic Expression of Cdc25A Accelerates the G1/S Transition and Leads to Premature Activation of Cyclin E- and Cyclin A-Dependent Kinases Mol Cell Biol. 1999 Sep; 19(9): 6183–6194.

Ikura T, Ogryzko VV, Grigoriev M, Groisman R, Wang J, Horikoshi M, Scully R, Qin J, Nakatani Y. Involvement of the TIP60 histone acetylase complex in DNA repair and apoptosis. Cell. 2000 Aug 18;102(4):463-73.

Ikura T, Tashiro S, Kakino A, Shima H, Jacob N, Amunugama R, Yoder K, Izumi S, Kuraoka I, Tanaka K, Kimura H, Ikura M, Nishikubo S, Ito T, Muto A, Miyagawa K, Takeda S, Fishel R, Igarashi K, Kamiya K. DNA damage-dependent acetylation and ubiquitination of H2AX enhances chromatin dynamics. Mol Cell Biol. 2007 Oct;27(20):7028-40. Epub 2007 Aug 20.

Ikura M, Furuya K, Matsuda S, Matsuda R, Shima H, Adachi J, Matsuda T, Shiraki T, Ikura T. Acetylation of Histone H2AX at Lys 5 by the TIP60 Histone Acetyltransferase Complex Is Essential for the Dynamic Binding of NBS1 to Damaged Chromatin. Mol Cell Biol. 2015 Dec;35(24):4147-57. doi: 10.1128/MCB.00757-15. Epub 2015 Oct 5.

Jacquet K, Fradet-Turcotte A, Avvakumov N, Lambert JP, Roques C, Pandita RK, Paquet E, Herst P, Gingras AC, Pandita TK, Legube G, Doyon Y, Durocher D, Côté J. The TIP60 Complex Regulates Bivalent Chromatin Recognition by 53BP1 through Direct H4K20me Binding and H2AK15 Acetylation. Mol Cell. 2016 May 5;62(3):409-421. doi: 10.1016/j.molcel.2016.03.031.

Jeyaprakash AA, Klein UR, Lindner D, Ebert J, Nigg EA, Conti E. Structure of a Survivin-Borealin-INCENP core complex reveals how chromosomal passengers travel together. Cell. 2007 Oct 19;131(2):271-85.

Jha HC, Lu J, Saha A, Cai Q, Banerjee S, Prasad MA, Robertson ES. EBNA3C-mediated regulation of aurora kinase B contributes to Epstein-Barr virus-induced B-cell proliferation through modulation of the activities of the retinoblastoma protein and apoptotic caspases. J Virol. 2013 Nov;87(22):12121-38. doi: 10.1128/JVI.02379-13.

Jian Ming Jeremy Ng, Minghui Jessica Chen, Jacqueline Y.K. Leung, Zhao Feng Peng, Jayapal Manikandan, Robert Z. Qi, Meng Inn Chuah, Adrian K. West, James C. Vickers, Jia Lu, Nam Sang Cheung, Roger S. Chung. Transcriptional insights on the regenerative mechanics of axotomized neurons in vitro. J Cell Mol Med. 2012 Apr;16(4):789-811. doi: 10.1111/j.1582-4934.2011.01361.

Kamura T, Hara T, Kotoshiba S, Yada M, Ishida N, Imaki H, Hatakeyama S, Nakayama K, Nakayama KI. Degradation of p57Kip2 mediated by SCFSkp2-dependent ubiquitylation. Proc Natl Acad Sci U S A. 2003 Sep 2;100(18):10231-6.

Kandli M, Feige E, Chen A, Kilfin G, Motro B. Isolation and characterization of two evolutionarily conserved murine kinases (Nek6 and nek7) related to the fungal mitotic regulator, NIMA. Genomics. 2000 Sep 1;68(2):187-96.

Kang TH, Park DY, Choi YH, Kim KJ, Yoon HS, Kim KT. Mitotic histone H3 phosphorylation by vaccinia-related kinase 1 in mammalian cells. Mol Cell Biol. 2007 Dec;27(24):8533-46.

Karg T, Warecki B, Sullivan W. Aurora B-mediated localized delays in nuclear envelope formation facilitate inclusion of late-segregating chromosome fragments. Mol Biol Cell. 2015 Jun 15;26(12):2227-41. doi: 10.1091/mbc.E15-01-0026.

Kassar-Duchossoy L, Gayraud-Morel B, Gomes D, Rocancourt D, Buckingham M, Shinin V, et al. MRF4 determines skeletal muscle identity in Myf5: Myod double-mutant. Nature 2004; 431:466-71.

Katayama H, Sasai K, Kawai H, Yuan ZM, Bondaruk J, Suzuki F, Fujii S, Arlinghaus RB, Czerniak BA, Sen S. Phosphorylation by aurora kinase A induces Mdm2-mediated destabilization and inhibition of p53. Nat Genet. 2004 Jan;36(1):55-62.

Katayama H, Wang J, Treekitkarnmongkol W, Kawai H, Sasai K, Zhang H, Wang H, Adams HP, Jiang S, Chakraborty SN, Suzuki F, Arlinghaus RB, Liu J, Mobley JA, Grizzle WE, Wang H, Sen S. Aurora kinase-A inactivates DNA damage-induced apoptosis and spindle assembly checkpoint response functions of p73. Cancer Cell. 2012 Feb 14;21(2):196-211. doi: 10.1016/j.ccr.2011.12.025.

Kato J, Matsushime H, Hiebert SW, Ewen ME, Sherr CJ. Direct binding of cyclin D to the retinoblastoma gene product (pRb) and pRb phosphorylation by the cyclin D-dependent kinase CDK4. Genes Dev. 1993 Mar;7(3):331-42.

Kawashima SA, Tsukahara T, Langegger M, Hauf S, Kitajima TS, Watanabe Y. Shugoshin enables tension-generating attachment of kinetochores by loading Aurora to centromeres. Genes Dev. 2007 Feb 15;21(4):420-35.

Kettenbach AN, Schlosser KA, Lyons SP, Nasa I, Gui J, Adamo ME, Gerber SA. Global assessment of its network dynamics reveals that the kinase Plk1 inhibits the phosphatase PP6 to promote Aurora A activity. Sci Signal. 2018 May 15;11(530). pii: eaaq1441. doi: 10.1126/scisignal.aaq1441.

Khazaei MR, Püschel AW. Phosphorylation of the par polarity complex protein Par3 at serine 962 is mediated by aurora a and regulates its function in neuronal polarity. J Biol Chem. 2009 Nov 27;284(48):33571-9. doi: 10.1074/jbc.M109.055897.

Kim Y, Starostina NG, Kipreos ET. The CRL4Cdt2 ubiquitin ligase targets the degradation of p21Cip1 to control replication licensing. Genes Dev. 2008 Sep 15;22(18):2507-19. doi: 10.1101/gad.1703708.

Kim JW, Jang SM, Kim CH, An JH, Kang EJ, Choi KH. New molecular bridge between RelA/p65 and NF-κB target genes via histone acetyltransferase TIP60 cofactor. J Biol Chem. 2012 Mar 2;287(10):7780-91. doi: 10.1074/jbc.M111.278465. Epub 2012 Jan 16.

Kimura K, Hirano M, Kobayashi R, Hirano T. Phosphorylation and activation of 13S condensin by Cdc2 in vitro. Science. 1998 Oct 16;282(5388):487-90.

Kimura M, Takagi S, Nakashima S. Aurora A regulates the architecture of the Golgi apparatus. Exp Cell Res. 2018 Jun 1;367(1):73-80. doi: 10.1016/j.yexcr.2018.03.024.

Kinoshita K, Noetzel TL, Pelletier L, Mechtler K, Drechsel DN, Schwager A, Lee M, Raff JW, Hyman AA. Aurora A phosphorylation of TACC3/maskin is required for centrosome-dependent microtubule assembly in mitosis. J Cell Biol. 2005 Sep 26;170(7):1047-55.

Kitagawa D, Vakonakis I, Olieric N, Hilbert M, Keller D, Olieric V, Bortfeld M, Erat MC, Flückiger I, Gönczy P, Steinmetz MO. Structural basis of the 9-fold symmetry of centrioles. Cell. 2011 Feb 4;144(3):364-75. doi: 10.1016/j.cell.2011.01.008.

Kitajima S1, Kudo Y, Ogawa I, Tatsuka M, Kawai H, Pagano M, Takata T. Constitutive phosphorylation of aurora-a on ser51 induces its stabilization and consequent overexpression in cancer. PLoS One. 2007 Sep 26;2(9):e944.

Kouros-Mehr H, Slorach EM, Sternlicht MD, Werb Z. GATA-3 maintains the differentiation of the luminal cell fate in the mammary gland. Cell. 2006 Dec 1;127(5):1041-55.

Kramer ER, Scheuringer N, Podtelejnikov AV, Mann M, Peters JM. Mitotic regulation of the APC activator proteins CDC20 and CDH1. Mol Biol Cell. 2000 May;11(5):1555-69.

Krenn V, Musacchio A. The Aurora B Kinase in Chromosome Bi-Orientation and Spindle Checkpoint Signaling. Front Oncol. 2015 Oct 16;5:225. doi: 10.3389/fonc.2015.00225.

Krystyniak A, Garcia-Echeverria C, Prigent C, Ferrari S. Inhibition of Aurora A in response to DNA damage. Oncogene. 2006 Jan 19;25(3):338-48.

La Thangue NB. DRTF1/E2F: an expanding family of heterodimeric transcription factors implicated in cell-cycle control Trends Biochem Sci. 1994 Mar;19(3):108-14.

Laughon A. DNA binding specificity of homeodomains. Biochemistry. 1991 Dec 3;30(48):11357-67.

Lakich MM, Diagana TT, North DL, Whalen RG. MEF-2 and Oct-1 bind to two homologous promoter sequence elements and participate in the expression of a skeletal muscle-specific gene. J Biol Chem. 1998 Jun 12;273(24):15217-26

Lan W, Zhang X, Kline-Smith SL, Rosasco SE, Barrett-Wilt GA, Shabanowitz J, Hunt DF, Walczak CE, Stukenberg PT. Aurora B phosphorylates centromeric MCAK and regulates its localization and microtubule depolymerization activity. Curr Biol. 2004 Feb 17;14(4):273-86.

Lane HA, Nigg EA. Antibody microinjection reveals an essential role for human polo-like kinase 1 (Plk1) in the functional maturation of mitotic centrosomes. J Cell Biol. 1996 Dec;135(6 Pt 2):1701-13.

Larsson N, Marklund U, Gradin HM, Brattsand G, Gullberg M. Control of microtubule dynamics by oncoprotein 18: dissection of the regulatory role of multisite phosphorylation during mitosis. Mol Cell Biol. 1997 Sep;17(9):5530-9.

Le Grand F, Rudnicki MA. Skeletal muscle satellite cells and adult myogenesis. Curr Opin Cell Biol. 2007 Dec;19(6):628-33. Epub 2007 Nov 8.

Lee K, Rhee K. PLK1 phosphorylation of pericentrin initiates centrosome maturation at the onset of mitosis. J Cell Biol. 2011 Dec 26;195(7):1093-101. doi: 10.1083/jcb.201106093.

Lee M, Kim IS, Park KC, Kim JS, Baek SH, Kim KI. Mitosis-specific phosphorylation of Mis18α by Aurora B kinase enhances kinetochore recruitment of polo-like kinase 1. Oncotarget. 2017 Nov 27;9(2):1563-1576. doi: 10.18632/oncotarget.22707.

Lee W, Haslinger A, Karin M, Tjian R. Activation of transcription by two factors that bind promoter and enhancer sequences of the human metallothionein gene and SV40. Nature. 1987 Jan 22-28;325(6102):368-72.

Lee WH, Bookstein R, Hong F, Young LJ, Shew JY, Lee EY. Human retinoblastoma susceptibility gene: cloning, identification, and sequence. Science. 1987 Mar 13;235(4794):1394-9.

Lees JA, Buchkovich KJ, Marshak DR, Anderson CW, Harlow E. The retinoblastoma protein is phosphorylated on multiple sites by human cdc2. EMBO J. 1991 Dec;10(13):4279-90.

Leland H. Hartwell, Joseph Culotti, and Brian Reid Genetic Control of the Cell-Division Cycle in Yeast, I. Detection of Mutants Proc Natl Acad Sci U S A. 1970 Jun; 66(2): 352–359.

Lénárt P, Petronczki M, Steegmaier M, Di Fiore B, Lipp JJ, Hoffmann M, Rettig WJ, Kraut N, Peters JM. The small-molecule inhibitor BI 2536 reveals novel insights into mitotic roles of polo-like kinase1. Curr Biol. 2007 Feb 20;17(4):304-15.

Lens SM, Wolthuis RM, Klompmaker R, Kauw J, Agami R, Brummelkamp T, Kops G, Medema RH. Survivin is required for a sustained spindle checkpoint arrest in response to lack of tension. EMBO J. 2003 Jun 16;22(12):2934-47.

Lentini L1, Amato A, Schillaci T, Di Leonardo A. Simultaneous Aurora-A/STK15 overexpression and centrosome amplification induce chromosomal instability in tumour cells with a MIN phenotype. BMC Cancer. 2007 Nov 13;7:212.

Levine MS, Bakker B, Boeckx B, Moyett J, Lu J, Vitre B, Spierings DC, Lansdorp PM, Cleveland DW, Lambrechts D, Foijer F, Holland AJ. Centrosome Amplification Is Sufficient to Promote

Spontaneous Tumorigenesis in Mammals. Dev Cell. 2017 Feb 6;40(3):313-322.e5. doi: 10.1016/j.devcel.2016.12.022.

Li Y, Kao GD, Garcia BA, Shabanowitz J, Hunt DF, Qin J, Phelan C, Lazar MA. A novel histone deacetylase pathway regulates mitosis by modulating Aurora B kinase activity. Genes Dev. 2006 Sep 15;20(18):2566-79.

Lindahl T, Barnes DE. Repair of endogenous DNA damage. Cold Spring Harb Symp Quant Biol. 2000;65:127-33.

Liu X, Tesfai J, Evrard YA, Dent SY, Martinez E. c-Myc transformation domain recruits the human STAGA complex and requires TRRAP and GCN5 acetylase activity for transcription activation. J Biol Chem. 2003 May 30;278(22):20405-12. Epub 2003 Mar 26.

Liu X, Li Z, Song Y, Wang R, Han L, Wang Q, Jiang K, Kang C, Zhang Q. AURKA induces EMT by regulating histone modification through Wnt/β-catenin and PI3K/Akt signaling pathway in gastric cancer. Oncotarget. 2016 May 31;7(22):33152-64. doi: 10.18632/oncotarget.8888.

Li, Z., Van Calcar, S., Qu, C., Cavenee, W.K., Zhang, M.Q., and Ren, B. A global transcriptional regulatory role for c-Myc in Burkitt's lymphoma cells. Proc. Natl. Acad. Sci. USA (2003); 100, 8164–8169.

Losada A, Yokochi T, Kobayashi R, Hirano T. Identification and characterization of SA/Scc3p subunits in the Xenopus and human cohesion complexes. J Cell Biol. 2000 Aug 7;150(3):405-16.

Lowe M, Rabouille C, Nakamura N, Watson R, Jackman M, Jämsä E, Rahman D, Pappin DJ, Warren G. Cdc2 kinase directly phosphorylates the cis-Golgi matrix protein GM130 and is required for Golgi fragmentation in mitosis. Cell. 1998 Sep 18;94(6):783-93.

Lu L, Han H, Tian Y, Li W, Zhang J, Feng M, Li Y. Aurora kinase A mediates c-Myc's oncogenic effects in hepatocellular carcinoma. Mol Carcinog. 2015 Nov;54(11):1467-79. doi: 10.1002/mc.22223.

Machida YJ, Hamlin JL, Dutta A. Right place, right time, and only once: replication initiation in metazoans. Cell. 2005 Oct 7;123(1):13-24.

Macůrek L, Lindqvist A, Lim D, Lampson MA, Klompmaker R, Freire R, Clouin C, Taylor SS, Yaffe MB, Medema RH. Polo-like kinase-1 is activated by aurora A to promote checkpoint recovery. Nature. 2008 Sep 4;455(7209):119-23. doi: 10.1038/nature07185.

Mallm JP, Rippe K. Aurora Kinase B Regulates Telomerase Activity via a Centromeric RNA in Stem Cells. Cell Rep. 2015 Jun 16;11(10):1667-78. doi: 10.1016/j.celrep.2015.05.015.

Mattera L, Escaffit F, Pillaire MJ, Selves J, Tyteca S, Hoffmann JS, Gourraud PA, Chevillard-Briet M, Cazaux C, Trouche D. The p400/Tip60 ratio is critical for colorectal cancer cell

proliferation through DNA damage response pathways. Oncogene. 2009 Mar 26;28(12):1506-17. doi: 10.1038/onc.2008.499. Epub 2009 Jan 26.

McGarry TJ, Kirschner MW. Geminin, an inhibitor of DNA replication, is degraded during mitosis. Cell. 1998 Jun 12;93(6):1043-53.

Meraldi P, Lukas J, Fry AM, Bartek J, Nigg EA. Centrosome duplication in mammalian somatic cells requires E2F and Cdk2-cyclin A. Nat Cell Biol. 1999 Jun;1(2):88-93.

Meraldi P1, Honda R, Nigg EA. Aurora-A overexpression reveals tetraploidization as a major route to centrosome amplification in p53-/- cells. EMBO J. 2002 Feb 15;21(4):483-92.

Meyer N, Penn LZ. Reflecting on 25 years with MYC. Nat Rev Cancer. 2008 Dec;8(12):976-90. doi: 10.1038/nrc2231.

Merino VF, Nguyen N, Jin K, Sadik H, Cho S, Korangath P, Han L, Foster YMN, Zhou XC, Zhang Z, Connolly RM, Stearns V, Ali SZ, Adams C, Chen Q, Pan D, Huso DL, Ordentlich P, Brodie A, Sukumar S. Combined Treatment with Epigenetic, Differentiating, and Chemotherapeutic Agents Cooperatively Targets Tumor-Initiating Cells in Triple-Negative Breast Cancer. Cancer Res. 2016 Apr 1;76(7):2013-2024. doi: 10.1158/0008-5472.CAN-15-1619. Epub 2016 Jan 19.

Mo F1,2, Zhuang X1,2, Liu X1,2,3,4,5, Yao PY5, Qin B1,2,5, Su Z5,6, Zang J1,2,3,4, Wang Z1,2,3,4, Zhang J1,2,7, Dou Z1,2,3,4, Tian C1,2,3,4, Teng M1,2,3,4, Niu L1,2,3,4, Hill DL8, Fang G1,2, Ding X5,6, Fu C1,2,3,4, Yao X1,2,3,4. Acetylation of Aurora B by TIP60 ensures accurate chromosomal segregation. Nat Chem Biol. 2016 Apr;12(4):226-32. doi: 10.1038/nchembio.2017.

Monaco L, Kolthur-Seetharam U, Loury R, Murcia JM, de Murcia G, Sassone-Corsi P. Inhibition of Aurora-B kinase activity by poly(ADP-ribosyl)ation in response to DNA damage. Proc Natl Acad Sci U S A. 2005 Oct 4;102(40):14244-8.

Morgan DO. Regulation of the APC and the exit from mitosis. Nat Cell Biol. 1999 Jun;1(2):E47-53.

Mori D, Yano Y, Toyo-oka K, Yoshida N, Yamada M, Muramatsu M, Zhang D, Saya H, Toyoshima YY, Kinoshita K, Wynshaw-Boris A, Hirotsune S. NDEL1 phosphorylation by Aurora-A kinase is essential for centrosomal maturation, separation, and TACC3 recruitment. Mol Cell Biol. 2007 Jan;27(1):352-67.

Mori D, Yamada M, Mimori-Kiyosue Y, Shirai Y, Suzuki A, Ohno S, Saya H, Wynshaw-Boris A, Hirotsune S. An essential role of the aPKC-Aurora A-NDEL1 pathway in neurite elongation by modulation of microtubule dynamics. Nat Cell Biol. 2009 Sep;11(9):1057-68. doi: 10.1038/ncb1919.

Morin PJ, Sparks AB, Korinek V, Barker N, Clevers H, Vogelstein B, Kinzler KW. Activation of beta-catenin-Tcf signaling in colon cancer by mutations in beta-catenin or APC. Science. 1997 Mar 21;275(5307):1787-90.

Morris L, Allen KE, La Thangue NB. Regulation of E2F transcription by cyclin E-Cdk2 kinase mediated through p300/CBP co-activators. Nat Cell Biol. 2000 Apr;2(4):232-9.

Mostocotto C, Carbone M, Battistelli C, Ciotti A, Amati P, Maione R. Poly(ADP-ribosyl)ation is required to modulate chromatin changes at c-MYC promoter during emergence from quiescence. PLoS One. 2014 Jul 21;9(7):e102575. doi: 10.1371/journal.pone.0102575.

Murata-Hori M, Wang YL. The kinase activity of aurora B is required for kinetochore-microtubule interactions during mitosis. Curr Biol. 2002 Jun 4;12(11):894-9.

Nabeshima Y, Hanaoka K, Hayasaka M, Esumi E, Li S, Nonaka I. Myogenin gene disruption results in perinatal lethality because of severe muscle defect. Nature 1993; 364:532-5.

Nath S, Somyajit K, Mishra A, Scully R, Nagaraju G. FANCJ helicase controls the balance between short- and long-tract gene conversions between sister chromatids. Nucleic Acids Res. 2017 Sep 6;45(15):8886-8900. doi: 10.1093/nar/gkx586.

Nevins JR. E2F: a link between the Rb tumor suppressor protein and viral oncoproteins. Science. 1992 Oct 16;258(5081):424-9.

Ng JM, Chen MJ, Leung JY, Peng ZF, Manikandan J, Qi RZ, Chuah MI, West AK, Vickers JC, Lu J, Cheung NS, Chung RS. Transcriptional insights on the regenerative mechanics of axotomized neurons in vitro. J Cell Mol Med. 2012 Apr;16(4):789-811. doi: 10.1111/j.1582-4934.2011.01361.

Nigg EA. Cyclin-dependent protein kinases: key regulators of the eukaryotic cell cycle. Bioessays. 1995 Jun;17(6):471-80.

Noton E, Diffley JF. CDK inactivation is the only essential function of the APC/C and the mitotic exit network proteins for origin resetting during mitosis. Mol Cell. 2000 Jan;5(1):85-95.

Ohashi S1, Sakashita G, Ban R, Nagasawa M, Matsuzaki H, Murata Y, Taniguchi H, Shima H, Furukawa K, Urano T. Phospho-regulation of human protein kinase Aurora-A: analysis using anti-phospho-Thr288monoclonal antibodies. Oncogene. 2006 Dec 14;25(59):7691-702.

Ohi R, Sapra T, Howard J, Mitchison TJ. Differentiation of cytoplasmic and meiotic spindle assembly MCAK functions by Aurora B-dependent phosphorylation. Mol Biol Cell. 2004 Jun;15(6):2895-906.

Ohishi T, Muramatsu Y, Yoshida H, Seimiya H. TRF1 ensures the centromeric function of Aurora-B and proper chromosome segregation. Mol Cell Biol. 2014 Jul;34(13):2464-78. doi: 10.1128/MCB.00161-14.

Ohtani K, DeGregori J, Nevins JR. Regulation of the cyclin E gene by transcription factor E2F1. Proc Natl Acad Sci U S A. 1995 Dec 19;92(26):12146-50.

Okano S1, Lan L, Caldecott KW, Mori T, Yasui A. Spatial and temporal cellular responses to single-strand breaks in human cells. Mol Cell Biol. 2003 Jun;23(11):3974-81.

Olguin HC, Olwin BB. Pax-7 up-regulation inhibits myogenesis and cell cycle progression in satellite cells: a potential mechanism for self-renewal. Dev Biol. 2004 Nov 15;275(2):375-88.

Ott MO, Bober E, Lyons G, Arnold H, Buckingham M. Early expression of the myogenic regulatory gene, myf-5, in precursor cells of skeletal muscle in the mouse embryo. Development 1991; 111:1097-107.

Otto T, Horn S, Brockmann M, Eilers U, Schüttrumpf L, Popov N, Kenney AM, Schulte JH, Beijersbergen R, Christiansen H, Berwanger B, Eilers M. Stabilization of N-Myc is a critical function of Aurora A in human neuroblastoma. Cancer Cell. 2009 Jan 6;15(1):67-78. doi: 10.1016/j.ccr.2008.12.005.

Ou O, Huppi K, Chakka S, Gehlhaus K, Dubois W, Patel J, Chen J, Mackiewicz M, Jones TL, Pitt JJ, Martin SE, Goldsmith P, Simmons JK, Mock BA, Caplen NJ. Loss-of-function RNAi screens in breast cancer cells identify AURKB, PLK1, PIK3R1, MAPK12, PRKD2, and PTK6 as sensitizing targets of rapamycin activity. Cancer Lett. 2014 Nov 28;354(2):336-47. doi: 10.1016/j.canlet.2014.08.043.

Padilla-Nash HM1, Heselmeyer-Haddad K, Wangsa D, Zhang H, Ghadimi BM, Macville M, Augustus M, Schröck E, Hilgenfeld E, Ried T. Jumping translocations are common in solid tumor cell lines and result in recurrent fusions of whole chromosome arms. Genes Chromosomes Cancer. 2001 Apr;30(4):349-63.

Pardee AB. A restriction point for control of normal animal cell proliferation. Proc Natl Acad Sci U S A. 1974 Apr;71(4):1286-90.

Pardee AB. G1 events and regulation of cell proliferation. Science. 1989 Nov 3;246(4930):603-8.

Park J, Song EJ. Deubiquitinase USP35 as a novel mitotic regulator via maintenance of Aurora B stability. BMB Rep. 2018 Jun;51(6):261-262.

Parker JS, Mullins M, Cheang CUM, Leung S, Voduc D, Vickery T, Davies S, Fauron C, He X, Hu Z, Quackenbush JF, Stijleman IJ, Palazzo J, Marron JS, Nobel AB, Mardis E, Nielsen TO, Ellis MJ, Perou MC, and Bernard PS. Supervised risk predictor of breast cancer based on intrinsic subtypes. J Clin Oncol. 2009 Mar 10; 27(8): 1160-1167. doi:10.1200/JCO.2008.18.1370

Patapoutian A, Yoon JK, Miner JH, Wang S, Stark K, Wold B. Disruption of the mouse MRF4 gene identifies multiple waves of myogenesis in the myotome. Development 1995; 121:3347-58.

Pérez de Castro I1, Aguirre-Portolés C, Martin B, Fernández-Miranda G, Klotzbucher A, Kubbutat MH, Megías D, Arlot-Bonnemains Y, Malumbres M. A SUMOylation Motif in Aurora-A: Implications for Spindle Dynamics and Oncogenesis. Front Oncol. 2011 Dec 14;1:50. doi: 10.3389/fonc.2011.00050.

Persico A, Cervigni RI, Barretta ML, Corda D, Colanzi A. Golgi partitioning controls mitotic entry through Aurora-A kinase. Mol Biol Cell. 2010 Nov 1;21(21):3708-21. doi: 10.1091/mbc.E10-03-0243.

Perna D, Fagà G, Verrecchia A, Gorski MM, Barozzi I, Narang V, Khng J, Lim KC, Sung WK, Sanges R, Stupka E, Oskarsson T, Trumpp A, Wei CL, Müller H, Amati B. Genome-wide mapping of Myc binding and gene regulation in serum-stimulated fibroblasts. Oncogene. 2012 Mar 29;31(13):1695-709. doi: 10.1038/onc.2011.359. Epub 2011 Aug 22.

Petronczki M, Lénárt P, Peters JM. Polo on the Rise-from Mitotic Entry to Cytokinesis with Plk1. Dev Cell. 2008 May;14(5):646-59. doi: 10.1016/j.devcel.2008.04.014.

Pfleger CM, Kirschner MW. The KEN box: an APC recognition signal distinct from the D box targeted by Cdh1. Genes Dev. 2000 Mar 15;14(6):655-65.

Pinyol R, Scrofani J, Vernos I. The role of NEDD1 phosphorylation by Aurora A in chromosomal microtubule nucleation and spindle function. Curr Biol. 2013 Jan 21;23(2):143-9. doi: 10.1016/j.cub.2012.11.046.

Plotnikova OV, Nikonova AS, Loskutov YV, Kozyulina PY, Pugacheva EN, Golemis EA. Calmodulin activation of Aurora-A kinase (AURKA) is required during ciliary disassembly and in mitosis. Mol Biol Cell. 2012 Jul;23(14):2658-70. doi: 10.1091/mbc.E11-12-1056.

Plotnikova OV, Pugacheva EN, Dunbrack RL, Golemis EA. Rapid calcium-dependent activation of Aurora-A kinase. Nat Commun. 2010 Sep 7;1:64. doi: 10.1038/ncomms1061.

Plotnikova OV, Pugacheva EN, Golemis EA. Aurora A kinase activity influences calcium signaling in kidney cells. J Cell Biol. 2011 Jun 13;193(6):1021-32. doi: 10.1083/jcb.201012061.

Pouwels J, Kukkonen AM, Lan W, Daum JR, Gorbsky GJ, Stukenberg T, Kallio MJ. Shugoshin 1 plays a central role in kinetochore assembly and is required for kinetochore targeting of Plk1. Cell Cycle. 2007 Jul 1;6(13):1579-85.

Pugacheva EN, Jablonski SA, Hartman TR, Henske EP, Golemis EA. HEF1-dependent Aurora A activation induces disassembly of the primary cilium. Cell. 2007 Jun 29;129(7):1351-63.

Puget N, Knowlton M, Scully R. Molecular analysis of sister chromatid recombination in mammalian cells. DNA Repair (Amst). 2005 Feb 3;4(2):149-61.

Puig-Butille JA1, Vinyals A2, Ferreres JR3, Aguilera P4, Cabré E2, Tell-Martí G4, Marcoval J3, Mateo F5, Palomero L5, Badenas C1, Piulats JM5, Malvehy J4, Pujana MA5, Puig S4, Fabra À6. AURKA Overexpression Is Driven by FOXM1 and MAPK/ERK Activation in Melanoma CellsHarboring BRAF or NRAS Mutations: Impact on Melanoma Prognosis and Therapy. J Invest Dermatol. 2017 Jun;137(6):1297-1310. doi: 10.1016/j.jid.2017.01.021.

Prendergast GC, Hopewell R, Gorham BJ, Ziff EB. Biphasic effect of Max on Myc cotransformation activity and dependence on amino- and carboxy-terminal Max functions. Genes Dev. 1992 Dec;6(12A):2429-39.

Qian YW, Erikson E, Li C, Maller JL. Activated polo-like kinase Plx1 is required at multiple points during mitosis in Xenopus laevis. Mol Cell Biol. 1998 Jul;18(7):4262-71.

Rawls A, Morris JH, Rudnicki M, Braun T, Arnold HH, Klein WH, et al. Myogenin's functions do not overlap with those of MyoD or Myf-5 during mouse embryogenesis. Dev Biol 1995; 172:37-50.

Rawls A, Valdez MR, Zhang W, Richardson J, Klein WH, Olson EN. Overlapping functions of the myogenic bHLH genes MRF4 and MyoD revealed in double mutant mice. Development 1998; 125:2349-58.

Reyes C, Serrurier C, Gauthier T, Gachet Y, Tournier S. Aurora B prevents chromosome arm separation defects by promoting telomere dispersion and disjunction. J Cell Biol. 2015 Mar 16;208(6):713-27. doi: 10.1083/jcb.201407016.

Richards MW, Burgess SG, Poon E, Carstensen A, Eilers M, Chesler L, Bayliss R. Structural basis of N-Myc binding by Aurora-A and its destabilization by kinase inhibitors. Proc Natl Acad Sci U S A. 2016 Nov 29;113(48):13726-13731.

Rieder CL, Salmon ED. The vertebrate cell kinetochore and its roles during mitosis. Trends Cell Biol. 1998 Aug;8(8):310-8.

Robbins AR1, Jablonski SA, Yen TJ, Yoda K, Robey R, Bates SE, Sackett DL. Inhibitors of histone deacetylases alter kinetochore assembly by disrupting pericentromeric heterochromatin. Cell Cycle. 2005 May;4(5):717-26.

Robinson PJ, An W, Routh A, Martino F, Chapman L, Roeder RG, Rhodes D. 30 nm chromatin fibre decompaction requires both H4-K16 acetylation and linker histone eviction. J Mol Biol. 2008 Sep 12;381(4):816-25. doi: 10.1016/j.jmb.2008.04.050.

Rosenfeld MG. POU-domain transcription factors: pou-er-ful developmental regulators. Genes Dev. 1991 Jun;5(6):897-907.

Ruderman NB, Kapeller R, White MF, Cantley LC. Activation of phosphatidylinositol 3-kinase by insulin. Proc Natl Acad Sci U S A. 1990 Feb;87(4):1411-5.

Rudnicki MA, Braun T, Hinuma S, Jaenisch R. Inactivation of MyoD in mice leads to upregulation of the myogenic HLH gene Myf-5 and results in apparently normal muscle development. Cell 1992; 71:383-90.

Rudnicki MA, Schnegelsberg PN, Stead RH, Braun T, Arnold HH, Jaenisch R. MyoD or Myf-5 is required for the formation of skeletal muscle. Cell 1993; 75:1351-9.

Ruvkun G, Finney M. Regulation of transcription and cell identity by POU domain proteins. Cell. 1991 Feb 8;64(3):475-8.

Ryan AK, Rosenfeld MG. POU domain family values: flexibility, partnerships, and developmental codes. Genes Dev. 1997 May 15;11(10):1207-25

Sakuraba K, Yasuda T, Sakata M, Kitamura YH, Shirahata A, Goto T, Mizukami H, Saito M, Ishibashi K, Kigawa G, Nemoto H, Sanada Y, Hibi K. Down-regulation of Tip60 gene as a potential marker for the malignancy of colorectal cancer. Anticancer Res. 2009 Oct;29(10):3953-5.

Sarkissian M1, Mendez R, Richter JD. Progesterone and insulin stimulation of CPEB-dependent polyadenylation is regulated by AuroraA and glycogen synthase kinase-3. Genes Dev. 2004 Jan 1;18(1):48-61.

Saxton RA, Sabatini DM. mTOR Signaling in Growth, Metabolism, and Disease. Cell. 2017 Mar 9;168(6):960-976. doi: 10.1016/j.cell.2017.02.004.

Schlosser I, Hölzel M, Mürnseer M, Burtscher H, Weidle UH, Eick D. A role for c-Myc in the regulation of ribosomal RNA processing. Nucleic Acids Res. 2003 Nov 1;31(21):6148-56.

Scott PH, Brunn GJ, Kohn AD, Roth RA, Lawrence JC Jr. Evidence of insulin-stimulated phosphorylation and activation of the mammalian target of rapamycin mediated by a protein kinase B signaling pathway. Proc Natl Acad Sci U S A. 1998 Jun 23;95(13):7772-7.

Sebastian B, Kakizuka A, Hunter T. Cdc25M2 activation of cyclin-dependent kinases by dephosphorylation of threonine-14 and tyrosine-15. Proc Natl Acad Sci U S A. 1993 Apr 15;90(8):3521-4.

Seki A, Coppinger JA, Jang CY, Yates JR, Fang G. Bora and the kinase Aurora a cooperatively activate the kinase Plk1 and control mitotic entry. Science. 2008 Jun 20;320(5883):1655-8. doi: 10.1126/science.1157425.

Shandilya J, Medler KF, Roberts SG. Regulation of AURORA B function by mitotic checkpoint protein MAD2. Cell Cycle. 2016 Aug 17;15(16):2196-2201.

Shen-Li H, O'Hagan RC, Hou H Jr, Horner JW 2nd, Lee HW, DePinho RA. Essential role for Max in early embryonic growth and development. Genes Dev. 2000 Jan 1;14(1):17-22.

Shintani S, Mihara M, Li C, Nakahara Y, Hino S, Nakashiro K, Hamakawa H. Up-regulation of DNA-dependent protein kinase correlates with radiation resistance in oral squamous cell carcinoma. Cancer Sci. 2003 Oct;94(10):894-900.

Shirayama M, Zachariae W, Ciosk R, Nasmyth K. The Polo-like kinase Cdc5p and the WD-repeat protein Cdc20p/fizzy are regulators and substratesof the anaphase promoting complex in Saccharomyces cerevisiae. EMBO J. 1998 Mar 2;17(5):1336-49.

Shogren-Knaak M, Ishii H, Sun JM, Pazin MJ, Davie JR, Peterson CL. Histone H4-K16 acetylation controls chromatin structure and protein interactions. Science. 2006 Feb 10;311(5762):844-7.

Shtutman M, Zhurinsky J, Simcha I, Albanese C, D'Amico M, Pestell R, Ben-Ze'ev A. The cyclin D1 gene is a target of the beta-catenin/LEF-1 pathway. Proc Natl Acad Sci U S A. 1999 May 11;96(10):5522-7.

Shu SK, Liu Q, Coppola D, Cheng JQ. Phosphorylation and activation of androgen receptor by Aurora-A. J Biol Chem. 2016 Oct 21;291(43):22854.

Shukla A, Kong D, Sharma M, Magidson V, Loncarek J. Plk1 relieves centriole block to reduplication by promoting daughter centriole maturation. Nat Commun. 2015 Aug 21;6:8077. doi: 10.1038/ncomms9077.

Singh SK, Wu W, Zhang L, Klammer H, Wang M, Iliakis G. Widespread dependence of backup NHEJ on growth state: ramifications for the use of DNA-PK inhibitors. Int J Radiat Oncol Biol Phys. 2011 Feb 1;79(2):540-8. doi: 10.1016/j.ijrobp.2010.08.018. Epub 2010 Oct 13.

Sirzén F, Nilsson A, Zhivotovsky B, Lewensohn R. DNA-dependent protein kinase content and activity in lung carcinoma cell lines: correlation with intrinsic radiosensitivity.

Soucek T, Pusch O, Hengstschläger-Ottnad E, Adams PD, Hengstschläger M. Deregulated expression of E2F-1 induces cyclin A- and E-associated kinase activities independently from cell cycle position. Oncogene. 1997 May 15;14(19):2251-7.

Soufi A, Garcia MF, Jaroszewicz A, Osman N, Pellegrini M, Zaret KS. Pioneer transcription factors target partial DNA motifs on nucleosomes to initiate reprogramming. Cell. 2015 Apr 23;161(3):555-568. doi: 10.1016/j.cell.2015.03.017. Epub 2015 Apr 16.

Sourisseau T, Maniotis D, McCarthy A, Tang C, Lord CJ, Ashworth A, Linardopoulos S. Aurora-A expressing tumour cells are deficient for homology-directed DNA double strand-breakrepair and sensitive to PARP inhibition. EMBO Mol Med. 2010 Apr;2(4):130-42. doi: 10.1002/emmm.201000068.

Speliotes EK, Uren A, Vaux D, Horvitz HR. The survivin-like C. elegans BIR-1 protein acts with the Aurora-like kinase AIR-2 to affect chromosomes and the spindle midzone. Mol Cell. 2000 Aug;6(2):211-23.

Srivastava M, Nambiar M, Sharma S, Karki SS, Goldsmith G, Hegde M, Kumar S, Pandey M, Singh RK, Ray P, Natarajan R, Kelkar M, De A, Choudhary B, Raghavan SC. An inhibitor of nonhomologous end-joining abrogates double-strand break repair and impedes cancer progression. Cell. 2012 Dec 21;151(7):1474-87. doi: 10.1016/j.cell.2012.11.054.

Squatrito M, Gorrini C, Amati B. Tip60 in DNA damage response and growth control: many tricks in one HAT. Trends Cell Biol. 2006 Sep;16(9):433-42. Epub 2006 Aug 9.

Stephens PJ, Greenman CD, Fu B, Yang F, Bignell GR, Mudie LJ, Pleasance ED, Lau KW, Beare D, Stebbings LA, McLaren S, Lin ML, McBride DJ, Varela I, Nik-Zainal S, Leroy C, Jia M, Menzies A, Butler AP, Teague JW, Quail MA, Burton J, Swerdlow H, Carter NP, Morsberger LA, Iacobuzio-Donahue C, Follows GA, Green AR, Flanagan AM, Stratton MR, Futreal PA, Campbell PJ. Massive genomic rearrangement acquired in a single catastrophic event during cancer development. Cell. 2011 Jan 7;144(1):27-40. doi: 10.1016/j.cell.2010.11.055.

Su R, Gong JN, Chen MT, Song L, Shen C, Zhang XH, Yin XL, Ning HM, Liu B, Wang F, Ma YN, Zhao HL, Yu J, Zhang JW. c-Myc suppresses miR-451¬YWTAZ/AKT axis via recruiting HDAC3 in acute myeloid leukemia. Oncotarget. 2016 Nov 22;7(47):77430-77443. doi: 10.18632/oncotarget.12679.

Sumara I, Vorlaufer E, Gieffers C, Peters BH, Peters JM. Characterization of vertebrate cohesin complexes and their regulation in prophase. J Cell Biol. 2000 Nov 13;151(4):749-62.

Sun L, Hodeify R, Haun S, Charlesworth A, MacNicol AM, Ponnappan S, Ponnappan U, Prigent C, Machaca K. Ca2+ homeostasis regulates Xenopus oocyte maturation. Biol Reprod. 2008 Apr;78(4):726-35.

Sun Y, Jiang X, Chen S, Fernandes N, Price BD. A role for the Tip60 histone acetyltransferase in the acetylation and activation of ATM. Proc Natl Acad Sci U S A. 2005 Sep 13;102(37):13182-7. Epub 2005 Sep 2.

Sun Y, Jiang X, Price BD. Tip60: connecting chromatin to DNA damage signaling. Cell Cycle. 2010 Mar 1;9(5):930-6. Epub 2010 Mar 11.

Sutani T, Yuasa T, Tomonaga T, Dohmae N, Takio K, Yanagida M. Fission yeast condensin complex: essential roles of non-SMC subunits for condensation and Cdc2 phosphorylation of Cut3/SMC4. Genes Dev. 1999 Sep 1;13(17):2271-83.

Sykes SM, Mellert HS, Holbert MA, Li K, Marmorstein R, Lane WS, McMahon SB. Acetylation of the p53 DNA-binding domain regulates apoptosis induction. Mol Cell. 2006 Dec 28;24(6):841-51.

Taga M, Hirooka E, Ouchi T. Essential roles of mTOR/Akt pathway in Aurora-A cell transformation. Int J Biol Sci. 2009 Jun 19;5(5):444-50.

Tang J, Cho NW, Cui G, Manion EM, Shanbhag NM, Botuyan MV, Mer G, Greenberg RA. Acetylation limits 53BP1 association with damaged chromatin to promote homologous recombination. Nat Struct Mol Biol. 2013 Mar;20(3):317-25. doi: 10.1038/nsmb.2499. Epub 2013 Feb 3.

Tang Y, Luo J, Zhang W, Gu W. Tip60-dependent acetylation of p53 modulates the decision between cell-cycle arrest and apoptosis. Mol Cell. 2006 Dec 28;24(6):827-39.

Takitoh T, Kumamoto K, Wang CC, Sato M, Toba S, Wynshaw-Boris A, Hirotsune S. Activation of Aurora-A is essential for neuronal migration via modulation of microtubule organization. J Neurosci. 2012 Aug 8;32(32):11050-66.

Taubert S, Gorrini C, Frank SR, Parisi T, Fuchs M, Chan HM, Livingston DM, Amati B. E2F-dependent histone acetylation and recruitment of the Tip60 acetyltransferase complex to chromatin in late G1. Mol Cell Biol. 2004 May;24(10):4546-56.

Tsvetkov LM, Yeh KH, Lee SJ, Sun H, Zhang H. p27(Kip1) ubiquitination and degradation is regulated by the SCF(Skp2) complex through phosphorylated Thr187 in p27. Curr Biol. 1999 Jun 17;9(12):661-4.

Turner R, Tjian R. Leucine repeats and an adjacent DNA binding domain mediate the formation of functional cFos-cJun heterodimers. Science. 1989 Mar 31;243(4899):1689-94.

Uribesalgo I, Buschbeck M, Gutiérrez A, Teichmann S, Demajo S, Kuebler B, Nomdedéu JF, Martín-Caballero J, Roma G, Benitah SA, Di Croce L. E-box-independent regulation of transcription and differentiation by MYC. Nat Cell Biol. 2011 Oct 23;13(12):1443-9. doi: 10.1038/ncb2355.

Van Den Broeck A, Nissou D, Brambilla E, Eymin B, Gazzeri S. Activation of a Tip60/E2F1/ERCC1 network in human lung adenocarcinoma cells exposed to cisplatin. Carcinogenesis. 2012 Feb;33(2):320-5. doi: 10.1093/carcin/bgr292. Epub 2011 Dec 9.

Venuti JM, Morris JH, Vivian JL, Olson EN, Klein WH. Myogenin is required for late but not early aspects of myogenesis during mouse development. J Cell Biol 1995; 128:563-76.

Verrijzer CP, Alkema MJ, van Weperen WW, Van Leeuwen HC, Strating MJ, van der Vliet PC.The DNA binding specificity of the bipartite POU domain and its subdomains. EMBO J. 1992 Dec;11(13):4993-5003.

Vicente-Manzanares M, Sánchez-Madrid F. Role of the cytoskeleton during leukocyte responses. Nat Rev Immunol. 2004 Feb;4(2):110-22.

Vigneron S, Sundermann L, Labbé JC, Pintard L, Radulescu O, Castro A, Lorca T. Cyclin A-cdk1-Dependent Phosphorylation of Bora Is the Triggering Factor Promoting Mitotic Entry. Dev Cell. 2018 Jun 4;45(5):637-650.e7. doi: 10.1016/j.devcel.2018.05.005.

Vo TTL1, Park JH1, Seo JH2, Lee EJ1, Choi H1, Bae SJ1, Le H1, An S1, Lee HS1, Wee HJ1, Kim KW1,3. ARD1-mediated aurora kinase A acetylation promotes cell proliferation and migration. Oncotarget. 2017 Jul 18;8(34):57216-57230. doi: 10.18632/oncotarget.19332.

Waizenegger IC, Hauf S, Meinke A, Peters JM. Two distinct pathways remove mammalian cohesin from chromosome arms in prophase and from centromeres in anaphase. Cell. 2000 Oct 27;103(3):399-410.

Walter AO1, Seghezzi W, Korver W, Sheung J, Lees E. The mitotic serine/threonine kinase Aurora2/AIK is regulated by phosphorylation and degradation. Oncogene. 2000 Oct 5;19(42):4906-16.

Wagner AJ, Meyers C, Laimins LA, Hay N. c-Myc induces the expression and activity of ornithine decarboxylase. Cell Growth Differ. 1993 Nov;4(11):879-83.

Wang F, Dai J, Daum JR, Niedzialkowska E, Banerjee B, Stukenberg PT, Gorbsky GJ, Higgins JM. Histone H3 Thr-3 phosphorylation by Haspin positions Aurora B at centromeres in mitosis. Science. 2010 Oct 8;330(6001):231-5. doi: 10.1126/science.1189435.

Wang G, Chen Q, Zhang X, Zhang B, Zhuo X, Liu J, Jiang Q, Zhang C. PCM1 recruits Plk1 to the pericentriolar matrix to promote primary cilia disassembly before mitotic entry. J Cell Sci. 2013 Mar 15;126(Pt 6):1355-65. doi: 10.1242/jcs.114918.

Wang H, Peng B, Pandita RK, Engler DA, Matsunami RK, Xu X, Hegde PM, Butler BE, Pandita TK, Mitra S, Xu B, Hegde ML. Aurora kinase B dependent phosphorylation of 53BP1 is required for resolving merotelic kinetochore-microtubule attachment errors during mitosis. Oncotarget. 2017 Jul 25;8(30):48671-48687. doi: 10.18632/oncotarget.16225.

Wang Y, Sun H, Wang Z, Liu M, Qi Z, Meng J, Sun J, Yang G. Aurora-A: a potential DNA repair modulator. Tumour Biol. 2014 Apr;35(4):2831-6. doi: 10.1007/s13277-013-1393-8.

Wang Y, Wang Z, Qi Z, Yin S, Zhang N, Liu Y, Liu M, Meng J, Zang R1, Zhang Z, Yang G. The negative interplay between Aurora A/B and BRCA1/2 controls cancer cell growth and tumorigenesis via distinct regulation of cell cycle progression, cytokinesis, and tetraploidy. Mol Cancer. 2014 Apr 28;13:94. doi: 10.1186/1476-4598-13-94.

Wang ZM, Yang H, Livingston DM. Endogenous E2F-1 promotes timely G0 exit of resting mouse embryo fibroblasts. Proc Natl Acad Sci U S A. 1998 Dec 22;95(26):15583-6.

Warecki B, Sullivan W. Micronuclei Formation Is Prevented by Aurora B-mediated Exclusion of HP1a from Late-Segregating Chromatin in Drosophila. Genetics. 2018 Jul 9. pii: genetics.301031.2018. doi: 10.1534/genetics.118.301031.

Wei H1, Yu X2. Functions of PARylation in DNA Damage Repair Pathways. Genomics Proteomics Bioinformatics. 2016 Jun;14(3):131-139. doi: 10.1016/j.gpb.2016.05.001.

Wei Y, Yu L, Bowen J, Gorovsky MA, Allis CD. Phosphorylation of histone H3 is required for proper chromosome condensation and segregation. Cell. 1999 Apr 2;97(1):99-109.

Wilkins BJ, Rall NA, Ostwal Y, Kruitwagen T, Hiragami-Hamada K, Winkler M, Barral Y, Fischle W, Neumann H. A cascade of histone modifications induces chromatin condensation in mitosis. Science. 2014 Jan 3;343(6166):77-80. doi: 10.1126/science.1244508.

Windhofer F, Wu W, Wang M, Singh SK, Saha J, Rosidi B, Iliakis G. Marked dependence on growth state of backup pathways of NHEJ. Int J Radiat Oncol Biol Phys. 2007 Aug 1;68(5):1462-70.

Wu CC, Yang TY, Yu CT, Phan L, Ivan C, Sood AK, Hsu SL, Lee MH. p53 negatively regulates Aurora A via both transcriptional and posttranslational regulation. Cell Cycle. 2012 Sep 15;11(18):3433-42. doi: 10.4161/cc.21732.

Wu R, Jurek M, Sundarababu S, Weinstein DE. The POU gene Brn-5 is induced by neuregulin and is restricted to myelinating Schwann cells. Mol Cell Neurosci. 2001 Apr;17(4):683-95.

X. Ivanov, Z. Mladenov, S. Nedyalkov, and T. G. Todorov. Experimental investigations into avian leucoses. Transmission, haematology and morphology of avian myelocytomatosis. Bulletin de Institut de Pathology Comparative Animaux, vol. 10, pp. 5–38, 1964.)

Xiao H, Chung J, Kao HY, Yang YC. Tip60 is a co-repressor for STAT3. J Biol Chem. 2003 Mar 28;278(13):11197-204. Epub 2003 Jan 27.

Xu DR, Huang S, Long ZJ, Chen JJ, Zou ZZ, Li J, Lin DJ, Liu Q. Inhibition of mitotic kinase Aurora suppresses Akt-1 activation and induces apoptotic cell death in all-trans retinoid acid-resistant acute promyelocytic leukemia cells. J Transl Med. 2011 May 21;9:74. doi: 10.1186/1479-5876-9-74.

Yan W, Cao QJ, Arenas RB, Bentley B, Shao R. GATA3 inhibits breast cancer metastasis through the reversal of epithelial-mesenchymal transition. J Biol Chem. 2010 Apr 30;285(18):14042-51. doi: 10.1074/jbc.M110.105262. Epub 2010 Feb 26.

Yang D, Liu H, Goga A, Kim S, Yuneva M, Bishop JM. Therapeutic potential of a synthetic lethal interaction between the MYC proto-oncogene and inhibition of aurora-B kinase. Proc Natl Acad Sci U S A. 2010 Aug 3;107(31):13836-41. doi: 10.1073/pnas.1008366107.

Yang SH, Sharrocks AD, Whitmarsh AJ. MAP kinase signalling cascades and transcriptional regulation. Gene. 2013 Jan 15;513(1):1-13. doi: 10.1016/j.gene.2012.10.033.

Yao JE, Yan M, Guan Z, Pan CB, Xia LP, Li CX, Wang LH, Long ZJ, Zhao Y, Li MW, Zheng FM, Xu J, Lin DJ, Liu Q. Aurora-A down-regulates IkappaBalpha via Akt activation and interacts with insulin-like growth factor-1 induced phosphatidylinositol 3-kinase pathway for cancer cell survival. Mol Cancer. 2009 Nov 5;8:95. doi: 10.1186/1476-4598-8-95.

Yasui Y1, Urano T, Kawajiri A, Nagata K, Tatsuka M, Saya H, Furukawa K, Takahashi T, Izawa I, Inagaki M. Autophosphorylation of a newly identified site of Aurora-B is indispensable for cytokinesis. J Biol Chem. 2004 Mar 26;279(13):12997-3003.

Ye XS, Fincher RR, Tang A, Osmani AH, Osmani SA. Regulation of the anaphase-promoting complex/cyclosome by bimAAPC3 and proteolysis of NIMA. Mol Biol Cell. 1998 Nov;9(11):3019-30.

Yu CT, Wu JC, Liao MC, Hsu SL, Huang CY. Identification of c-Fos as a mitotic phosphoprotein: regulation of c-Fos by Aurora-A. J Biomed Sci. 2008 Jan;15(1):79-87.

Yu F, Jiang Y, Lu L, Cao M, Qiao Y, Liu X, Liu D, Van Dyke T, Wang F, Yao X, Guo J, Yang Z. Aurora-A promotes the establishment of spindle assembly checkpoint by priming the Haspin-Aurora-B feedback loop in late G2 phase. Cell Discov. 2017 Jan 10;3:16049. doi: 10.1038/celldisc.2016.49.

Yun Li, Gary D. Kao, Benjamin A. Garcia, Jeffrey Shabanowitz, Donald F. Hunt, Jun Qin, Caroline Phelan, and Mitchell A. Lazar. A novel histone deacetylase pathway regulates mitosis by modulating Aurora B kinase activity. Genes Dev. 2006 Sep 15; 20(18): 2566–2579. doi: 10.1101/gad.1455006.

Z. Mladenov, U.Heine, D.Beard, and J.W. Beard. Strain MC29 avian leukosis virus. Myelocytoma, endothelioma, and renal growths: pathomorphological and ultrastructural aspects. Journal of the National Cancer Institute, vol. 38, no. 3, pp. 251–285, 1967.

Zammit PS, Relaix F, Nagata Y, Ruiz AP, Collins CA, Partridge TA, Beauchamp JR. Pax7 and myogenic progression in skeletal muscle satellite cells. J Cell Sci. 2006 May 1;119(Pt 9):1824-32. Epub 2006 Apr 11.

Zeller KI, Zhao X, Lee CW, Chiu KP, Yao F, Yustein JT, Ooi HS, Orlov YL, Shahab A, Yong HC, Fu Y, Weng Z, Kuznetsov VA, Sung WK, Ruan Y, Dang CV, Wei CL. Global mapping of c-Myc binding sites and target gene networks in human B cells. Proc Natl Acad Sci U S A. 2006 Nov 21;103(47):17834-9. Epub 2006 Nov 8.

Zhao Y, Cheng D, Wang S, Zhu J. Dual roles of c-Myc in the regulation of hTERT gene. Nucleic Acids Res. 2014;42(16):10385-98. doi: 10.1093/nar/gku721. Epub 2014 Aug 28.

Zhang CZ, Leibowitz ML, Pellman D. Chromothripsis and beyond: rapid genome evolution from complex chromosomal rearrangements. Genes Dev. 2013 Dec 1;27(23):2513-30. doi: 10.1101/gad.229559.113.

Zhang CZ, Spektor A, Cornils H, Francis JM, Jackson EK, Liu S, Meyerson M, Pellman D. Chromothripsis from DNA damage in micronuclei. Nature. 2015 Jun 11;522(7555):179-84. doi: 10.1038/nature14493.

Zhang M, Atkinson RL, Rosen JM. Selective targeting of radiation-resistant tumor-initiating cells.Proc Natl Acad Sci U S A. 2010 Feb 23;107(8):3522-7. doi: 10.1073/pnas.0910179107.

Zhang W, Behringer RR, Olson EN. Inactivation of the myogenic bHLH gene MRF4 results in upregulation of myogenin and rib anomalies. Genes Dev 1995; 9:1388-99.

Zhao Y, Hu X, Wei L, Song D, Wang J, You L, Saiyin H, Li Z, Yu W, Yu L, Ding J, Wu J. PARP10 suppresses tumor metastasis through regulation of Aurora A activity. Oncogene. 2018 May;37(22):2921-2935. doi: 10.1038/s41388-018-0168-5.

Zhao ZS, Lim JP, Ng YW, Lim L, Manser E. The GIT-associated kinase PAK targets to the centrosome and regulates Aurora-A. Mol Cell. 2005 Oct 28;20(2):237-49.

Zheng F, Yue C, Li G, He B, Cheng W, Wang X, Yan M, Long Z, Qiu W, Yuan Z, Xu J, Liu B, Shi Q, Lam EW, Hung MC, Liu Q. Nuclear AURKA acquires kinase-independent transactivating function to enhance breast cancer stem cell phenotype. Nat Commun. 2016 Jan 19;7:10180. doi: 10.1038/ncomms10180.

Zhu C, Mills KD, Ferguson DO, Lee C, Manis J, Fleming J, Gao Y, Morton CC, Alt FW. Unrepaired DNA breaks in p53-deficient cells lead to oncogenic gene amplification subsequent to translocations. Cell. 2002 Jun 28;109(7):811-21.